



The Molecular Composition and Geochemical Applications of Asphaltenes

A thesis submitted to the Newcastle University in partial fulfilment of the requirements for the degree of Doctor of Philosophy in the Faculty of Science, Engineering and Agriculture

Aminu Bayawa Muhammad

School of Civil Engineering & Geosciences
Newcastle University, UK

October 2009

Declaration

I hereby certify that the work described in this thesis is my own, except where otherwise acknowledged, and has not been submitted previously for a degree at this or any other University.

Aminu Bayawa Muhammad

Dedication

I dedicate this work to my father, Late Muhammad Ibrahim Bayawa; my mother, Malama Hadiza Bayawa and all my teachers. Thank you!

Abstract

Asphaltenes are the heaviest components of petroleum and bitumen consisting of a complex mixture of heteroaromatic substances that have been associated with various deposition problems in both upstream and downstream sectors of the petroleum industry. This thesis describes characterisation of asphaltenes from a variety of sources and geographical areas using FTIR, NMR, as well as selective chemical degradation methods in combination with GC/MS & GC/IRMS with the aim of understanding how their compositions vary with source and geochemical history.

Asphaltenes were observed to co-precipitate with substances such as waxes that are components of the maltene fraction. Quantitative removal of the co-precipitated substances requires Soxhlet extraction of the asphaltenes for several hours. The extraction time was found to vary with different asphaltenes. The so-called occlusion or physical entrapment of biomarkers in the cage-like structure of the asphaltenes is more than likely a consequence of the co-precipitation of the waxes.

Analysis of mid-infrared spectra of the asphaltenes revealed that petroleum asphaltenes consist predominantly of aliphatic moieties bonded to condensed aromatic structures with relative proportions of aromatic carbon in range of 30 to 40% for non-biodegraded petroleum asphaltenes as revealed by ^{13}C NMR. Biodegraded asphaltenes are less aromatic with relative aromatic carbon being 27% or less although the aromatic moieties tend to have relatively greater degree of condensation than asphaltenes from on-degraded oils. Although *n*-alkyl and *iso*-alkyl groups are the dominant aliphatic moieties, naphthenic groups, mainly in form of homohopanooids and steroids, are significantly present. Oxygen functionalities are mainly in form of hydroxyl, ether, ester, and carboxyl as well as conjugated ketone groups. Ester groups were detected only in coal and black shale asphaltenes. Carboxyl groups were detected in all the asphaltenes irrespective of source and geographical region, although they were particularly prominent in black shale and coal asphaltenes even at a relatively high rank of $R_o = 1.5\%$. Nitrogen functionalities were present as pyridinic and pyrrolic heteroaromatic systems in addition to tertiary aromatic amines.

With increasing thermal stress, asphaltenes were observed to evolve towards an equilibrium structure or composition in which aromatic moieties become dominant over aliphatic moieties as a result of increasing condensation and dealkylation. Distribution of alkyl moieties shifts towards increasing proportions of the lower molecular weight homologues with increasing thermal maturity. The thermal stress also results in loss of oxygen functionalities mainly from ester and carboxyl groups. At the molecular level, isomerisation of bound hopanooids and steroids to form an equilibrium composition was observed with increasing maturity. However, while isomerisation of bound hopanooids in asphaltenes appear to be in phase with the corresponding isomerisation of hopanes in the maltene fraction, the isomerisation of bound steroids lags significantly behind the corresponding isomerisation of the steranes in the maltenes.

There is good potential in using multivariate pattern recognition tools in oil/oil correlations based on asphaltene bulk composition as measured using FTIR. Notwithstanding some misclassification, the techniques tend to correlate asphaltenes with common source. Similarly, the aliphatic moieties of asphaltenes also reflect the organic matter sources of the asphaltenes. The *n*-alkyl moieties from asphaltenes with common source not only show similar

distributions, but also similar $\delta^{13}\text{C}$ trends even in asphaltenes from biodegraded oils. Likewise, bound hopanoids also reflect the organic matter source such that asphaltenes with common source show similar hopanoid distributions. The aliphatic moieties therefore have good potential that may be comparable to the conventional hydrocarbon-based biomarkers in oil/oil correlations.

In general, the composition of asphaltenes is controlled by the source organic matter and its thermal evolution. The effect of biodegradation is not yet completely understood but, with the exception of steroids, it does not appear to affect the aliphatic composition of the asphaltenes. There is therefore a significant potential in using asphaltenes in discrimination/correlation of oils particularly where the hydrocarbons in the maltene fraction are lost to biodegradation.

Acknowledgement

All thanks are to Allah (SWT), the most gracious, the most merciful, for life, sustenance, health and everything enabling to undertake this study.

I wish to thank my supervisor, Dr Geoff D Abbott for advice and support whenever I needed them. Your friendship and guidance have been source of motivation to me throughout these years. Thank you so much!

I am very grateful to Dr Claire Fialips for the invaluable assistance she gave me on FTIR. In addition she purchased the GRAMS/AI and showed me how to use it. Thank you! I am also grateful to Dr Steve Robertson who first suggested using FTIR to me.

I am also grateful to Mr Bernie Bowler, Mr Ian Harrison, Mr Paul Donohoe and Phil Green. Special thanks to Dr David Apperley and Mr Fraser Markwell of Solid-state NMR Service at Durham University for running my samples for nothing!

My mother; Malama Hadiza Bayawa appears to be the only person who listens, understands and believes my story. I can't imagine myself without you! Thank you for the unconditional understanding and endless prayers.

My wives; Rabi'ah Abubakar Shinkafi and Hadiza Abubakar D/Daji, and children; Fatima, Aisha, Maryam and of course Ahmad (who I am yet to hug!), have been wonderful and very supportive. God bless you for your endless love. You are always close to my heart.

My friends; Dr Yusuf Saidu and Malam Muhammad Gidado Liman, have been very helpful in looking after my interests at Sokoto while I was way on this programme. I am grateful for your friendship.

I appreciate the moral support and company of my pals; Bello Adamu, Sani Yahya, Aminu Mohammed, Murtala Mohammed, Uzochukwu Ugochuchu, Ojiugo Okafor, Bashir Aliyu, Umar Ba and Nykky Allen. You made me laugh when I was about to cry!

Finally, I am grateful to the management of Usmanu Danfodiyo University Sokoto, Nigeria for granting me study leave, and Petroleum Technology Development Fund (PTDF), Nigeria for sponsorship, to undertake this programme.

*Aminu B Muhammad
20 October 2009*

Table of Content

The Molecular Composition and Geochemical Applications of Asphaltenes	i
Declaration.....	ii
Dedication	i
Abstract.....	ii
Acknowledgement	iv
Table of Content.....	v
Chapter 1 Introduction and Literature Review	1
1.1 Introduction	1
1.2 Definition, Stability and Precipitation Behaviour.....	2
1.2.1 Asphaltenes: what are they?.....	2
1.2.2 Solubility and stability nature of asphaltenes in oils.....	4
1.2.3 Precipitation behaviour of asphaltenes	5
1.3 Molecular Size and Weight	6
1.4 Chemical Composition and Structure	7
1.5 Biomarkers in Asphaltenes.....	9
1.6 Research Problem	11
1.7 Aim and Objectives	11
1.8 Relevance	11
1.9 Scope and Delimitation	12
Chapter 2 Materials and Methods.....	13
2.1 Introduction	13
2.2 Description of Samples	13
2.2.1 Black shales	14
2.2.2 Northsea oils	16
2.2.3 Oman oils	17
2.2.4 Kuwait oils.....	17
2.2.5 Qatar oils.....	18
2.2.6 Yemen oil.....	18
2.2.7 Other oils.....	18
2.2.8 Coal samples	19
2.3 Methods of Sample Preparation.....	19
2.3.1 Powdering of rock and coal samples.....	19
2.3.2 Extraction of bitumen from the black shale and coal samples	19
2.3.3 Precipitation and purification of asphaltenes.....	20
2.3.4 Fractionation of maltenes	21
2.3.5 Urea adduction.....	22
2.3.6 Ruthenium ion catalysed oxidation (RICO) of asphaltenes.....	22
2.3.7 Potassium permanganate oxidation of asphaltenes.....	23
2.3.8 <i>n</i> -Butylsilane reduction	23
2.3.9 Extraction of acids from oils and bitumen	25
2.3.10 Esterification of acids	25
2.3.11 Preparation of samples for FTIR analysis	26

2.4	Analytical Methods	27
2.4.1	Total carbon, hydrogen, nitrogen and sulphur analysis.....	27
2.4.2	Total organic carbon analysis.....	27
2.4.3	Rock-Eval pyrolysis	28
2.4.4	Gas chromatography (GC).....	28
2.4.5	Gas chromatography/mass spectrometry (GC/MS).....	29
2.4.6	Compound specific isotope ratio analysis (CSIR)	29
2.4.7	Fourier transform infrared spectroscopy (FTIR)	31
2.4.8	Solid-state nuclear magnetic resonance spectroscopy.....	31
Chapter 3	Characterisation of the Samples	33
3.1	Introduction	33
3.2	Methodology.....	33
3.3	Results and Discussion	33
3.3.1	Black shale samples.....	33
3.3.2	Coal samples	41
3.3.3	Oil samples	46
3.4	Summary and Conclusions	59
Chapter 4	Adsorption and Occlusion in Asphaltenes	60
4.1	Introduction	60
4.2	Methodology.....	62
4.2.1	Selection of samples	62
4.2.2	Analytical procedure	62
4.3	Results and Discussion	64
4.3.1	Determination of time required for efficient extraction of asphaltenes.....	64
4.3.2	Determination of an ideal asphaltenes degradation reagent.....	67
4.3.3	Comparative analysis of maltene, adsorbed and 'occluded' biomarkers.....	71
4.3.4	Simulation of occlusion of hydrocarbons in asphaltenes	78
4.4	Summary and Conclusions	80
Chapter 5	Bulk Composition and Structure of Asphaltenes by FTIR and NMR.....	81
5.1	Introduction	81
5.2	Methodology.....	83
5.2.1	Samples and sample preparation.....	83
5.2.2	Pre-processing and curve fitting of FTIR spectra	85
5.2.3	Chemometric multivariate statistical analysis	87
5.3	Results and Discussion	87
5.3.1	Assignment of bands.....	87
5.3.2	Coal asphaltenes: evolution with maturity	94
5.3.3	Black shale (source-rock) asphaltenes	98
5.3.4	Petroleum asphaltenes	102
5.3.5	Chemometric discrimination and correlation of asphaltenes	108
5.4	Summary and Conclusions	119
Chapter 6	Bound Biomarkers in Asphaltenes Released by Ruthenium Ion Catalysed Oxidation	121
6.1	Introduction	121

6.2	Methodology.....	123
6.2.1	Selection and preparation of samples	123
6.2.2	Identification of compounds and data analysis	124
6.2.3	Chemometrics	125
6.3	Results and Discussion	125
6.3.1	Method development and verification	125
6.3.2	<i>n</i> -Alkanoic acids.....	127
6.3.3	α,ω - <i>n</i> -Alkandioic acids	134
6.3.4	Branched alkanoic acids	137
6.3.5	Hopanoic acids (HA)	138
6.3.6	Steranoic acids (SA).....	145
6.3.7	Effect of biodegradation	148
6.3.8	Asphaltene versus maltene biomarkers.....	152
6.3.9	Effect of thermal maturation on asphaltene biomarkers	157
6.3.10	Assessment of solvent effect on asphaltene biomarkers	159
6.3.11	Correlation using asphaltenes biomarkers	161
6.4	Summary and Conclusions	163
Chapter 7	Summary and Future Work.....	165
7.1	Overall Conclusions.....	165
7.2	Future Work	167

Chapter 1 Introduction and Literature Review

1.1 Introduction

Considerable amount of work has been published on asphaltenes indicating a great deal of scientific interest on these materials (Mullins et al., 2007; Sheu, 2002; Sheu and Mullins, 1995; Bunger and Li, 1981). The interest in these chemical substances is not only out of scientific curiosity in wanting to know what they are but mainly for the wide range of problems they have been found to be associated with as a result of their chemical composition and propensity to precipitate out of solution and form deposits. These problems cover both upstream and downstream sectors of the petroleum industry and include obstruction of reservoirs, plugging of wells and pipelines, separation difficulties and fouling as well as catalyst deactivation/poisoning and environmental pollution during processing (Ancheyta, 2007; Shedid and Zekri, 2006; Kokal and Sayegh, 1995; Galoppini, 1994). They have also been found to stabilise oil-water emulsions which are difficult to process at surface facilities (Khadim and Sarbar, 1999). It is clear therefore that the detrimental effect of asphaltenes in the petroleum industry is widespread, hence they are termed the “the cholesterol of petroleum” (Kokal and Sayegh, 1995). This is clearly illustrated in Figure 1.1.

Consequently, understanding these substances is very important more so for the fact that onshore reserves of the conventional crude is on the decline and hence more attention is now being directed to deep water offshore reserves and in such environments any flowline plugging problem will be expensive to clear (Creek, 2005; Saniere et al., 2004). This further justifies the increasing in work on these substances as summarised in Figure 1 of Ancheyta et al. (2002) and several published books (Mullins, 2007; Sheu and Mullins, 1995). Most of the published works revolve around their characterisation and stability/precipitation properties with the main aim of developing convenient and efficient ways of alleviating the problems they cause. This chapter gives a broad overview of some relevant work on these important materials.



Figure 1.1: Asphaltenes are likened to cholesterol in human body that precipitates and deposits to plug the pipeline leading to shut down of the system for repairs (Headen et al., 2007; Creek, 2005).

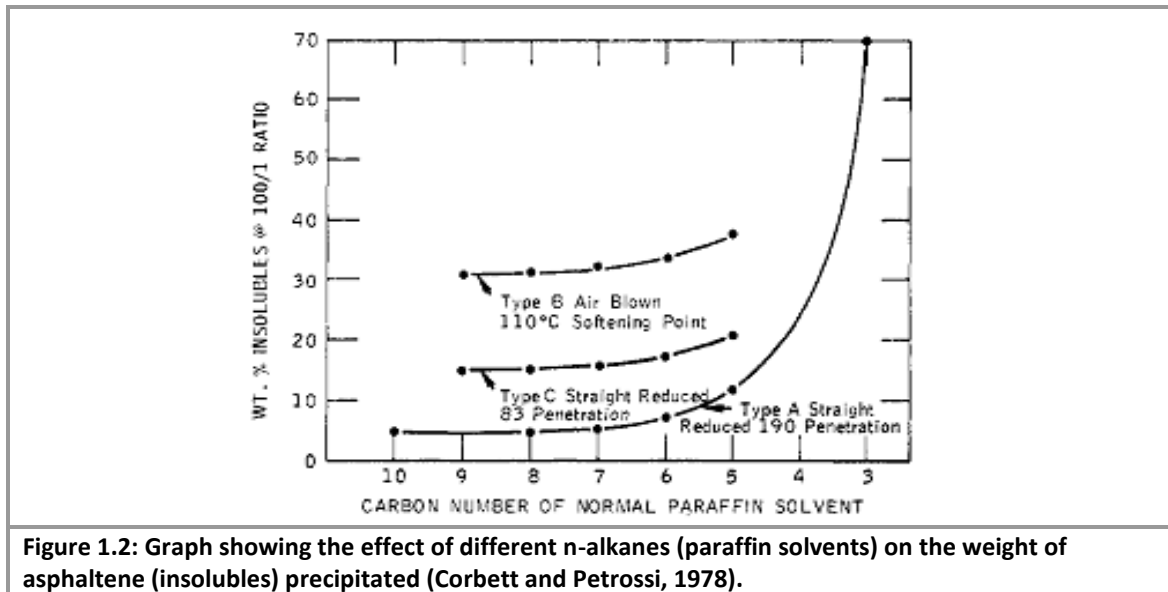
1.2 Definition, Stability and Precipitation Behaviour

1.2.1 Asphaltenes: what are they?

Asphaltene are chemical substances in petroleum or bitumen defined by their solubility properties. Although solubility of asphaltenes at ambient condition is a function of their molecular weight and polarity (Long, 1981), Speight and Moschopedis (1981) classified them as being soluble in polar solvents (such as benzene, dichloromethane, tetrahydrofuran etc) with surface tension higher than 25 dyne cm^{-1} and insoluble in liquids (principally hydrocarbons) with surface tension less than 25 dyne cm^{-1} (Speight and Moschopedis, 1981). Nevertheless, the principal solvents used in precipitation of asphaltenes are the lower alkanes (Speight, 2004); particularly *n*-pentane, *n*-hexane and *n*-heptane, notwithstanding the fact that, for economic reasons, in the downstream sector of the petroleum industry liquid propane is also used (Speight, 1999).

It is clear from the above definition that the intrinsic composition of asphaltene as a class of compounds is dependent on many factors. The solubility of a chemical compound is not only a function of its chemical nature (elemental composition, its structure and functionality) but also its molecular weight, the nature of the solvent as well as the temperature. This is evident in even as simple class of homologues as the alkanes (Jennings and Weispfennig, 2005). Consequently, it is very difficult to include/exclude compounds from the class. Nevertheless, asphaltenes as a pseudo-class of compounds are still defined and studied per se often with more restrictions placed to limit the 'membership' of the class as much as possible (Creek, 2005; Speight, 2004). Thus Creek (2005) summarised that asphaltenes by definition should meet the following three criteria: "(i) precipitates from oil when diluted 20:1 or more with paraffin solvents (*n*-C₅, *n*-C₇, ...) but is soluble in toluene; (ii) can be filtered (not extruded) at 1-1.5 μm ; and (iii) does not include contributions from resins and waxes" (Creek, 2005).

Nevertheless, despite restrictions, such as above, in defining asphaltenes, what is and what is not a member of the asphaltene 'class' could still be variable. The effect of different *n*-alkane solvents used in precipitating asphaltenes on the bulk composition of the asphaltenes precipitated has been studied by a number of workers. Corbett and Petrossi (1978) observed that the relative proportion of asphaltene precipitated is a function of the solvent used (Figure 1.2). In general, the relative amount of asphaltene precipitated is not only dependent on the nature of the oil or bitumen but has also been observed to decrease with increasing molecular weight of the *n*-alkane used in the precipitation in an asymptotic fashion (Figure 1.2). *n*-Hexane and lower homologues have been found to precipitate higher proportion of resins as well thereby resulting in overestimation of the asphaltenes (Long, 1981; Corbett and Petrossi, 1978) hence the common adoption of *n*-heptane in precipitation of asphaltenes (Hammami *et al.*, 1995).



However, even when a specific solvent is consistently employed in precipitation of asphaltenes other factors have been observed to influence the relative proportion, and therefore composition, of asphaltenes precipitated (Speight, 2004). Alboudwarej *et al.* (2002), for example, observed that the yield of asphaltenes obtained when *n*-heptane is used is significantly dependent on contact time and heptane-to-bitumen ratio (Figure 1.3). The yield increases with contact time, with equilibrium reached at about 24 hours. The yield also increases with proportion of *n*-heptane used, with optimum reached at 25 cm³ of *n*-heptane per 1g of oil or bitumen. It is therefore a common practice to use about 40 cm³ for 1 gram of oil with contact time of about 24 hours for the precipitation of asphaltenes (Alboudwarej *et al.*, 2002; Speight, 1984), although Speight (2004) recommends equilibration period of 8 to 10 hours.

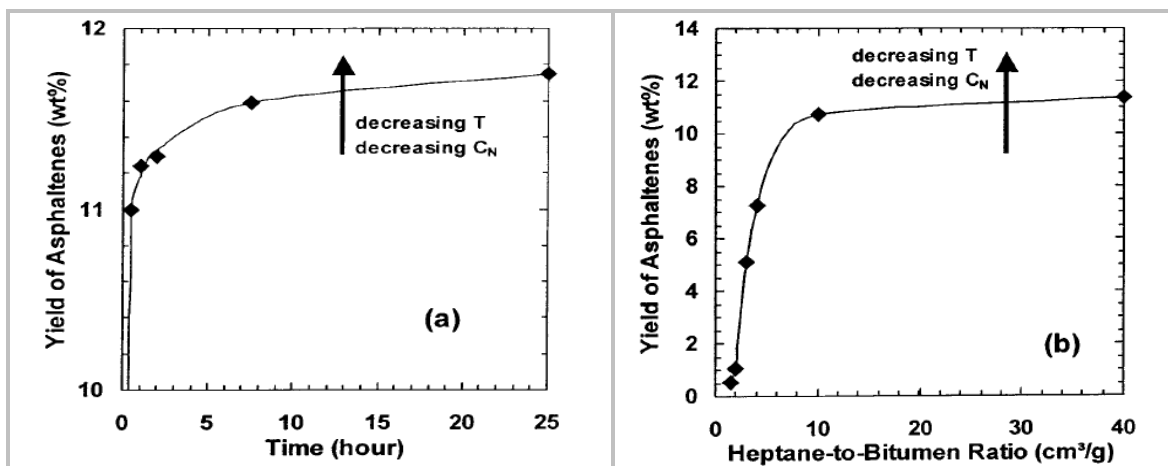


Figure 1.3: Linear plots showing variation in yield of asphaltene against time the mixture is allowed to equilibrate (a), and the yield versus oil to solvent ration employed (b). The plots show about 20 hours is required for equilibration and about 30 ml of solvent

Generally, asphaltenes form a pseudo-class of somewhat complex chemical substances with no clear boundary with resins and thus the composition is significantly influenced by a wide range of factors. Nonetheless, they are precipitated with lower *n*-alkanes employing a ratio of 40 cm⁻¹ per gram oil and equilibration period of up to 24 hours followed by Soxhlet extraction to remove co-precipitated non asphaltene substances.

1.2.2 Solubility and stability nature of asphaltenes in oils

One of the fundamental issues in asphaltenes science is their physical state in the oil. Are they intrinsically soluble or insoluble in an oil medium? This is important in developing a physical model for prediction of asphaltene stability (Cimino *et al.*, 1995). In this regard, two conflicting descriptive models are generally used to describe the physical state of asphaltenes in oils (Donaggio *et al.*, 2001; Neves *et al.*, 2001; Cimino *et al.*, 1995). The first model considers asphaltenes in crude oils as lyophilic dispersions of molecules. In this model the asphaltene molecules, and/or aggregates, are inherently dissolved in the oil (maltene) matrix more or less as are other smaller molecules are (Figure 1.4 (a)). The model does not give any special role to the resins; they are just part of the predominantly hydrocarbon solubilising medium. The whole system is therefore a homogeneous one phase solution of molecules in delicate harmony. This model implies that precipitation of the asphaltenes is simply a phase splitting process where a phase rich in asphaltenes and a phase rich in the solvent are formed and coexist in equilibrium (Donaggio *et al.*, 2001).

The second model (i.e. the lyophobic model) invokes a system where the asphaltenes are intrinsically insoluble components that are dispersed and stabilised in the medium by the peptising action of other components (i.e. resins) as illustrated in Figure 1.4 (b). The resins are believed to be adsorbed on the asphaltene surface and through steric effect, stabilise the asphaltenes against flocculation and precipitation. Precipitation of the asphaltenes, according to this model, involves partitioning of the resins between the surface of the asphaltenes and the oil medium resulting in desorption of the peptising resins from the asphaltene surface (Speight, 2004; Andersen and Speight, 2001). It is however still not clear whether the asphaltenes are molecularly peptised (Hammami and Ratulowski, 2007; Speight, 2004) or peptised in form of submicrometer aggregate particles (Pereira *et al.*, 2007); both molecules and aggregate could however exist in equilibrium (Cimino *et al.*, 1995).

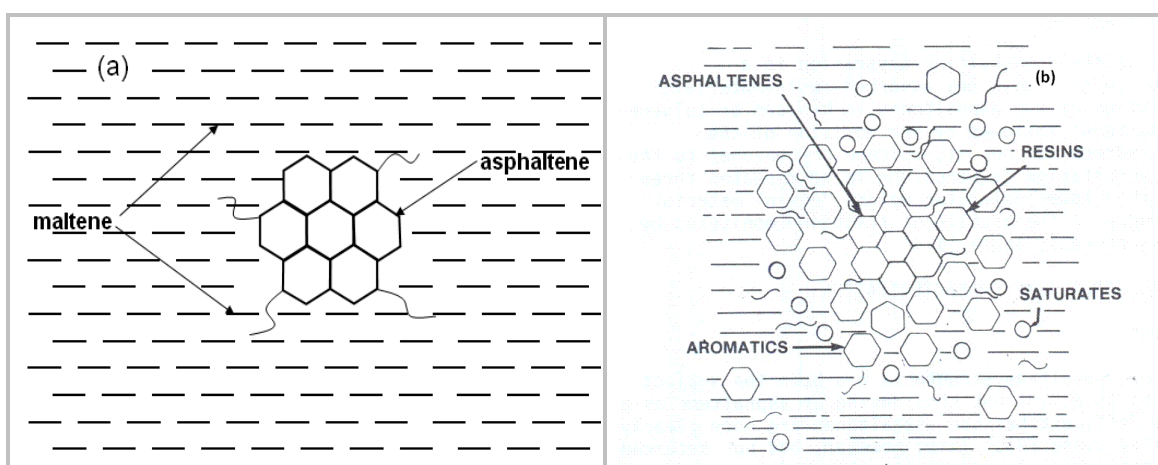


Figure 1.4: Pictorial representation of the two descriptive models of asphaltenes in oil matrix; (a) the lyophilic model with no specific role for resins, and (b) the lyophobic model with resins as peptising agents.

Neither of the models, however, can account for all the observed phase properties of asphaltenes (Donaggio *et al.*, 2001) and it is possible that all the models could be true to some extent. Castillo *et al.* (2001), based on fractionation studies, postulate that asphaltenes consist of the most insoluble fraction, which constitutes the colloidal phase, and the remaining sparingly soluble fraction, which constitutes the dispersing components that adsorb on the colloidal phase and stabilise the system in solution. This is somewhat supported by the work of

Gutierrez *et al.* (2001), Acevedo *et al.* (2004) and Alboudwarej *et al.* (2002). Cimino *et al.* (1995) suggest a thermodynamic equilibrium between asphaltene molecules and asphaltene micelles.

In general however, it is agreed that the stability of asphaltenes in oil matrix appears to be based on delicate compositional equilibrium which depends on many factors, the most important of which are composition and pressure, and to a lesser extent temperature (Hammami and Ratulowski, 2007; Andersen and Speight, 2001). Altering the composition (e.g. by mixing with incompatible hydrocarbon fluids, miscible flooding, CO₂ flooding, gas lift operation), for example, could destabilise the equilibrium resulting in desorption of the peptising agents from the asphaltenes and therefore precipitation of the asphaltenes from solution (Hammami and Ratulowski, 2007). Resins are generally associated with peptisation of the asphaltenes in solution (Speight, 1984).

The importance of the resins in stabilisation of asphaltenes in oils has been a subject of investigations (Pereira *et al.*, 2007; Gonzalez *et al.*, 2006; Andersen and Speight, 2001; Carnahan *et al.*, 1999). Carnahan *et al.* (1999), for example, observed that although stability of asphaltenes varies with the nature of the resins, it increases linearly with the amount of the resins. These findings are also supported by the results of Hammami *et al.* (1998). Leon *et al.* (2000), however, did not observe any positive relationship between bulk composition of the dispersion medium and the stability of asphaltenes in crude oils. Pereira *et al.* (2007), on the other hand, concluded from their findings that resins, depending on their nature, could have both stabilising and destabilising effect on asphaltenes; resins with low tendency to self-associate could stabilise asphaltenes, otherwise destabilisation could occur as adsorbed resins could be providing attractive surfaces for aggregation to proceed. There is also evidence that electrostatic repulsion probably contributes to stabilisation of the asphaltenes in solution (Neves *et al.*, 2001).

1.2.3 Precipitation behaviour of asphaltenes

Irrespective of the physical form in which asphaltenes exist in the oil/maltene matrix, it has been established that in the presence of nonpolar solvents (i.e. *n*-alkanes), asphaltenes tend to aggregate, form clusters and flocculate thereby precipitating out of solution. This is true even in dilute solutions. Furthermore, the precipitation process is accompanied by adsorption and co-precipitation of other non-asphaltene components such as resins and hydrocarbon waxes (Ekulu *et al.*, 2005). Hence the characteristics, including texture, of the asphaltenes precipitated tend to also depend on the type and quantity of the solvent used (Hammami *et al.*, 1995).

Empirical observations suggest that the precipitation of asphaltenes occurs in stages in accord to the so-called Yen Model (Mullins, 2007). Evdokinov *et al.* (2006), using different techniques, show that asphaltene monomers start to aggregate, possibly into dimers and trimers, at concentrations below 10 mg/l. This appears to be followed by the formation of the so-called nanoaggregates possibly from the dimers and trimers. The threshold concentration above which the nanoaggregates form is termed the critical nanoaggregation concentration (CNAC) so far detected only using High Q-ultrasonic spectroscopy (Figure 1.5 (a)) (Andreatta *et al.*, 2007; Andreatta *et al.*, 2005a; Andreatta *et al.*, 2005b). Although the CNAC varies with

different oils from as high as *ca* 400 mg/l to as low as 50 to 150 mg/l (Badre *et al.*, 2006), the apparent specific volumes of the nanoaggregates is in the order of $0.8 \text{ cm}^3/\text{g}$.

The next stage of the aggregation process is the formation of even bigger aggregates, often referred to as micelles, apparently from the nanoaggregates. This is said to occur above threshold concentration called the critical micelle concentration (CMC) (Figure 1.5 (b)). Though this has not been detected by ultrasound spectroscopy, it has been observed through many other methods including calorimetry (Andersen and Christensen, 2000; Andersen and Birdi, 1991), vapour pressure osmometry (Yarranton *et al.*, 2000), NIR spectroscopy (Oh *et al.*, 2003; Mullins, 1990), small-angle scattering (Shue and Storm, 1995), surface and interfacial tension measurements (Yarranton *et al.*, 2000; Mohamed *et al.*, 1999; Shue and Storm, 1995). In general, it was observed that the CMC is dependent on the nature of the asphaltenes and the solvent used. Furthermore, the size of the aggregates formed increases with decrease in asphaltene concentration and increase with amount of the precipitating solvent added (Neves *et al.*, 2001).

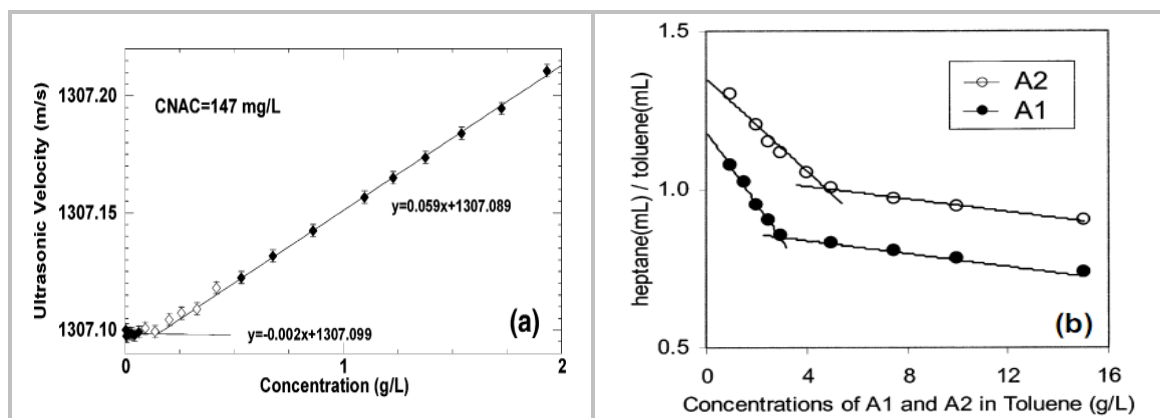


Figure 1.5: Plots showing the detection of the concentration thresholds at which the two known aggregation stages set in; (a) Critical nanoaggregation concentration (Andreatta *et al.*, 2005b), and (b) critical micelles concentration for two different asphaltenes (A1 & A2) (Oh *et al.*, 2003).

Physical examination of the aggregation of asphaltenes shows that growth of the aggregates follows a pattern: from spots to string to small flocs and finally to large fractal-like flocs. The lag time before appearance of the precipitate appears to be concentration dependent with higher concentration having shorter lag time (Angle *et al.*, 2006; Speight and Moschopedis, 1981).

1.3 Molecular Size and Weight

Many investigations have been carried out on the size, shape and molecular weight of asphaltenes. The results are however anything from being consistent and are thus subject of intense debate (Herod *et al.*, 2008; Mullins *et al.*, 2008; Badre *et al.*, 2006) which is a clear indication of the variability and complexity of these materials (Speight and Moschopedis, 1981). Different methods for molecular weight determination tend to give grossly different results and consensus is yet to be achieved (Mullins, 2009; Strausz *et al.*, 2008; Bungler and Li, 1981).

In a review on the molecular nature of asphaltenes, Speight and Moschopedis (1981) reported asphaltene molecular weight values of up to 300,000 amu using ultracentrifuge method; and between 80,000 to 140,000 amu using osmotic pressure and monomolecular film methods.

Other techniques such as ebullioscopic method, viscosity determinations, light adsorption coefficients, cryoscopic method, and vapour pressure osmometry give much lower values in the range of 1,000 to 5,000 amu. There is however a general recognition of the fact that asphaltenes form aggregates, whose formation is not only dependent on the nature of the asphaltenes but also on solvent polarity, concentration and temperature. The observed high molecular weights could therefore be of such aggregates (Speight and Moschopedis, 1981).

Mass spectrometric methods using various ionisation techniques including field ionisation, field desorption, electrospray, atmospheric pressure photoionisation, and laser desorption give molecular weights in the range between 400 to 1400 amu with mean value at about 800 amu (Mullins, 2009; Mullins et al., 2008). This is corroborated by results using other methods such as time-resolved fluorescence depolarisation, Taylor dispersion diffusion, fluorescence correlation spectroscopy and nuclear magnetic diffusion. Although this may seem conclusive, some workers still contend that the molecular weight is in the range of several thousands, and methods that show otherwise (as outlined above) detect only the low molecular weight components and are incapable of detecting the macro components (Morgan et al., 2009; Herod et al., 2008; Strausz et al., 2008).

The general geometry of the asphaltene ring system is a largely pericyclic sheet of 4 to 10 (Badre *et al.*, 2006) or 10 to 20 (Groenzin and Mullins, 1999) fused rings although coal asphaltenes are said to be significantly smaller than petroleum asphaltenes. Fluorescence depolarisation method has been used by Groenzin and Mullins (1999) to observe a strong correlation between the size of fused ring system of asphaltenes and the absolute size of the molecule. The asphaltene diameter varies between 10 and 20 Å (Groenzin and Mullins, 1999) although Badre *et al.* (2006) reported an absolute molecular size of *ca* 12 Å for petroleum asphaltenes and even smaller size for coal asphaltenes.

1.4 Chemical Composition and Structure

Asphaltenes principally consist of carbon, hydrogen, nitrogen, oxygen and sulphur. The proportion of each element however varies slightly with source and the precipitating solvent used (Speight and Moschopedis, 1981). Carbon and hydrogen vary within a narrow range of $82\pm 3\%$ and $8.1\pm 0.7\%$, respectively. Nitrogen, oxygen and sulphur are however more variable: 0.6 to 3.3%, 0.3 to 4.9% and 0.3 to 10.3% respectively. The H/C ratio is generally low (1.15 ± 0.05) suggesting condensed aromatic structures with heteroatomic units (Speight and Moschopedis, 1981).

Various methods, including infrared spectroscopy, X-ray diffraction and chemical degradation, have been employed to investigate the structure of asphaltenes (Yen et al., 1984; Yen et al., 1961). Although some aspects of the structure of asphaltenes is still being debated (Section 1.3), there appears to be agreement that it consists of an aromatic core with appendages (and contentiously bridges?) made of aliphatic chains (Speight and Moschopedis, 1981).

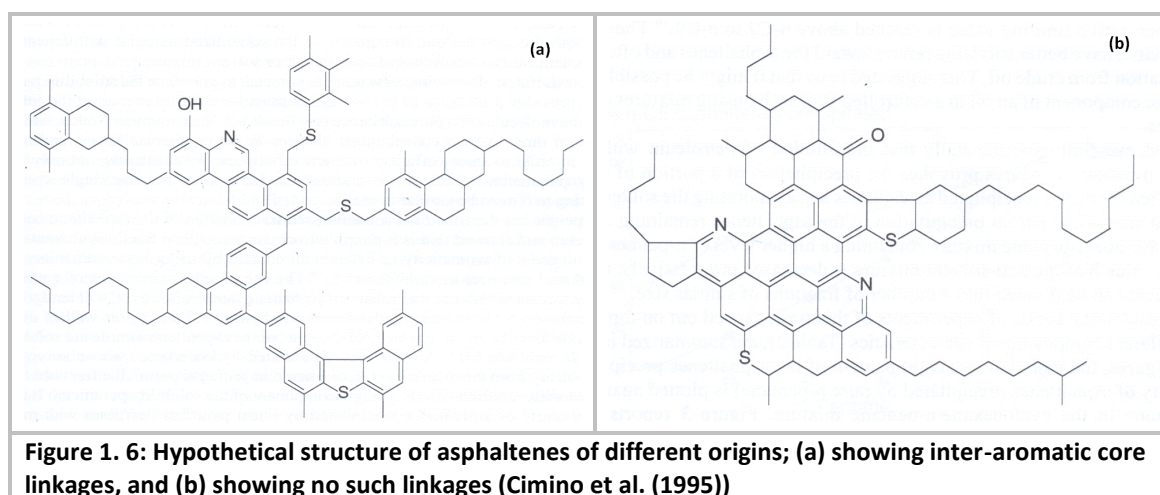
Spectroscopic methods including NMR and IR, suggest the aromatic core consists of condensed aromatic rings (Figure 1.6). The geometry of the aromatic core has been shown by carbon X-ray Raman spectroscopy to be the more stable pericondensed rather than catacondensed ring system (Bergmann et al., 2003; Gordon et al., 2003). However, rather than pure hydrocarbon, the core is heteroatomic with other elements, principally oxygen, nitrogen and sulphur, dispersed in the aromatic core.

Oxygen occurs predominantly in the form of phenolic hydroxyl group and quinones together with ketones (Speight and Moschopedis, 1981). The distribution of nitrogen and sulphur has been studied using X-Ray Absorption Near Edge Structure (XANES), a very sensitive and selective method that discriminates between different nitrogen and sulphur species (Mitra-Kirtley and Mullins, 2007; George and Gorbaty, 1989). It has been found that all the sulphur exist in the form of thiophene, sulphide and sulphoxide with the relative proportion of each being dependent on the nature of the asphaltenes. In the eight samples (from USA, Canada, Kuwait and France) studied by Waldo (1992), it was observed that sulphoxide is dominant (44%) in only one sample; others show about 10% or less. The overall dominant sulphur species, however, are the reduced sulphide (16-43%) and thiophene (36-67%) with the latter always being greater than the former in the ratio 1.2 to 3.4. Other sulphur species such as sulphone and sulphate are about 4% or less.

In contrast, almost all the nitrogen in asphaltenes is in the form of aromatic pyrrolic and pyridinic species with little or no saturated amine. In the seven asphaltenes samples from different sources studied by Mitra-Kirtley et al. (1993b), 65 to 80% of the nitrogen is in pyrrolic form while pyridinic nitrogen varies between about 20 to 30%. The saturated amine is generally less than 4%. Furthermore, unlike in kerogen and bitumen, no pyridonic nitrogen (and quaternary nitrogen) was observed in petroleum asphaltenes (Mitra-Kirtley et al., 1993a; Mitra-Kirtley et al., 1993b).

The nature of the appendages attached to asphaltene condensed heteroaromatic core has also been investigated. Coleman (1995) using NMR and IR has estimated that the average chain length per alkyl side chain varies with sample but is between about 3 to 7. This is corroborated by the work of Peng et al. (1999a), who, using Ruthenium Ion Catalysed Oxidation (RICO), show the predominance of short chain alkyl groups although homologues up to C₃₂ were also observed. The presence of the high molecular weight alkyl homologues as side chains in asphaltenes has also been shown using pyrolysis-GC/MS (del Rio *et al.*, 1995). The alkyl groups in asphaltenes are linked to the aromatic core via a number of different bonds. Ether, ester and sulphide linkages have all been identified. The vast majority of the alkyl groups, however, appear to be bonded through C–C linkage (Peng *et al.*, 1997).

The most controversial issues concerning asphaltene science, apart from molecular weight but related to it, is whether asphaltene macromolecules are monomeric or polymeric. The polymeric hypothesis is supported by Peng et al. (1997) who observed that the high molecular weight asphaltene (HMA) fraction of Athabasca asphaltene, unlike the low molecular weight asphaltene (LMA) fraction, consist of core fragments linked via S-bridges and upon desulphurisation, the HMA breakdown into the composite cores with significant decrease in molecular weight corresponding to generation of the monomeric units. This is, however, in direct contradiction with the conclusions of Badre et al. (2006) and other workers (see Mullins *et al.* (2007)) who argued that the so-called polymeric structure is inconsistent with their observations from various techniques (see Section 1.3).



1.5 Biomarkers in Asphaltenes

Biomarkers are geochemical fossils – trace organic compounds in sedimentary organic matter (SOM), such as bitumen, kerogen, coal and oil, which are directly derived from their biological precursors (see Figure 1.7 for example). These compounds are often indicative of the biota from which the SOM formed and consequently are widely used in geochemical investigations (Killops and Killops, 2005; Peters et al., 2005b; Peters et al., 2005a; Hunt, 1995).

As in all other fractions of crude oils, biomarkers have been found in asphaltenes. In general, asphaltene biomarkers can be grouped into broad two classes. The first group consists of biomarkers that are chemically bound via covalent bonds and are therefore part of the asphaltenes structural network. These are probably the ‘true’ asphaltene biomarkers. The other group consists of biomarkers that are essentially not asphaltenic compounds and are simply physically trapped within the asphaltene structural network, possibly, during formation of the asphaltenes, and/or following precipitation of the asphaltenes from solution.

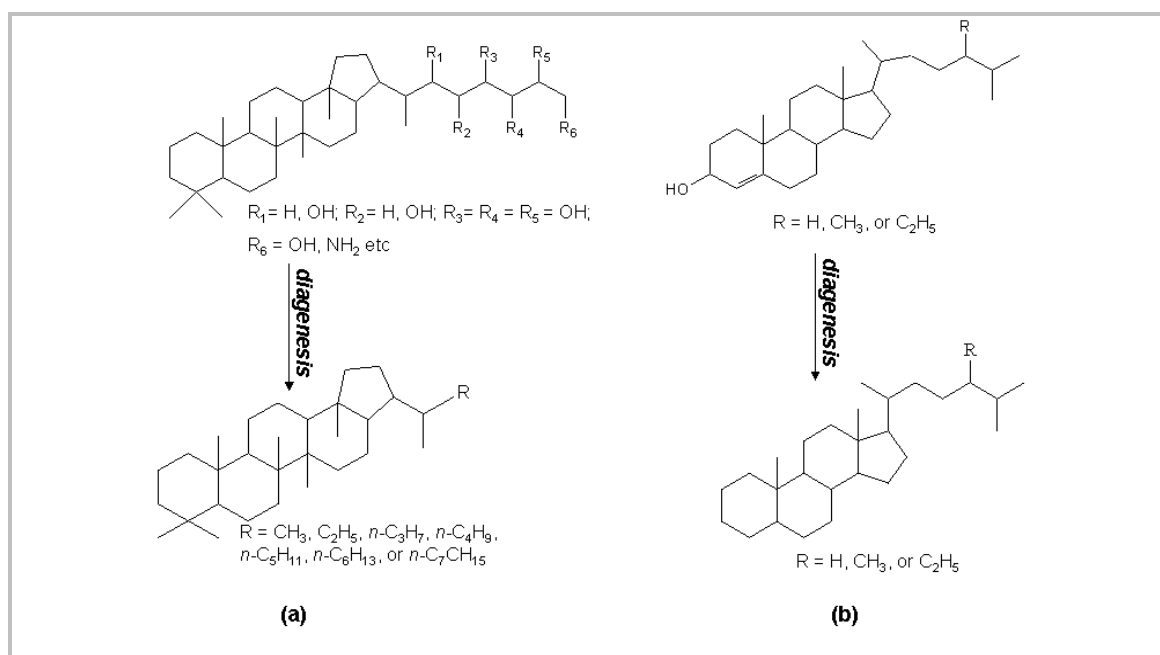


Figure 1.7: Illustration of transformation of biological compounds into geochemical fossils (biomarkers). (a) Shows bactraihopanepolyols resulting in hopanes, and (b) sterols resulting in steranes (Peters et al., 2005a).

Investigation of trapped biomarkers appears to have been first made by C. M. Ekweozor (Ekweozor, 1986; Ekweozor, 1984) using chemical degradation (sodium/naphthalene) to break down the asphaltenes and release the trapped biomarkers. A possible problem with Ekweozor's method however lies in the precipitation/purification of the asphaltenes. The asphaltenes were precipitated according to the method of Speight (1984) without further Soxhlet extraction to removed adsorbed maltene components. This problem was however addressed by Liao and co-workers (Liao et al., 2006a; Liao and Geng, 2002) with the revival of the occlusion hypothesis (see Chapter 4 for further discussion). These authors used hydrogen peroxide/acetic acid reagent for the chemical degradation of the Soxhlet-extracted asphaltenes aromatic moieties in order to release the physically trapped biomarkers (Liao et al., 2006b).

Almost all molecular components found in the maltene fraction of oils have been also found in asphaltenes as physically trapped or co-precipitated components. Bowden *et al.* (2006) observed the presence of *n*-alkanes, steranes, hopanes and tricyclic terpanes in asphaltenes fraction of Jet Rock as well as other fractions of the bitumen extract albeit with clear differences in concentration and distribution. They noted asphaltenes and resin fractions contain much lower proportion of biomarkers than free hydrocarbon and kerogen fractions. However, extended tricyclic terpanes (>C₃₀) are relatively more prominent in the asphaltenes and resins than in the free aliphatic fractions (Bowden *et al.*, 2006). Both sterane and hopane isomerisations have been noted to be hindered in asphaltenes and other macromolecules. In addition, diasteranes do not appear to be present in asphaltenes (Bowden et al., 2006; Peng et al., 1997).

Biomarkers covalently bound to asphaltenes have also been investigated using a wide range of methods depending, and more or less specific, to the nature of the chemical bond involved (Peng et al., 1997; Mojelsky et al., 1992). GC amenable compounds (often after derivatisation or conversion to hydrocarbons), include linear/branched alkanoids such as alkanes, alkanolic acids etc, have been observed through these procedures. Traditional biomarkers such as

steroids, hopanoids as well as tricyclic and tetracyclic terpenoids have also been observed. These biomarkers, particularly those obtained through ruthenium ion catalysed oxidation, have been shown to have potential in oil/oil correlations (Ma *et al.*, 2008). The bound biomarkers, particularly those bound via C–C bond linkage, are considered in more detail in Chapter 6.

1.6 Research Problem

Despite the great deal of work on asphaltenes, the transformation and variation of composition of asphaltenes from similar and different oils and source rocks are still unclear. Many important questions still unanswered include: What is the relationship amongst asphaltenes from different sources? Are there any differences/similarities amongst asphaltenes of different ages, maturities and depositional environments? Are there any differences between source rock and reservoir oil asphaltenes? Answers to these questions could greatly help in understanding asphaltenes and in developing correct models for predicting their properties as well as in using them for geochemical applications such as correlations, palaeoenvironmental investigations etc.

1.7 Aim and Objectives

The main aim of this work is to characterise the composition of the asphaltenes from different geochemical histories in order to have a deeper insight into their probable differential origins and explore possible geochemical applications for such differences. Specific objectives of the project include:

1. to investigate the adsorption/occlusion hypothesis of asphaltenes with the aim of ascertaining the validity of the hypothesis
2. to investigate the bulk composition of asphaltenes using mid-infrared Fourier transform infrared spectroscopy
3. to characterise aliphatic moieties particularly the bound biomarkers in asphaltenes
4. to investigate variations in composition of asphaltenes with their geochemical histories
5. to explore the potential of using the bulk composition of asphaltenes in discrimination/correlation of asphaltenes from similar and/or different sources
6. to exploit the bound biomarker content of asphaltenes in discrimination/correlation of asphaltenes

1.8 Relevance

This work provides fairly deep information on genesis and composition of asphaltenes. This is of geochemical importance as asphaltenes, being resistant macromolecules, could preserve information of correlation and palaeoenvironmental importance. Furthermore, more data on the variability of chemical compositions of asphaltenes would in turn enhance accuracy in modelling their physical properties in solutions and their behaviour in refinery processes; and this is vital information in designing ways to tackle production, transport and refinery problems associated with them.

1.9 Scope and Delimitation

The work is confined to characterisation of the chemical composition and structure of asphaltenes for the purpose of achieving the stated objectives. Consequently, asphaltenes from source rocks (black shales), coal and petroleum will be used in this work. However, physical properties, including molecular weights, of asphaltenes will not be covered.

For the purpose of this work, asphaltenes are considered to be components of petroleum (including heavy oils or bitumens) and bitumens from coal and black shales that are insoluble in *n*-pentane, *n*-hexane or *n*-heptane but excluding co-precipitated components such as hydrocarbon waxes and resins which are removed by Soxhlet extraction with the precipitation solvent for at least 48 hours.

Chapter 2 Materials and Methods

2.1 Introduction

This chapter gives a brief description of the samples used in this study and the methods used to prepare the samples for analysis. The conditions of instruments used to acquire the data/results presented are also fully described. The chapter is therefore divided into three major sections accordingly. Note, however, information on some of the samples is not provided because of data protection agreements.

2.2 Description of Samples

In general, a total of 57 samples, including 19 black shales, 34 oils and 4 coal samples were used in this work. The oil samples were obtained from different geographical areas and ages (Table 2.1). Twenty two of the oils were obtained courtesy of Fugro-Robertson Ltd. Dr Howard Armstrong of Durham University, UK provided the Tanezzuft and Batra black shale samples. The Kimmeridge mudstone and the 4 coal samples were provided by my supervisor, Dr Geoff D Abbott. These samples are briefly described below.

Table 2. 1: List of oils used in the study

Sample ID	Reservoir age	Source rock age	Field	Country
A39	-	Jurassic	-	Abu Dhabi
AR3	-	-	-	U. States
B58	Miocene- Pliocene	Oligocene/Miocene	Habigong	Bangladesh
BN	-	Jurassic	-	U. Kingdom
C26	Ordovician	Ordovician	Midale	Canada
C30	Ordovician	Ordovician	Midale	Canada
CH	-	-	-	Canada
K77	Cretaceous	Jurassic	Raudhatain	Kuwait
K78	Cretaceous	Jurassic	Sabriyah	Kuwait
NA1	-	-	Gaj	Serbia
NA2	-	-	Gaj	Serbia
NB	-	-	-	Nigeria
O28	Cretaceous	Cretaceous	Natih	Oman
O31	Cretaceous	Cretaceous	Natih	Oman
PR1	-	-	-	U. States
Q49	Cretaceous	Jurassic	Al Shaheen	Qatar
Q61	Late Jurassic	Jurassic	Bul Hanine	Qatar
U01	-	Jurassic	Kittiwake	U. Kingdom
U02	Carboniferous	Jurassic	Flora	U. Kingdom
U04	L. Plaeocene	-	-	U. Kingdom
U05	-	Jurassic	Kittiwake	U. Kingdom
U07	Jurassic	Jurassic	Fergus	U. Kingdom
U14	Upper Jurassic	Jurassic	Ettrick	U. Kingdom
U16	-	Jurassic	Captain	U. Kingdom
U32	Tertiary	Jurassic	Nelson	U. Kingdom
U54	Upper Jurassic	Jurassic	Ettrick	U. Kingdom
U56	Jurassic	Jurassic	Alder	U. Kingdom
U59	Statjord	Jurassic	Bruce	U. Kingdom
U68	U. Paleocene	Jurassic	-	Norway
U84	Paleocene	Jurassic	Nelson	U. Kingdom
U89	-	Jurassic	Britannia	U. Kingdom
U93	Jurassic	Jurassic	Gannet west	U. Kingdom
UFN	-	Jurassic	-	U. Kingdom
Y32	Cretaceous	Jurassic	Hemiar	Yemen

2.2.1 Black shales

The Tanezzuft black shale (Lower Silurian) core samples were obtained from well H29 logged on the 18th of December, 2005 in the H field NC-115 concession in Murzuq Basin which is located in the southwest of Libya, about 500 km from Tripoli (Figure 2.1 (a)). Forty eight samples were collected from the core on 19th of December, 2005 at about 10 cm intervals from the base of the 5 m thick 'hot' black shale (Figure 2.1(b)). The base of the formation starts at depth of about 4884 ft (1488.64 m). The 16 rock samples used for asphaltene studies were selected following preliminary analysis of the 48 samples as described in Chapter 3.

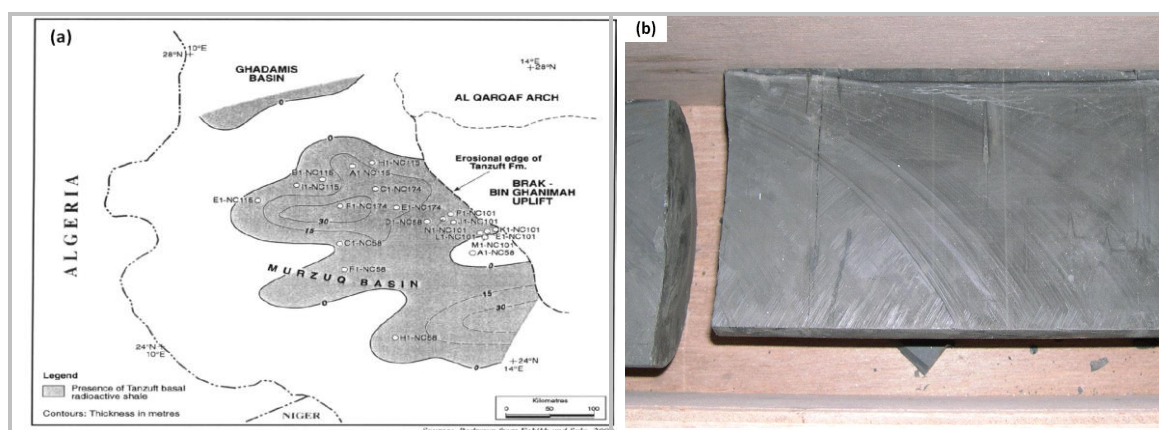


Figure 2. 1: A map showing distribution of the Tanezzuft black shale in Murzuq Basin relative to other basins in Libya (Hallett, 2002); (b) A photograph of a section of the basal 'hot' black shale (4858 - 4861 feet) from HC29-NC115 core (courtesy of Dr H Armstrong)

Physical examination of the shales (Figure 2.1 (b)) shows that the first *ca* 1 m (from the base), consists of black shale with silty laminae and pyrite-rich silty blebs. This is followed by approximately another 1 m section of intensely fractured black shale with sandy nodules near the top. The middle section contains rounded pyritic sandstone blebs (about 1 cm long and 0.5 cm wide), and graptolite fragments streaks and lenses of siltstone/fine sandstone are present but rare. The upper *ca* 2 m section consists of typical black shale with faint silty streaks and lenses on mm to sub-millimetre scale (Turner, 2006, personal communication).

The basal Tanezzuft 'hot' shale in Murzuq basin has been estimated to have a generation potential of over 40 billion barrels of oil (Aziz, 2000) although by 2000 only about 5200 million barrels was discovered in place, out of which only about 31% is recoverable. This accounts for only 3.9% of total Libyan oil reserves (Hallett, 2002). By the year 2007 however the discovered recoverable reserves was in excess of 1.9 billion barrels (Sarkawi et al., 2007).

The Batra 'hot' black shales, on the other hand, are Lower Palaeozoic, Late Ordovician shales deposited following Hirnantian to early Silurian deglaciation resulting in increased photic zone primary productivity with establishment of anoxic stratified water column resulting good preservation of the organic matter (Armstrong et al., 2009). The two samples, B348 and B372 (from core depths of 34.8 & 37.2 m above the base of the formation, respectively) used in this work were from 18 m section of the formation from Wadi Batn el Ghul well BG14. The samples are immature ($T_{max} = 419\text{ }^{\circ}\text{C}$) with Type II ($HI = 267\text{ mgHC/gC}$; $TOC = 3.89\%$) marine organic matter (Armstrong et al., 2009; Muhammad, 2004). The black shale samples used in this study are listed in Table 2.2.

Table 2. 2: List of black shale samples used in the study

Sample	Height above base (m)	Age	Basin	Formation	Country
T01	0.0	Silurian	Murzuq	Tanezzuft	Libya
T02	9.1	Silurian	Murzuq	Tanezzuft	Libya
T05	36.4	Silurian	Murzuq	Tanezzuft	Libya
T07	54.6	Silurian	Murzuq	Tanezzuft	Libya
T10	81.9	Silurian	Murzuq	Tanezzuft	Libya
T15	131.0	Silurian	Murzuq	Tanezzuft	Libya
T19	171.0	Silurian	Murzuq	Tanezzuft	Libya
T24	222.2	Silurian	Murzuq	Tanezzuft	Libya

T28	263.8	Silurian	Murzuq	Tanezzuft	Libya
T32	318.4	Silurian	Murzuq	Tanezzuft	Libya
T35	345.7	Silurian	Murzuq	Tanezzuft	Libya
T38	373.0	Silurian	Murzuq	Tanezzuft	Libya
T39	382.1	Silurian	Murzuq	Tanezzuft	Libya
T43	422.1	Silurian	Murzuq	Tanezzuft	Libya
T46	452.1	Silurian	Murzuq	Tanezzuft	Libya
T48	472.1	Silurian	Murzuq	Tanezzuft	Libya
KMS	-	Jurassic	-	Kimmaridge	U. Kingdom
B348	34.8	Ordovician	Batn el Ghul	Batra	Jordan
B372	37.2	Ordovician	Batn el Ghul	Batra	Jordan

2.2.2 Northsea oils

A total of sixteen (16) Northsea oils, out of which only two (2) were biodegraded, were used in this study. The oils were obtained from different wells and reservoirs (Appendix 1A). Brief descriptions of these oils are given below based on their respective locations.

Three samples; two from Palaeocene reservoir (U78 & U84) and one from Tertiary reservoir (U32), were from Nelson Field. The field consists of four Blocks, namely 22/11, 22/6a, 22/7 and 22/12a, in the UK Central Northsea. The oil accumulation is mainly in the Palaeocene Forties Sandstone member. The Field has about 420 to 450 MMB of low sulphur recoverable oil with density of about 40.6 °API (Kunka et al., 2003). The Nelson oil is believed to be sourced from the mature Jurassic Kimmeridge Clay Formation in the East and the West Forties Basins mainly about 50 to 10 Ma ago during Middle Eocene and Miocene (Kunka et al., 2003; Will and Peattie, 1990).

Only one sample (U07) was obtained from Fergus Field. The field is a small satellite field located in north-eastern part of Block 39/2a, about 5 km SE of the much bigger Fife Field. The field has 16.3 million barrels of initial oil in place. The recoverable reserve is however estimated at 11.3 million stock tank barrels (MMSTB). The reservoir is the Late Jurassic Fife Sandstone Member. The oil is sweet and light (36.4 °API) and was sourced from the Upper Jurassic organic rich shale of the Kimmeridge Clay Formation in the southern Central Graben (Shepherd et al., 2003).

Furthermore, one oil sample (U02) was obtained from Flora Field. The field splits between Blocks 31/26a and 31/26c of the UK sector of the Northsea. It is about 325 km southeast of Aberdeen and about 14 km northeast of the Fergus oilfield. The reservoir is the Upper Carboniferous Flora Sandstone. The oil, light (38.2°API) and undersaturated, is a mixture of oils sourced mainly from Upper Jurassic Kimmeridge Clay Formation in the Central Graben to the north of the field and the laterally equivalent Farsund and Mandal Formations of the Dutch é Basin to the east. The field was discovered in 1997 with 69 MMSTB in place (Hayward et al., 2003).

The Captain Field (about 38 km²) is the source of one oil sample (U16). The field is located in Block 13/22a, about 129 km northeast of Aberdeen. The reservoir is the Late Aptian (Early Cretaceous) Captain Sandstone member of the Valhall/Wick Sandstone Formation. The oil,

originally considered to be a typical Northsea black oil, was biodegraded in the Tertiary and is relatively heavy with 19 - 21 °API gravity. It was sourced from Kimmeridge Clay Formation from both the West Halibut Basin and Smith Bank Graben possibly in the early Tertiary. The Field was discovered with 1000 MMB oil-in-place (Pinnock and Clitheroe, 2003).

Other oils from the Northsea that have been used in this study are listed in Appendix 1A.

2.2.3 Oman oils

The two oils (O28 & O31) from Oman were obtained from the Natih oil field (Figure 2.2 (a)). The field was discovered in 1963 and has about 475 million m³ of oil in place (Alsharhan and Nairn, 1997). The Natih Formation (344 to 450 m thick) is dominantly open-marine carbonates and is lithologically divided into 7 units (namely Unit A to G) with the middle part of Unit B and basal part of Unit E as the source rocks and Units A, C, D and E as the reservoirs (Terken, 1999; Alsharhan and Nairn, 1997). The most important source rock however is the 50 m-thick Unit B with average TOC of about 5% and hydrogen index of 200 to 600 mgHC/gTOC indicating good to excellent quality Type I/II kerogen with potential for petroleum generation (Terken, 1999). The oils have about 32 °API gravity and 1.0 to 1.13% sulphur content (Alsharhan and Nairn, 1997) with geochemical characteristics that are distinct from other oils in Oman (Grantham et al., 1990; Grantham et al., 1988).

2.2.4 Kuwait oils

The two Kuwait oils, K77 and K78 (Appendix 1A) were obtained from Raudhatain and Sabriyah oil fields located in the northern region of Kuwait (Figure 2.2 (b)). Raudhatain field, discovered in 1955 produces 28 - 40 °API oil from Cretaceous reservoir; and Sabriyah field, discovered in 1956, produces 28 - 32 °API oil from mid Cretaceous Burgan and Mauddud reservoirs (Abdullah and Connan, 2002; Carman, 1996).

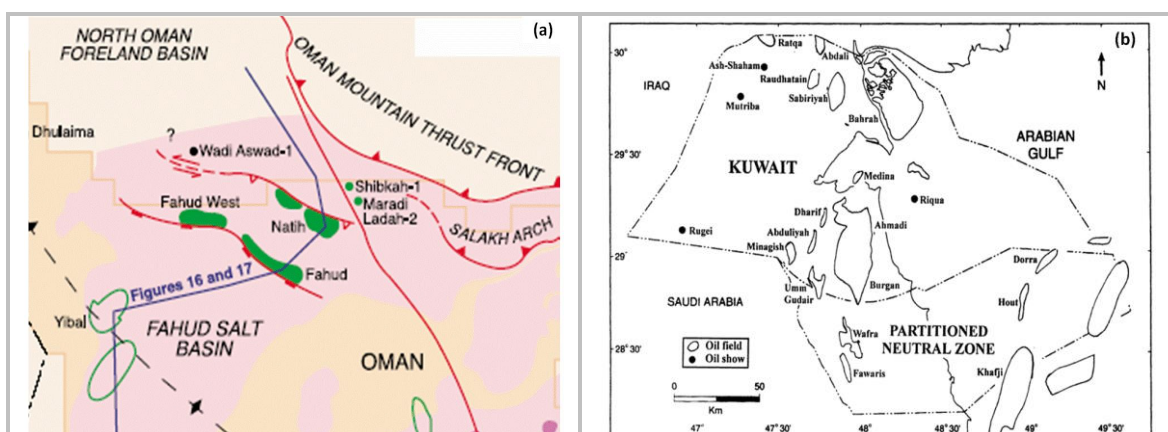


Figure 2. 2: Map showing the location of (a) the Natih field, the source of the two oils from Oman (Abdullah and Connan, 2002); and (b) the Raudhatain & Sabriyah fields from which the Kuwait oil samples were obtained (Terken, 1999).

The 120 – 275 m thick Late Jurassic Sulaiy Formation and the overlaying 120 – 360 m thick Early Cretaceous Minagish Formation (both dominated by limestone lithology) are considered as the potential source rocks for these oils (Abdullah and Kinghorn, 1996) although this is still not established (Abdullah and Connan, 2002).

2.2.5 Qatar oils

The two oils, Q49 & Q61, from Qatar were obtained from offshore fields namely Al Shaheen and Bul Hanine (Figure 2.3 (a)) respectively. The Al Shaheen Field, in Block 5 offshore Oman, was discovered in 1974 although production started in 1994. It has five reservoirs although the dominant one is the mid-Cretaceous Kharab Formation. The oil produced is heavy and sour with density of 30 °API and sulphur content of about 1.9% (Al-Siddiqi and Dawe, 1999). The Bul Hanine Field, on the other hand, was discovered in 1965 but production started in 1972. The Late Jurassic Arab D limestone is the most prolific reservoir here with initial oil in place of 2.4 billion barrels with 36 °API gravity (Alsharhan and Nairn, 1997).

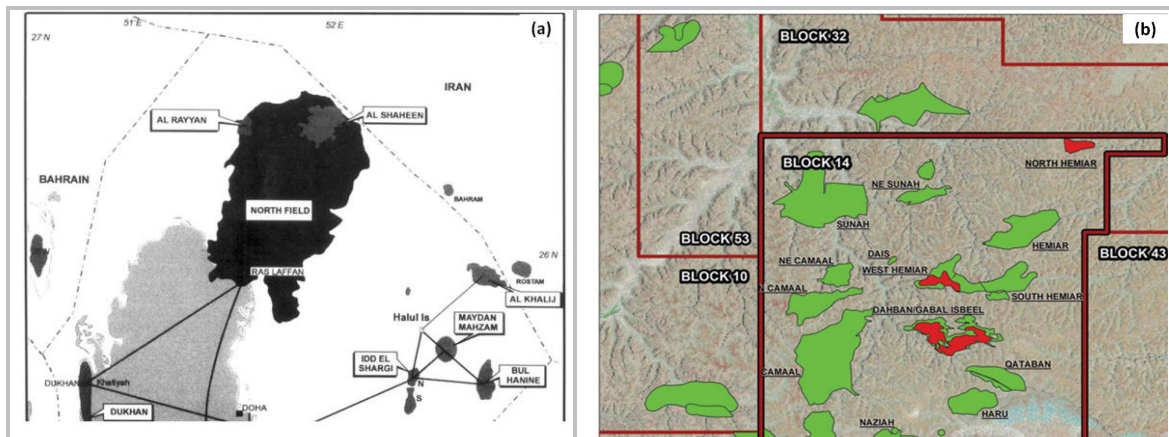


Figure 2. 3: Maps showing the location of (a) the two oil fields, Al Shaheen and Bul Hanine, from where the two oils from Qatar were obtained; and (b) location of Hemiar oil field from where the single oil sample from Yemen was obtained (Murphy, 2007).

The Upper Jurassic Jubailah (0.5 - 3.5% TOC) and Hanifa (1.0 - 6% TOC) Formations have been established as the main source rocks for almost all the oils in Qatar oil fields (Alsharhan and Nairn, 1997). However, the basal part of the Arab D reservoir, underlying the Hanifa and Jubaila formations, is organic rich (0.43 - 8.55% TOC) and mature to be a possible additional source rock for the oils (Al-Saad and Ibrahim, 2005).

2.2.6 Yemen oil

The oil Y32 was obtained from Hemiar field discovered in 1991 (Special, 1998). The field is located in about the middle of eastern half of Yemen in a group with six other fields (Alsharhan and Nairn, 1997). It produces heavy oils with gravity in the range of 18.0 to 22.0 °API (Special, 1998). All the Yemen oils are believed to be sourced from Amran Group - a Middle Jurassic single bituminous black shale although there are other potential source rocks (Alsharhan and Nairn, 1997).

2.2.7 Other oils

Details of ten oil samples are not fully disclosed as requested by the supplier. Two of these oils (AR3 & PR1) were from the Gulf of Mexico; three oils (C26, C30 & CH) are from Canada, and one each from Bangladesh (B58) and Abu Dhabi (A39). Two heavy oils (NA1 & NA2) were from Pannonian Basin, Serbia (Stojanovic et al., 2009). A bitumen sample (NB) from Southwest (Ondo State) Nigerian bitumen deposit was generously provided by Mr Abubakar B/Kebbi of Waziri Umaru Polytechnic, B/Kebbi. The bitumen has been characterised by Adebisi and Omode (2007).

2.2.8 Coal samples

The four coal samples (C04, C56, C69 & C15) used were provided by Dr Geoff D Abbott, Newcastle University, UK. Sample C15 was obtained from Harvey Beaumont seam, County Durham. It is Westphalian A and B Coal Measures in the Northumberland Coalfield and has been to contain about 0.85 to 2.25% total sulphur and 0.3 to 1.7% pyritic sulphur (Turner and Richardson, 2004). Samples C04, C56 and C69, on the other hand, were obtained from Brent coal, Northsea from depths of 1891.60, 2781.50 and 3293.10 m, respectively. The vitrinite reflectances (R_o) of the coals were previously determined to be 0.40, 0.56, 0.69 and 1.50% for C04, C56, C69 and C15, respectively.

2.3 Methods of Sample Preparation

This section describes the various procedures used in processing the 'raw' samples into a form that is amenable for analysis. Often procedures were adopted to reduce the complexity of the analytical samples to help identification of the components.

2.3.1 Powdering of rock and coal samples

Prior to extraction of bitumen from black shales or coals, the rock/coal samples are powdered. This increases the surface area of the sample thereby increasing the degree of contact between the sample and the extraction solvent. The powdering of the rock samples was done using a Tema mill and the powdered samples were stored in glass jars. The mill was washed with detergent, rinsed with distilled water and then dried before powdering each sample.

2.3.2 Extraction of bitumen from the black shale and coal samples

There are three methods for extraction of bitumen from carbonaceous samples: (1) In Soxhlet extraction method 'fresh' solvent (from continuous evaporation and condensation) at temperature above ambient temperature is continuously recycled through the powdered rock to extract the soluble components. (2) In Accelerated Solvent Extraction (Buckley et al., 1998), hot solvent is forced through the powdered rock at high pressure to effect extraction. (3) In ultrasonic extraction, on the other hand, high frequency (>20 kHz) sound waves are continuously passed through the rock/solvent mixture to aid dissolution of the soluble components into the solvent. Although all the methods have comparable efficiencies, the last two are faster.

The kind and quantity of the extractable components are dependent on the kind of solvent used and the timing of extraction. Different solvents are used by different laboratories. In general, however, fairly polar organic solvents or solvent mixtures are used. In common use is an azeotropic mixture of dichloromethane (DCM) and methanol (MeOH) (93:7, v/v). The timing of extraction also varies from about 24 to 72 hours depending on the extractability of the sample.

In this work Soxhlet extraction was used. All materials, e.g. cellulose thimbles, cotton wool, were Soxhlet extracted (DCM, 24 hours) prior to their use in sample extraction. A known weight (± 0.1 mg) of the powdered sample was extracted for 48 hours (72 hours for coal) with 200 ml of DCM/MeOH mixture (93:7, v/v). Small amounts of activated copper turnings were added in the solvent to remove any free elemental sulphur which degrades GC columns. The

solvent was removed from the extract by rotary evaporation (30 °C, 25 mmHg) followed by drying under a stream of nitrogen until a constant weight was obtained.

2.3.3 Precipitation and purification of asphaltenes

(a) *Precipitation of Asphaltenes*

As discussed in Chapter 1, asphaltenes are defined based on solubility properties (Speight and Moschopedis, 1981). The quantity and quality of asphaltenes vary with both the kind of solvent employed and the precipitation procedure adopted (Alboudwarej et al., 2002). Normal pentane, hexane and heptane are the common hydrocarbon solvents used for precipitation of asphaltenes from oils and bitumens although the latter is more commonly used. The precipitation procedure is usually based on the method of Speight (1984) which involves triple re-dissolution and re-precipitation after initial precipitation from oil or bitumen. In this work, *n*-hexane was mainly used for the precipitation of the asphaltenes for cost reasons and for the fact that the observed difference in yield between hexane and heptane is not as significant as that between pentane and hexane. However, *n*-pentane and *n*-heptane were also used to precipitate asphaltenes from three samples for comparison.

Briefly, a known weight of oil/bitumen was added to a conical flask. It was then treated with a 40-fold (w/v) excess of *n*-hexane in small increments portions with regular swirling. Bitumen and heavy oils were dissolved in 1 cm³ DCM before precipitating the asphaltenes with *n*-hexane. The mixture was then stirred for at least 2 hours and then allowed to equilibrate for 24 hours. The asphaltenes were recovered from the mixture by centrifugation at 3500 rev/min for 10 to 15 minutes. The asphaltenes were then re-dissolved in a minimum amount of DCM (about 1 to 2 cm³) and re-precipitated with 40-fold *n*-hexane. After about 30 minutes of stirring, the asphaltenes were recovered by centrifugation. This was repeated two more times and finally the asphaltenes were transferred into a pre-weighed glass vial with minimal volume of DCM. The excess solvent was removed by evaporation leaving about 1 cm³ which was then allowed to stand at ambient temperature until evaporation was completed leaving a residues of solid asphaltenes.

(b) *Purification of asphaltenes*

Although Speight (1984) recommend only the triple re-dissolution and re-precipitation described above for purification of asphaltenes from the co-precipitated resins and waxes, this was observed to be inadequate (Alboudwarej et al., 2002). Consequently additional procedures such as ultrasonication, Soxhlet extraction etc. are used to remove the co-precipitated substances from the asphaltenes. Alboudwarej et al. (2002) compared some of these procedures (except the latter) and concluded in favour of Soxhlet extraction of the asphaltene for 72 hours. This procedure was therefore adopted in this work.

The dried asphaltenes were crushed with a spatula and extracted for between 24 and 240 hours in pre-extracted (DCM, 24 hours) Whatman cellulose thimbles (1 x 10 cm) using the solvent used in the precipitation process. However, for the study of adsorption/occlusion properties of asphaltenes (Chapter 4), acetone was used for extraction of the asphaltenes to be consistent with the method of Liao et al. (2006b).

2.3.4 Fractionation of maltenes

Prior to instrumental analysis such as GC and GC/MS, maltenes are often separated into broad compound classes namely: aliphatic hydrocarbons consisting of acyclic and cyclic alkanes (naphthenes); aromatic hydrocarbons consisting of pure aromatics, including polycyclic aromatic compounds (PAHs) and naphtho-aromatic compounds; and resins, which consist of both aliphatic and aromatic heteroatomic (mainly N, S and O) organic compounds. The separation generally improves instrument sensitivity and aids in the identification of the compounds.

Traditionally column and thin layer chromatographic methods are used for fractionation of oils/bitumen and maltenes. These methods are relatively time consuming however. This led to the development of a rapid fractionation method (Bennett and Larter, 2000) that allows handling as many as ten samples at the same time. The method is a two-step process involving initial separation of resins from hydrocarbons on SPE column. The hydrocarbon fraction is then separated into aliphatic and aromatic fractions using argentation column chromatography with silver nitrate/Kieselgel 60G ($\text{AgNO}_3/\text{SiO}_2$) column (Bennett and Larter, 2000). This method was adopted for the analyses described in this thesis.

In general, each ISOLUTE C18 column (500 mg/3 cm³; Kinesis Ltd.) was first cleaned with 4 cm³ DCM, flushed with air and dried (60 °C, 24 hours). Sample (50 to 60 mg) was weighed directly on the column and hydrocarbon and resin fractions were recovered with 4 cm³ *n*-hexane and 4 cm³ DCM respectively. Deuterated *n*-hexadecane (Sigma-Aldrich) and 4-methyl biphenyl (Sigma-Aldrich) were added in the hydrocarbon fraction as internal standards. The fraction was then concentrated to about 0.5 cm³ under stream of nitrogen gas. 100 to 150 µl was then loaded on to the $\text{AgNO}_3/\text{SiO}_2$ column pre-cleaned with 4 cm³ *n*-hexane. Aliphatic and aromatic fractions were recovered with 3 cm³ *n*-hexane and 4 cm³ DCM respectively. The fractions were concentrated under stream of nitrogen gas to about 0.5 cm³ and transferred into GC vials for analysis. In each batch of 8 samples a blank control and a standard (Brent oil) sample was also separated.

Slight modifications to the above procedure were made to conveniently separate some unusual samples. It was observed that desorbed components obtained from Soxhlet extraction of asphaltenes were not completely soluble in *n*-hexane and could not be suspended even after ultrasonication; and so could not be loaded on the C18 column for fractionation into hydrocarbon and resin fractions. To address this problem, DCM, instead of *n*-hexane, was used as eluent on $\text{AgNO}_3/\text{SiO}_2$ column, instead of C18 column. The fraction so obtained was dried under nitrogen gas and then re-dissolved in *n*-hexane, in which it dissolves. This solution was then loaded on another $\text{AgNO}_3/\text{SiO}_2$ column and aliphatic and aromatic fractions were collected as outlined above. This procedure was adopted after successful initial trials with one oil sample.

The $\text{AgNO}_3/\text{SiO}_2$ column was prepared as follows (Bennett and Larter, 2000): About 30 g Kieselgel 60G (Merck) was thoroughly mixed with 60 cm³ 5% aqueous AgNO_3 (100%, Sigma-Aldrich) solution in a conical flask. The flask, containing the slurry, was completely wrapped with aluminium foil (to protect the AgNO_3 from photolysis) with only small holes to allow escape of water vapour. The slurry was left to dry in a drying cabinet (85 °C, 7 days). The dry

lumps were then crushed into fine powder in a mortar and pestle. The powder was transferred back into the flask, covered with foil and kept in drying cabinet until required.

The column was prepared in ISOLUTE Empty Reservoir (3 cm³, Kinesis Ltd.). An ISOLUTE Frit (20 µm, 3 cm³/9 mm; Kinesis Ltd) was inserted into the reservoir and about 550 mg of the AgNO₃/SiO₂ adsorbent added. This was covered with another Frit. The adsorbent was then compacted to a thickness of about 1 cm with the help of a specially made cylindrical aluminium rod.

2.3.5 Urea adduction

Compound specific isotope ratio (CSIR) analysis requires good purification of the samples to avoid contamination of the isotopic data by co-eluting compounds. Consequently, in CSIR analysis of linear aliphatic hydrocarbons, cyclics are often separated from the acyclics, particularly *n*-alkanes. For this purpose, there are essentially two main methods in common usage namely: urea adduction and molecular sieving. Urea adduction has been used widely to separate *n*-alkanes from the cyclics and *iso*-alkanes (Murphy, 1969). The method is based on the observed phenomenon that as urea precipitates out of solution it exclusively traps *n*-alkanes within its crystal lattice (forming clathrates) while the branched and cyclic compounds remain in solution. The method has been found to give comparable results to those from molecular sieving (Xu and Sun, 2005; Murphy, 1969) and was thus adopted in this study.

About 10 to 20 mg of aliphatic fraction or methyl esters was dissolved in about 0.5 cm³ DCM in 20 cm³ vial. Then about 10 cm³ of saturated urea (99.5%, BDH) solution in methanol was added. The mixture was placed in a refrigerator (below 0 °C, 6 hours). After the crystallisation was complete, the supernatant solution, containing the cyclic and branched compounds, was decanted and the crystals washed with cold *n*-hexane (10 cm³, x3) and then dried under stream of nitrogen gas. Then about 20 cm³ of deionised water was added to dissolve the crystals and then the released occluded linear compounds were extracted with *n*-hexane (10 cm³, x3). The solvent was removed from the extract by rotary evaporation to about 2 cm³ and then further dried to about 0.5 cm³ under nitrogen before being transferred to GC vials for analysis.

Where the cyclic compounds are of interest, for example in the identification hopanoic and steranoic acid methyl esters, the decanted solution is treated with 20 cm³ of water, extracted and concentrated as described above.

2.3.6 Ruthenium ion catalysed oxidation (RICO) of asphaltenes

RICO is a chemical technique that selectively oxidises aromatic ring structures into CO₂ with the aliphatic moieties converted to fatty acids. It has been widely used to elucidate the aliphatic composition of geopolymers (Peng et al., 1999b; Stock and Tse, 1983). The active reagent, ruthenium tetroxide (RuO₄), has been prepared and used in different forms (Lee and van den Engh, 1973). The *in situ* preparation, in which only catalytic amount of the ruthenium salt is used, is however more convenient and is now widely used for chemical oxidation of asphaltenes and other forms of sedimentary organic matter (Ma et al., 2008; Peng et al., 1999a; Mojelsky et al., 1992). The method has good selectivity with respect to the products formed (Stock and Tse, 1983) and could therefore be used in reconstruction of the original structure.

The procedure adopted in this work is as follows: About 50 mg of the asphaltenes was dissolved in 4 cm³ DCM and 4 cm³ acetonitrile (BDH) was added. Then 5 cm³ of 12% aqueous sodium periodate (NaIO₄) and then about 5 mg RuCl₃.XH₂O (Sigma-Aldrich) were added. After 24 hours of magnetic stirring at room temperature (*ca* 20 °C), about 10 cm³ of DCM and 10 cm³ methanol (to destroy excess oxidising agent) were added and the mixture was centrifuged (3500 rpm, 15 minutes). The supernatant was decanted and the residue washed with 10 cm³ of DCM and 10 cm³ of water. The washings were combined with the supernatant and the organic phase, containing free carboxylic acids, was recovered. The solvent was removed from the organic phase by rotary evaporation (25 °C, 25 mmHg). Traces of water were removed by adding 5 cm³ of acetone and re-evaporating. Before analysis, the acids were derivatised into methyl esters as described in Section 2.3.10.

2.3.7 Potassium permanganate oxidation of asphaltenes

Potassium permanganate is a very strong oxidising agent which has been used in degradation polycyclic hydrocarbons (Gates-Anderson et al., 2001) and geopolymers such as kerogen and coal (Vitorovic et al., 1984; Ward et al., 1945). However it barely attacks saturated hydrocarbons (Lee and Spitzer, 1969; Stewart, 1965). This selectivity was taken advantage of in this work in order to break down the aromatic structure of asphaltene without attacking the saturated hydrocarbons that might have been trapped within the asphaltenes.

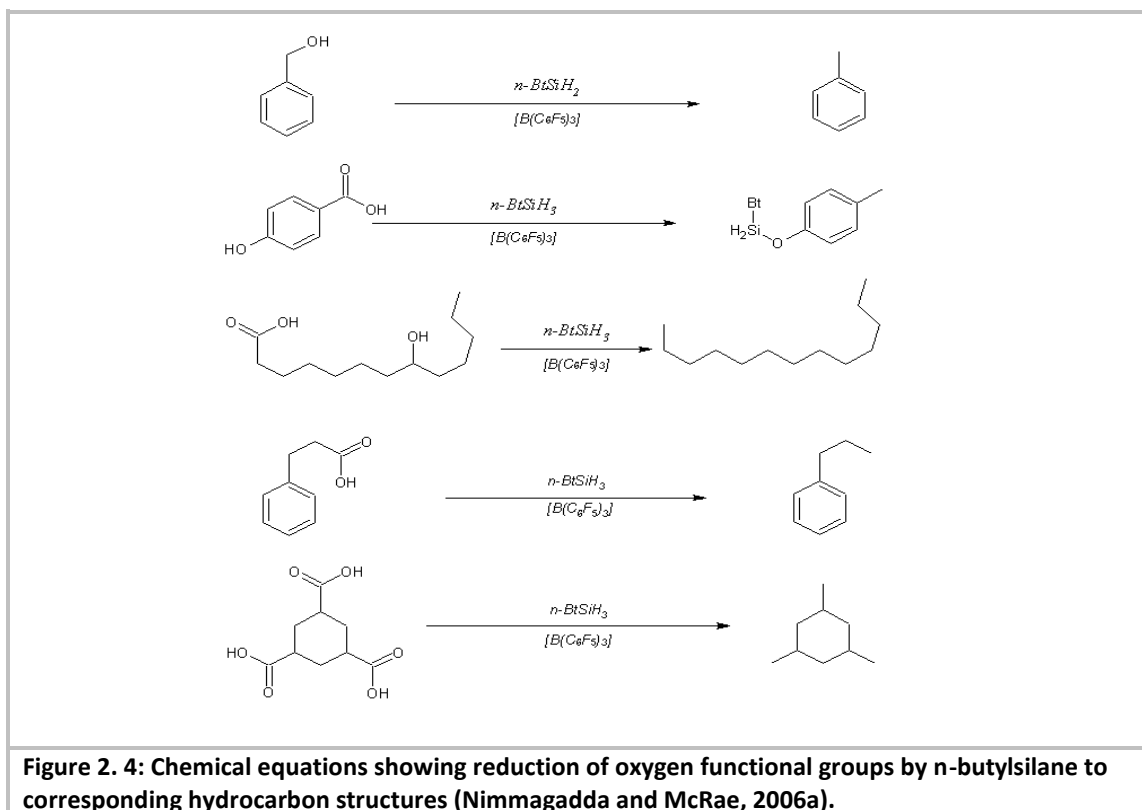
The potassium permanganate oxidation of asphaltene was done as follows: About 100 mg of the asphaltenes was dissolved in 5 cm³ dichloromethane in a 100 cm³ conical flask. To this were added 20 cm³ of ~0.1M aqueous potassium permanganate and 5 cm³ of 3% sulphuric acid. After 24 hours of continuous stirring at room temperature, 30 cm³ of deionised water was added and the mixture was extracted with dichloromethane (50 cm³, x3). Internal standard (deuterated hexadecane) was added to the combine extracts before the solvent was rotoevaporated to about 5 cm³ and then to about 1 cm³ under nitrogen. This was then treated with 40 cm³ *n*-hexane and the insoluble material was removed by centrifugation (3,500 rev/minute, 10 minutes). The *n*-hexane soluble material was recovered and solvent reduced to 1 cm³ and aliphatic hydrocarbons isolated by column chromatography as described in Section 2.3.4.

2.3.8 *n*-Butylsilane reduction

This is a very versatile method that reduces most of the oxygen-based functionalities such as hydroxyl, carbonyl, carboxylic acid, and ester (Nimmagadda and McRae, 2006b; Nimmagadda and McRae, 2006a) into the corresponding hydrocarbon and ether (in case of ester) as illustrated in Figure 2.4, without any effect of carbon skeleton of the compound involved. The method has been used to elucidate the backbone structure of fulvic acids by reduction of the polar functional groups thereby making it amenable for GC/MS analysis (Nimmagadda and McRae, 2007).

In this work, the method was used to reduce carbonyl and carboxylic functional groups in asphaltenes sample in order to eliminate aliphatic side chains with terminal carboxylic group as an alternative/additional source of α,ω -dicarboxylic acids observed in RICO products (Section 6.3.3 (c)). For this purpose, 137.4 mg of the asphaltene sample (NBA) from the Nigerian biodegraded bitumen (NB) was dissolved in 3 cm³ dry toluene (Sigma-Aldrich) in a 100

ml three-neck round-bottomed flask. This was fitted with a condenser and the two side arms and condenser closed with septa. The system was flushed with nitrogen for about 30 minutes. Then about 10 mg of tris(pentafluorophenyl)borane $[B(C_6F_5)_3]$ (Sigma-Aldrich) dissolved in 2 cm^3 toluene was introduced via a syringe. After about 30 minutes of mixing with a magnetic stirrer, 500 μl *n*-butylsilane ($\geq 97.0\%$, Sigma-Aldrich) was introduced. The reaction was allowed to proceed at room temperature for 24 hours under static nitrogen atmosphere maintained with the help of a balloon (Leonard et al., 1995).



After the 24 hours of reaction, the solvent was removed by rotary evaporation and the asphaltenes were precipitated as described in Section 2.3.3. The reduction was repeated on the precipitated residual asphaltenes as described above. After this about 101.3 mg asphaltenes were recovered by precipitation. Portions of the asphaltene, before and after reduction, were prepared and analysed by FTIR as described in Sections 2.3.11 and 2.4.7 respectively, and the remaining analysed by RICO (Section 2.3.5) followed by GC/MS (Section 2.4.5).

The reduction procedure used here is modified from Nimmagadda and McRae (2007) after successful trials on model compounds: A mixture of stearic acid (53.2 mg), cholesterol (43.4 mg) and ergosterol (48.6 mg) was treated, as described above, with 5 mg $[B(C_6F_5)_3]$ and 300 μl *n*-butylsilane. After 24 hours the reaction mixture was diluted to 20 ml with DCM. 3 cm^3 was then column chromatograph (5 g silica) and the hydrocarbon products eluted with 70 cm^3 *n*-hexane and analysed on GC/MS. Dry toluene was used as solvent for the reaction instead of dry dichloromethane as using the later requires the reaction to be done in the dark to avoid photolytic production of HCl from DCM which has been observed to seriously retard the reaction (Nimmagadda and McRae, 2006a).

2.3.9 Extraction of acids from oils and bitumen

Acidic compounds in crude oils and bitumen (commonly referred to as naphthenic acids) occur mainly as carboxylic acids consisting of aromatic and aliphatic (both cyclic and acyclic) structures. They occur in relatively small proportions depending on the maturity and biogeochemical history of the oil; often immature and biodegraded crudes tend to have relatively high proportions of the acids (Lochte and Littman, 1955). Consequently, the free acid contents of some of the oil samples were analysed to investigate whether there was any significant contributions from the free acids to the RICO acid products.

Methods employed for extraction of the acids from the crude oils and bitumen are based on the principles of acid/base reaction in which direct saponification (Behar and Albrecht, 1984; Costantinides and Arich, 1967) or a base adsorbent is used to chemisorbed the acids (perhaps as salts) from the oil medium. The acids are then recovered from the adsorbent using a stronger acid solvent to reverse the process. The most common adsorbent used is potassium or sodium hydroxide on silica (Ramljak et al., 1977; Douglas and Powell, 1969) or silicic acid (Farrimond et al., 2002; McCarthy and Duthie, 1962). However, recently our laboratory has developed and optimised a new method based on quaternary amine ion exchange chromatography (Jones et al., 2001). Although the method is lengthy, requiring up to 24 hours for completion, up to about ten separations can be handled simultaneously which makes it a method of choice where many samples are to be analysed. This method was therefore adopted in this work.

About 400 mg of oil sample was placed in a vial and 10 μl of surrogate standard (β -cholanolic acid (Sigma-Aldrich), 1 mg/cm³) was added. This was then applied to a pre-cleaned (10 cm³ hexane followed by 10 ml 1:1 hexane/DCM) SAX quaternary amine (10 g) SPE 6 cm³ column (International Sorbent Technology) with the help of small aliquots of DCM and hexane. The non-acid components were then eluted with 20 cm³ of hexane/DCM mixture (1:1) followed by 25 cm³ of DCM. The acids were eluted with 30 cm³ of 2% (v/v) formic acid (Sigma-Aldrich) in diethyl ether (Sigma-Aldrich) followed by 20 cm³ of 5% (v/v) formic acid in diethyl ether. The acid solution was then evaporated to about 1 cm³ using rotary evaporator at room temperature. This was then transferred into a vial, dried under a stream of nitrogen, and allowed to stand overnight until the odour of formic acid no longer detected. Before analysis, the acids were derivatised as described in Section 2.3.10. Deuterated hexadecane was added as internal standard.

2.3.10 Esterification of acids

Carboxylic acids are polar compounds with strong intermolecular hydrogen bonds. This makes them fairly non-volatile and therefore non-GC amenable and hence the need for derivatisation to improve their volatility. Although there are many GC amenable derivatives of carboxylic acids (e.g. silyl esters, methyl esters, etc), their esters with alkanols, and particularly methanol (methyl esters), are not only the most common (making identification much easier), they are also easy to prepare.

There are a number methods of preparing methyl esters of carboxylic acids (Christie, 2006; Knapp, 1979). In geochemical studies diazomethane and boron trifluoride are the most common methods employed. The former is particularly rapid and efficient especially in the presence of catalytic amount of methanol. It however requires dedicated/special apparatus

and requires special training for safety reasons. Boron trifluoride, on the other hand, is inefficient in methylation of aromatic acids. In this work sulphuric acid was used to catalyse the esterification of the acids in methanol (Christie, 2006).

About 1 ml DCM was used to transfer the acids into a boiling tube. Then 7 cm³ of 2 % concentrated sulphuric acid (98%, BDH) in methanol was added with few anti-bumping granules. The mixture was refluxed on a test tube heater for 3 hours. After cooling, 10 cm³ water was added and the methyl esters were extracted with DCM (10 cm³, x3). The esters were dried over sodium sulphate (>99%, Sigma-Aldrich), and the excess solvent removed using a rotary evaporator (20 °C, 25 mmHg) to about 2 cm³ and reduced further to about 0.5 cm³ under nitrogen. The esters were transferred into a GC vial for analysis. Deuterated hexadecane (~2 mg/cm³) was added (50 µl) as internal standard.

The esterification method was adopted following trial on standard compounds. A mixture of stearic acid (3.9 mg) and isophthalic acid (4.9 mg) was esterified and treated as described above, and analysed on GC. The conversion was found to be 100% and 93.8% respectively after 2 hour of reflux.

2.3.11 Preparation of samples for FTIR analysis

There are many sampling techniques that can be used for FTIR analysis of samples depending on the nature of the sample (Smith, 1996). However, by far the most common methods employed KBr pellets (transmission mode) and Diffuse Reflectance (DR). The most important advantage of the former is that the absorbance so obtained is directly proportional to the concentration of the absorbing species according to the Beer-Lambert law. Quantification is easy and straightforward if absorptivity is known. This sampling technique was therefore used for analysis of the asphaltenes using FTIR.

The samples were prepared as follows: About 5 mg of the asphaltene was mixed with ~ 495 mg of potassium bromide (99.5% IR Spectroscopic grade, Sigma-Aldrich) to give an optimal concentration of about 1% (w/w). The mixture was grounded into a fine powder with agate mortar and pestle (International Crystal Laboratory) until crystals of KBr are no longer visible and the mixture tends to stick to the mortar (Smith, 1996). The powder was wrapped in aluminium foil and kept in dessiccator until required for analysis. A blank, consisting of only KBr, was also prepared similarly. The mortar and pestle were washed with DCM and wiped with tissue before every sample was prepared. All samples were analysed within one week of being prepared.

The pellets were prepared using a 15 ton manually operated hydraulic press (Specac Ltd). About 200 mg of the sample/KBr powder prepared above was placed in a 13 mm standard die (Specac Ltd) sandwiched between two 13 mm dies. The die system was centrally placed on the lower bolster pressing face and the top bolster pressing face was lowered to tightly hold the die component in place. The pressure release screw was then closed and 5 ton pressure was applied for 5 minutes before it was increased to 10 ton where it was held for 15 minutes. After this the pellet was recovered, wrapped in aluminium foil and kept in desiccator until required. The pellets were not oven dried to avoid thermally induced chemical changes in the samples. A blank pellet (KBr without sample) was prepared and treated similarly.

2.4 Analytical Methods

2.4.1 Total carbon, hydrogen, nitrogen and sulphur analysis

This involves quantification of relative amounts of carbon, hydrogen, nitrogen, and sulphur in powdered rock, coal and asphaltene samples. The analysis was done as a preliminary characterisation to find the relative proportions of the major elements in the samples. About 100 mg of the powdered sample was weighed into special ceramic cup and 100 mg of tungsten (VI) oxide (Elementar R22), which facilitates the combustion process, was added. A standard sample (sulfadiazine) was prepared similarly; about 75 mg of sulfadiazine (99.0%min., Sigma-Aldrich; 47.99%C, 22.37%N & 12.81%S) was weighed into a cup without the accelerator. The blank was an empty ceramic cup.

The analysis was done with Elementar Vario Max CNS instrument fitted with auto-sampler. The instrument was first calibrated by several analyses of a standard sample. Furthermore, a standard was analysed after every ten analytical samples. The average value obtained from the analysis of two blanks was subtracted the averages of both the standard and the analytical samples. Replicate analysis ($n=16$) of the standard sample (sulfadiazine) revealed the standard deviation were respectively $\pm 0.46\%$, $\pm 0.23\%$ and $\pm 0.76\%$; and relative error were 0.44%, 0.55% and 2.09% for carbon, nitrogen and sulphur respectively.

Analysis of carbon, hydrogen, nitrogen and sulphur in asphaltenes was carried out by Mr J R Baron using a Carlo Erba 1108 Elemental Analyser controlled with CE Eager 200 software at Advanced Chemical and Materials Analysis (ACMA), Newcastle University, UK. The results of the elemental analysis are in Appendix 2A.

2.4.2 Total organic carbon analysis

Total organic carbon (TOC) is the common form in which the relative amounts of organic matter in sediments is expressed. It is determined using many methods although dry combustion is the most accurate, reliable and rapid (Bisutti et al., 2004). The variant of the method used in this work involves complete combustion of the decarbonated sample at 1000 – 1100°C in stream of O₂ to convert any organic carbon (OC) into CO₂ which was then quantified.

The powdered rock sample was first decarbonated as follows: About 100 mg of the sample was weighed into ceramic filtering crucible (Alpha AR 8028) and 2 cm³ of 50% (v/v) HCl (BDH AnalaR, 38.4%, & 1.18 specific gravity) was added and allowed to stand in hood. When all the acid solution percolated through the crucible, about 2 cm³ of deionised water was added to wash off the excess acid. This was repeated five more times before the samples were dried in an oven (105 °C) for at least 5 hours. Each sample was prepared and analysed in duplicate.

The TOC was determined using a LECO CS-244 Carbon and Sulphur Determinator. The instrument was first calibrated using eight LECO carbon and sulphur steel calibrating samples (%C = 0.834 \pm 0.005 %S = 0.0044 \pm 0.0003). A ring of the calibrating sample was placed in a ceramic crucible and 1.2 g of tungsten accelerator (SL 266, Sci Lab Analytical) was added to facilitate combustion. This was combusted in the determinator at O₂ flow pressure of 2.4-2.6 bar. The analytical samples were analysed similarly; in addition the tungsten accelerator about 0.6 g of iron chip accelerator (AR 077, Sci Lab Analytical) was however added to facilitate

ignition. A calibrating sample was analysed after analysis of every six analytical samples to ensure the determinator performs within calibration. Repeatability and bias of the method based on replicate analysis ($n = 17$) of the calibrating sample were $0.8497 \pm 0.0050\%$ and 0.6870% , respectively.

2.4.3 Rock-Eval pyrolysis

Rock-Eval pyrolysis is used to identify the type and maturity of organic matter and assess its petroleum potential. The method involves gradual thermal cracking of sedimentary organic matter in the absence of O_2 and then measurement of the amount of the products (pyrolysates) evolved. Depending on the instrument used the pyrolysates are divided into S1, the 'free' component (~bitumen); S2, the kerogen component; and S3, the carbon dioxide from organic matter. These are used to calculate the hydrogen index (HI), a measure of type/quality of the organic matter; and the petroleum generation index (PI). The temperature at the peak of S2 generation is also recorded as Tmax. Both Tmax and PI are measures of maturity of the organic matter. Rock-Eval pyrolysers of versions latter than Rock-Eval II (e.g. Oil Show Analyzer) do not measure S3 but splits the S1 into gas and oil components.

In this work Oil Show Analyser Multichrom CH10 was used for analysis of the black shale and coal samples. About 100 mg of the powdered sample was weighed into pyrolysis crucible. The analysis was done in accordance with the method of Peters (1986). Briefly, the sample was gradually heated in a helium atmosphere to 300 °C where it was held for 3 minutes. The temperature was then programmed at 25°C/minute to 550°C. The pyrolysates were quantified, using flame ionisation detector (FID), as volatile gas component and oil component (S1), and pyrolysed non-volatile organic matter (S2). Tmax (in °C) was also recorded.

Each sample was analysed in duplicate and the average value calculated. Blank (an empty crucible) and in-house reference standard (352/123; TOC=5.15%, S1=0.27 mg/gRock, S2=13.59 mg/gRock & Tmax=430°C) were analysed prior to every 22 crucibles of samples. In general, bias of the method was less than 1% for all parameters and repeatability, based on replicate analysis ($n=10$) of sample T1, was $432 \pm 2^\circ\text{C}$ for Tmax, 8.41 ± 0.36 mg/gRock for S1 (taken as sum of the gas and oil peaks) and 45.07 ± 2.34 mg/gRock for S2. Hydrogen index (HI) and petroleum generation index (PI) were computed from equations 2.1 and 2.2, respectively.

$$HI = \frac{S2}{TOC} \times 100 \quad 2.1$$

$$PI = \frac{S1}{S1 + S2} \quad 2.2$$

2.4.4 Gas chromatography (GC)

GC is a molecular separation technique for separation of mixtures of organic compounds that can be volatilised without decomposition. The technique involves sweeping the mixture over a stationary phase (held in a column) with a mobile phase (carrier gas). The differential interaction between the components of the mixture and the two phases results in differential speeds through the column and therefore differential time at which they exit the column. As the components more or less individually exit the column, they are detected using a detector

such a flame ionisation detector or a thermal conductivity detector. The signal is used to produce a response versus retention time graph (chromatogram) with peaks representing individual components.

In this work, GC was mainly used for preliminary analysis prior to GC/MS or GC/IRMS for quality control purposes. The instrument used was an HP 5890 series II gas chromatograph equipped with an HP-5 capillary column (30 m x 0.25 mm) with 0.25 μm thick dimethyl polysiloxane stationary phase. The GC oven was temperature programmed to 50 $^{\circ}\text{C}$ where it was held for 2 minute, and ramped at 4 $^{\circ}\text{C}/\text{minute}$ to 300 $^{\circ}\text{C}$ where it was held 20 minutes. Hydrogen was used as the carrier gas at approximate flow rate of 2 ml/minute with initial pressure of 100 kPa. Acquisition of the data was with Atlas software on an HP desktop computer.

2.4.5 Gas chromatography/mass spectrometry (GC/MS)

GC/MS is a technique in which GC is joined to mass spectrometer (MS). The GC separates a mixture into individual compounds and as each compound elutes out of the GC column, it passes into the mass spectrometer where the molecules are ionised (often by electron impact). Some of the primary ions so generated may further undergo fragmentation generating secondary ions the kind of which is dependent on the structure of the compound. These ions are separated and analysed by the spectrometer giving a unique signature of the original compound that can be used to reconstruct its molecular structure (Kitson et al., 1996). This is the full scan mode. In selected ion monitoring (SIM) mode only a few fragment ions of interest are monitored with added advantage of sensitivity but the mass spectra is lost.

Aliphatic and aromatic hydrocarbon fractions of oils and bitumen and as well as methyl esters of carboxylic acids were analysed using GC/MS. The instrument was a Hewlett-Packard 6890 GC, with split/splitless injector (280 $^{\circ}\text{C}$), linked to a Hewlett-Packard 5973MSD mass spectrometer set at electron ionisation energy of 70 eV; source temperature of 230 $^{\circ}\text{C}$; quadrupole temperature of 150 $^{\circ}\text{C}$; multiplier voltage of 2000 V; and interface temperature of 310 $^{\circ}\text{C}$. The acquisition was controlled by a HP computer on Chemstation platform. All samples were analysed in selected ion monitoring mode (SIM) set to monitor ions of interest with a dwell time 35 ms per ion. A few samples were, however, analysed in full scan mode covering the range 50 to 550 amu in order to obtain the mass spectra of compounds for identification.

The GC was equipped with a fused silica capillary column (30 m x 0.25 mm i.d) coated with 0.25 μm dimethyl polysiloxane (HP-5ms) phase. The GC was temperature programmed as follows: held for 5 minutes at 40 $^{\circ}\text{C}$, and then ramped at 4 $^{\circ}\text{C}/\text{minute}$ to 300 $^{\circ}\text{C}$ where it was held for 20 minutes. The carrier gas was helium with a flow rate of approximately 1 $\text{cm}^3/\text{minute}$ and initial pressure of 50 kPa while split at 30 ml/minute. The sample (1 μl) in DCM or *n*-hexane was injected by an HP7683 autosampler and the split opened after 1 minute to vent the solvent.

2.4.6 Compound specific isotope ratio analysis (CSIR)

CSIR analysis is a technique used to measure the relative proportions of the stable isotopes of an element in a chemical compound. This isotopic signature may give an insight into the biosynthetic path for the compound and possibly the organism that synthesised the compound. It therefore provides an additional tool for possible discrimination of compounds

of different sources. The most common method used for CSIR analysis is the GC/IRMS. The GC separates the mixture into the composite individual compounds. As each compound elutes, it is combusted into CO₂ that is then passed to mass spectrometer which then separates and measures the relative proportion of the two main isotopically different CO₂ molecules based on their molar masses (44 for ¹²CO₂ versus 45 for ¹³CO₂). The isotopic signature of the compound, expressed in the per mil (‰) unit, is universally calculated relative to the international standard Vienna Pee Dee belemnite (VPDB) from equation 2.3. The technique was used in this work to determine the δ¹³C of *n*-alkanes and *n*-alkanoic acid methyl esters from some samples for the purpose of comparison and discrimination.

$$\delta^{13}\text{C} = \left(\frac{\left(\frac{^{13}\text{C}}{^{12}\text{C}} \right)_{\text{sample}}}{\left(\frac{^{13}\text{C}}{^{12}\text{C}} \right)_{\text{standard}}} - 1 \right) \times 1000\text{‰} \quad 2.3$$

The GC/IRMS analysis was performed on a Thermo Electron Trace Ultra GC equipped with split/splitless injector (280 °C) via a Combustion III Interface linked to a Thermo Electron Delta V Plus IR-MS set at electron ionisation energy of 70 eV; source temperature of 230 °C; quad temperature of 150 °C; multiplier voltage of 2000 V and interface temperature of 310 °C. The acquisition was controlled by a Dell computer using Isodat software, initially in carbon mode monitoring the 13/12 ratio of CO₂.

The sample (1 µl) in hexane was injected by a CTC autosampler and the split opened after 1 minute. The GC was temperature programmed from 50 to 320 °C at 5 °C/minute and held at 320 °C for 6 minutes. The carrier gas was helium at 1 ml/minute, initial pressure of 50 kPa and split at 20 ml/min. The solvent peak was diverted to the FID and CO₂ reference gas was pulsed into the mass spectrometer and after 7 minutes the back flush valve directed the split sample via the combustion furnace (940 °C) and reduction furnace (650 °C) into the mass spectrometer and the isotope ratio measured. Chromatographic separation was performed on a fused silica capillary column (30 m x 0.25 mm i.d.) coated with 0.25 µm dimethyl polysiloxane (HP-5) stationary phase. The acquired data were processed using the Isodat dynamic background integration Workspace software to give the peak retention times and isotope ratios as δ¹³C values. The data were also stored on DVD for any further processing, integration or printing.

Accuracy of the measurements was monitored by analysing a standard mixture of methyl esters of fatty acid (C₁₆ to C₂₅) of known δ¹³C values before and after analysis of analytical samples. The error and deviation are generally within acceptable limits (Table 2.1).

Table 2.3: Summary of statistical analysis of standard methyl esters of aliphatic acid mixture $\delta^{13}\text{C}$ analysis

Carbon number	C16	C17	C18	C19	C20	C21	C22	C23	C24	C25	C26	C27	C28	C29	C30
Actual values	-30.5	-31.0	-31.0	-33.1	-32.2	-29.0	-32.8	-31.7	-33.2	-28.5	-32.9	-28.5	-32.1	-31.0	-33.1
Measurement 1	-31.2	-32.1	-32.0	-34.0	-33.3	-30.1	-33.6	-32.2	-34.2	-29.0	-33.5	-29.0	-32.9	-31.7	-33.6
Measurement 2	-31.1	-30.6	-30.9	-33.3	-32.8	-29.8	-33.2	-32.2	-33.9	-29.3	-33.7	-29.3	-32.8	-29.2	-35.0
Measurement 3	-30.9	-31.1	-31.2	-33.4	-32.7	-29.5	-33.1	-31.6	-32.9	-28.4	-32.7	-28.7	-32.2	-31.1	-33.5
Mean	-31.1	-31.3	-31.4	-33.6	-32.9	-29.8	-33.3	-32.0	-33.7	-28.9	-33.3	-29.0	-32.6	-30.7	-34.0
Standard Dev.	0.2	0.8	0.6	0.4	0.3	0.3	0.3	0.3	0.7	0.5	0.5	0.3	0.4	1.3	0.8
Rel. error (%)	1.9	0.9	1.2	1.4	2.3	2.8	1.5	0.9	1.4	1.4	1.2	1.8	1.7	-1.1	2.8

2.4.7 Fourier transform infrared spectroscopy (FTIR)

FTIR is a powerful analytical method for identification and quantification of many functionalities in a chemical system (Smith, 1996; Nakanishi, 1962). The method has various sampling techniques (Smith, 1996) of which transmission and diffuse reflectance (DRIFTS) are widely used. In the former, an IR beam (I_o) incident on sample (in KBR pellet or sealed cell) is partly absorbed and partly transmitted (I). The absorbance (A_o) is directly proportional to concentration (c) of the absorbing group in accordance with the Beer-Lambert's law (equation 2.4). This quantification however requires absorptivity (i.e. the proportionality constant, ϵ), which varies with the chemical environment of the absorbing group.

$$A = -\log_{10}\left(\frac{I}{I_o}\right) = \epsilon c \quad 2.4$$

The asphaltene samples were analysed in transmission modes. The pellet was held in place using a special pellet holder which was then slotted in place on the Smart Transmission E.S.P holder. A pure KBr pellet was used as background which was automatically subtracted from each spectrum. Repeatability of the method was based on replicate (x3) analysis of a sample (K78) each prepared as other analytical samples (2.3.11). Precision of the measurements was determined by triplicate analysis of a single sample (U54).

The instrument used was Thermo Nicolet Nexus 870 FTIR spectrometer (Thermo Nicolet Corp.) with DTGS KBR detector and XT-KBr beam splitter with aperture of 69 and Autogain mode. The spectral quality check facility was set on for automatic detection of any abnormality during analysis. Each spectrum was acquired in mid-infrared region ($400 - 4000 \text{ cm}^{-1}$) by co-adding 70 scans at a resolution of 4 cm^{-1} . The data acquisition was carried out with OMNIC 6.1a (Thermo Nicolet Corp.) software on Dell desktop computer.

2.4.8 Solid-state nuclear magnetic resonance spectroscopy

Nuclear magnetic resonance spectroscopy is a very powerful analytical technique in structure elucidation of chemical compounds. The technique exploits the magnetic properties of spinning nuclei (e.g. ^{13}C and ^1H) and the effect of that on the electron clouds of the nearby atom in the molecule to derive information on the structure of the chemical compound (Lambert and Mazzola, 2003). Although NMR was originally developed to study compounds in the liquid phase, development of solid-state NMR has widened the applications of the technique to the study of insoluble materials such as polymers, coal, kerogen etc. (Sfini and Legrand, 1990; Tekely et al., 1990; Vassallo et al., 1987). Bulk structural parameters of asphaltenes have also been investigated using the technique (Calemma et al., 1998; Calemma et al., 1995). In

this work the technique was employed to complement FTIR bulk characterisation of the asphaltenes.

The solid-state NMR analysis was performed at Durham University, EPSRC National Solid-state NMR Research Service, on a Varian VNMRS 400 spectrometer using a double-resonance (H-X) MAS probe equipped with a 4 mm rotor. The resonance frequencies for ^1H and ^{13}C NMR were 399.88 and 100.56 MHz, respectively. The Soxhlet extracted asphaltene samples were used without further preparation. The sample rotor was spun at 12 kHz. A pulse repetition delay of 2 s was used and a cross polarization (CP) contact time of 0.50 ms was applied for all the experiments. Modulated (TPPM) decoupling was carried out at a nutation frequency of 76 kHz. Spectral referencing is with respect to external neat tetramethylsilane.

Chapter 3 Characterisation of the Samples

3.1 Introduction

Sedimentary organic matter and carbonaceous materials (including bitumen, kerogen, oil and coal) are products of geological transformation of terrestrial and marine biomass. Although the original biological composition is significantly altered through the transformation processes (i.e. diagenesis, catagenesis and metagenesis), the resulting substances may still contain 'fossilised' information that can be used to distinguish the substances based on their sources, depositional condition and environment as well as degree of transformation (Killops and Killops, 2005; Tissot and Welte, 1984). Consequently, over the years geochemical tools have been developed for characterisation of sedimentary organic matter (Peters et al., 2005a; Peters et al., 2005b; Hunt, 1995). This chapter describes a comprehensive use of these traditional organic geochemical tools to characterise the samples used in this work in order to provide foundation for discussion of the information obtained from the asphaltene presented in the subsequent chapters of the thesis.

3.2 Methodology

All the samples were characterised based on the chemical composition of the aliphatic and aromatic fractions of the oils and bitumen after precipitation of the asphaltenes (Section 2.3.3). The maltenes were fractionated into aliphatic hydrocarbon, aromatic hydrocarbon and resin fractions as described in Section 2.3.4. The fractions were analysed by GC and GC/MS (Section 2.4.4 and 2.4.5). Identification of compounds of interest was achieved using the mass spectra and relative retention times with the help of literature (Peters et al., 2005a).

In addition to visual examination of the chromatograms, various source, age and maturity related biomarker indices were computed using peak areas of the compounds from the relevant selected ion mass chromatogram as recommended by Peters *et al.* (2005a). Interpretation of the results obtained was based on established procedures as reported in the literature (Peters et al., 2005a). Furthermore, the multivariate statistical tools in Minitab[®] 15 Statistical Software (Minitab Inc.) platform were used to comprehensively analyse the multivariate data.

3.3 Results and Discussion

3.3.1 Black shale samples

(a) Bulk geochemistry

Table 3.1 summaries the elemental analysis and Rock-Eval pyrolysis results from the 48 samples from Tanezzuft black shales. The black shale is generally carbon rich with average total carbon of 21 wt % and a minimum of over 11 %. With TOC value of about 20 wt %, most of the total carbon is organic; the 'carbonate' carbon being only 0.80 ± 0.14 wt %. The observed maximum TOC value (25.26%) is about 34 % higher than the value reported by Aziz (2000) and Lünig *et al.* (2000) as the maximum in the concession NC115. Furthermore, with minimum value of about 8 wt % and mean value of 9.75 wt %, sulphur is relatively high. However,

compared to carbon and sulphur, nitrogen, with uniform value of about 1 wt %, is relatively low in these samples.

Table 3.1: Summary of bulk elemental analysis and Rock-Eval pyrolysis results of the Tanezzuft black shale sample ($n = 48$)*

	C (%)	N (%)	S (%)	TOC (wt %)	Tmax	S1	S2	HI	PI
Mean	20.49	0.81	9.75	19.70	432.0	9.69	47.81	243.0	0.17
Stdev	2.38	0.10	1.76	2.24	2.0	1.15	5.22	14.0	0.01
Max	26.94	1.07	17.48	25.26	439.0	13.39	62.18	276.0	0.19
Min	11.46	0.42	7.61	11.25	429.0	5.64	31.02	222.0	0.15

*C, N, S and TOC are in wt %; Tmax in °C; S1 and S2 in mgHC/gRock; and HI in mgHC/gTOC. Stdev = Standard deviation; Max = Maximum value; Min = Minimum value.

The Rock-Eval pyrolysis parameters are surprisingly low considering the high TOC values recorded (Table 3.1). This is clear from the relatively low hydrogen index (HI) values with maximum value of 276 mgHC/gTOC and average value of about 243 mgHC/gTOC. Moreover, with uniform values of about 0.2, the petroleum generation index (PI) is also low and agrees with the Tmax values, which show a maximum Tmax value of 439 °C and average value of 432 °C.

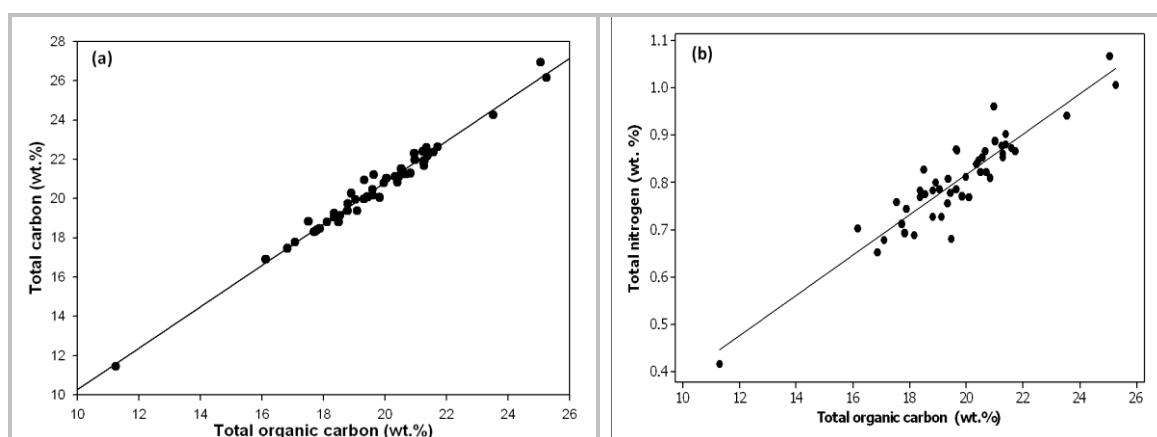
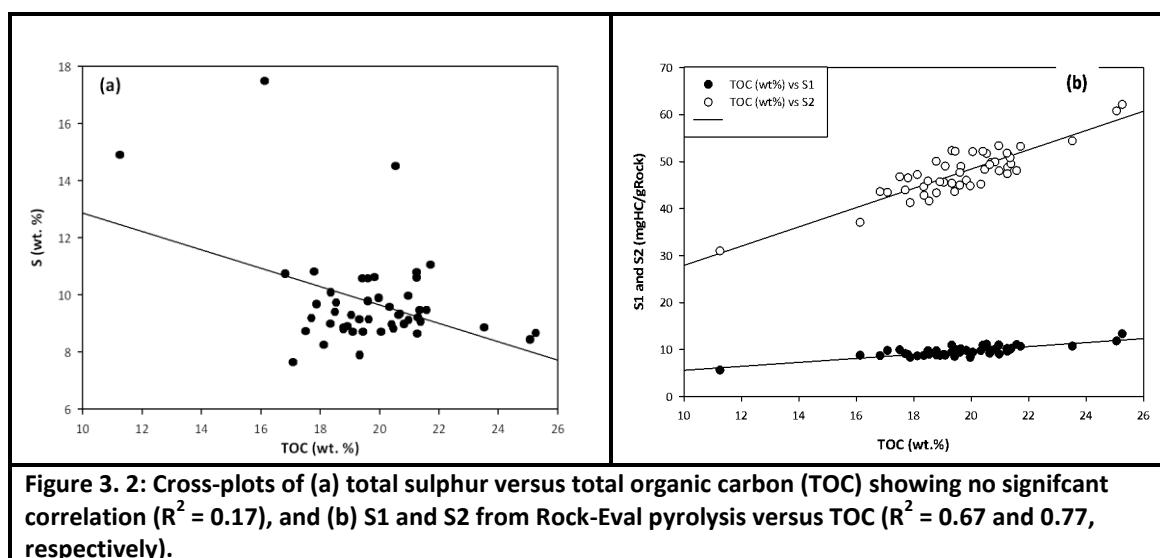
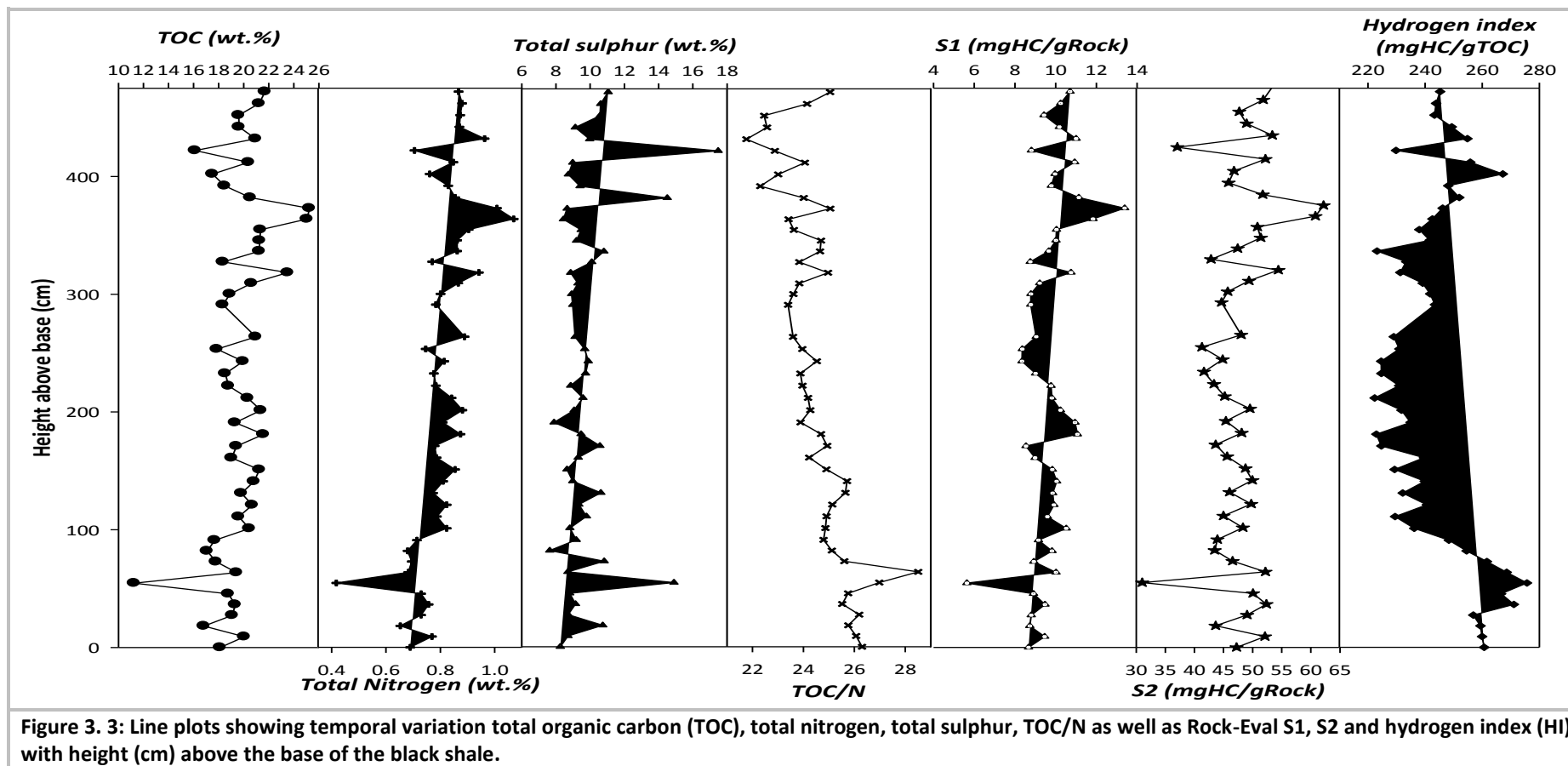


Figure 3. 1: Cross-plots of (a) total carbon versus total organic carbon (TOC) ($R^2 = 0.98$), and (b) total nitrogen versus TOC ($R^2 = 0.85$) showing positive correlation between the parameters.

The total carbon and nitrogen correlate with TOC (Figure 3.1). A similar relationship between TOC and total nitrogen was observed by Nara *et al.* (2005) in 23 ka old Lake Hovsgol sediments. The total sulphur versus TOC relationship, on the other hand, does not appear to correlate with TOC (Figure 3.2). This lack of relationship is common in both recent and ancient sediments (Hofmann *et al.*, 2000; Leventhal, 1995; Berner, 1984). Furthermore, both Rock-Eval pyrolysis S1 and S2 also positively correlate with TOC ($R^2 = 0.67$, $R^2 = 0.76$; $p < 0.05$) as shown in Figure 3.2.



Temporally, the total carbon, TOC and total nitrogen show similar variation and general increase up-section (Figure 3.3). It is interesting to note that although the total sulphur does not correlate with TOC (Figure 3.3), the three highest values of total sulphur correspond to minima and maxima of TOC (Figure 3.3). Furthermore, there is also a general increase in the total sulphur up-section although to a lesser extent compared to the TOC and total nitrogen. Conversely, the TOC/N ratio shows an even more pronounced general decrease up-section (Figure 3.3). Based on the observed temporal variation in the bulk geochemistry of the samples, sixteen samples were selected for molecular geochemical study and asphaltene compositional investigation by FTIR (Chapter 5). These samples represent the major spikes in TOC and sulphur and other intermediate samples.



(b) Molecular geochemistry

Results of molecular analysis of aliphatic and aromatic fractions of the selected 6 samples give further details on the geochemistry of the Tanezzuft 'hot' black shale. Figure 3.4 show a typical TIC of the aliphatic fractions. The chromatogram is dominated by *n*-alkanes (C₁₀ to C₃₃) with positively skewed (maxima between C₁₂ and C₁₇) unimodal distribution. Isoprenoids, particularly pristane (Pr) and phytane (Ph), are relatively low in all the samples.

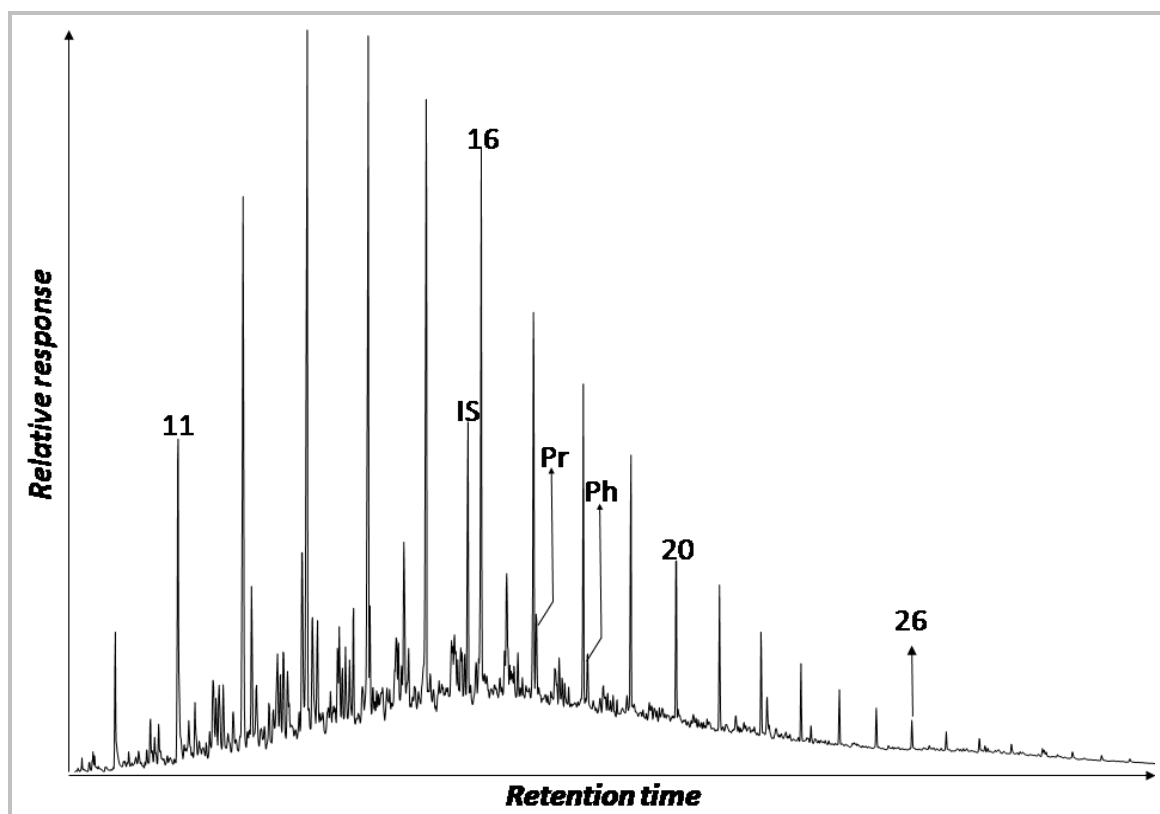


Figure 3. 4: TIC of the aliphatic fraction showing the *n*-alkane, the dominance of the C₁₂ to C₁₆ homologues and relatively small isoprenoids (integer = carbon number of the *n*-alkane, Pr = Pristane & Ph = Phytane).

Figure 3.5 shows a typical distribution of the cyclic terpanes from *m/z* 191 mass chromatogram of the aliphatic fraction. The distribution is dominated by the tricyclic terpanes (Figure 3.5 (a)) followed by the hopanes, Ts (i.e. C₂₇ 18 α (H)-22,29,30-trisnorneohopane), C₂₉ and C₃₀ hopanes. The 17 α (H),21 β (H) isomers are dominant over other isomers. The homohopanes are generally low and C₃₄ and C₃₅ homohopanes are only barely detectable in some samples. Sample T46 has barely detectable cyclic terpanes particularly the hopanes. Amongst the homohopanes, the 22S isomers are slightly dominant over their biological 22R counterparts (Figure 3.5 (b)). This terpane distribution is similar to that observed in the coeval Saudi Arabian Qusaiba Member which is the main source of Palaeozoic petroleum of the Central Province of Saudi Arabia (Cole et al., 1994).

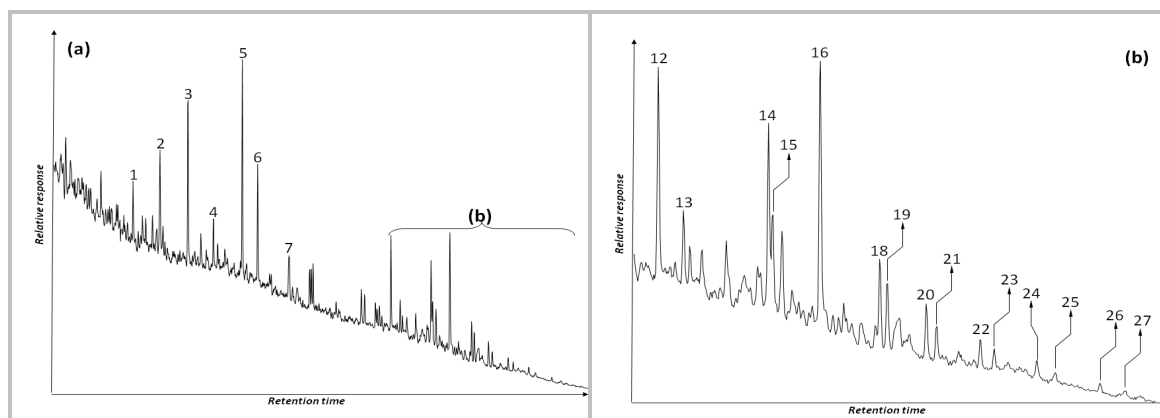


Figure 3. 5: m/z 191 mass chromatogram showing tricyclic, tetracyclic and pentacyclic terpenes in aliphatic fractions of Tanezzuft 'hot' shale bitumen. (See Appendix 6A for Assignment).

The m/z 217 mass chromatogram comprising the regular and rearranged steranes is dominated by the C_{21} 5(H) α ,14 β (H),17 β (H) (i.e. pregnane) and C_{22} 5(H) α ,14 β (H),17 β (H) (i.e. homopregnane) isomers (Figure 3.6 (a)). The C_{29} sterane is the dominant homologue (albeit slightly over C_{27}) amongst the C_{27} to C_{29} extended steranes. The rearranged diasteranes are also abundant and dominated by the 13 β (H),17 α (H) isomers. There is a general slight dominance of the 20S epimer over the biological 20R amongst the C_{27} to C_{29} homologues (Figure 3.6). The C_{28}/C_{29} steranes ratio with average value of 0.45 (Appendix 3A) being less than 0.5 is in agreement with Lower Palaeozoic source rocks (Grantham and Wakefield, 1988). The steranes are in general proportionally greater than the hopanes as illustrated by sterane/hopane ratio being in the range of 1.5 to 4.0 (Appendix 3A).

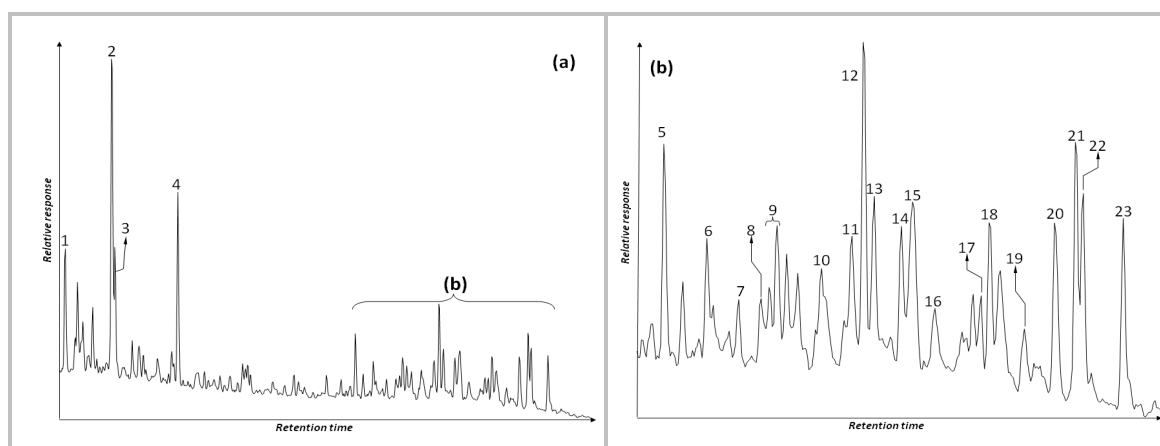


Figure 3. 6: A typical m/z 217 mass chromatogram showing typical distribution of the steranes in aliphatic fractions of Tanezzuft 'hot' shale bitumen. (See Appendix 6B for Assignment)

(c) Thermal maturity

Maturity is the extent of thermal transformation of sedimentary organic matter. It is estimated using optical, Rock-Eval and molecular tools (Hunt, 1995; Peters, 1986; Tissot and Welte, 1984). The shales' average Tmax and PI values of 435 °C and 0.10 respectively indicate the organic matter is in the early maturity stage (Peters, 1986). This is supported by the unimodal distribution of the *n*-alkanes (Figure 3.4) and distributions of the steranes and hopanes (Figures 3.5 and 3.6) as well as the molecular maturity parameters (Appendix 3B). Both

average values of 20S/(20S+20R) sterane and 22S/(22S+22R) homohopane ratios (0.51 and 0.54 respectively, Appendix 3B), are below the respective equilibrium values of 0.55 and 0.60 which are established at the early maturity stage (Seifert and Moldowan, 1986). Furthermore, the CPI values being generally greater than 1 (Appendix 3A) indicate the early maturity of the shales (Peters et al., 2005a; Bray and Evans, 1961). Although the aromatic methylphenanthrene (MPI), the associated calculated vitrinite reflectance (R_c) and PP-1 values (Appendix 3B) may suggest higher maturity, this is possibly an over estimation similar to observations of Radke *et al.* (1982) and Cassani *et al.* (1988) that the distribution of these compounds is often affected by migration and lithology.

(d) *Depositional condition and environment*

Anoxia is a condition of zero (or low) oxygen that develops following water stratification and depletion, without replacement, of dissolved oxygen due to aerobic oxidation of biomass. It is characterised by fine lamination of sediment, due to absence of benthic feeders, and pyrite framboids formed from reaction of hydrogen sulphide with reactive iron (Wignall, 1994). The Tanezzuft black shales have all these characteristics indicating deposition under stratified anoxic water column. This probably explains the relatively high amounts of sulphur observed in the shales (Table 3.1) and is supported by the anomalously high TOC/N ratio.

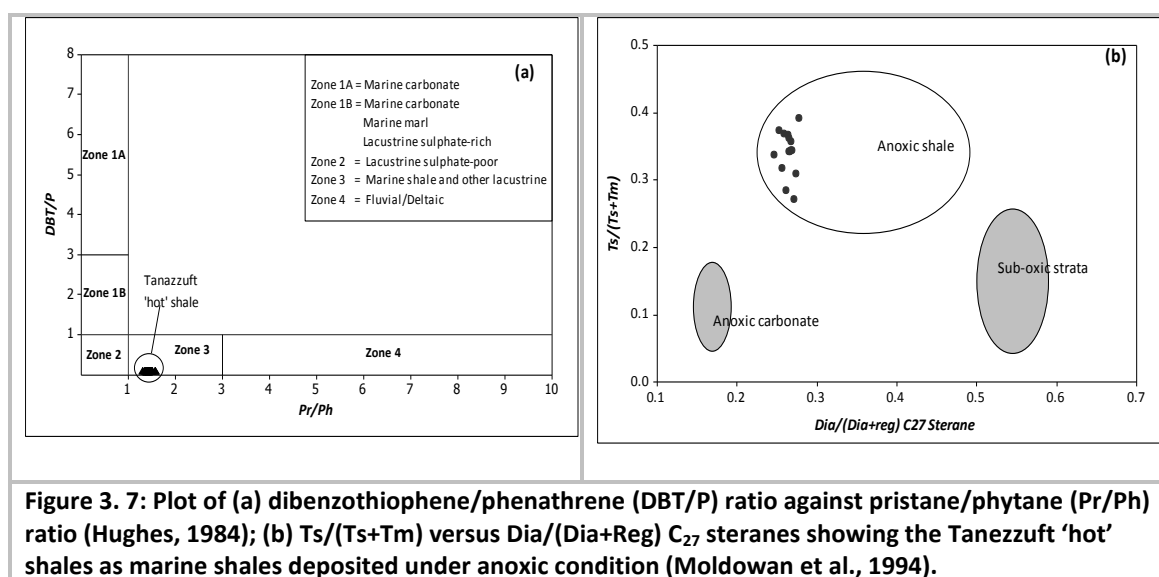


Figure 3. 7: Plot of (a) dibenzothiophene/phenanthrene (DBT/P) ratio against pristane/phytane (Pr/Ph) ratio (Hughes, 1984); (b) Ts/(Ts+Tm) versus Dia/(Dia+Reg) C₂₇ steranes showing the Tanezzuft 'hot' shales as marine shales deposited under anoxic condition (Moldowan et al., 1994).

Although it has been observed that sediments deposited under oxic condition show S/TOC ratio of about 0.40 while values greater than 0.40 with positive intercept of the sulphur-axis is characteristic of deposition in anoxic condition, sometimes anoxic sediments display an independent relationship between sulphur and TOC (Dean and Arthur, 1989; Berner, 1984). This situation has been observed in both recent (e.g. Black Sea (Berner and Raiswell, 1983) and ancient (e.g. Cretaceous, (Dean and Arthur, 1989)) sediments. It occurs when pyrite formation is limited by availability of detrital reactive iron minerals; a situation found in distal settings where the sediment is mainly calcareous (Berner, 1984) or when sulphate reduction overwhelms the reactive iron supply. This was possibly the situation during deposition of the Tanezzuft basal 'hot' shales. As shown in Figure 3.2 there is no correlation between the sulphur and TOC (*cf.* Leventhal, (1995) and Hofmann *et al.*, (2000)) indicating the sediments were

deposited in anoxic condition in which reactive iron was limited or overwhelmed. This is further supported by molecular data.

The position of the samples in Figure 3.7 (a) and (b) is consistent with marine shales deposited in anoxic depositional setting (Moldowan et al., 1994; Hughes, 1984). Furthermore, Moldowan et al. (1994) have shown, using data from marginally mature Toarcian source rocks, that the relative position of samples on Pr/(Pr+Ph) versus C₂₇ Dia/(Dia+Reg) steranes can be used to discriminate among anoxic carbonates, anoxic shales and suboxic strata. Figure 3.8 (b) is a similar plot for samples analysed in this work and the position of the samples clearly corresponds to anoxic shales as shown by other proxies discussed above.

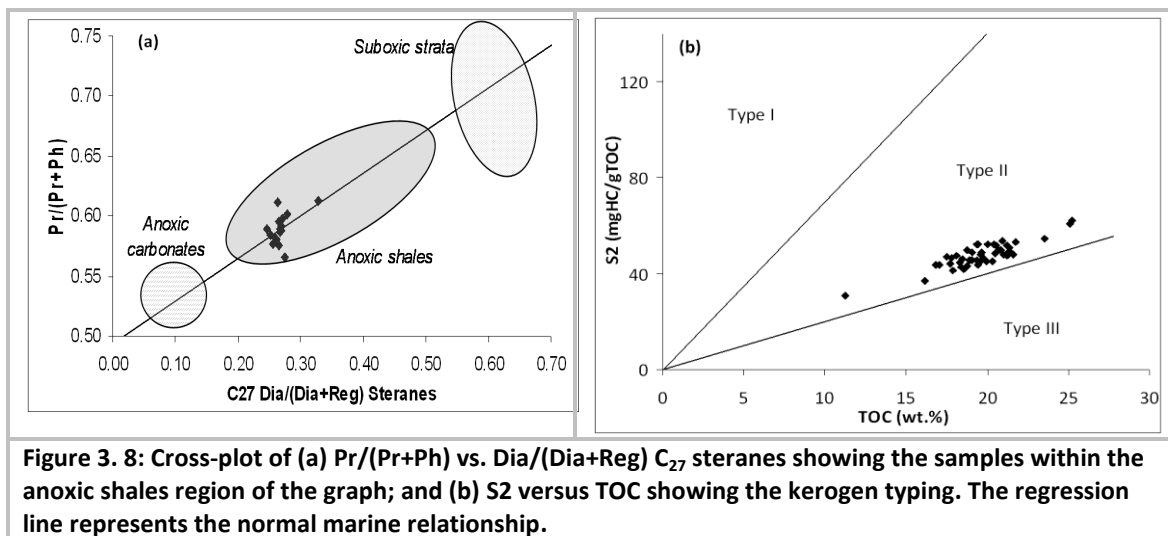


Figure 3. 8: Cross-plot of (a) Pr/(Pr+Ph) vs. Dia/(Dia+Reg) C₂₇ steranes showing the samples within the anoxic shales region of the graph; and (b) S₂ versus TOC showing the kerogen typing. The regression line represents the normal marine relationship.

(e) Nature of the organic matter

Although the type and source of organic matter in black shales or sedimentary rock has been traditionally studied by direct examination under microscope, other geochemical proxies that adequately give this information have been developed. For example, hydrogen index (HI) is commonly used to interrogate the nature of sedimentary organic matter (Peters, 1986). Accordingly, the Type II/III kerogen, observed in this 'hot' black shale (Figure 3.8 (b)), is often interpreted as a mixture of Type II, predominantly phytoplankton-based organic matter, and Type III, fairly oxidised marine organic matter and/or land plant-derived organic matter, kerogens (Hunt, 1995; Langford and Blanc-Valleron, 1990). Neither of these is however acceptable considering that: (1) land plant did not evolve until Devonian (Gray, 1993); (2) as discussed in Section 3.3.1 (d), the sediments were deposited under anoxic condition which provided good condition for preservation of the organic matter.

Furthermore, although bacterial reworking of the original phytoplankton organic matter using sulphates and nitrates as electron sink may lead to the observed low HI, this was unlikely to be the case. The very low presence of hopanes, as proxies of bacterial contribution, as shown in both absolute concentrations and sterane/hopane ratios, suggests a bacterial contribution was minimal.

Tanezzuft black shale has been observed to be particularly rich in graptolites (Aziz, 2000) which have been observed to be abundant in these samples (Section 2.2.1). Graptolite has been shown to consist mainly of aromatic structure (in fact more aromatic than vitrinite) with aliphatic groups (Bustin et al., 1989). This graptolite-rich organic matter type is likely to be responsible for the unusually low hydrogen index in these samples.

3.3.2 Coal samples

(a) Bulk geochemistry

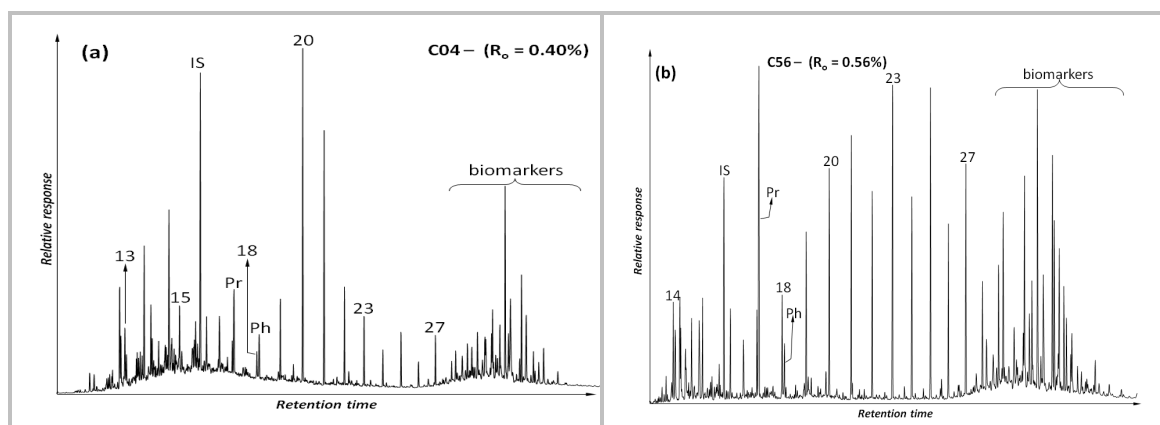
Table 3.2 show results from bulk characterisation of the four samples studied in this work. The elemental compositions show that the total carbon content increases with maturity of the coal. Similarly the Tmax increases from C04 to C15 in agreement with vitrinite reflectance.

Table 3. 2: Bulk geochemical parameters of the coal samples

Sample	Ro	C (%)	H (%)	N (%)	S (%)	S1	S2	Tmax (°C)	HI
C04	0.40	24.85	1.74	0.38	2.55	7.7	38.8	424	156
C56	0.56	48.58	3.25	0.96	3.90	8.0	70.3	434	145
C69	0.69	76.88	6.06	1.71	2.65	20.3	157.0	440	204
C15	1.50	82.38	4.55	1.64	3.91	3.2	111.3	459	135

(b) Molecular geochemistry

The molecular characterisation of the aliphatic fraction of the coal bitumens reveals that the saturated hydrocarbon composition is dominated by *n*-alkanes, isoprenoids and cyclic biomarkers (Figure 3.9).



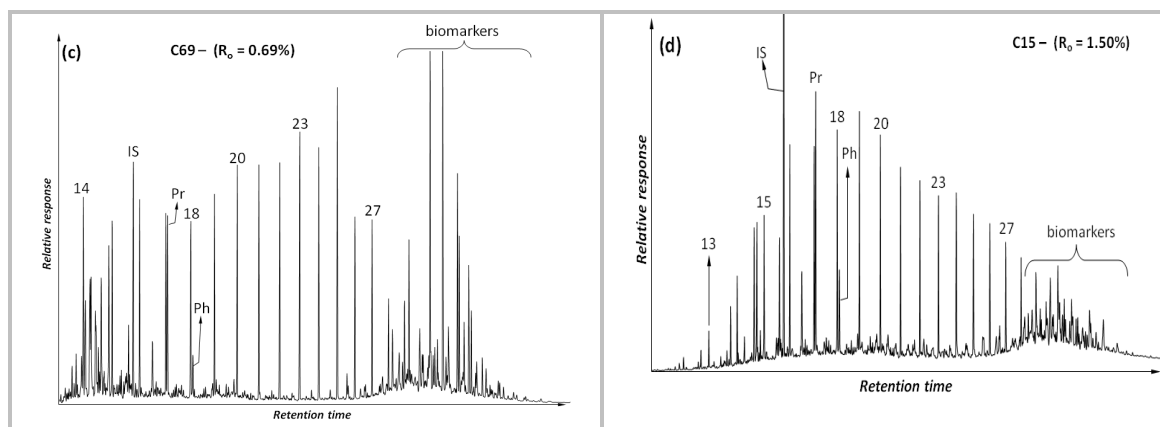


Figure 3. 9: TIC of aliphatic fractions of the coal bitumens showing differences and similarities in distribution of the dominant hydrocarbons. The integers represent the carbon numbers of the *n*-alkanes, Pr = pristane, Ph = phytane, and IS = internal standard.

There are however differences amongst the coals in the distribution of the dominant compounds. C04 has a pronounced bimodal distribution with dominance of C₂₀ and C₂₁ homologues (Figure 3.9) and C15 has a unimodal distribution with dominance of the C₁₆ to C₂₀ homologues. C56 and C69, on the other hand, show distributions somewhat intermediate between C04 and C15 although C56 has a more pronounced dominance of *n*-alkanes with odd carbon number between C₂₀ to C₂₈ compared to C69.

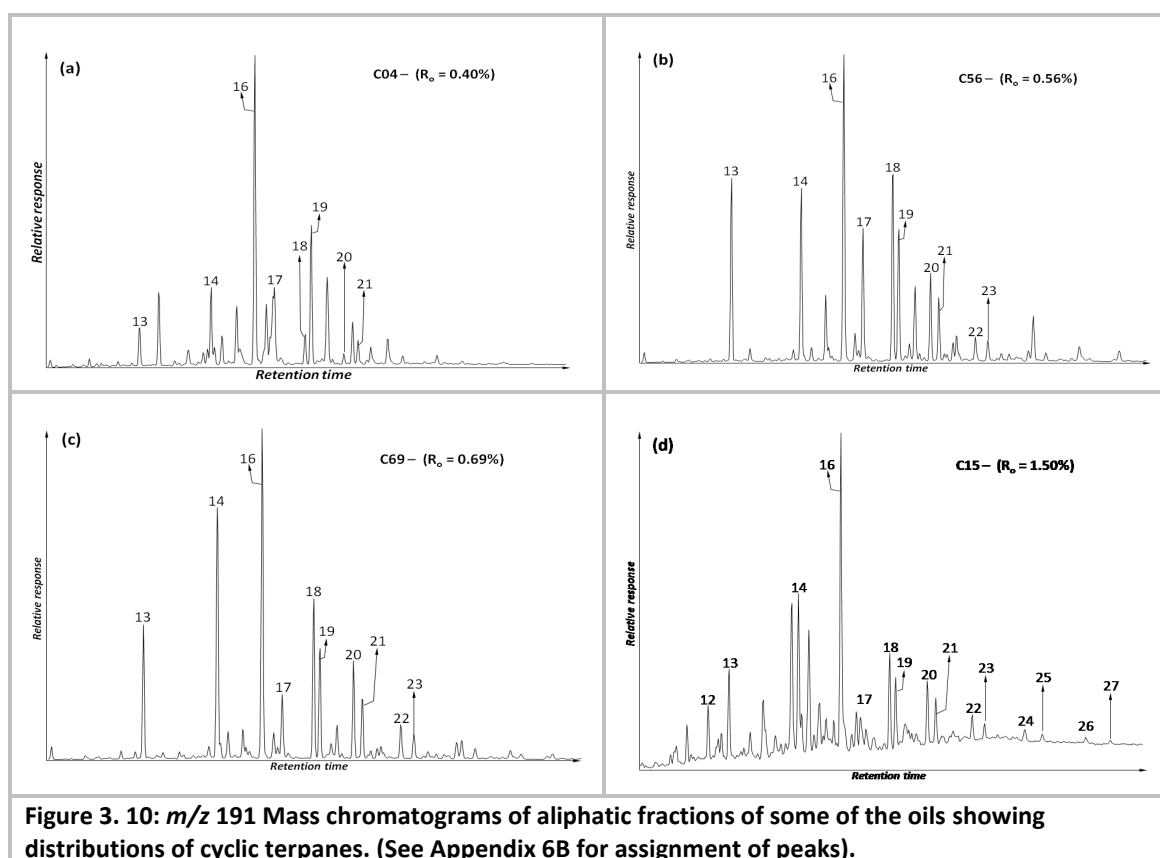
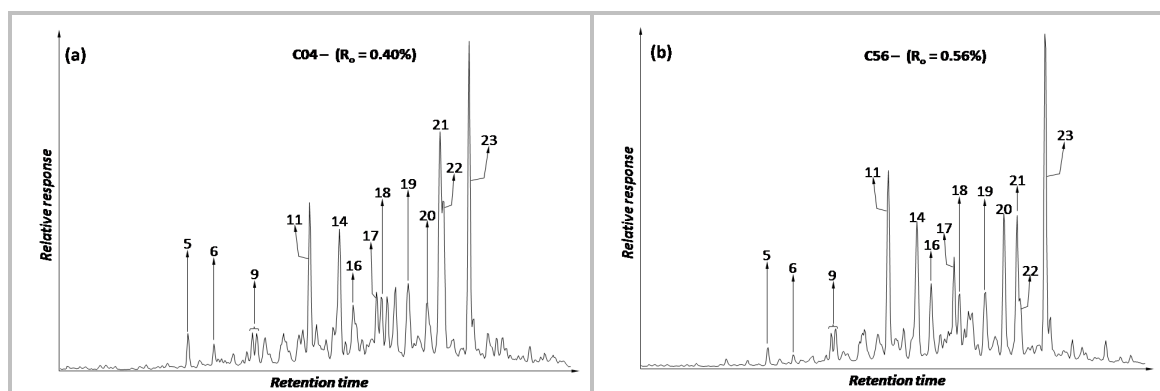


Figure 3.10 shows the distribution of the terpanes in the four coal samples. The tricyclanes and tetracyclanes are generally very low except in C15. Ts (C_{27} 18 α (H)-22,29,30-trisnorneohopane) is significantly present in C15 and barely detectable in other coals. Tm (C_{27} 17 α (H)-22,29,30-trisnorhopane), on the other hand, although present in all the samples, is relatively more pronounced in C56 and C69. The hopanes are dominated by the C_{29} and C_{30} homologues and 17 α (H),21 β (H) isomers. Homologues up to C_{35} were however detected in all the samples and particularly in C15. The 17 β (H),21 α (H) isomers are significantly present in C04 and C56. Amongst the homohopanes, the 22S epimers are greater than the corresponding 22R except in C04 where the opposite is the case.



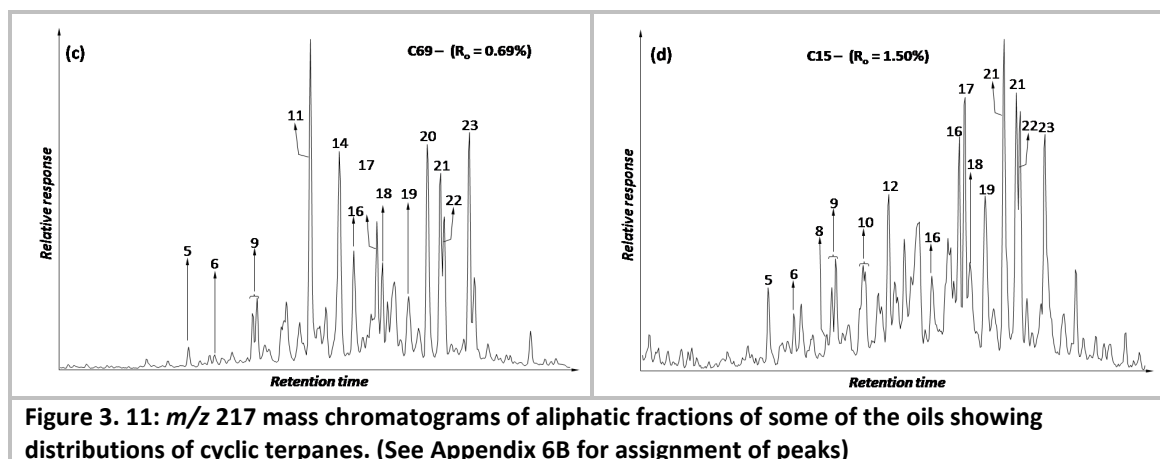


Figure 3. 11: m/z 217 mass chromatograms of aliphatic fractions of some of the oils showing distributions of cyclic terpanes. (See Appendix 6B for assignment of peaks)

The sterane distribution consisting of the C_{27} to C_{29} homologues is shown in Figure 3.11. The 24-ethylcholestanes (C_{29} homologues) are the dominant homologues, constituting of up to 60% in three of the sample and about 47% in C15. The cholestanes (C_{27} homologues) are the next most abundant except in C15 where 24-methylcholestanes (C_{28} homologues) are second dominant steranes. The diasteranes are relatively high in all the samples and are dominated by the $13\beta(H),17\alpha(H)$ isomers.

(c) Thermal maturity

The four coal samples have different maturities as shown by their respective vitrinite reflectance (Table 3.3); the maturity increases in the order $C15 > C69 > C56 > C04$. This is substantiated by both elemental data and Rock-Eval-based maturity parameter T_{max} (Peters, 1986) as shown in Table 3.3. The relative carbon content of the coals increase with R_o and there is a good positive correlation between R_o and T_{max} ($R^2 = 0.95$, $p < 0.05$). Molecular maturity parameters further support these results.

The $T_s/(T_s+T_m)$ ratio, although affected by organic matter source (Moldowan et al., 1986), may also reflect level of maturity (Peters et al., 2005a). It is low in the three less mature samples and up to 0.35 for the most mature C15. The $\beta\alpha/\alpha\beta$ ratio also shows progressive decrease with maturity from C04 to C69 in accord with conversion of the less stable $17\beta(H),21\alpha(H)$ isomer to the more stable $17\alpha(H),21\beta(H)$ isomer (Seifert and Moldowan, 1980). The index is however partly source and depositional environment dependent (Peters et al., 2005a) which may explain why C15 has an usually high value relative to other samples despite being the most matured (Table 3.3).

Table 3. 3: Some molecular maturity parameters calculated from the compounds and biomarkers in aliphatic fractions of the coals

Sample	R_o	CPI	CPI1	OEP1	OEP2	$T_s/(T_s+T_m)$	$\beta\alpha/\alpha\beta-C_{29}$	$22S/(S+R)-C_{31}$	$22S/(S+R)-C_{32}$	$20S/(S+R)-C_{29}$
C04	0.40	2.49	1.61	1.39	2.15	0.10	0.83	0.19	0.20	0.18
C56	0.56	2.22	1.76	1.69	1.69	0.02	0.39	0.60	0.58	0.33
C69	0.69	1.80	1.31	1.18	1.31	0.06	0.11	0.59	0.60	0.52

C15	1.50	1.22	0.96	0.90	1.07	0.36	0.38	0.57	0.59	0.57
-----	------	------	------	------	------	------	------	------	------	------

The homohopane-based 22S/(22S+22R) maturity proxy (Table 3.3) indicates that the 22R↔22S isomerisation equilibrium (0.57 to 0.62, (Seifert and Moldowan, 1980)) has been established in the three most mature coal samples. This is shown in Figure 3.12(a) in agreement with the fact that such equilibrium has been observed to be attained at $R_o = 0.6\%$ and sometimes slightly less (Zumberge, 1987). The slight difference between the C_{31} - and C_{32} -based %22S values is not unusual as it has been previously observed (Zumberge, 1987). The maturity difference amongst the coals is however more clearly shown by sterane-based 20S/(20S+20R) from 5 α (H),14 α (H),17 α (H) ethylcholestanes (C_{29}), the value of which increases with R_o as illustrated in Figure 3.12(a). The order shows gradual increase in the value with R_o until it levels out at about 0.55; equilibrium value is established at about 0.52 to 0.55 (Moldowan et al., 1986).

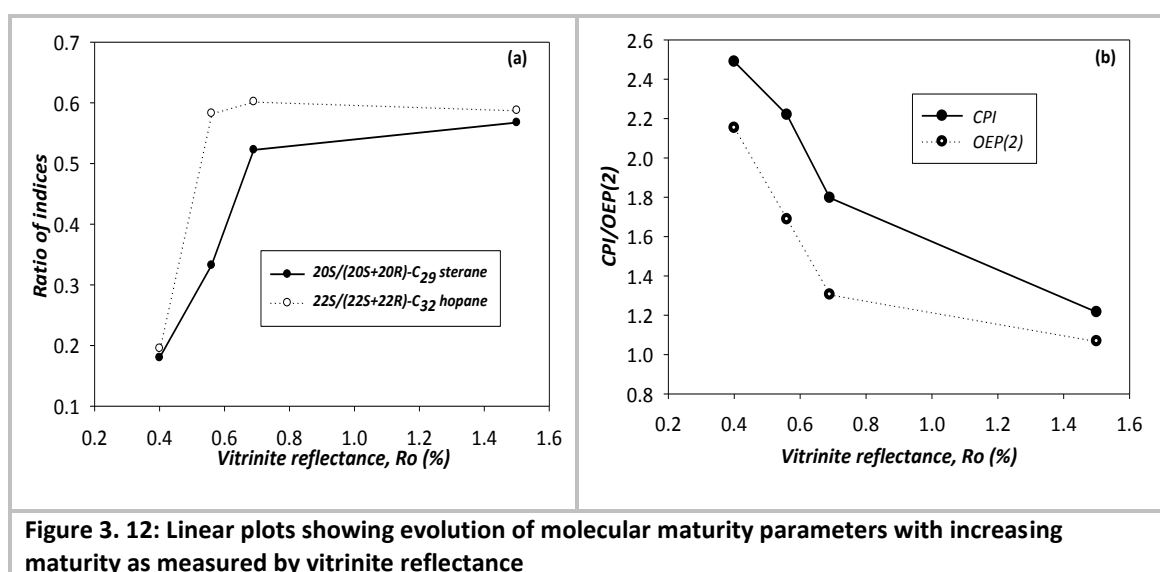


Figure 3. 12: Linear plots showing evolution of molecular maturity parameters with increasing maturity as measured by vitrinite reflectance

The progressive maturation of the coal samples is further reflected in the evolution of other maturity-dependent parameters. For example, both CPI and OEP, which measure the odd to even carbon ratio of the n -alkanes, fall towards equilibrium value of 1 with increasing maturity (Figure 3.12(b)) in agreement with observations of Bray and Evans (1961) and Scalan and Smith (1970). The slight disparity between CPI and OEP2 versus CPI1 and OEP1 might be because the former applies to higher molecular weight homologues compared to the later parameters. This suggests the former indices might be more suitable for assessment of relative odd to even carbon predominance in coals.

(d) *Source and depositional environment*

The relatively high Pr/Ph ratio (Table 3.4) is indicative of terrigenous organic matter under oxic depositional environment (Peters et al., 2005a; Didyk et al., 1978). The difference in the values of the parameter among the samples further suggest different source for the four coals. This is further reflected in Pr/ C_{17} ratio and Ph/ C_{18} although both are influenced by with maturity. The CPI being significantly greater than 1, although also influenced by maturity, indicates land plant organic particularly for the samples with low maturity. The dominance of ethylcholestane (C_{29} sterane) further support the high plant organic matter source as is the case for coals.

Table 3.4: Results of some molecular source parameters computed from biomarkers in aliphatic fractions of the coal bitumens.

Sample	Pr/Ph	Pr/C ₁₇	Ph/C ₁₈	C ₂₉ /C ₃₀ αβ	Ts/(Ts+C ₂₉ αβ)	C ₃₁ R/C ₃₀ αβ	Dia/(Dia+Reg)C ₂₇	C ₂₇ /(C ₂₇ +C ₂₈ +C ₂₉)	C ₂₈ /(C ₂₇ +C ₂₈ +C ₂₉)	C ₂₉ /(C ₂₇ +C ₂₈ +C ₂₉)
C04	1.97	3.68	2.33	0.23	0.19	0.44	0.46	0.15	0.17	0.68
C56	7.57	5.63	0.64	0.52	0.02	0.42	0.44	0.22	0.16	0.62
C69	4.83	1.30	0.26	0.80	0.04	0.33	ND	0.16	0.17	0.67
C15	2.92	1.53	0.50	0.46	0.50	0.21	0.46	0.13	0.41	0.46

Furthermore, the relative distribution of the sterane homologues (Table 3.4) indicates that the three less mature samples were sourced from similar organic matter which is obviously different from that of C15 as illustrated by the relative positions of the samples in ternary diagram (Figure 3.13). Although $C_{31}R/C_{30} > 0.25$ is said to indicate marine depositional environment (Peters et al., 2005a), the ratio is obviously influenced by maturity and therefore decreases as 22R stereomer isomerises to 22S as clearly shown in Figure 3.15 ($R^2 = 0.95$, $p < 0.05$).

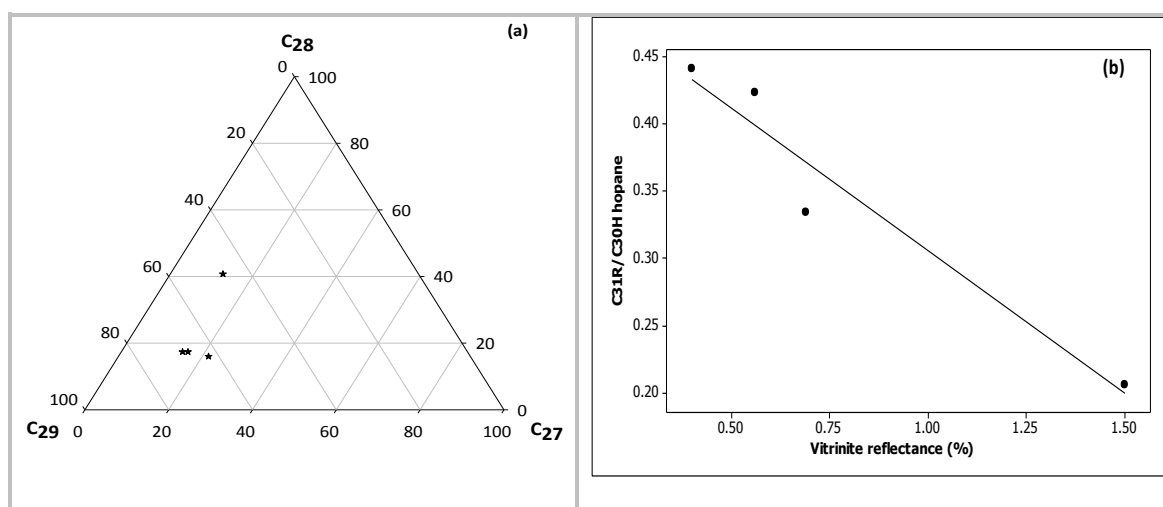


Figure 3. 13: (a) Ternary diagram showing the respective position of the four coal samples with respect to relative proportions of the cholestane (C₂₇), methylcholestane (C₂₈) and ethylcholestane (C₂₉); (b) Scatter plot showing influence of maturity on C₃₁R/C₃₀ ratio ($R^2=0.94$)

The relatively high proportion of diasteranes relative to regular steranes as depicted by Dia/(Dia+Reg) ratio (Table 3.6) suggests prevalence of clay minerals (Sieskind et al., 1979; Rubinstein et al., 1975) and/or acidic and oxic condition (Brincat and Abbott, 2001; Moldowan et al., 1986), necessary for conversion of the regular steranes to diasteranes, in the depositional environment.

3.3.3 Oil samples

(a) *Molecular geochemistry*

Examination of the TICs from the analysis of the aliphatic hydrocarbon fractions reveals that the dominant chemical compounds in all the non-biodegraded oils are the *n*-alkanes ranging from C₁₀ to C₃₆₊ homologues with positively skewed unimodal distribution and maxima around C₁₄ to C₁₆ homologues (Figure 3.14). An exception is sample NA2 from Serbia that shows nearly equal proportion of *n*-alkanes from C₁₃ to C₃₀. The isoprenoids are also present albeit in different proportions; abundant in some of the oils and relatively low in others as depicted in Pr/C₁₇ and Ph/C₁₈ ratios (Appendix 3C). There seems to be slight dominance of odd carbon *n*-alkanes over even carbon members in the carbon range from C₂₅ to C₃₄ which disappears in C₂₃ to C₃₀ as depicted by CPI and CPI(1) (see also OEP values) respectively (Appendix 3C). The terrigenous/aquatic ratio (TAR) is very low indicating the dominance of the lower homologues (C₁₅ to C₁₉) over the high molecular weight members (C₂₇ to C₃₁).

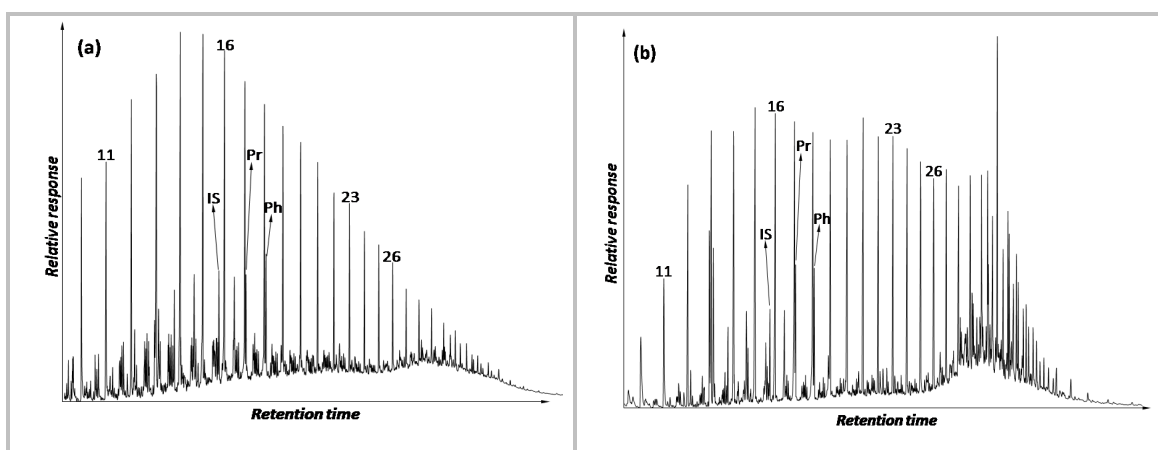
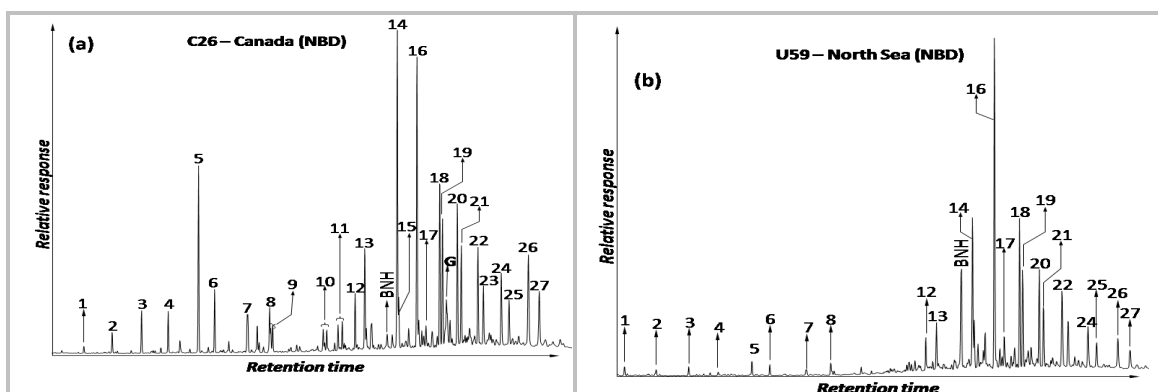
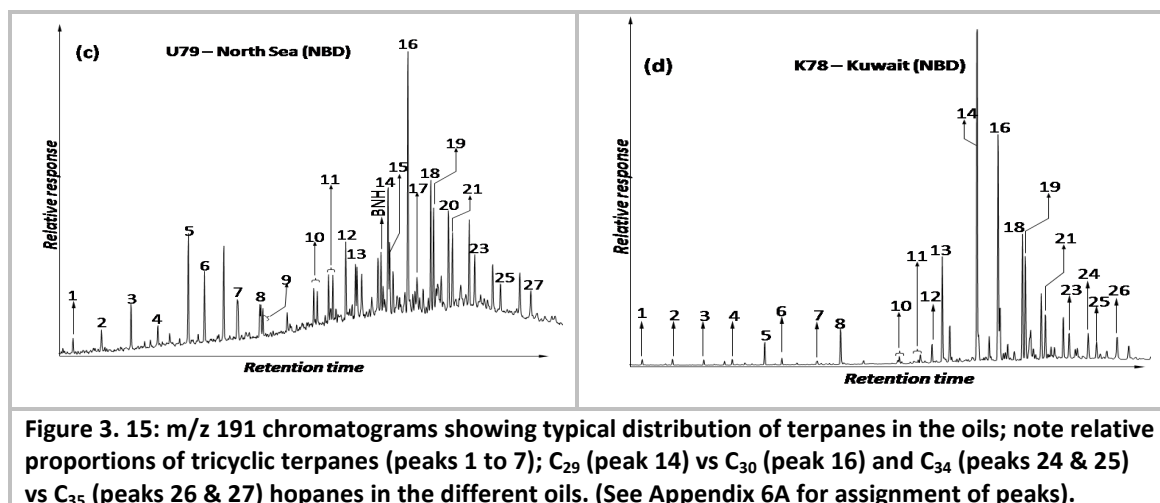


Figure 3. 14: TIC showing (a) typical distribution of *n*-alkanes and isoprenoids in most of the non-biodegraded oils, (b) an unusual distribution of the compounds in a non-biodegraded Serbian oil (NA2).

On the other hand, major cyclic compounds identified in the aliphatic hydrocarbon fractions of the oils are the terpanes and steranes. The terpanes, consisting of tricyclic, tetracyclic and pentacyclic terpanes are present in variable proportions in different oil samples. The tricyclic terpanes range for C₁₉ to C₂₉ with 13β(H),14α(H) configuration and 22S and 22R doublets for C₂₅ to C₂₉ homologues. However, only C₂₄ tetracyclic terpane was identified. Most of the samples (about 60%) have relatively high proportion of the tricyclic and tetracyclic terpanes with no clear separation amongst the sample with respect to geography or age. However, in almost all samples, except in A39, the C₂₃ homologue is the major tricyclic terpane followed by C₂₄ (Figure 3.15)

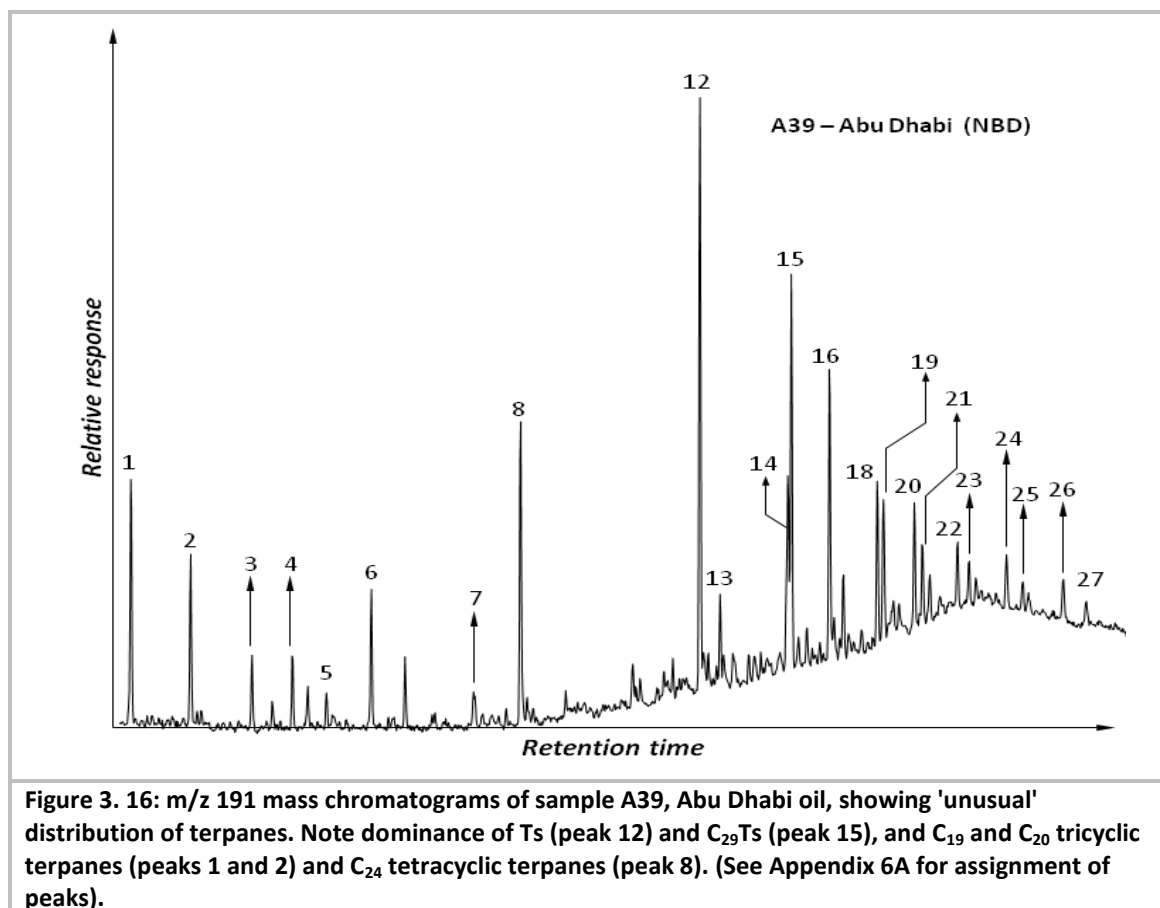




The pentacyclic terpanes are the most abundant of the terpanes in all the oils. Homologues identified range from C₂₇ to C₃₅ in two stereomeric configurations although 17 α (H),21 β (H) isomers are the dominant isomers with 17 β (H),21 α (H) isomers occurring in relatively small proportions; measurable only with respect to C₂₉ and C₃₀ homologues. Only two isomers of C₂₇ and one of C₂₈ pentacyclic terpanes were identified namely: 18 α (H)-22,29,30-trisnorhopane (Ts), 17 α (H)-22,29,30-trisnorhopane (Tm), and 17 α (H),21 β (H)-28,30-bisnorhopane (BNH). The later however has been observed to co-elute with its 17 β (H),21 β (H) isomer in most analytical conditions (Moldowan et al., 1984). The BNH was observed in Northsea oils, the two oils from Canada (C26 and C30) and one Gulf of Mexico oil (PR1) albeit in different relative abundance even amongst the Northsea oils as reflected in BNH/(BNH+C₃₀) ratio (Appendix 3C).

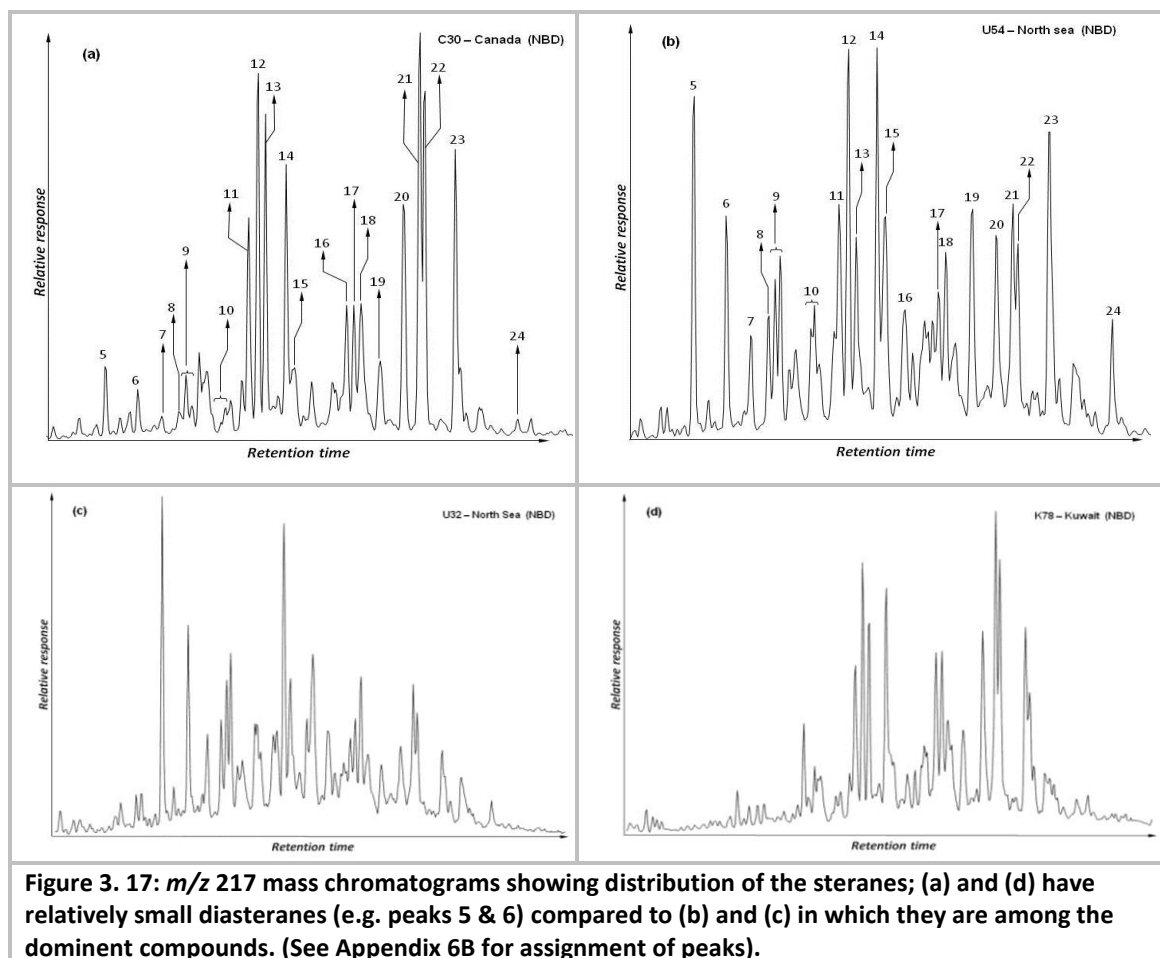
In almost all the oils, except A39 from Abu Dhabi (Figure 3.16), C₂₉ 17 α (H),21 β (H) and C₃₀ 17 α (H),21 β (H) are the most abundant homologues amongst the terpanes. The relative proportions of the two homologues vary amongst the samples. In most of the samples C₃₀ is dominant over C₂₉ (e.g. the Northsea oils). The two homologues are nearly equal in the oils from Canada and Qatar (Figure 3.15), and C₂₉ is clearly dominant over C₃₀ in the two Kuwait oils as reflected in values of C₂₉/C₃₀ ratio (Appendix 3C). Furthermore, the C₃₁ to C₃₅ pentacyclic terpanes (i.e. the homohopanes), each consisting of the 22S and 22R epimers, are dominated by the C₃₁ homologues. The relative proportion of the homohopanes gradually decrease with increasing carbon number except in some samples (e.g. K77, C26 and U01) in which C₃₅ is equal to or greater than the C₃₄ homologue as revealed by values of C₃₅/C₃₄ ratio of the oils (Appendix 3C). In addition to the terpanes, the m/z 191 mass chromatograms of the oils from Serbia (NA1 and NA2) and Canada (C26 and C30) show the presence of gammacerane (Figure 3.15).

The Abu Dhabi oil (Sample A39) is unusual (compared to the other oils), with respect to distribution of the tricyclic, tetracyclic and pentacyclic terpanes (Figure 3.16). The distribution of the terpanes in this oil is dominated by Ts followed by C₂₉Ts. Furthermore, unlike other oils where C₁₉ tricyclic terpane occur in small amounts compared to other tricyclics, in A39 it is the dominant tricyclic terpane, followed by the C₂₀ homologue. In addition, C₂₄ tetracyclic terpanes is also unusually abundant (compared to other oils) - being the third most abundant amongst the tricyclic and tetracyclic terpanes.



Steranes ranging from C₂₇ to C₂₉ were also identified in all the oils samples (Figure 3.17). In addition, C₂₁ and C₂₂ steranes are also present in all the oils, and C₃₀ sterane in the Northsea oils (Figure 3.17). The C₂₁ and C₂₂ steranes consist of 5 α (H),14 β (H),17 β (H) isomers. The C₂₇ to C₂₉ homologues broadly consists of the regular steranes and the diasteranes. The diasteranes are generally dominated by 13 β (H),17 α (H) isomers although the 13 α (H),17 β (H) isomers are also present. Each stereomer has 20S and 20R epimer. In general, the proportion of the diasteranes relative to the regular steranes varies with sample. Nevertheless, in the Northsea oils, the C₂₇ diasteranes are the dominant steranes (over 60%) as shown in Dia/(Dia+Reg) sterane ratio (Appendix 3C). Conversely, low proportions of the diasteranes were observed in Canadian oils (C26 and C30), Oman oils (O28 and O31) and particularly in the two Kuwait oils (K77 and K78).

As for the diasteranes, the C₂₇ to C₂₉ regular steranes occur in variable proportion amongst the oils. In almost all the oils, however, the dominant homologue, albeit slightly, is either C₂₇ or C₂₉ a (Appendix 3C). The Oman oils (O28 and O31) however have nearly equal proportions of all the homologues. The homologues consists of the two main isomers observed in oils namely; 5 α (H),14 β (H),17 β (H) and 5 α (H),14 α (H),17 α (H) consisting of the biological R and the geological S epimers due to configuration at C20 position. In most samples the geoisomers 5 α (H),14 β (H),17 β (H) are slightly dominant over their biological 5 α (H),14 α (H),17 α (H) counterparts as depicted by $\beta\beta/(\beta\beta+\alpha\alpha)$ ratio (Table 3.5). 5 α (H),14 α (H),17 α (H) 20R propylcholestane was also tentatively identified in the Northsea oils (Figure 3.17).



(b) Biodegradation

Biodegradation is the microbial alteration of petroleum composition that often happens when hydrocarbons are exposed to microbes (mainly bacteria) under the correct condition. In general, biodegradation of petroleum shows selectivity with respect to different compounds; thus, petroleum compounds are eliminated at different rates. Consequently, the extent of biodegradation of petroleum can be estimated by examination of the pattern of removal of the composite compounds (Peters et al., 2005a).

About six of the oils used in this study are variably biodegraded. Figure 3.18 contains the TIC of these oils. Two of these oils (BN and U16) are from the Northsea, one each from Canada (CH), Serbia (NA1), Gulf of Mexico (AR3) and Nigeria (NB). In general, the n -alkanes are completely removed in all these oils. The isoprenoids are intact in AR3 and partially removed in BN and, to even greater extent, in CH. The compounds are completely removed in U16, NA1 and NB. Terpanes and steranes are generally unaffected in all the samples except NA1 and NB.

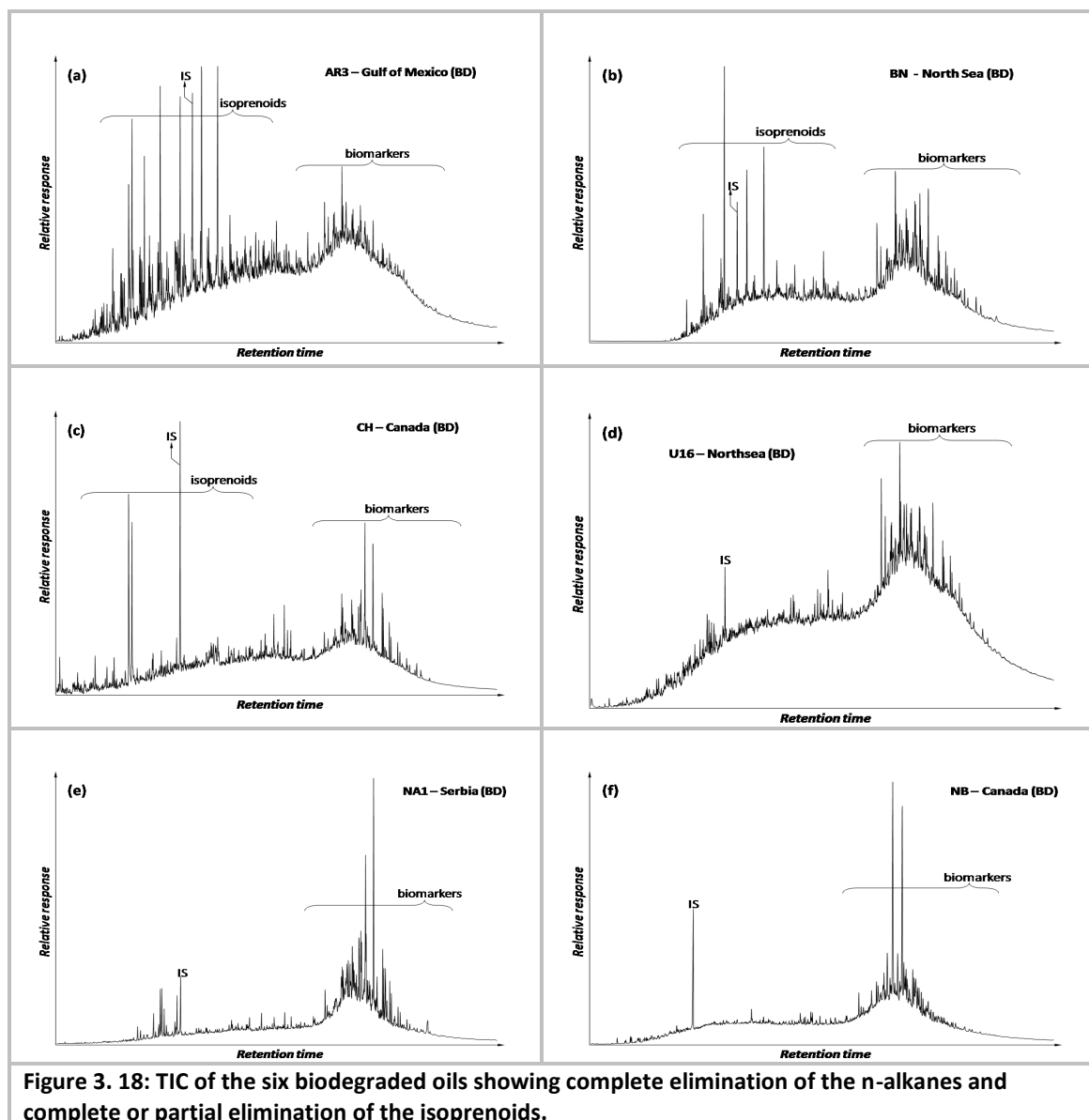
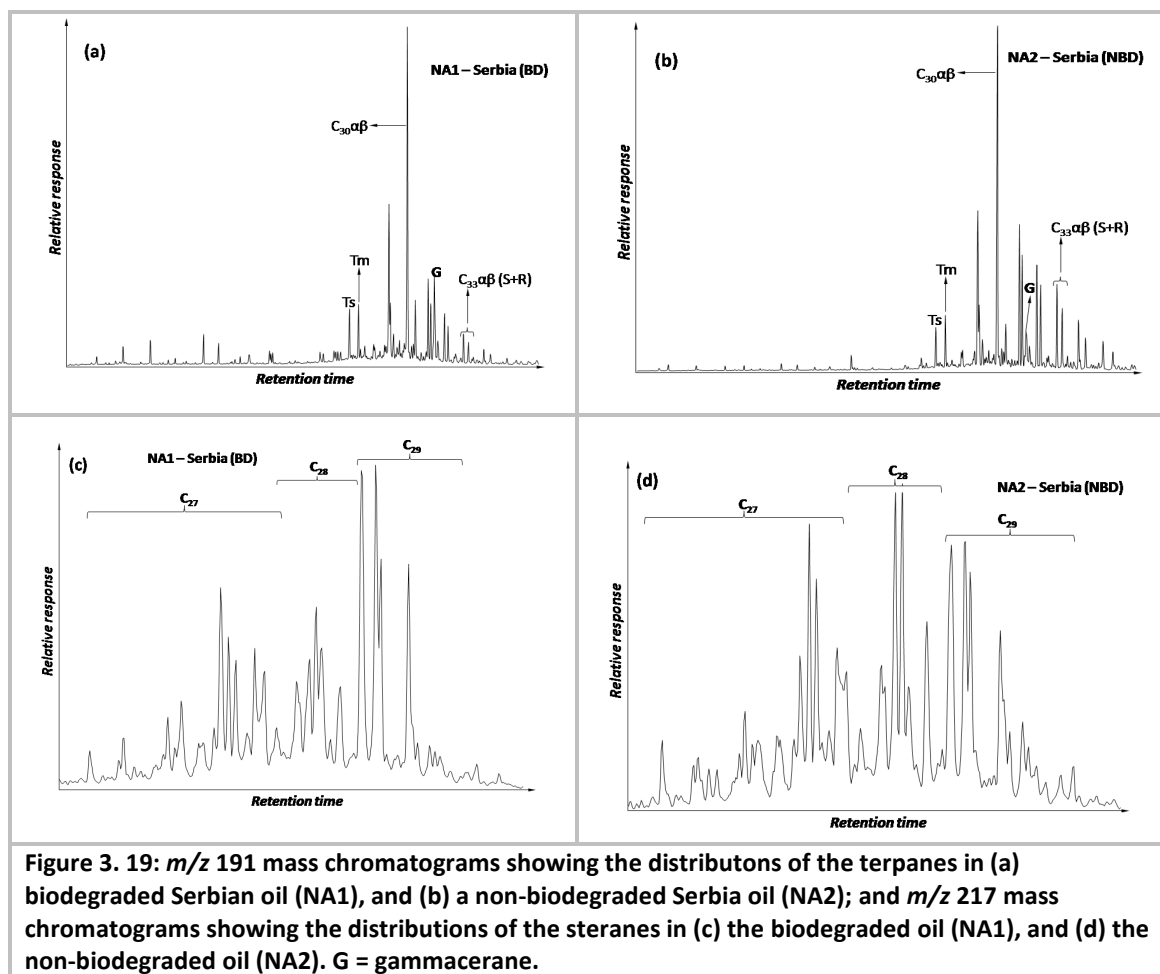
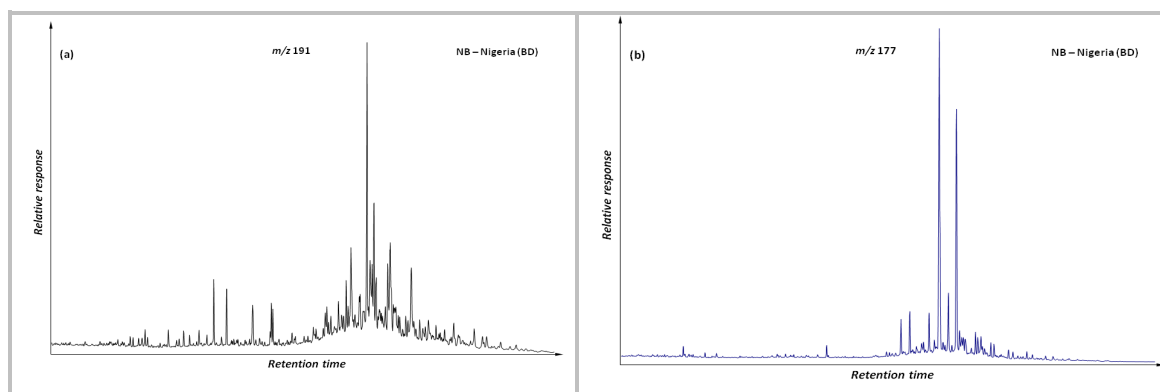
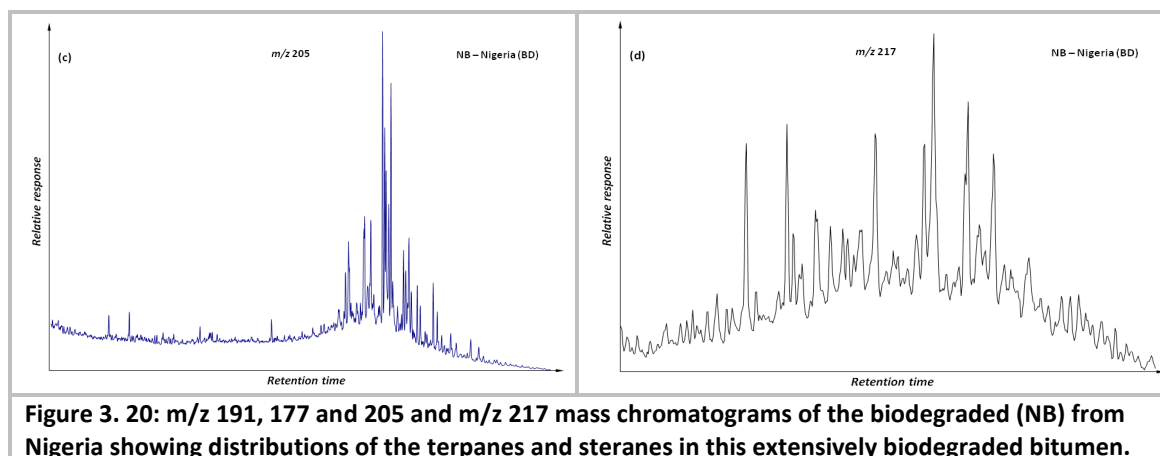


Figure 3.19 shows the m/z 191 chromatograms of the degraded and non-degraded Serbian oils. Note the enhanced tricyclic terpanes peaks relative to pentacyclics in the biodegraded oil (NA1) compared to the non-degraded oil (NA2) in agreement with the observation that the tricyclic are more resistant to biodegradation than the pentacyclics. Another major difference is also the enhanced gammacerane (G) peak compared to C_{31} $17\alpha(H),21\beta(H)$ homohopanes in the biodegraded oil (NA1) in agreement with the fact that gammacerane is more resistant to biodegradation than the hopanes (Peters et al., 2005a). Furthermore, it appears the biodegradation preferentially remove the higher molecular weight hopanes relative to the lower molecular homologues as shown by diminished peaks in the biodegraded oil compared to the non-degraded one. The lower homologue steranes (C_{27} and C_{28}) are partially removed relative to the C_{29} steranes resulting in dominance of the latter in the biodegraded oil (NA1) although C_{28} is the dominant homologue in the non-degraded oil.



The Nigerian bitumen (NB) is the most extensively biodegraded amongst all the biodegraded oils. In addition to the fact that all the *n*-alkanes and isoprenoids are completely removed, the terpanes and steranes are severely altered. The regular hopanes are almost completely removed (Figure 3.20). The dominant terpanes present are the C_{26} to C_{29} norhopanes. Other terpanes tentatively identified are the methylhopanes ranging from C_{30} to C_{34} showing m/z 205 as the base peak and methylnorhopanes. The later have m/z 205 as the base peak and m/z 355 indicative of norhopanes. Other unusual biomarkers observed in the NB aliphatic hydrocarbon fraction are what tentatively appear to be dimethylhopanes and trimethylnorhopanes with m/z 219 and m/z 233 as the base peaks respectively.





(c) Thermal Maturity

Thermal maturity is “the extent of heat-driven reactions that convert sedimentary organic matter in petroleum” (Peters et al., 2005a). Heat dependent molecular isomerisations and structural transformations have been widely employed to estimate maturity of source rocks at the time of expulsion of petroleum. These tools are particularly important where only oil samples, rather than source rock, are available (Peters et al., 2005a). Some of these thermal maturity parameters have been computed (Table 3.5) for the oils used in this work.

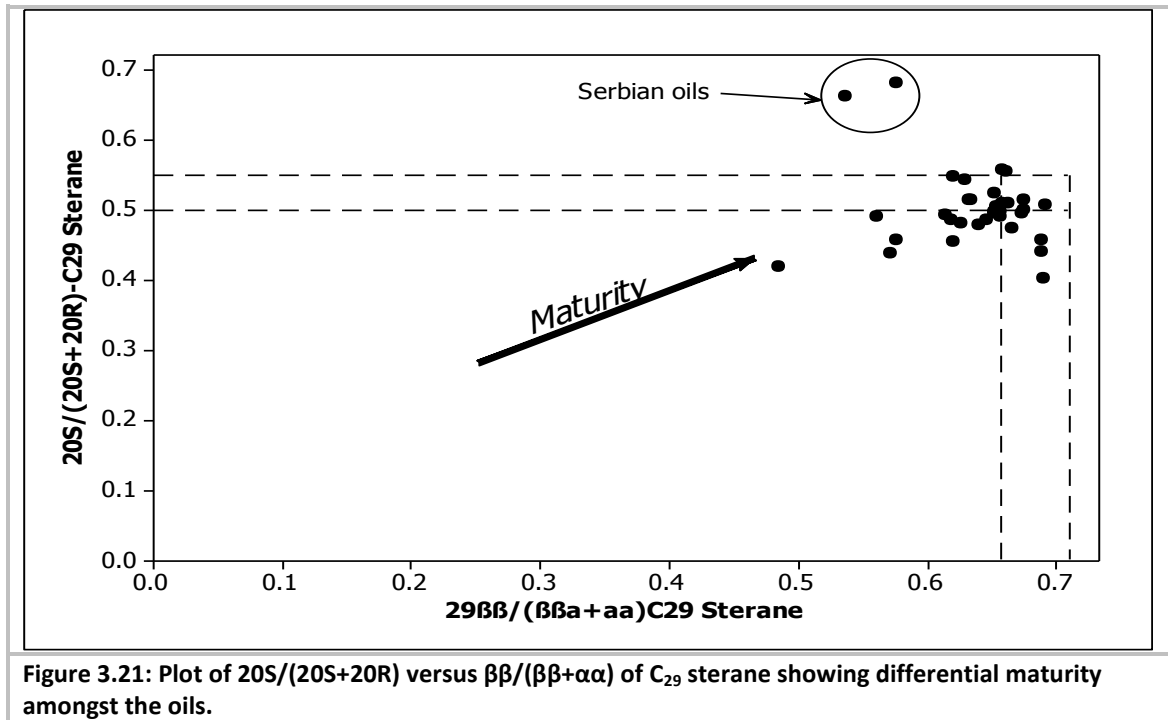
The homohopane isomerisation at C22 chiral centre involves heat-mediated conversion of the biological R isomer to the S isomer. The 22S/(22S+22R) ratio thus increases from zero until equilibrium is established at about 0.57 to 0.62 (Seifert and Moldwan, 1980). As is clear from Table 3.8, the equilibrium has been established in all the samples as expected since the equilibrium is established at early maturity. On the other hand, the 20S/(20S+20R) ratio varies from 0.40 to 0.55 amongst the samples although most of the samples have attained the equilibrium value. For this parameter equilibrium is established at ~0.52 and oil generation (early maturity) starts about 0.40 (Mackenzie et al., 1982). Notably, oils generated in the early maturity stage include the two oils from Kittiwake Oil Field in the Northsea and some other Northsea oils (Table 3.5).

Table 3. 5: Some molecular thermal maturity parameters computed from biomarkers

Sample	$C_{22}/C_{21}T3C$	$C_{24}/C_{23}-T3C$	$C_{23}T3C/C_{30}\alpha\beta$	$C_{24}T4C/C_{30}\alpha\beta$	$C_{25}Ts/(C_{29}Ts+C_{25}\alpha\beta)$	$22S/(22S+22R) C_{31}\alpha\beta$	$22S/(22S+22R) C_{32}\alpha\beta$	$20S/(20S+20R) C_{29}\alpha\alpha$	$\beta\beta/(\beta\beta+\alpha\alpha) C_{29}$ sterane
A39	0.99	0.44	0.49	1.07	0.60	0.50	0.57	0.55	0.66
B58	0.48	4.27	0.01	0.05	0.25	0.58	0.60	0.52	0.65
BN	1.14	0.62	0.14	0.10	0.32	0.57	0.57	0.51	0.69
C26	0.88	0.35	0.56	0.16	0.11	0.58	0.60	0.50	0.68
C30	0.94	0.35	0.56	0.17	0.11	0.58	0.60	0.50	0.67
K77	0.67	0.32	0.10	0.17	0.06	0.55	0.59	0.50	0.66
K78	0.71	0.28	0.09	0.14	0.04	0.54	0.59	0.50	0.65
O28	0.23	0.68	0.32	0.12	0.17	0.58	0.59	0.55	0.62
O31	0.41	0.57	0.32	0.15	0.16	0.58	0.59	0.48	0.62
Q43	0.71	0.37	0.12	0.17	0.24	0.57	0.60	0.50	0.65
Q61	0.68	0.40	0.13	0.23	0.27	0.56	0.60	0.51	0.66
U32	0.42	0.72	0.22	0.09	0.37	0.56	0.59	0.51	0.66
U54	0.35	0.60	0.05	0.04	0.30	0.58	0.58	0.42	0.49
U59	0.47	0.70	0.04	0.04	0.22	0.59	0.59	0.46	0.58
U68	0.31	0.80	0.14	0.09	0.32	0.58	0.58	0.49	0.61
U79	0.39	0.58	0.38	0.11	0.34	0.56	0.58	0.50	0.65
U84	0.40	0.72	0.19	0.10	0.40	0.58	0.58	0.51	0.68
Y32	0.36	0.66	0.06	0.05	0.29	0.58	0.58	0.51	0.63
U01	0.51	0.96	0.18	0.18	0.50	0.56	0.56	0.44	0.69
U05	0.51	1.05	0.19	0.20	0.53	0.56	0.57	0.40	0.69
U02	0.30	0.66	0.07	0.07	0.30	0.58	0.59	0.49	0.56
U04	0.00	0.71	0.14	0.11	0.36	0.56	0.60	0.49	0.66
U07	0.35	0.74	0.10	0.09	0.30	0.58	0.59	0.49	0.65
U46	0.37	0.93	0.14	0.12	0.43	0.57	0.58	0.45	0.62
U56	0.40	0.74	0.15	0.12	0.41	0.56	0.58	0.46	0.69
U93	0.42	0.75	0.07	0.07	0.34	0.58	0.58	0.47	0.67
AR3	0.39	0.67	0.22	0.06	0.30	0.56	0.58	0.54	0.63
CH	0.56	0.48	0.53	0.08	0.09	0.57	0.60	0.48	0.63
M5	1.03	1.02	0.00	0.00	0.17	0.56	0.58	0.51	0.63
NA1	0.18	0.71	0.08	0.04	0.19	0.58	0.58	0.66	0.54
NA2	1.01	0.83	0.02	0.04	0.24	0.56	0.59	0.68	0.58
Pr1	0.55	0.62	0.20	0.07	0.15	0.57	0.59	0.44	0.57
FN	0.33	0.80	0.08	0.06	0.27	0.57	0.60	0.57	0.66
U89	0.35	0.71	0.16	0.10	0.48	0.33	0.58	0.58	0.61
U14	0.36	0.57	0.07	0.04	0.32	0.58	0.58	0.39	0.48
NB	1.05	0.97	1.88	0.49	0.38	0.52	0.62	ND	ND

The two oils from Serbia are rather unusual with respect to their values of 20S/(20S+20R) ratio (> 0.65). Values of the parameter above the equilibrium value of 0.55 are usually because of preferential biodegradation of the 20R isomer relative to the 20S isomer (Rullkötter and Wendisch, 1982). However, since NA2 is not biodegraded and has nearly the same value as the biodegraded NA1, the higher value might be related to the organofacies of the source rock of the oils. This is clear from Figure 3.21 which, in addition to showing the two samples as outliers, also shows the $\beta\beta/(\beta\beta+\alpha\alpha)$ ratio equilibrium is yet to be established despite

20S/(20S+20R) ratio being above the equilibrium value. Figure 3.21 also shows most of the samples have reached full maturity with respect to the two maturity parameters. Samples outside the equilibrium region are mainly the Northsea oils, U54, U59, U02, U46 etc and PR1 from Gulf of Mexico. This suggests these oils were generated in the early part of the 'oil window'.



(d) *Depositional environment and condition*

The molecular composition (especially biomarkers) of oils has been widely used to successfully delineate the environment and condition under which the source rock that generated the oils was deposited (Peters et al., 2005a; Peters et al., 1986). Using these tools, the oils can be grouped into two/three main groups based on lithology of source rock; namely carbonate, shale and marl (Peters et al., 2005a). Oils from carbonate source rock show characteristic low relative proportion of diasteranes as depicted by low C₂₇ Dia/(Dia+Reg) ratio (Hughes, 1984) and high C₂₉/C₃₀ hopane ratio (Ten Haven et al., 1988). The oils also have high C₃₅ homohopane relative to the C₃₄ homologue (McKirdy et al., 1983) as semi-quantitatively shown in C₃₅/C₃₄ ratio and homohopane index (%C₃₅). In general, most oils sourced from marine carbonate source rock show C₃₅/C₃₄ > 0.8 and C₂₉/C₃₀ > 0.6 (Peters et al., 2005a). Furthermore, Pr/Ph ratio is 1 or less for these oils (Moldowan et al., 1985; Hughes, 1984).

On the other hand, shale-sourced oils display their expected characteristics. For example, all the Northsea oils, sourced from argillaceous Kimmeridge Clay Formation, have high diasteranes (Dia/(Dia+Reg) sterane = 0.45 to >0.7); low C₂₉/C₃₀ ratio being generally less than 0.6 and high pristane relative to phytane (Pr/Ph > 0.9). The C₃₅/C₃₄ ratio however varies from 0.73 to 1.43, although for over 50% of the Northsea oils it is greater or equal to 1.

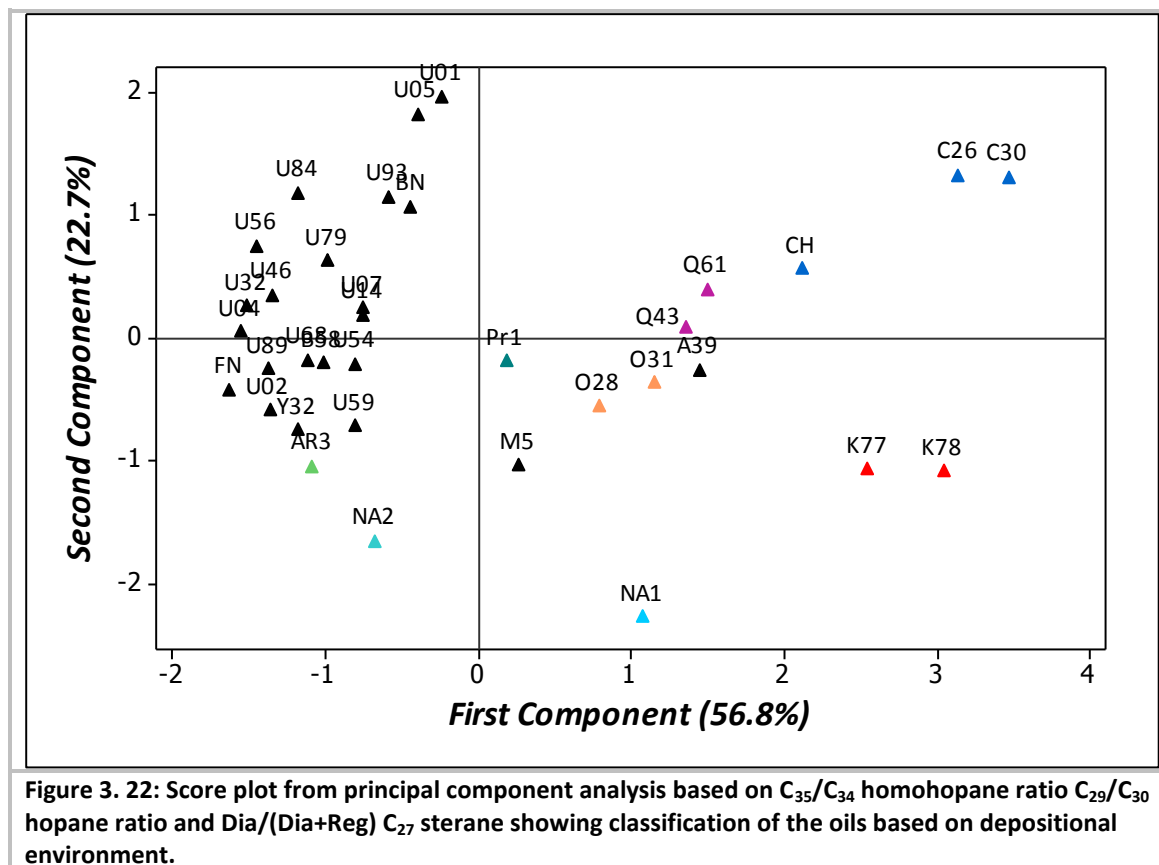
The two oils (U01 & U05) from Kittiwake oil field (Northsea) have particularly high C_{35}/C_{34} compared to other Northsea oils. High C_{35} homohopane has also been found to be an indicator of highly reducing conditions during deposition of the sediment (Peters and Moldowan, 1991) as is supported by positive correlation between the homohopane index and hydrogen index (Rangel et al., 2000). In such conditions, the precursor extended C_{35} hopanoid is reduced and/or incorporated in kerogen, resulting in preservation of the extended side chain, rather than oxidised and decarboxylated resulting in homohopanes with shorter side chains (e.g. C_{34} , C_{33} etc). The index however is affected by maturity; it decreases with increasing maturity (Peters and Moldowan, 1991). This may explain the variability in the observed index amongst the Northsea oils. Otherwise, it may indicate variable extent of establishment of anoxia in different sections of the Kimmeridge Clay depositional settings.

The two oils from Qatar (Q43 & Q61) however do not seem to respect the above interpretation. Although the oils have a C_{29}/C_{30} ratio being greater than 0.90, characteristic of marine carbonates, they nevertheless have relatively high diasteranes - a property commonly associated with clay-rich sediments such as shale. In fact, the Dia/(Dia+Reg) ratio of the oils (over 0.5) is higher than that of some Northsea oils known to be sourced from Kimmeridge Clay Formation. Consequently, the oils (Q43 & Q61) may apparently have been sourced from a marine shale rather than marine carbonate. This apparent discrepancy, however, is resolved from the lithology of the source rock. The source rock for these oils has been established as the Jubailah formation and the underlying Hanifa formation (Alsharhan and Nairn, 1997). Both of these source rocks are argillaceous (clay-rich) limestone (Alsharhan and Nairn, 1997). The source rocks, therefore, although carbonate, contains clay minerals that have been observed to catalyse conversion of regular steranes to the re-arranged diasteranes (Rubinstein et al., 1975).

Based on the above general pattern of biomarker characteristics, six other oils (about which no information of the source was available) are possibly sourced from marine carbonate source rocks. These include the three oils from Canada (C26 & C30), which show signatures of marine carbonate namely low Dia/(Dia+Reg) ratio (<0.40), high C_{29}/C_{30} ratio (>0.80) and high C_{35}/C_{34} ratio (>1.20) as shown in Appendix 3C. Similarly, PR1 and M5, from the Gulf of Mexico, show characteristics of marine carbonate sourced oils albeit less strongly due to relatively lower C_{29}/C_{30} ratio and relatively high Dia/(Dia+Reg) ratio with respect to PR1. This may imply argillaceous carbonate source rock for this oil, as may also be the case with respect to sample A39 from Abu Dhabi.

Thus it is clear that these three parameters are useful in the classification of oils based on their depositional environment. Consequently, in addition to dibenzothiophene/phenanthrene (DBT/P) ratio (Hughes, 1984), they were used collectively in principal component analysis to classify the samples. The results show that the first two principal components (PC1 and PC2) account for about 80% of the variation with C_{29}/C_{30} , Dia/(Dia+Reg) and DBT/P giving the major contributions to PC1 and C_{35}/C_{34} being the major contributor to PC2. Figure 3.22 is the score plot of the two major components (PC1 and PC2) showing clear discrimination between various depositional settings. The marine carbonate-sourced oils are on the positive side of PC1 and marine shale-sourced oils on negative side. Furthermore, oils with $C_{35}/C_{34} > 1.0$, reflecting anoxic setting, are in the positive half of PC2, while those with lower values are in

the negative half. In general, oils with the same source have similar scores and are therefore located closely. This classification is in agreement with the method of Hughes (1984) with respect to marine carbonates as shown in Figure 3.23. However, most of the marine shale oils are wrongly classified as lacustrine sulphate-poor possibly due to the effect of maturity on Pr/Ph ratio.



The marine depositional environment of the oils is further emphasised by the proportion of $C_{31}R$ homohopane relative to C_{30} hopane. Marine carbonate, shale and marl have $C_{31}R/C_{30}$ greater than 0.25 (Peters et al., 2005a) as is the case with almost all the oils used in this work (Appendix 3C). The only outlier in this respect is sample NA1 from Serbia ($C_{31}R/C_{30} = 0.17$). This oil however is biodegraded. As discussed above, the hopanes, in addition to other biomarkers, are altered by the biodegradation. It has been observed that lower homologues in the hopane range from C_{27} to C_{32} are biodegraded more slowly than the higher homologues (Rullkötter and Wendisch, 1982). Consequently, it is reasonable that the observed low C_{31}/C_{30} ratio in NA1 is because of preferential degradation of C_{31} relative to C_{30} and thus the value of the parameter in unbiodegraded oil could be higher than the observed 0.17 as is the case in NA2 (Appendix 3C).

Furthermore, in addition to all the Northsea oils, the two oils from Canada and one oil from Gulf of Mexico (PR1) show the presence of 28,30-bisnorhopane (BNH). The relative proportion of this compound however varies even among the Northsea oil as shows by $\text{BNH}/(\text{BNH}+C_{30})$ ratio (Appendix 3C). BNH is thought to be produced by chemoautotrophic bacteria that thrives at the oxic-anoxic boundary and thus has been associated with some anoxic depositional settings (Peters et al., 2005a). The presence of this biomarker in the Northsea oils is in agreement with anoxic deposition condition under which the Kimmeridge Clay was deposited

and suggests similar condition was established during deposition of the source rock from which PR1 oil and the two oils from Canada were sourced. The variability in the value of the $BNH/(BNH+C_{30})$ ratio amongst the Northsea samples (Appendix 3C) could be a consequence of differential maturity as it has been observed to decrease with increasing maturity among Monterey oils (Curiale et al., 1985).

The establishment of an anoxic depositional setting during deposition of source rock is further corroborated with respect to the oils from Canada and Serbia by the presence of gammacerane in the hydrocarbon fraction of the oils. Although the origin of this compound has not been established (Peters et al., 2005a), nonetheless, it is thought to be a diagenetic product of gammaceran- 3β -ol (i.e. tetrahymanol) (Ten Haven et al., 1989; Venkatesan, 1989) mainly produced by bacteriovorous ciliates which thrives at the interface between oxic and anoxic regions of stratified water column (Sinninghe Damsté et al., 1995a). The presence of this biomarker therefore indicates source rock of the oils was deposited in stratified water column, often due to hypersalinity, under highly reducing conditions (Moldowan et al., 1985).

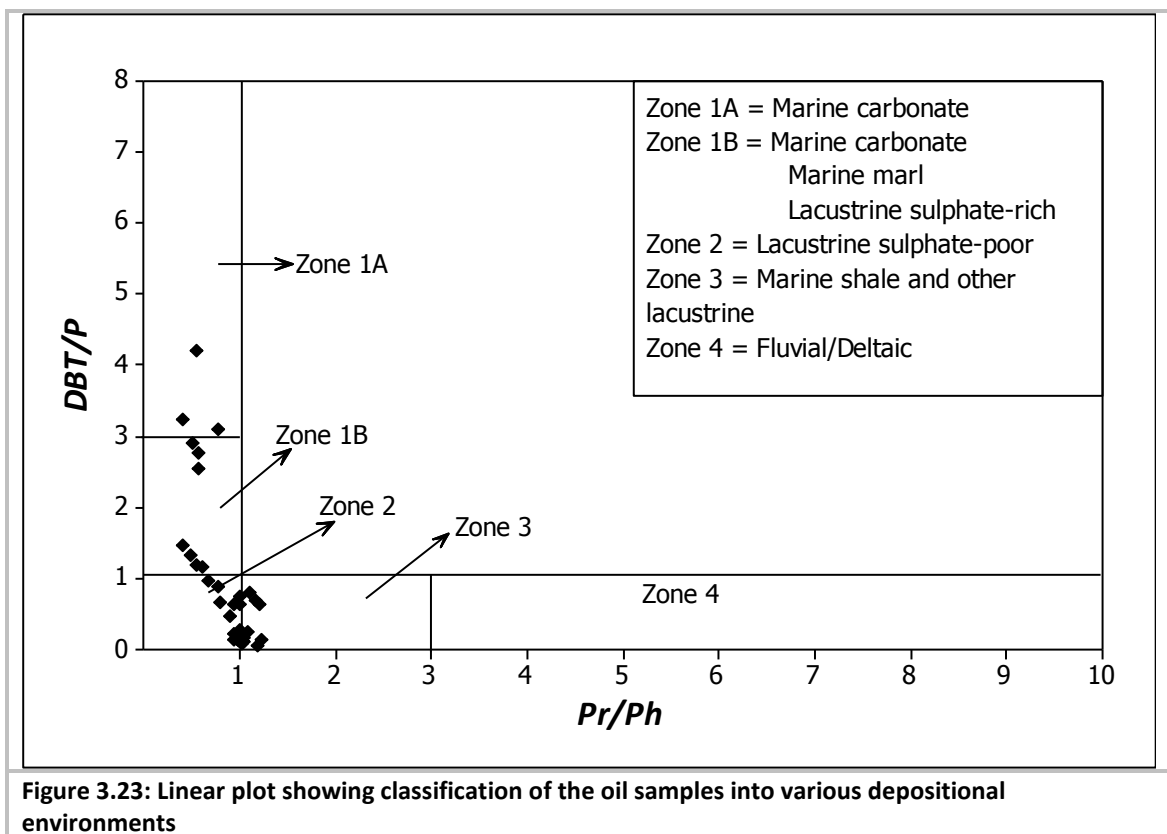


Figure 3.23: Linear plot showing classification of the oil samples into various depositional environments

(e) Organic matter input

The predominant type organic matter from which oils are generated can be broadly classified into marine, terrigenous and lacustrine organic matter. A combination of geology and composition of petroleum can be used to have an insight into the nature of precursor organic matter from which the oil was derived. In general, oils generated from source rocks deposited earlier than the Silurian are sourced from marine organic matter. This is because land plants, the main contributors to terrigenous organic matter did not evolve until the Silurian. Thus, the two oils from Canada are sourced from marine organic matter. Similarly, the Northsea oils,

although sourced from Jurassic Kimmeridge Clay, the presence, in these oils, of C₃₀ sterane, a diagenetic product of 24-*n*-propylcholestrols produced by marine Chrysophyte algae, indicate marine phytoplankton organic matter input (Moldowan et al., 1985).

3.4 Summary and Conclusions

Samples of varying geochemical histories were obtained in order to investigate how the composition of asphaltenes is influenced by the varying histories of the samples. Traditional geochemical characterisation of the three black shale samples reveals they were deposited in marine environment with maturity ranging from immature to marginally mature. Similarly, the coal samples range from immature, early mature, mature and late mature; these are suitable for investigating the influence of thermal history on the asphaltenes.

Characterisation of the oils reveals, although their maturity does not vary very much, that they were principally sourced from marine carbonates, marls and shales. Furthermore, the oils consist of both biodegraded and non-biodegraded oils. The latter were characterised to have varying degree of biodegradation and therefore suitable for assessing how such properties affect the composition of asphaltene.

Chapter 4 Adsorption and Occlusion in Asphaltenes

4.1 Introduction

Asphaltenes are materials consisting of a wide range of macromolecules of different sizes and shapes but are principally considered to consist of condensed aromatic cores with side chain appendages (Badre *et al.*, 2006) and possibly interlinked by polymethylene bridges through carbon-carbon, sulphide, ether as well as ester bonds (Strausz *et al.*, 1999a). This macromolecular structure of asphaltenes is at the heart of the “occlusion hypothesis”.

The “occlusion hypothesis” is based on the premise that, because of their macromolecular and/or solubility properties, asphaltenes can trap smaller molecules within their structural framework and thus in essence exclude them from the bulk of the oil matrix (maltene). This is based on the assumption that either a typical asphaltene is (i) polymeric with a cage-like or clathrate structure (Mujica *et al.*, 2000), and/or (ii) molecules exist in aggregates in an oil medium. Thus, during the formation of such cage-like structures or aggregates, some of the surrounding smaller molecules, including biomarkers, are securely engulfed or trapped. The entrapped molecules are therefore protected from secondary alteration processes (Liao and Geng, 2002; Ekweozor, 1984).

The implication of this hypothesis is that, if asphaltenes were formed in source rocks, molecular fossils (biomarkers) of the source organic matter will remain entrapped within the asphaltene structural framework even after severe biodegradation of the oil because asphaltenes, being the most resistant fraction of the oil, protect the entrapped biomarkers. This therefore makes asphaltenes potentially of vital geochemical importance in oil-source and oil-oil correlation, environmental forensics and palaeoenvironmental studies particularly in such cases (Liao *et al.*, 2006a; Liao *et al.*, 2006b; Liao and Geng, 2002).

The occlusion hypothesis appears to have been first put forward by C. M. Ekweozor (Ekweozor, 1986; Ekweozor, 1984) about 25 years ago and recently revived by Z. Liao and co-workers (Liao *et al.*, 2006a; Liao and Geng, 2002). In both cases it seems to be a consequence of empirical observation that there was an apparent difference between the distributions (or of computed indices) of maltene saturate biomarkers and the corresponding “free” (i.e. extractable) biomarkers recovered from asphaltenes after breaking up the asphaltenes by chemical degradation methods. Despite this it is still not confirmed whether the so-called occluded compounds are products of occlusion, and not merely remnants of adsorbed components of maltene. Although Ekweozor (1984) acknowledged the possibility of generation of the observed biomarkers through chemical processes, Liao and Geng (2002) concluded that the compounds they observed were ‘free’ compounds occluded within the asphaltene structures and have no dynamic contact with the maltenes.

An attempt was made to simulate occlusion and test whether or not the observed saturated hydrocarbons from the chemical degradation of Soxhlet-extracted asphaltenes were products of occlusion (Liao *et al.*, 2005). In the experiment, 100 mg of deuterated *n*-eicosane ($C_{20}D_{42}$) was added to a toluene solution of pre-extracted asphaltenes (200 mg in 20 ml toluene). The findings showed that over 98% of the $C_{20}D_{42}$ was recovered from the extracts. However, no

C₂₀D₄₂ was detected in the occluded fraction following chemical degradation of the asphaltenes with H₂O₂/acetic acid reagent although “trapped” hydrocarbons were observed (Liao *et al.*, 2005). Consequently, they conclude that asphaltenes are microporous substances that form aggregates within which biomarkers are trapped and protected from secondary alteration processes.

Several questions arise from this however. It is not clear whether toluene mimics or is comparable to maltene in solubilisation of asphaltenes. Obviously, toluene and maltene have different solvent properties, and in particular resins have been reported to play an important roles in the solubilisation and stabilisation of asphaltenes in the petroleum medium (Pereira *et al.*, 2007; Speight, 2004; Andersen and Speight, 2001). Second, it has been established that the concentration above which asphaltenes exist as nanoaggregates in toluene, varies between 40 to 400 mg/l (Andreatta *et al.*, 2007; Badre *et al.*, 2006). Consequently, the asphaltene concentration (10,000 mg/l) used by Liao *et al.* (2005) in the experiment is well above the critical nanoaggregate concentration (CNAC) and so any marker compound added in such aggregate solution of asphaltenes would not be occluded since the asphaltenes were already in an aggregated state. This might therefore explain why the marker compound was not detected in the occluded fraction.

Furthermore, it is known that during the precipitation process, asphaltenes adsorb and co-precipitate non-asphaltene substances, such as resins, hydrocarbons and particularly waxes, which are otherwise components of maltene. Thus, in analysis of the occluded compounds, the asphaltenes are Soxhlet extracted to remove the co-precipitated components before further analysis (Liao *et al.*, 2006b; Creek, 2005; Alboudwarej *et al.*, 2002). However, variable timing is used for the extraction and it is not clear what time of extraction is enough to selectively remove the adsorbed/co-precipitated compounds from the asphaltenes. Moreover, the acetone extraction was developed to separate the so-called low molecular weight asphaltenes from high molecular weight fraction (Peng *et al.*, 1997) and may therefore be unsuitable for removal of the adsorbed components.

Still more, the procedures used to release the compounds that may be trapped (occluded) within the asphaltenes 3D structure are based on chemical degradation of the asphaltenes. The aim is to selectively breakdown the asphaltenes macromolecules without 'damaging' the compounds trapped within them which are then recovered and analysed. Although other reagents such as potassium/naphthalene (Ekweozor, 1984) and NaIO₄/NaH₂PO₄ (Liao and Geng, 2002) have been used, Liao and co-workers appear to favour hydrogen peroxide in acetic acid as a mild degradation reagent (Liao *et al.*, 2006b). Nevertheless, the suitability of the reagent, with respect to its selectivity in breaking down the asphaltenes without affecting the occluded components, has not been established.

Consequently, it is the aim of this section of the work to re-evaluate critically the occlusion hypothesis. Leading from the above review, the following specific objectives will be addressed.

1. to determine the timing of Soxhlet extraction suitable for removing adsorbed and co-precipitated compounds from asphaltenes

2. to test the efficiency of conventional chemical oxidations methods for the selective degradation of asphaltenes in order to release the 'occluded' hydrocarbons
3. to investigate whether 'occlusion' is a consequence of adsorption and co-precipitation or an inherent process during the early formation of asphaltenes
4. to compare and contrast the free, adsorbed, and 'occluded' biomarker distribution in context of oil/oil correlation exercises

4.2 Methodology

4.2.1 Selection of samples

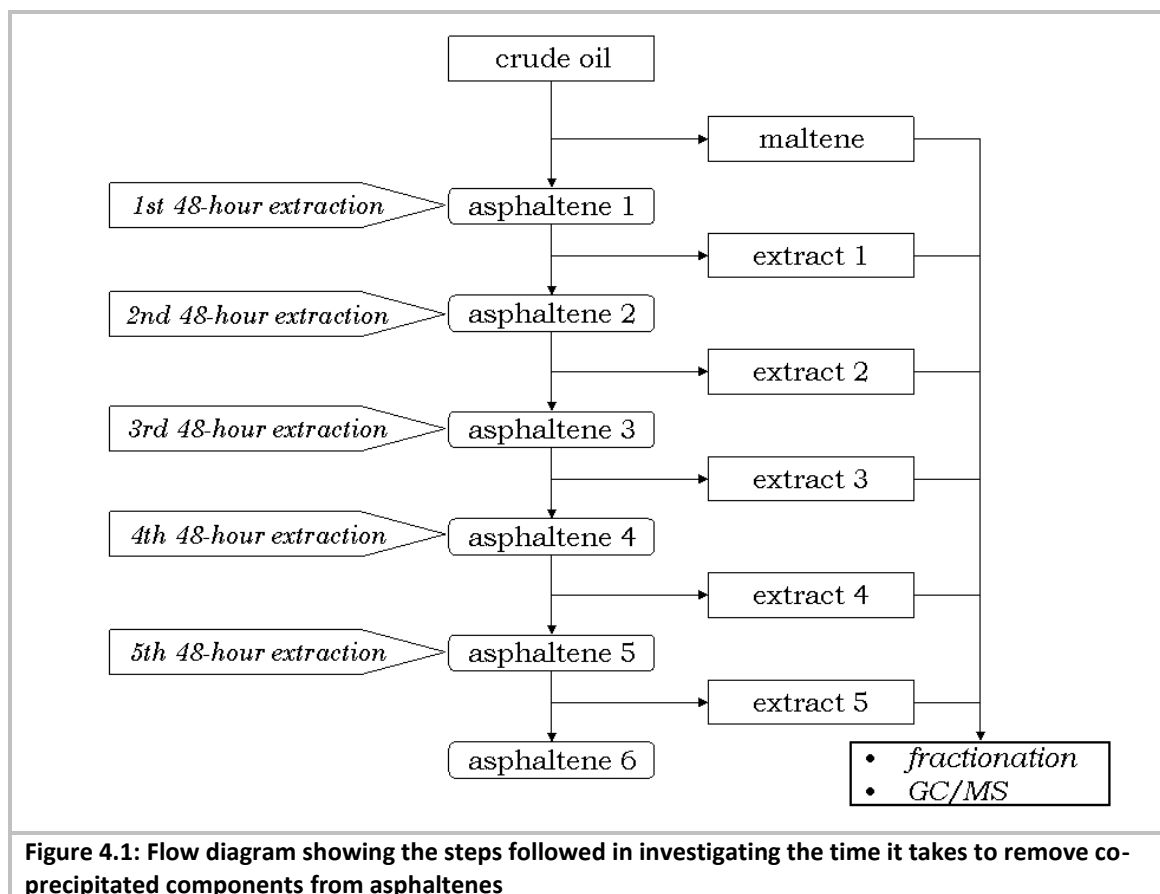
Twelve oil samples, ten of which are in pairs (from different geographical areas and source rocks) were chosen for this study. Each pair consists of oils from the same source, and in some cases obtained from the same field and reservoir. The samples were selected to examine the level of agreement and disagreement between members of a pair and members of different pairs.

4.2.2 Analytical procedure

The following analytical procedures were designed to address the respective objectives stated in Section 4.2.1.

(a) Suitable timing of Soxhlet extraction for cleaning asphaltenes

Three non-biodegraded oils from different geographical areas and basins namely B58 (Bangladesh), U56 (Northsea) and Y32 (Yemen) were selected for this study. The asphaltenes were recovered as described in Section 2.3.3(a). Each was Soxhlet extracted with acetone in six successive stages of 48 hours each (Section 2.3.3(b)). The extracts were collected, fractionated and the saturated hydrocarbon fractions analysed (Sections 2.3.4 and 2.4.6). The saturated hydrocarbon fractions from the maltenes were recovered and analysed as well. Figure 4.1 summarises the process.



(b) Suitability of asphaltenes degradation reagents

Following literature survey, experiments were conducted on the effect of (i) hydrogen peroxide (H_2O_2); (ii) potassium permanganate (KMnO_4); and (iii) ruthenium ion catalysed oxidation (RICO) reagent on authentic standards of aromatic and aliphatic compounds namely pyrene, tricosane and androstane. Thereafter, further experiments were undertaken to determine the feasibility of using the reagents for selective degradation asphaltenes in order to release the 'occluded' biomarkers.

(c) Simulation of occlusion of aliphatic hydrocarbons in asphaltenes

Marker compounds (deuterated hexadecane ($\text{C}_{16}\text{D}_{34}$) and androstane) were added to three oil samples namely BN and U54 from Northsea, UK and O28 from Oman. The oils were magnetically stirred for 30 days after which the asphaltenes were recovered (Section 2.3.3) and extracted using Soxhlet method with acetone for the appropriate time. The extracts and the products from the chemical degradation of the asphaltenes were analysed to determine whether the added marker compounds were exclusively present only in the extracts.

(d) Comparative analysis of free, adsorbed, and occluded hydrocarbons

Twelve oils were selected for comparative analysis of the composition and distribution of aliphatic hydrocarbons of maltene fractions to those of the corresponding adsorbed and occluded fractions. The asphaltenes were recovered from the oils as described in Section 2.3.3(a) and then Soxhlet extracted for 10 days to recover the adsorbed components (Section 2.3.3 (b)). Occluded saturated hydrocarbon components, on the other hand, were recovered

by using the most suitable chemical degradation method (i.e. aqueous potassium permanganate) based on the results of the work described in Section 4.2.2 (b). Finally, the saturated hydrocarbon fractions from the maltene, adsorbed and occluded fractions were recovered and analysed using chromatographic method and GC/MS (Sections 2.3.4. and 2.4.6).

4.3 Results and Discussion

4.3.1 Determination of time required for efficient extraction of asphaltenes

Generally, only about 6 to 10 % (w/w) of the original asphaltenes was recovered from the stepwise Soxhlet extraction of the asphaltenes. On the other hand, continuous extraction without solvent replacement, as was the case in stepwise extraction, gave relatively greater proportion (8 to 22%, w/w) of extractable components.

Although this may suggest the continuous extraction is more efficient than the stepwise extraction, the observation may however be because the composition of the extraction solvent, and therefore its solvent properties, is continuously altered by the extracted components from the previous extraction cycle. The resulting more polar solvent may perhaps extract relatively more of the adsorbed materials from the asphaltenes in subsequent extraction cycles. Nevertheless, irrespective of the method used, more extractable components were obtained from the Northsea oil (U56) asphaltenes compared to the other asphaltenes (Figure 4.2 (a)). B58 and Y32 asphaltenes show less variability in relative amounts of the extracts obtained from the two extraction procedures (i.e. continuous vs. stepwise extractions).

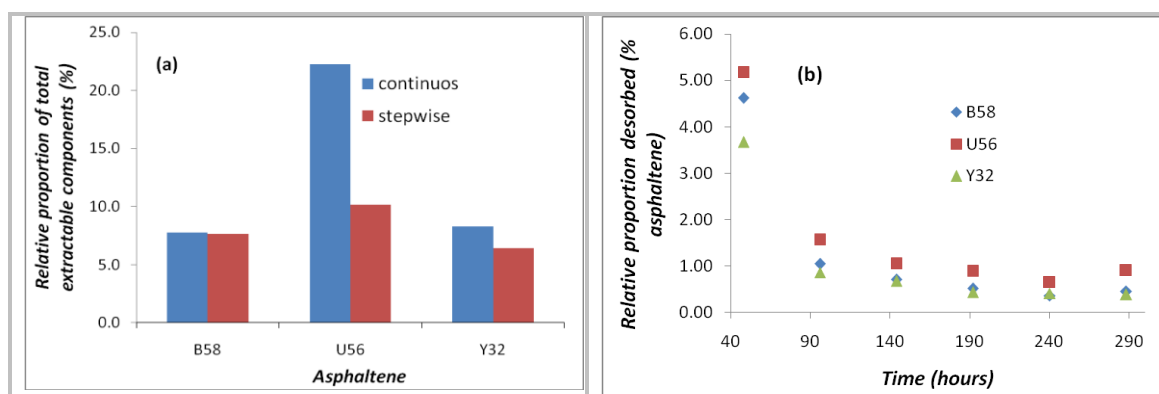


Figure 4.2: (a) Bar chart showing the relative proportions of extractable components desorbed from asphaltenes after 10 days of extraction using continuous and stepwise extraction; (b) Scatter plot show the evolution of the stepwise extraction with time with respect to the relative amounts of components desorbed.

All the asphaltenes irrespective of their sources display a similar asymptotic trend with regard to the relative proportions of the total amount of the original asphaltenes desorbed/recovered over time from the stepwise extraction process (Figure 4.2 (b)). The asymptotic nature of the extraction shows although there is gradual fall in the relative proportion of the extractable components, the amounts only tend to zero at infinite extraction time. In other words, there is theoretically no end time at which nothing would be desorbed from the asphaltenes.

Examination of compositions of the aliphatic hydrocarbon components of the fractions recovered from the stepwise Soxhlet extraction process reveals further information. The first extract recovered after 48 hours of extraction from all the asphaltenes is dominated by high molecular weight *n*-alkanes (waxes). The waxes exhibit symmetric unimodal distribution with maxima at C₃₂ to C₃₆ homologues but covering C₂₀ to C₄₄ range (Figure 4.3). Subsequent extracts from B58 and Y32 asphaltenes contain only trace amounts of *n*-alkanes (Figure 4.3). This suggests almost all the extractable waxes were practically removed from the asphaltenes within the first 48 hours of Soxhlet extraction although other non-aliphatic hydrocarbon components (possibly resins) were still being extracted in subsequent steps.

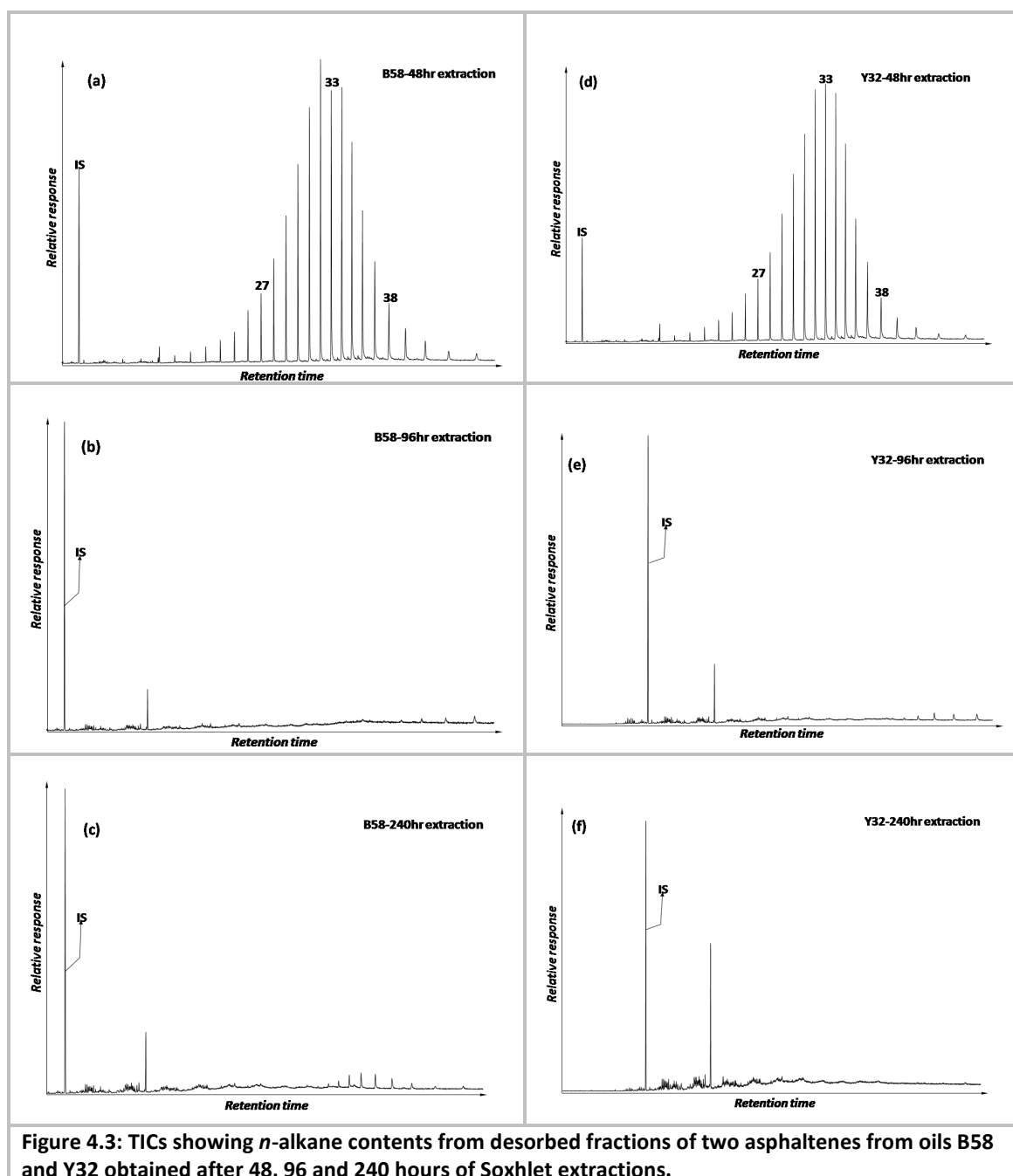
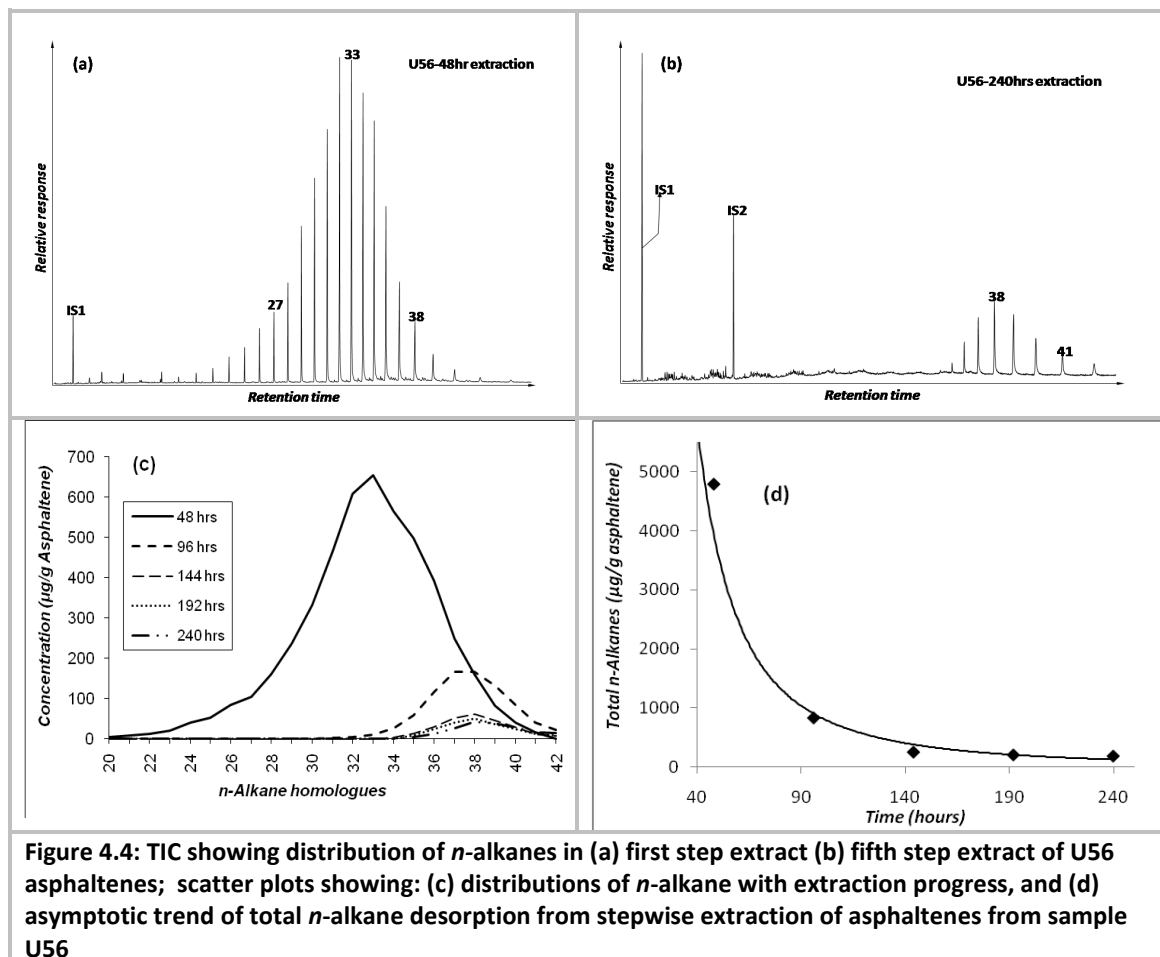


Figure 4.3: TICs showing *n*-alkane contents from desorbed fractions of two asphaltenes from oils B58 and Y32 obtained after 48, 96 and 240 hours of Soxhlet extractions.

The Soxhlet stepwise extracts from the asphaltenes of the Northsea oil (U56), on the other hand, display a different composition. Here although over 75% of the adsorbed saturated hydrocarbons were removed in the first 48 hours of extraction as shown in Figure 4.4,

subsequent extracts have significant amounts of waxes mainly in the range of C_{32} to C_{40} homologues; even at the fifth step (240 hours i.e. 10 days) of the extraction process. The wax composition of these subsequent extracts also exhibit symmetric unimodal distribution which is rather broad with maxima shifting towards higher molar weight (C_{37} or C_{38}) homologues (Figure 4.4).



The concentration profile of desorbed *n*-alkanes relative to asphaltenes is shown in Figure 4.4 (c). The regression curve (Figure 4.4 (d)) shows that the amounts of waxes desorbed from the asphaltenes decrease rapidly with time but never reach zeros (i.e. asymptotic trend). This shows the difficulty of complete removal of waxes from this asphaltene sample and suggests there may be no clear boundary between adsorbed and occluded components. It is noteworthy that although this is quantitatively observed in only U56 asphaltene, trace amounts of waxes were detected in all the extracts from B58 and Y32 asphaltenes (Figure 4.3).

These results show very important information not only on the time required to clean up asphaltenes but also on the nature and variability of the asphaltenes. First although asphaltenes appear to adsorb or co-precipitate similar kinds of *n*-alkanes, their strength or adsorptive power varies. While some asphaltenes appear to bind fairly strongly to the adsorbed aliphatic components others do so less strongly. The practical implication is at what extraction time are asphaltenes devoid of waxes as is required by Creek's definition of asphaltenes (Creek, 2005). Furthermore, what is the boundary between adsorbed and

'occluded' components particularly since the *n*-alkanes desorption profile is asymptotic trend with time.

Differential strength by which asphaltenes adsorb components has important implication for study of their structure. Purification of asphaltenes by mere triplicate re-dissolution/re-precipitation or few hours of extraction (Bowden et al., 2006; del Rio et al., 1995; Jones et al., 1988; Speight, 1984) is clearly inadequate as waxes may still remain adsorbed on the asphaltenes. Analysis of such asphaltenes samples by spectroscopic methods (e.g. IR and NMR) and pyrolysis for structural and compositional studies could lead to erroneous information because adsorbed or co-precipitated components could significantly contribute to the products that may be generated directly from the asphaltenes.

4.3.2 Determination of an ideal asphaltenes degradation reagent

As discussed in Chapter 1, asphaltenes consists of condensed polynuclear aromatic structures with aliphatic appendages (Speight and Moschopedis, 1981). In such structures 'occlusion' could either occur by engulfing smaller compounds within the macrostructure of an asphaltene molecule or by sandwiching the compounds within aggregates of the macromolecules. Either case, the 'occluded' compounds could be released by breaking the asphaltenes molecular structure or aggregates into smaller soluble molecules.

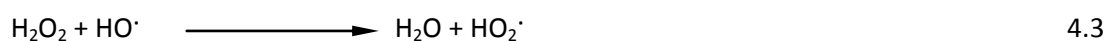
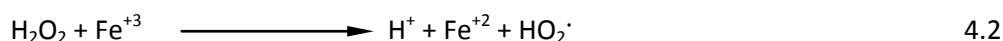
'Safe' release of 'occluded' compounds from asphaltenes requires the use of an agent that ideally should: (i) break up the aromatic core of the asphaltenes; (ii) not alter the occluded compounds; and (iii) preferably be effective at room temperature or less to avoid evaporative loss of occluded biomarkers. For this purpose three oxidising reagents known to degrade aromatic structures are considered. These include hydrogen peroxide, potassium permanganate and ruthenium tetroxide reagents and their suitability is assessed in the following sections.

(a) *Hydrogen peroxide solution*

Hydrogen peroxide (H_2O_2) has a standard redox potential of 1.76 V which is higher than that of potassium permanganate (1.70 V). Nevertheless, it is a relatively weak oxidising agent. Yet, unaided, H_2O_2 has been observed to slowly attack several types of compounds including aromatic hydrocarbons, mainly because it has both nucleophilic and electrophilic properties (Jones, 1999). However, in most of its applications, and particularly those involving oxidation of compounds that have no nucleophilic or electrophilic sites that could be easily attacked, H_2O_2 has to be activated to increase both its oxidation strength and selectivity (Jones, 1999).

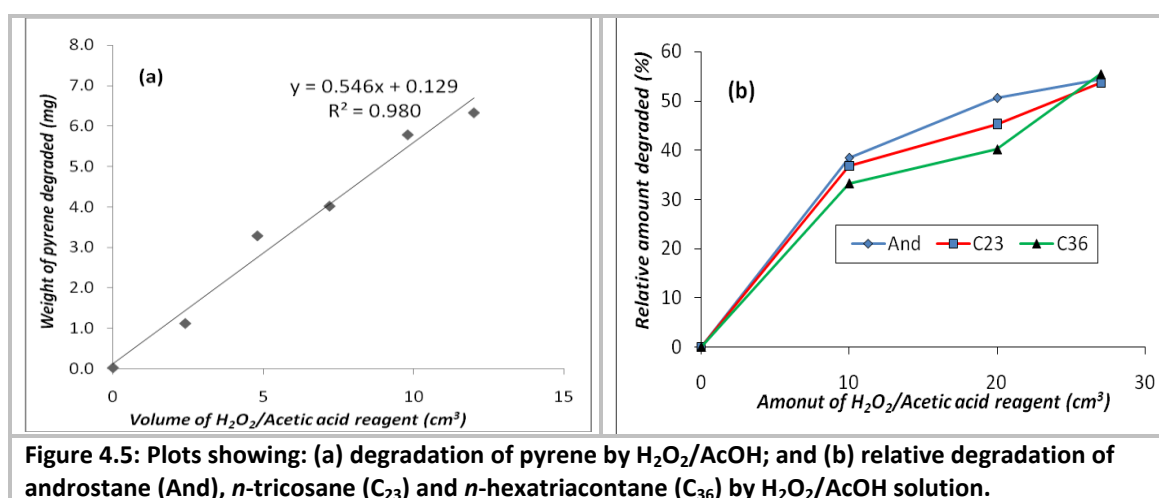
Consequently, many inorganic and organic substances are used to activate H_2O_2 . Among these substances iron salts and acetic acid are of particular importance. In Fenton's reagent, an iron (II)/(III) salt is added to hydrogen peroxide solution to catalyses the formation of hydroxyl radicals ($\text{HO}\cdot$) and perhydroxyl radicals ($\text{HO}_2\cdot$) as the active species (Jones, 1999) as shown in equations 4.1 to 4.3. The $\text{HO}\cdot$ is a very reactive specie capable of abstraction hydrogen from substrates (including hydrocarbons) generating free radicals that may be terminated or

undergo further chain reactions (equations 4.4 & 4.5). It is however not selective in its activity. Hence, Fenton's reagent is used in degradation of organic wastes (Gates-Anderson et al., 2001; Watts et al., 2000). Similar reactions could take place during treatment of asphaltenes with H_2O_2 as asphaltenes have been observed to contain significant amounts of iron in addition to other trace metals (Duyck et al., 2002).



Hydrogen peroxide is also commonly activated with carboxylic acids to form percarboxylic acid the most common of which is peracetic acid (Jones, 1999). Although industrially prepared peracetic acid is available, the reagent can be prepared *in situ* by direct mixing of acetic acid and hydrogen peroxide solution (e.g. (Liao et al., 2005)). Similarly, peracetic acid has been found to effectively oxidise several types of organic compounds, including aromatics, alkenes, alkynes, alkanes, alkanols as well as sulphur and nitrogen compounds through mechanism involving free radicals (N'guessan et al., 2004; Jones, 1999).

It therefore appears that contrary to claims of Liao and co-workers (Liao et al., 2006b; Liao and Geng, 2002), literature shows H_2O_2 -based reagents could degrade aliphatic hydrocarbon in addition to aromatics (N'guessan et al., 2006; N'guessan et al., 2004; Watts et al., 2000; Jones, 1999; Watts and Stanton, 1999; Augusti et al., 1998). There is therefore the possibility of alteration of the occluded saturated compounds that may be released via this method. However, in order to investigate this possibility further, experiments were conducted to investigate the effect of varying amounts of H_2O_2 /acetic reagent on mixture of representative aliphatic hydrocarbons (*n*-tricosane, *n*-hexatriacontane and androstane). The results show that about 45% of the hydrocarbons were lost to degradation relative to the control within 24 hours (Figure 4.5 (b)).



Nevertheless an attempt was made to use H_2O_2 /acetic acid reagent to degrade asphaltenes in order to recover the 'occluded' compounds. However to determine the amount of the reagent required to oxidise the aromatic moieties of the asphaltenes, further experiments were conducted on pyrene, as a representative aromatic hydrocarbon. The results reveal the compound was degraded at the rate of about $1.7\text{mg}/\text{cm}^3$ of the reagent (Figure 4.5 (a)). Extrapolation of this to asphaltenes, assuming that asphaltenes are about 30% aromatics (del Rio *et al.*, 1995), shows that degradation of 100 mg of asphaltenes requires about 17.6 ml of the reagent which is about twice the amount used by Liao *et al.* (2006). However, when asphaltene was treated with this proportion of the reagent, the asphaltene was observed to cluster together into lumps which did not dissolve or degrade even after 24 hours of continuous stirring. Based on these findings it was concluded that the reagent was not suitable for oxidative degradation of asphaltenes to release any occluded aliphatic hydrocarbons.

(b) *Potassium permanganate solutions*

Potassium permanganate (KMnO_4) solution has been widely used to degrade polyaromatic hydrocarbons (PAH), kerogen and coal to carboxylic acids (Gates-Anderson *et al.*, 2001; Rullkotter and Michaelis, 1990; Vitorović, 1980; Ward *et al.*, 1945). Literature on the use of KMnO_4 solution to degrade saturated hydrocarbons is however generally lacking. Nevertheless, Stewart (1965) and Lee (1969) observed that the reagent is barely effective in oxidative degradation of saturated hydrocarbons.

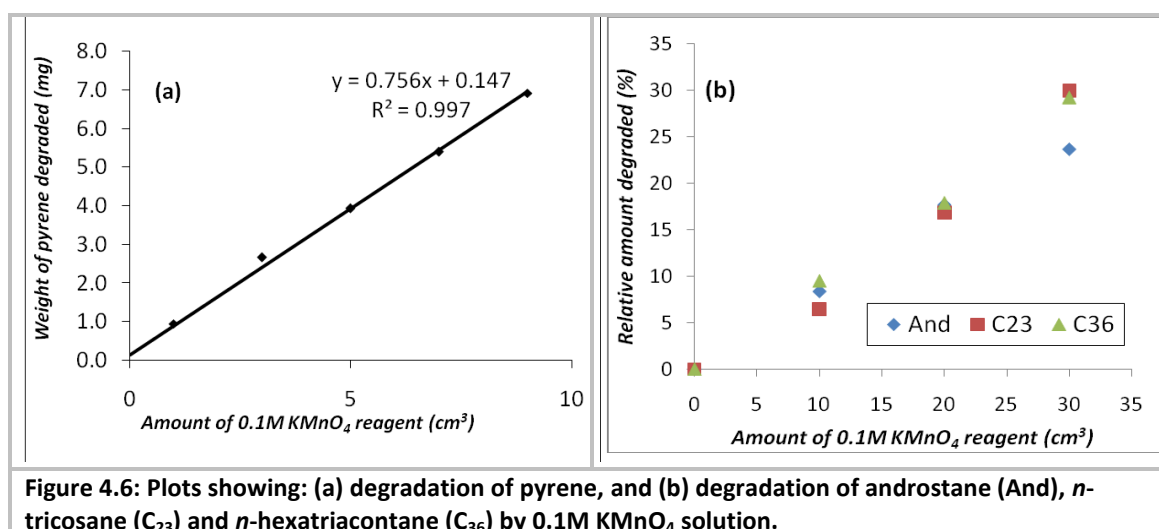


Figure 4.6: Plots showing: (a) degradation of pyrene, and (b) degradation of androstane (And), *n*-tricosane (C_{23}) and *n*-hexatriacontane (C_{36}) by 0.1M KMnO_4 solution.

Nonetheless, experiments were conducted to investigate the oxidative activity of the reagent on both aromatic, represented by pyrene, and saturated hydrocarbons, represented by *n*-tricosane (C_{23}), *n*-hexatriacontane (C_{36}) and androstane. The results show that about 0.18 to 1.19% of the aliphatic hydrocarbons were degraded per 1cm^3 of the reagent at room temperature in 24 hours (Figure 4.6 (b)). This is much lower than the 45% degraded by H_2O_2 /acetic acid reagent and confirms observations of Stewart (1965) and Lee (1969) that the reagent is barely effective against saturated hydrocarbons.

The action of acidic KMnO_4 solution on pyrene (an aromatic hydrocarbon) is rather different. The compound was degraded at about $0.9\text{mg}/\text{cm}^3$ of the reagent at room temperature (Figure 4.6 (b)). This suggests that about 35 ml of the reagent is required to degrade 100 mg of

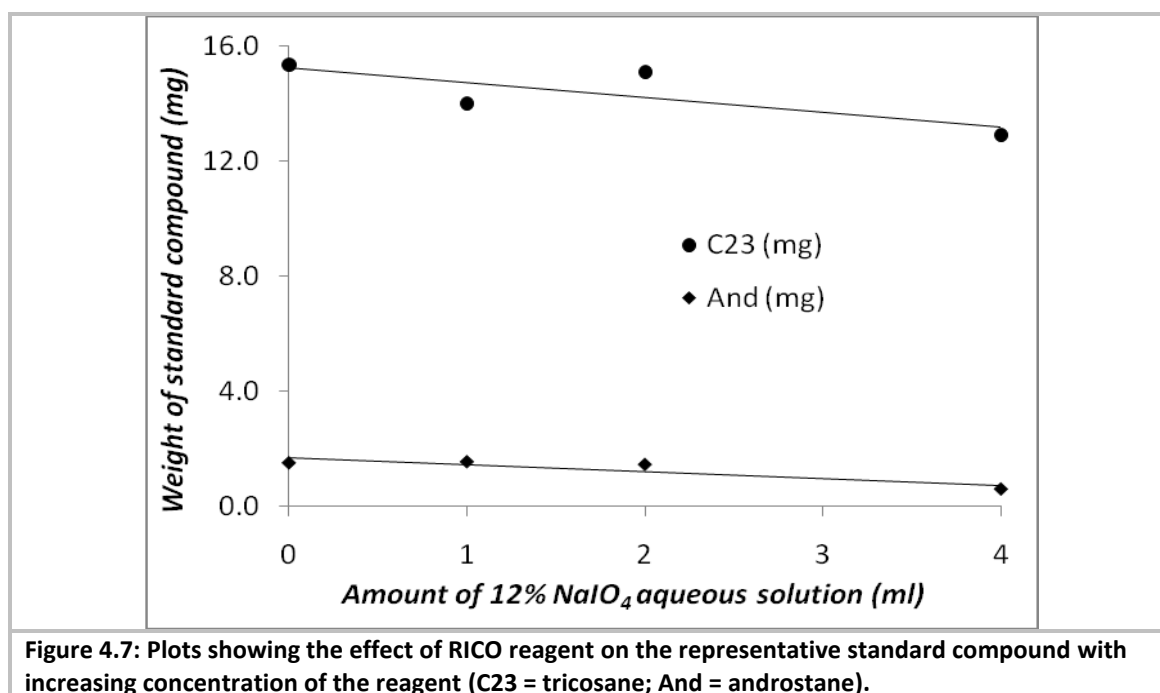
asphaltenes assuming it has 30% aromatic moieties. Treatment of an asphaltene sample with reagent resulted in complete dissolution and degradation of the asphaltenes.

(c) *Ruthenium ion catalysed oxidation*

Ruthenium ion catalysed oxidation (RICO) is a powerful technique for oxidative degradation of aromatic moieties. For example, Stock & Tse (1983) observed that while aromatic compounds were degraded with conversion of about 74 to 100%, more than 95% of saturated aliphatic hydrocarbon such as decane was recovered unchanged. Consequently, RICO is widely used to selectively degrade aromatic moieties in structural studies of coal, kerogen and asphaltenes (Peng *et al.*, 1999a; Standen *et al.*, 1991; Singleton *et al.*, 1985).

Nonetheless, to confirm the above observation and to further test the effect of RICO on cyclic saturated hydrocarbons, experiments were conducted accordingly. From these it was observed that while in all the experiments the aromatic hydrocarbon (pyrene) was completely degraded with none recovered, the saturated hydrocarbons, both acyclic *n*-tricosane and cyclic androstane, were quantitatively recovered (Figure 4.7).

Furthermore, the activity of the reagent was tested on asphaltenes. The results indicate complete degradation of the asphaltenes with the black asphaltenes solution in DCM changing to tan as observed by Peng *et al.* (1999a). However, recovering the 'occluded' saturated hydrocarbons was problematic. This required saponification of the aliphatic acids generated from the degradation of the aromatic moieties in order to solubilise them into the aqueous phase and then extract the released occluded hydrocarbons. However, separation of the two phases was found to be particularly difficult because of formation of foam by the long chain fatty acid salts formed from the saponification.



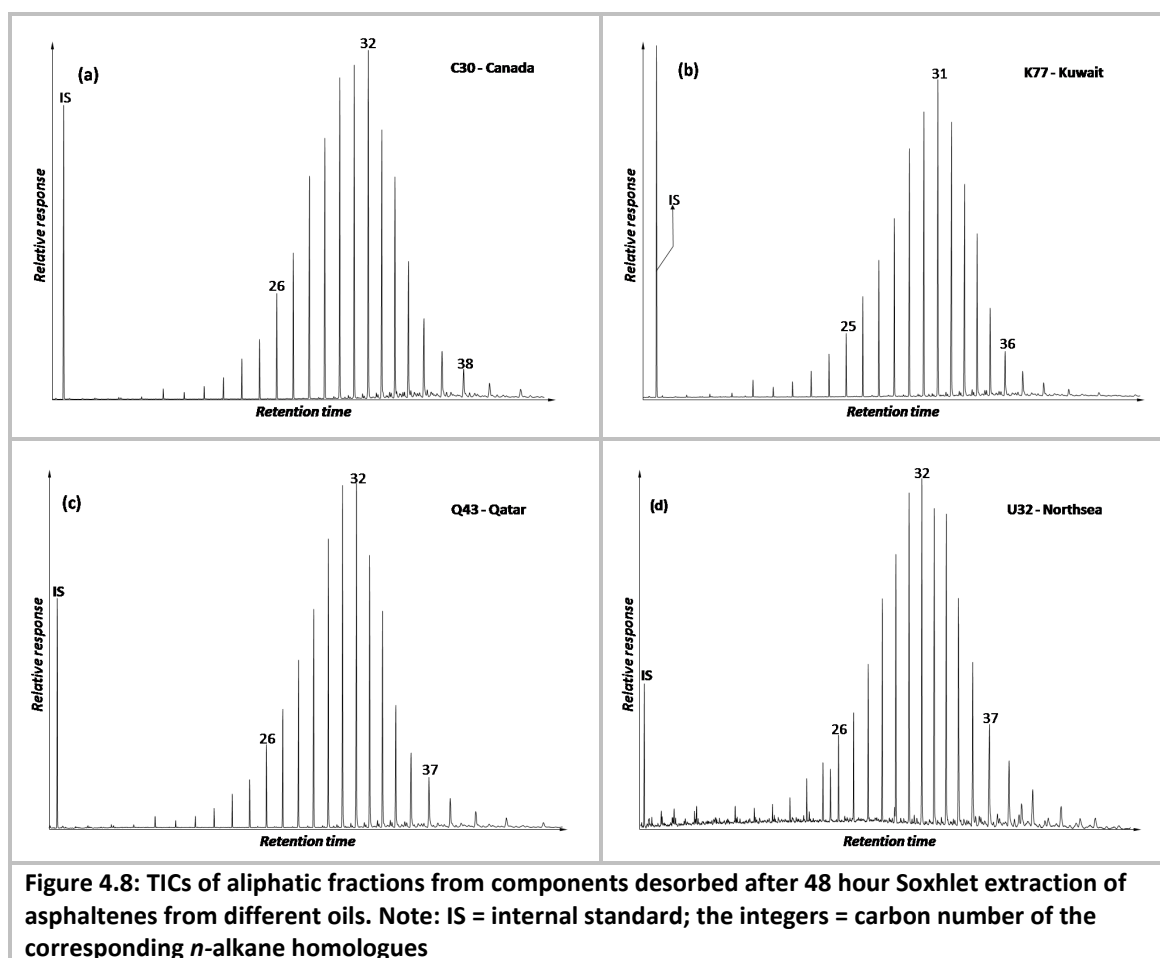
Consequently, although ruthenium ion catalysed oxidation was found to be the best oxidising agent in breaking down the asphaltene molecules/aggregates without affecting the saturated hydrocarbons, it was abandoned in preference of acidic potassium permanganate solution for

practical reason and for the fact that it is relatively more benign on the analytes compared to hydrogen peroxide/acetic acid reagent.

4.3.3 Comparative analysis of maltene, adsorbed and 'occluded' biomarkers

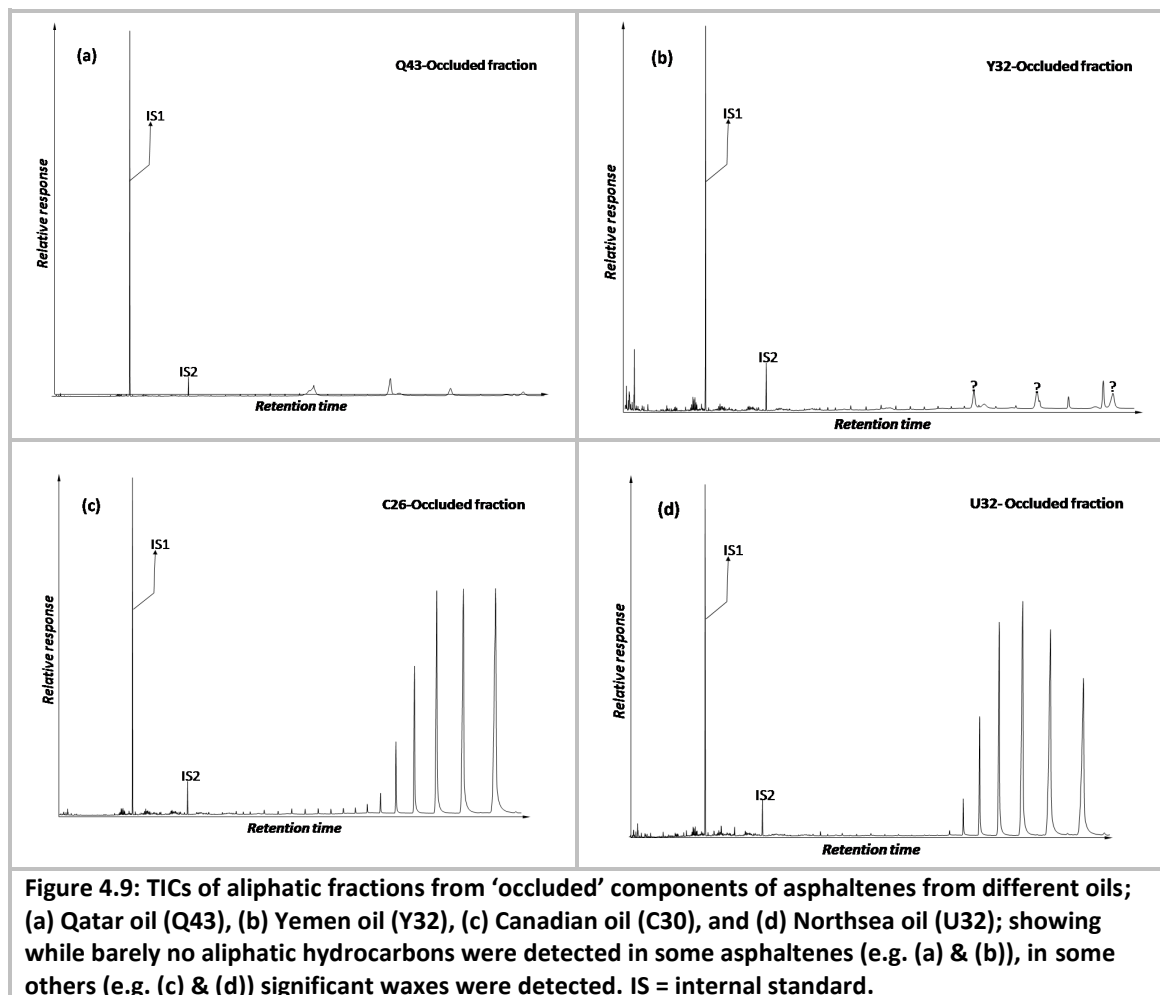
(a) *n*-Alkanes

As discussed in Section 4.3.1 the aliphatic fraction of components desorbed from asphaltenes by Soxhlet extraction is dominated by high molecular weight *n*-alkanes (waxes) ranging from C₂₀ to C₄₃. The distribution of the waxes from all the asphaltenes, irrespective of their sources, exhibits a symmetric unimodal distribution with maxima at C₃₃ to C₃₅ homologues (Figure 4.8). The isoprenoids pristane and phytane were not detected. This distribution is similar to the observation of Pan *et al.* (2002) although they used a different procedure. These authors conducted a series of dissolutions and precipitations (4 times) of the asphaltenes after initial precipitation from oil. Analysis of the aliphatic fraction from each step revealed a continuous increase in the proportions of the waxes while the lower molecular weight *n*-alkanes decrease such that the fourth fraction is dominated by the waxes in the range C₁₆ to C₄₂ with maxima at C₃₁ to C₃₃. Notably, in one of the samples (a biodegraded oil), although the maltene fraction contains only small amount of *n*-alkanes, the fourth and fifth fractions are dominated by waxes (Pan *et al.*, 2002).



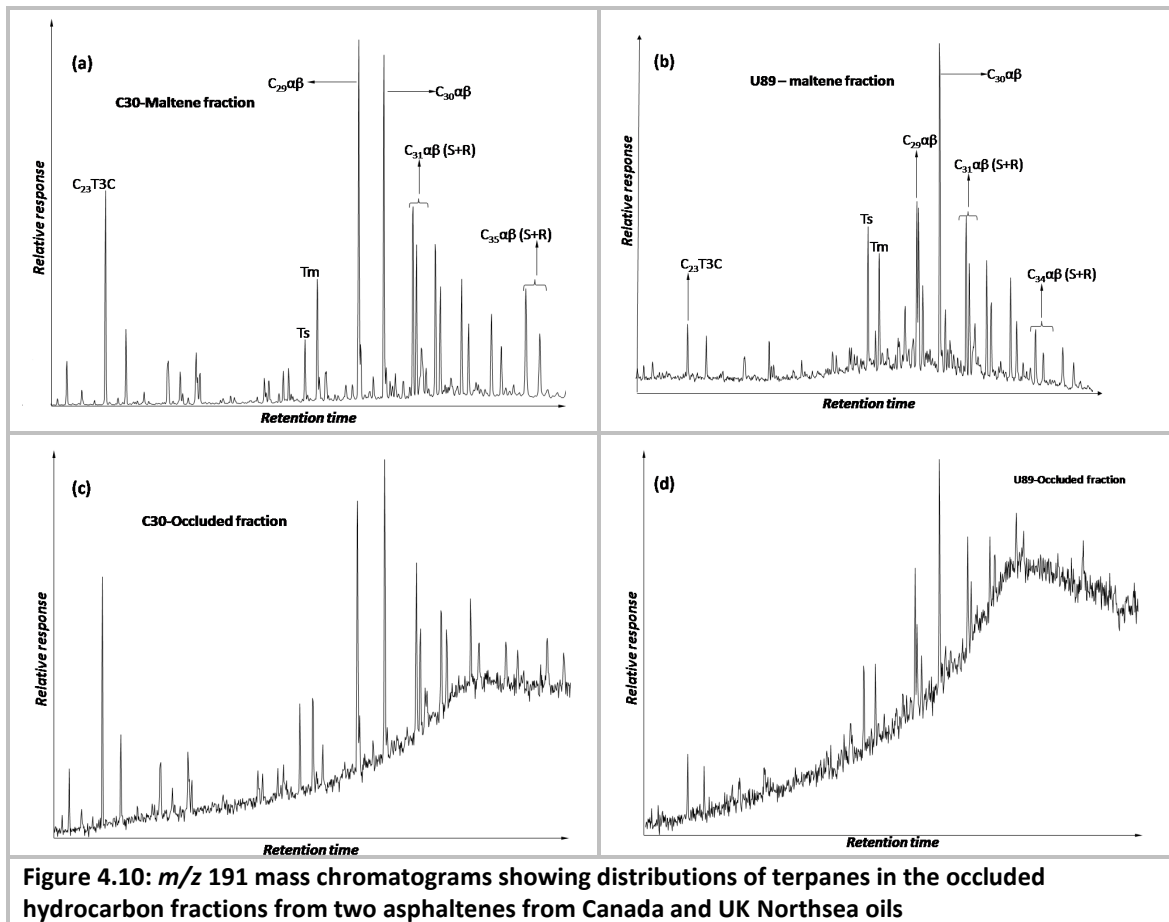
The *n*-alkane composition of the 'occluded' fraction of the asphaltenes is variable but in general only trace amount were detected in most of the samples. However, in some samples

such as asphaltenes from some Northsea and Canada oils, significant amount of waxes consisting mainly of C_{35} to C_{40} homologues were detected (Figure 4.9). The similarity in composition and distributions of these n -alkanes to those observed in the fifth extraction step of U56 asphaltenes (Section 4.3.1) suggests these n -alkanes are remnants of the adsorbed/co-precipitated waxes.



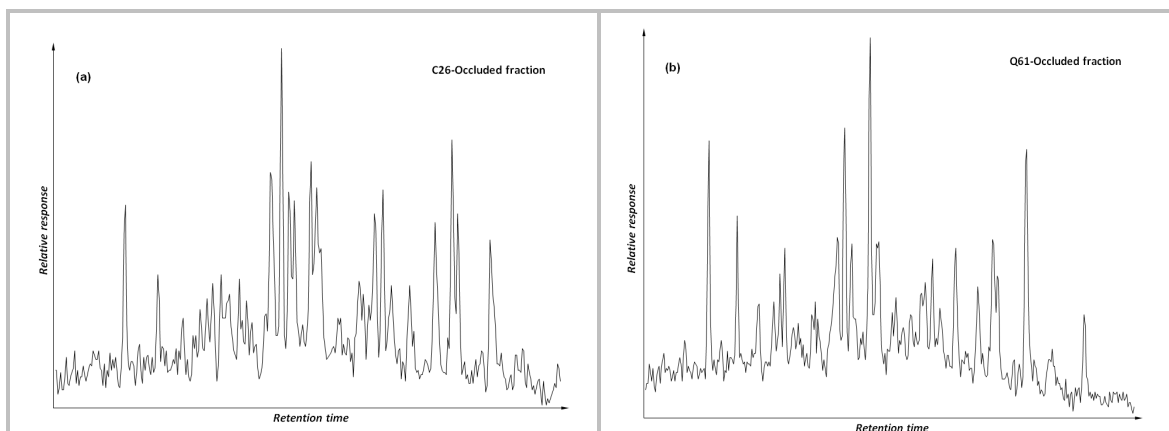
(b) Terpanes

All the terpanes detected in maltene fractions of oils were also detected in the corresponding adsorbed and occluded fractions. There is broadly a general agreement amongst the maltene, asphaltenes adsorbed and occluded fractions; samples, for example, that have relative high proportions of tricyclic terpanes in the free maltene, also exhibit high proportions of the compounds in the adsorbed and occluded asphaltenes fractions (Figure 4.10). In some samples, the C_{34} and C_{35} homohopanes were barely detectable. Similarly, although bisnorhopane (BNH) was detected in all the Northsea oils, it was not positively identified in the occluded fractions



(c) Steranes

Steranes were also present in both adsorbed and occluded hydrocarbon fractions. The homologues identified include C_{27} , C_{28} , C_{29} and, in some samples C_{30} steranes including both regular, $5(H)\alpha,14\alpha(H),17\alpha(H)$ and $5(H)\alpha,14\beta(H),17\beta(H)$, and diasteranes. The distributions of these compounds are similar to those from the corresponding free maltene oil fractions as shown in Figure 4.11 It is, however, noteworthy that the occluded fractions of asphaltens from oils (C_{26} and C_{30}) from Canada show enhanced diasteranes compared to other compounds.



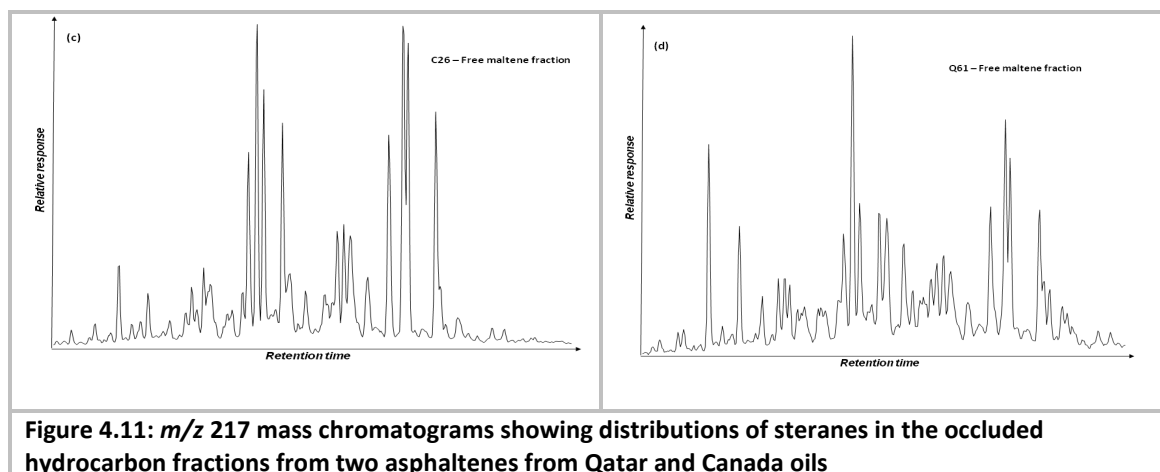


Figure 4.11: m/z 217 mass chromatograms showing distributions of steranes in the occluded hydrocarbon fractions from two asphaltenes from Qatar and Canada oils

(d) Maturity parameters

To compare and contrast the three fractions based on effect of maturation, typical parameters used for assessment of maturity of carbonaceous materials calculated from the three fractions (free maltene, adsorbed and occluded) are compared. $T_s/(T_s+T_m)$ shows no significant difference among the fractions in some of the samples (Q61, C30 and BN) (Table 4.1). Where significance difference was observed, it is rather not systematic and cannot therefore be attributed to either adsorption or occlusion. For example, for this parameter occluded-based > maltene-based > adsorbed-based for B58 while the reverse is the case for Y32 and U54 (also compare C26 and Q43) (Table 4.1).

Homohopane-based maturity parameter ($22S/(22S+22R)$) for both C_{31} and C_{32} homologues do not display any significant differences among the fractions (Table 4.1). The only exception is the biodegraded Northsea oil BN which shows low value (0.43) of the parameter from occluded fraction. On the other hand, although there is significant differences among different fraction with respect to C_{29} sterane-based maturity parameter ($20S/(20S+20R)$), the differences are not systematic or consistent and cannot therefore be reliably attributed to either adsorption or occlusion by the asphaltenes.

Comparison of the $\beta\beta/(\beta\beta+\alpha\alpha)$ parameter among the three fractions also shows the maltenes are generally in agreement with the corresponding occluded fractions in all the samples; and adsorbed fractions for some samples. The adsorbed fractions from Canadian oils C26 and C30; and Qatar oils Q43 and Q61, however, display significantly lower values of the parameter compared to the maltene and occluded fractions (Table 4.1).

Table 4.1: Some maturity-related parameters calculated from biomarker contents of maltene (M), adsorbed (A) and occluded (O) aliphatic contents.

Samples	Ts/Tm	C ₂₉ αβ/C ₂₉ Ts	αββ/(αββ+ααα) C ₂₇	20S/(20S+20R) C ₂₇ ααα	20S/(20S+20R) C ₂₉ ααα
BNA	1.26	0.54	0.46	0.42	0.41
BNM	1.23	0.55	0.67	0.57	0.49
BNO	1.33	0.38	0.45	0.45	0.45
C26A	0.79	0.17	0.52	0.57	0.43
C26M	0.59	0.16	0.65	0.53	0.47
C26O	0.80	0.26	0.49	0.41	0.46
C30A	0.64	0.24	0.59	0.50	0.41
C30M	0.65	0.17	0.65	0.46	0.50
C30O	0.67	0.22	0.56	0.44	0.47
Q43A	1.19	0.25	0.59	0.51	0.45
Q43M	1.20	0.36	nd	nd	0.50
Q43O	1.41	0.43	0.54	0.52	0.45
Q61A	1.36	0.42	0.62	0.49	0.44
Q61M	1.35	0.43	nd	nd	0.51
Q61O	1.38	0.43	0.42	0.30	0.34
U54A	1.25	0.43	0.41	0.39	0.36
U54M	0.99	0.40	0.42	0.48	0.36
U54O	0.81	0.43	0.43	0.44	0.33
Y32A	1.49	0.43	0.52	0.43	0.48
Y32M	1.04	0.44	0.68	0.54	0.57
Y32O	0.94	0.44	0.39	0.39	0.43
B58A	0.76	0.37	0.54	0.47	0.48
B58M	1.29	0.42	0.67	0.65	0.56
B58O	1.58	0.35	0.43	0.42	nd

About 50% of the samples (Y32, U54, Q61 and B58) in Table 4.1 show agreement amongst the maltene, adsorbed and occluded fractions with respect to C₂₉/C₂₉Ts maturity parameter. Other samples, however, show variable disagreement amongst the fractions on this parameter. For example, while for Q43, occluded-based > maltene-based > adsorbed-based; BN occluded-based < maltene-based ~ adsorbed-based (see also C30 and C26, Table 4.1). In general, the variability is also inconsistent and difficult to be attributed to either occlusion or adsorption.

(e) Source parameters

The ratio of C_{29} to C_{30} hopanes ($C_{29}/C_{30} \alpha\beta$) is an important parameter for the identification of depositional environments of petroleum source rocks (see Section 3.3.3). For most of the samples the values of the parameter are similar amongst the fractions (Table 4.2) and therefore lead to same conclusions with respect to the depositional environments of the oils. Exceptions are B58 and BN for which occluded and adsorbed fractions have significantly high values that may lead to erroneous classification of the oils as marine carbonate (*cf.* Section 3.3.3 (d)).

On the other hand, C_{31R}/C_{30} ratio is used to distinguish marine from non-marine depositional environments. The values of the parameter show agreement amongst the fractions for 75% of the samples analysed (Table 4.2). Nevertheless, even in samples that have significant differences in absolute values of the parameter amongst the fractions, the same conclusion would be arrived at with respect to the marine environment of the oils.

Table 4.2: Some source and age-related parameters calculated from biomarker contents of maltene (M), adsorbed (A) and occluded (O) aliphatic contents.

Samples	C ₃₀ /C ₂₉ αβ	C ₃₁ R/C ₃₀ αβ	C ₃₁ /C ₃₁ -C ₃₅	C ₃₂ /C ₃₁ -C ₃₅	C ₃₃ /C ₃₁ -C ₃₅	C ₃₄ /C ₃₁ -C ₃₅	C ₃₅ /C ₃₁ -C ₃₅	C ₃₅ /C ₃₄ αβ	C ₂₇ /C ₂₉ αββ	C ₂₇ /C ₂₇ -C ₂₉	C ₂₈ /C ₂₇ -C ₂₉	C ₂₉ /C ₂₇ -C ₂₉	Dia/(Dia+Reg)
BNA	2.09	0.37	0.41	0.24	0.19	0.17	0.00	0.00	0.93	0.36	0.26	0.38	0.27
BNM	1.72	0.38	0.29	0.22	0.19	0.15	0.15	1.04	1.06	0.37	0.28	0.35	0.38
BNO	1.28	0.34	0.29	0.17	0.19	0.20	0.15	0.74	1.15	0.40	0.24	0.35	0.32
C26A	0.80	0.41	0.31	0.26	0.13	0.12	0.18	1.54	0.55	0.31	0.13	0.56	0.14
C26M	0.92	0.45	0.31	0.22	0.14	0.13	0.19	1.43	0.85	0.40	0.14	0.47	0.10
C26O	0.91	0.44	0.28	0.25	0.14	0.15	0.18	1.19	0.85	0.39	0.16	0.46	0.26
C30A	1.04	0.34	0.29	0.25	0.16	0.14	0.16	1.19	0.64	0.34	0.13	0.53	0.09
C30M	0.97	0.42	0.28	0.21	0.16	0.14	0.21	1.48	0.73	0.35	0.17	0.48	0.10
C30O	1.12	0.39	0.29	0.23	0.18	0.13	0.17	1.29	0.71	0.33	0.19	0.47	0.26
Q43A	0.87	0.43	0.39	0.24	0.15	0.11	0.10	0.90	0.91	0.39	0.18	0.43	0.30
Q43M	1.07	0.52	0.36	0.25	0.18	0.11	0.11	1.04	0.67	0.34	0.16	0.50	0.53
Q43O	1.22	0.37	0.31	0.22	0.16	0.14	0.17	1.20	0.86	0.36	0.22	0.42	0.37
Q61A	1.23	0.40	0.36	0.26	0.15	0.11	0.12	1.10	0.72	0.35	0.15	0.49	0.34
Q61M	1.06	0.43	0.34	0.25	0.16	0.13	0.13	0.99	0.76	0.37	0.15	0.48	0.53
Q61O	1.19	0.40	0.32	0.23	0.19	0.12	0.13	1.08	0.69	0.33	0.19	0.48	0.34
U54A	2.10	0.33	0.36	0.23	0.19	0.13	0.09	0.69	1.12	0.39	0.26	0.35	0.36
U54M	1.96	0.38	0.34	0.23	0.20	0.11	0.10	0.91	0.98	0.36	0.27	0.37	0.34
U54O	2.22	0.37	0.32	0.21	0.20	0.13	0.13	1.07	0.96	0.36	0.27	0.37	0.37
Y32A	2.04	0.35	0.33	0.21	0.19	0.12	0.15	1.30	0.89	0.37	0.22	0.41	0.36
Y32M	2.27	0.34	0.37	0.25	0.19	0.11	0.08	0.74	0.86	0.38	0.19	0.44	0.39
Y32O	1.98	0.33	0.34	0.24	0.16	0.12	0.14	1.17	0.89	0.35	0.26	0.39	0.36
B58A	1.65	0.36	0.34	0.22	0.16	0.14	0.14	1.03	0.76	0.35	0.19	0.46	0.37
B58M	2.10	0.35	0.37	0.25	0.18	0.12	0.09	0.79	0.95	0.39	0.20	0.41	0.40
B58O	1.13	nd	0.35	0.45	0.20	0.00	0.00	0.47	0.93	0.32	0.33	0.35	0.39

Furthermore, the Dia/(Dia+Reg) sterane parameter used to differentiate between shale and carbonate petroleum source rocks also shows similar values amongst the fractions irrespective of the sample (Table 4.2). The Canadian samples (C26 and C30) however, have low values of the parameter for occluded fraction compared to the adsorbed and maltene fractions. For these samples, the diasteranes are relatively enriched in the occluded fraction (Table 4.2).

The ratio of C₂₇ to C₂₉ steranes is commonly used as an age discrimination parameter. The values of this parameter for all the fractions are comparable in almost all the samples (Table 4.2). The adsorbed fractions however have significantly low values compared to the maltene and occluded fractions in samples C26 and C30.

The above observations are generally true of other biomarker parameters (e.g. Figure 4.12). There is reasonable agreement between cyclic biomarker indices from the free, adsorbed and

'occluded' fractions of any given sample (Table 4.2); differences among values are rather unsystematic and could not be attributed to any physical phenomena under investigation (i.e. adsorption or occlusion). The differences could therefore be due to random error in analysis. Most importantly, same geochemical conclusions would be reached from the biomarker indices of the three fractions of a given oil sample in most cases.

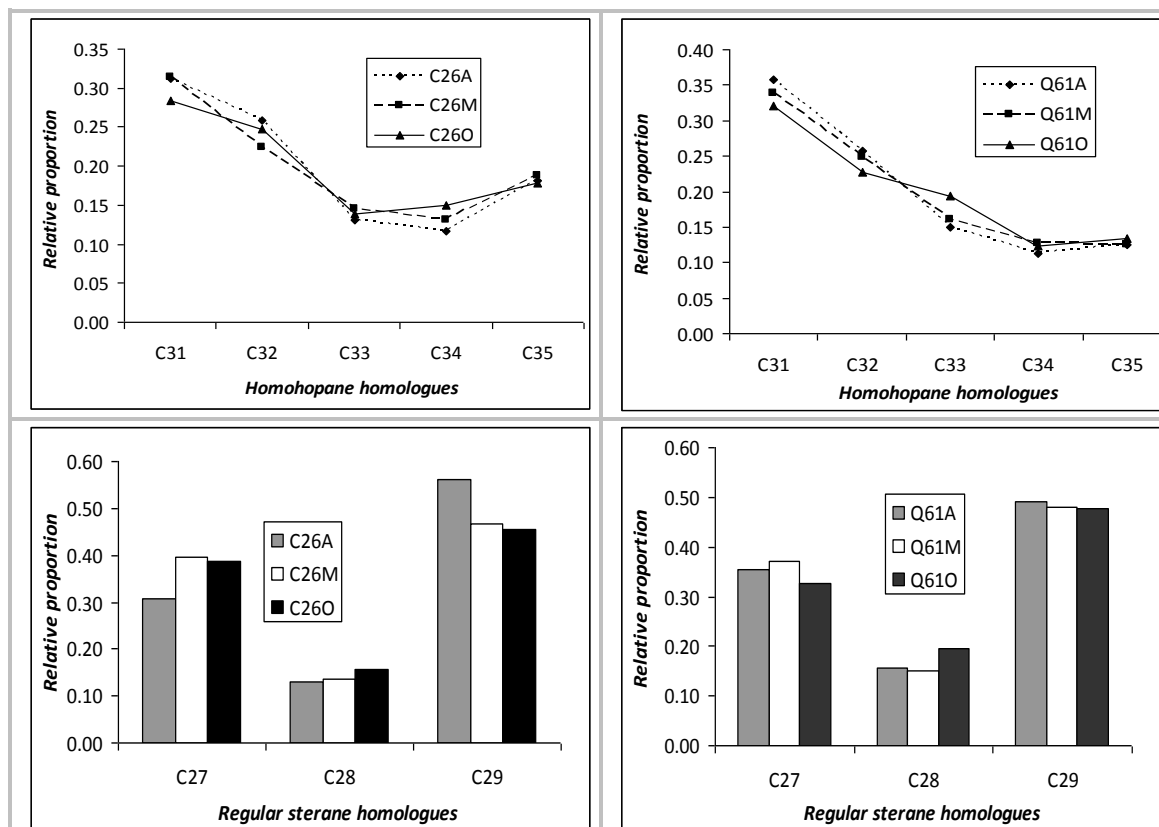


Figure 4.12: Top are line plots distributions of homohopanes and bottom are bar charts showing distribution of steranes from maltene (M), adsorbed (A) and occluded (O) fractions from two asphaltenes from Canada (C26) and Qatar (Q61) oils

4.3.4 Simulation of occlusion of hydrocarbons in asphaltenes

Results of the occlusion experiment revealed none of the added marker compounds was detected in the 'occluded' fraction following chemical degradation of the asphaltenes after ten days of Soxhlet extraction. This observation suggests that there was no dynamic contact between the occluded compounds and free compounds in the maltene. The occluded compounds appear to be encapsulated and the added marker compounds although dissolved in the maltene could not penetrate the asphaltene structural network or aggregate. This apparently supports the 'occlusion' hypothesis.

Although this is the most obvious interpretation of the observation, it however does not account for other observations such as:

1. Absence of smaller molecules in the occluded fraction. The smaller the compounds the greater the chance of being occluded since smaller compounds such as low molecular weight *n*-alkane occupy less space

- Absence of any systematic difference between the biomarkers in the so-called occluded fraction and free maltene fraction
- Stepwise extraction did not show any clear demarcation between adsorbed and occluded fractions
- Predominant presence of waxes in the occluded fractions of many asphaltenes. Stepwise Soxhlet extraction of the asphaltenes suggests such waxes are remnants (i.e. the 'tail end') of the waxes observed in the adsorbed fraction

The observations, and in particular 3 and 4, suggest the so-called occlusion is solubility controlled co-precipitation rather than entrapment and protection controlled by the structure or aggregation of asphaltenes molecules. Experimental solubility data show that the solubility of *n*-alkanes in a given solvent is dependent on the solvent, the molecular weight of the *n*-alkane and temperature (Jennings and Weispenning, 2005). In general, the lower the molecular weight of the solvent the more of the solute *n*-alkane it dissolves at any particular temperature. On the other hand, in any particular solvent (e.g. toluene) the solubility increases with temperature and decreases with molecular weight of the solute *n*-alkane (Figure 4.13). Note from Figure 4.13(a) that at 20 °C *n*-hexatricontane (C₃₆H₇₄) and higher homologues are practically insoluble in toluene which has similar solubility properties as *n*-heptane (Jennings and Weispenning, 2005).

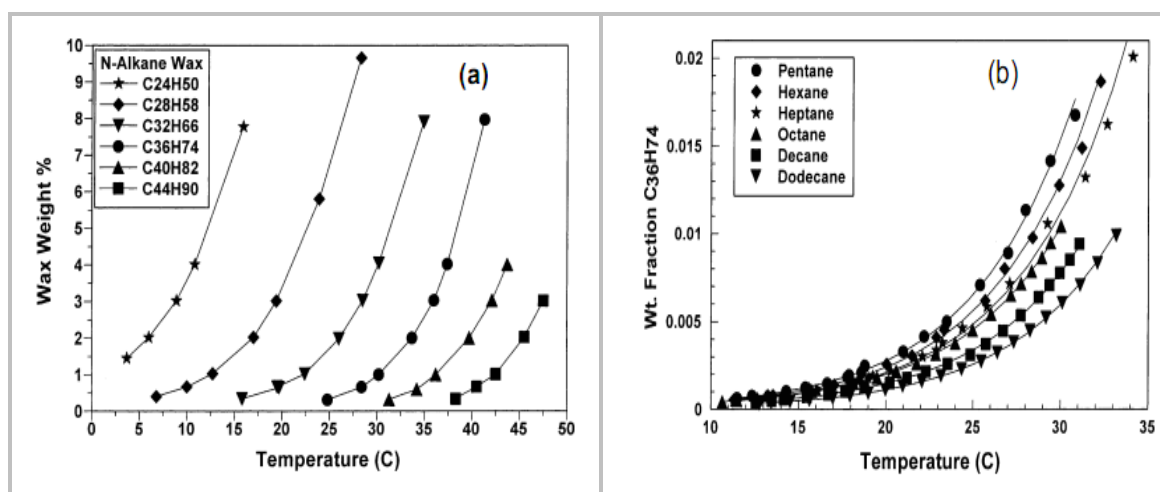


Figure 4.13: (a) shows the effect of molecular weight of *n*-alkanes and temperature on the solubility of the *n*-alkanes (b) shows the effect of solvent and temperature of solubility of *n*-hexatricontane (from Jennings & Weispenning (2005))

This supports the solubility influence on the precipitation properties of waxes and other components in petroleum. On addition of the precipitation solvent (e.g. *n*-hexane) equilibrium is established between the solubilised and precipitated phases based on solubility properties of the solutes. Greater proportions of the more soluble components (e.g. low molecular weight *n*-alkanes) remain in the solubilised phase while greater proportion of the less soluble components (e.g. waxes) are found in the precipitated phase. Thus relatively more waxes precipitate out with the asphaltenes. When the asphaltenes are re-dissolved and precipitated with fresh solvent, the solubilised phase is enriched in the waxes compared to the lower molecular weight homologues in the previous cycle. This explains the observation of Pan *et al.* (2002) that more high molecular weight *n*-alkanes relative to the lower molecular weights are

found with increasing washings. It also explains the observation in this work that maxima of waxes from stepwise extraction shifts towards higher molecular weight homologues and only these higher weights homologues were predominantly found in the so-called occluded fraction. This may also be why the marker compounds used in the occlusion experiment were not detected in the occluded fraction. It is believed that the cyclic biomarkers observed in the occluded fraction are remnants of those in the free maltene that co-precipitated with the asphaltenes.

4.4 Summary and Conclusions

Occlusion of compounds, in particular biomarkers, is a very promising hypothesis particularly in the study of extensively biodegraded oils if established. The hypothesis is critically investigated to assess its validity or otherwise. Specifically, the extent of Soxhlet extraction required to remove adsorbed/co-precipitated components from asphaltenes, and the most suitable chemical degradation method for recovering the occluded compounds were investigated. Furthermore, simulation experiments were conducted to test the occlusion hypothesis and hydrocarbon compositions of the maltene adsorbed and occluded fractions were compared to investigate whether the differences amongst the fractions are significant. Results of the investigation reveal the following:

1. Sequential stepwise Soxhlet extraction of asphaltenes reveals an asymptotic pattern not only with respect to the total amount of component desorbed but also with respect to the *n*-alkanes recovered which suggests there is no clear demarcation between adsorbed and occluded components
2. The adsorbed components from all the asphaltenes are dominated by waxes in the range C₂₀ to C₄₂. The occluded components, on the other hand, are also dominated by the waxes in the range C₃₆ to C₄₂ in some of the samples.
3. Among the three reagents investigated, acidified potassium permanganate solution was found to be practically the most suitable. Hydrogen peroxide solution with acetic acid was observed to significantly attack saturated hydrocarbons.
4. Comparative analysis of the saturated hydrocarbon components in maltene, adsorbed and occluded fractions revealed clear differences in distributions of the *n*-alkanes amongst the fractions. However, maturity and correlation indices calculated from the biomarkers of the fractions show general agreement amongst them. Where differences were observed, they were unsystematic and could not therefore be attributed to either adsorption or occlusion.
5. The so-called occlusion of compounds by asphaltenes is most likely a consequence of co-precipitation controlled by solubility properties of the compounds in addition to temperature and solvent properties.

Chapter 5 Bulk Composition and Structure of Asphaltenes by FTIR and NMR

5.1 Introduction

Infrared spectroscopy and nuclear magnetic resonance spectroscopy are among the most powerful tools available to the chemist for investigation of structure and composition of chemical substances. The infrared spectroscopy is based on the differential interaction of chemical bonds with the infrared radiation while the nuclear magnetic resonance spectroscopy exploits differential interaction of magnetic moments of atomic nuclei with radio frequencies.

The infrared is part of the spectrum of electromagnetic radiation between the high frequency end of the visible region to the low frequency end of the microwave region. Specifically, it covers the electromagnetic waves with wavelength between 0.78 to 1000 μm (13000 to 10 cm^{-1}). The IR region is further divided into near IR (NIR) covering 0.78 – 2.5 μm (13000 – 4000 cm^{-1}); mid IR (MIR) covering 2.5 – 25 μm (4000 – 400 cm^{-1}); and far IR (FIR) covering 25 – 1000 μm (400 – 10 cm^{-1}). Although all these regions have applications in the chemical sciences, MIR was specifically used in this study because of its application in determination of functional groups in chemical systems (Bellamy, 1975; Nakanishi, 1962).

The IR spectrum of a compound consists of a series of absorption (or emission) bands of variable intensities. Ideally, each absorption band in the spectrum corresponds to a vibrational transition within the molecule, and gives the position of absorption and intensity of the frequency at which the vibration occurs. Thus, as different bonds have different vibrational characteristics (because of differences in bond strength and masses of atoms connected); they absorb at different frequencies and therefore each absorption band provides structural information about the molecule. The absorptions are however affected by the chemical environment of the bond. Consequently, the IR spectrum is a molecular fingerprint with unique information on the molecule (Nakanishi, 1962).

IR, and in particular the preferred and more versatile (Thermo Nicolet, 2001) Fourier transform IR (FTIR) spectroscopy has been widely used in the study of carbonaceous materials (e.g.: Ibarra et al., (1996); Cerný (1996); Holmgren and Norden (1988); Haberhauer and Gerzabek (1999); Petersen et al. (2008); Christy et al. (1989); Calemma et al. (1995)). The studies cover applications ranging from quantitative estimation of bulk components to qualitative and quantitative interrogation of structural features. Wilt and Welch (1998), for example, used FTIR and partial least squares (PLS) analysis on crude oils to develop models for quantitative estimation of asphaltene content of the oils with excellent prediction potentials. Similarly, Sarya et al. (2007) successfully used combination of FTIR in the NIR region and chemometrics (PCA & PLS) to develop models for prediction of bulk properties (carbon residue, density, average molecular weight, sulphur, nitrogen, saturates, aromatics, resins and asphaltenes) of crude oils (see also (Aske et al., 2001; Wilt et al., 1998; Honigs et al., 1985)).

Most of the structural investigations of carbonaceous materials are, however, mainly on coal structural chemistry (e.g. Ibarra et al. (1996); Geng et al. (2009); Cerný, (1996); Holmgren & Nord, (1988); Guillen et al. (1992); Painter et al., (1981)). For example, Ibarra et al. (1996)

studied the maturity evolution of structural features of coals using FTIR. With the help of a curve fitting algorithm, they were able to deconvolute each spectrum into composite absorption bands more or less specific for individual chemical features that make up the coal structures. From this, among other things, they observed increasing aromaticity with increasing maturation and progressive conversion of aliphatic carboxylic groups into aromatic carbonyl groups (Ibarra et al., 1996).

Investigations of asphaltene structure using FTIR are rather inadequate. Most of the work is limited to obtaining spectra of the asphaltenes and, in some cases, computing therefrom ratios of some peaks without detailed investigation of the information such spectra may contain. An exception, however, is the work of Coelho et al. (2007). This work, although limited to aromatic features, employed FTIR analysis, together with curve fitting techniques and computational chemistry, to characterise the aromatic functionalities in the 2900 – 3100 cm^{-1} and 700 – 900 cm^{-1} regions of the asphaltenes and resins.

Investigation of asphaltenes using NMR, and particularly using solid-state NMR, is even scantier. However, the method has been extensively used to elucidate the distribution of carbon in coals (Wilson and Vassallo, 1985; Sullivan and Maciel, 1982). Traditionally quantitative determination of distribution of carbon in carbonaceous materials using dipolar dephasing cross polarisation ^{13}C NMR with magic angle spinning (CP/MAS ^{13}C NMR) require measurements at multiple dephasing time (Wilson and Vassallo, 1985) which is requires alot of spectrometer time. Wilson et al. (1984) has shown that it is possible to estimate some important structural parameters of coal using CP/MAS ^{13}C NMR at just two dipolar dephasing times; $t = 0$ and $t = 40 \mu\text{s}$. Measurement at $t = 0$ gives the total aliphatic and aromatic carbon from which the aromaticity factor, f_a can be calculated. The measurement at $t = 40 \mu\text{s}$, on the other hand, gives mainly signals from quaternary aromatic carbon and a combination of tertiary and primary aliphatic carbon (Wilson et al., 1984; Murphy et al., 1982) and allow for estimation of other structural parameters (equation 5.1 to 5.5) such as fractions of the aromatic carbon that is protonated (i.e. tertiary aromatic carbon, $f_a^{a,H}$) and nonprotonated (quaternary aromatic carbon, $f_a^{a,N}$); fraction of the total carbon that is protonated (f_a^H) and nonprotonated (f_a^N); as well as the fraction of the total hydrogen present in the aromatic systems (H_a) (Wilson et al., 1984).

$$f_a = \frac{A}{T} = \frac{N + P}{T} = \frac{1.21n + P}{T} = \frac{(1.21)(0.88)M + P}{T} \quad 5.1$$

$$f_a^{a,H} = \frac{P}{T} \quad 5.2$$

$$f_a^{a,N} = 1 - f_a^{a,H} \quad 5.3$$

$$f_a^H = f_a^{a,H} * f_a \quad 5.4$$

$$H_a = (C/H) * f_a^{a,H} * f_a \quad 5.5$$

Where A , N , P and T are the signal intensity of aromatic carbon at $t = 0$, signal intensity of nonprotonated aromatic carbon at $t = 0$, signal intensity of protonated aromatic carbon at $t = 0$, and is the total signal intensity of carbon at $t = 0$, respectively. M is the measured signal intensity of aromatic carbon at $t = 40 \mu\text{s}$.

Although the values of the parameters obtained for the equations above are less accurate than those obtained from measurements at multiple t (sometimes by up to 15%), the figures are good and are useful for comparison purposes.

Therefore this section of the work is generally aimed at the investigation of the bulk composition and structure of asphaltenes using FTIR and solid-state NMR. Specific objectives include:

1. to identify the various functional groups in asphaltenes
2. to investigate the changes in composition of asphaltenes with their thermal evolution
3. to investigate variations in chemical composition from different asphaltenes
4. to compare and contrast the chemical composition of asphaltenes from oils, black shales, and coals
5. to explore/develop a classification system of oils from asphaltene FTIR spectra

5.2 Methodology

5.2.1 Samples and sample preparation

Samples were selected to enable coverage of the above objectives. The samples selected for this study are shown in Table 5.1. They consist of asphaltenes from oils, coal bitumen and source rock bitumen. The results of the preliminary characterisation of these samples were presented in Chapter 3. The oils obtained from different geographical regions of the world including United Kingdom, North America, Middle East etc., and depositional environment including marine carbonate, marine marls, marine shales etc.

Coal samples, C04, C56, C69 and C15, with vitrinite reflectance 0.40, 0.56, 0.69 and 1.50% respectively were from Northsea coal deposits. These were selected to investigate the thermal evolution of the asphaltenes. The black shale samples were obtained from the Batra Formation, Jordan (2 samples); Kimmeridge Clay, UK (1 sample) and Tanezzuft Formation, Libya (16 samples) all deposited under marine stratified anoxic settings. However, while the Batra black shale and Kimmeridge Clay were immature, the Tanezzuft black shale was marginally mature. Bitumen from the coals and black shales samples were recovered by Soxhlet extraction as described in Section 2.3.2. The asphaltenes from the oils and bitumen were recovered and Soxhlet extracted to remove co-precipitated maltenes as outlined in Section 2.3.3.

Table 5.1: List of some the samples used in the FTIR and NMR analysis of asphaltenes

SN	Sample ID	Country	Field	Org. Matter	Dep. Environment
1	AR3	Gulf of Mexico	-	Marine	-
2	A39	Abu Dhabi	-	-	-
3	B58	Bangladesh	Habigong	Marine	Marine shale
4	BN	Northsea, UK	-	Marine	Marine shale
5	C26	Canada	Midale	Marine	Marine carbonate
6	C30	Canada	Midale	Marine	Marine carbonate
7	CH	Canada	-	Marine	Marine carbonate
8	FN	Northsea, UK	Veslefrikk	Marine	Marine shale
9	K77	Kuwait	Raudhatain	Marine	Marine carbonate
10	K78	Kuwait	Sabriyah	Marine	Marine carbonate
11	U01	Northsea, UK	Kittiwake	Marine	Marine shale
12	U05	Northsea, UK	Kittiwake	Marine	Marine shale
13	NA1	Serbia	Gaj	-	-
14	NA2	Serbia	Gaj	-	-
15	NB	Nigeria	-	-	-
16	O28	Oman	Natih	Marine	Marine marl
17	O31	Oman	Natih	Marine	Marine marl
18	Q43	Qatar	Al Shaheen	Marine	Marine marl
19	Q61	Qatar	Bul Hanine	Marine	Marine marl
20	U02	Northsea, UK	Flora	Marine	Marine shale
21	U56	Northsea, UK	Alder	Marine	Marine shale
22	U07	Northsea, UK	Fergus	Marine	Marine shale
23	U16	Northsea, UK	Captain	Marine	Marine shale
24	U54	Northsea, UK	Ettrick	Marine	Marine shale
25	U59	Northsea, UK	Bruce	Marine	Marine shale
26	U68	Northsea, UK	?	Marine	Marine shale
27	U84	Northsea, UK	Nelson	Marine	Marine shale
28	U89	Northsea, UK	Britannia	Marine	Marine shale
29	U93	Northsea, UK	Gannet West	Marine	Marine shale
30	Y32	Yemen	Hemiar	Marine	Marine shale

FTIR analyses were carried out in transmission mode (Section 2.4.10). Pellets of the asphaltene samples were prepared as described in Section 2.3.12. Precision of the FTIR measurements was gauged by statistical analysis of triplicate measurements on a pellet of sample U54. In order to assess the repeatability of the analysis triplicates of K78 (an oil asphaltene) and T28 (a black shale asphaltene) were prepared and analysed with the analytical samples. Relative standard error of the mean was calculated to estimate the level of error in the analysis. Asphaltenes were also precipitated from an oil (U56) using *n*-pentane, *n*-hexane and *n*-heptane respectively to investigate the effect of hydrocarbon solvent used in the precipitation on the chemical composition of the asphaltene.

5.2.2 Pre-processing and curve fitting of FTIR spectra

The FTIR spectra obtained from the asphaltenes were pre-processed (Beebe et al., 1998; Maddams, 1980) before curve-fitting and further analysis by multivariate chemometric methods. The spectra were baseline linearised using multi-point option and adjusted to zero absorbance. Smoothing, to reduce noise in the data, was performed using Savitzky-Golay algorithm (Savitzky and Golay, 1964) with second degree polynomial convolution function at 15 points on GRAMS/AI platform. However, to ensure the structural features of the spectra were not significantly altered by oversmoothing fine bands were monitored during the smoothing (Smith, 1996). Figure 5.1 compares the original (unsmoothed) spectrum and the smoothed spectra at different points.

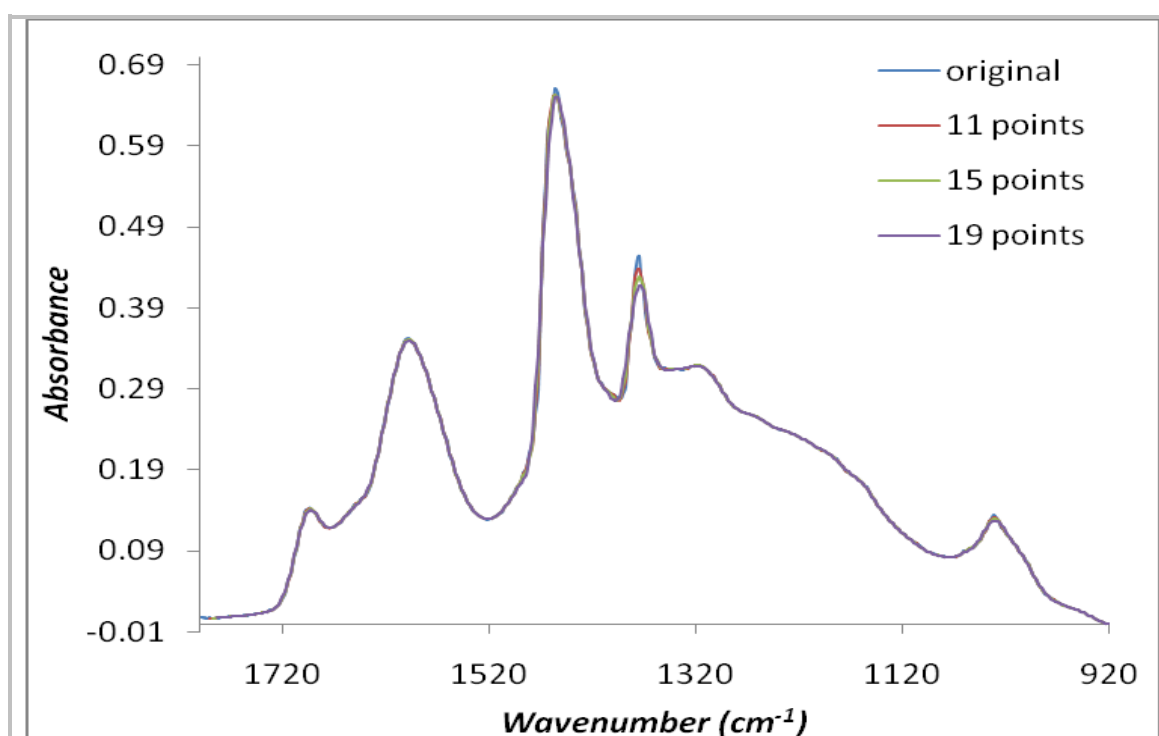


Figure 5. 1: Mid-infrared spectrum (1800 – 920 cm^{-1}) of the asphaltenes from C26 oil before and after smoothing at different points showing the shapes and positions of the bands in the original spectrum was not significantly altered by the 15 point smoothing used in preprocessing.

Curve fitting is a method used to separate overlapping peaks in a spectrum (Maddams, 1980). The procedure, which is based on least squares algorithm using GRAMS/AI software (Thermo Scientific, Inc.), was performed in three steps covering the spectral regions: 3100 – 2750 cm^{-1} , 1800 – 925 cm^{-1} and 925 – 680 cm^{-1} , respectively. In each case the number of bands that make up the composite bands and their positions (maxima) were identified with the aid of the second derivative of the spectra and literature (Painter et al., 1981; Maddams, 1980). The limits of the determined maxima were set to within $\pm 10 \text{ cm}^{-1}$. The width at half height of each band was estimated from the second derivative as the distance between inflection points (Painter et al., 1981). Since the shape of the bands was unknown, shape functions of equal Gaussian and Lorentzian functions were initially adopted and allowed to vary during the iterative procedure (Ibarra et al., 1996; Painter et al., 1981). Some typical curve-fitted sections of the mid-infrared spectra are shown in Figure 5.2.

Note that prior to the curve fitting, each spectrum was normalised to the percentage (w/w) of the asphaltene in KBr pellet. The FTIR measurement is governed by the Beer-Lambert law (equation 5.6). The absorbance (A) at a band by a chemical functionality is proportional to the area (A_b) of the band. Since thickness of the pellets prepared is fairly uniform and asphaltene have similar bulk chemical composition, both l and ϵ are assumed to remain constant (β) between samples. Therefore A_b is proportional to the concentration, c of the absorbing functionality. This allows similar chemical functionalities to be semi-quantitatively compared using the integrated areas of their respective bands (equation 5.7).

$$A = A_b = \epsilon lc = \beta c \tag{5.6}$$

$$A_b \propto \beta c \tag{5.7}$$

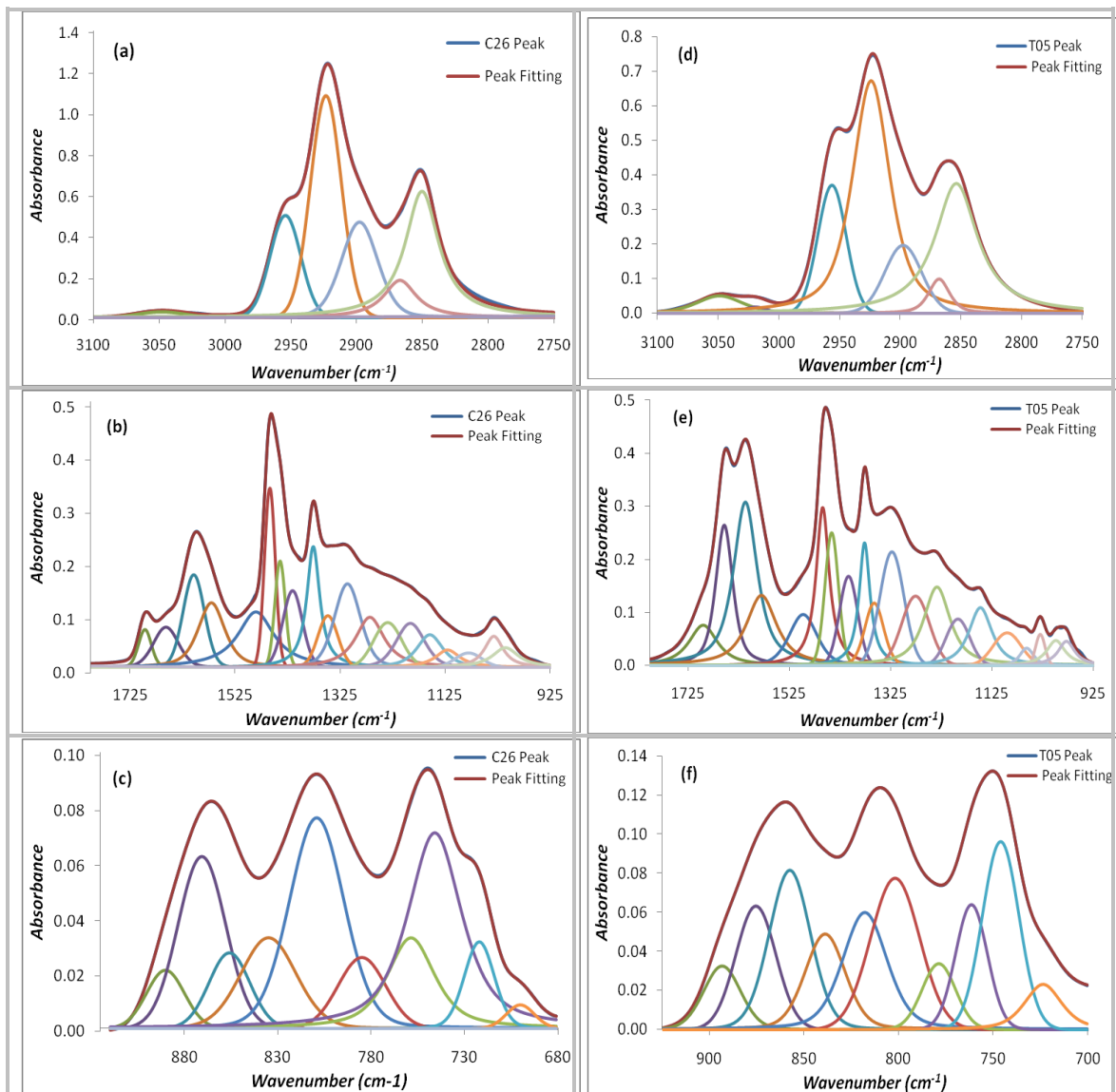


Figure 5.2: Typical curve fitting of mid-infrared spectra of petroleum asphaltenes showing deconvolution of bands in the three regions ((a) & (d)), (b) & (e) and (c) & (f) of the spectra of the Canadian asphaltenes (C26) and Tanezzuft black shale asphaltenes (T35).

5.2.3 Chemometric multivariate statistical analysis

Statistical chemometric tools were employed to provide comprehensive view of the covariate FTIR data mainly with the aim of developing classification methods of the oils based on the asphaltene FTIR data. Prior to this, all the spectra were normalised to the respective maximum absorbance to remove the effect of concentration on the data (Beebe *et al.*, 1998). Each of the three main regions (3100 - 2750, 1800 - 925, and 925 - 680 cm^{-1}) of the spectrum was analysed separately in the classification procedure. The multivariate statistical tools used to aid the classification were principal component analysis (PCA) followed by hierarchical cluster analysis (HCA) (Hair *et al.*, 2006; Adams, 1991; Smith, 1991).

In general, the high dimensionality of the data was reduced by PCA. The analysis transforms the original multicollinear spectral data into mutually orthogonal independent variables (i.e. principal components or PCs) such that PC1 extracts the maximum variance in the data and PC2 extracts the maximum variance of what remains and so on, so that the first few PCs extract most of the information in the original data (Tabachnick and Fidell 2007; Hair *et al.*, 2006; Beebe *et al.*, 1998). The score plot of PC1 against PC2 was used to initially explore the structure of the data and identify outliers. Then, the number of PCs accounting for most of the variance in the original data was identified from eigenvalue plot (eigenvalues vs. PCs). In order to eliminate the negative effect of multicollinearity in the original spectral data, the selected PCs were used as variables in HCA for more extensive classification (Hair *et al.*, 2006).

The best combination of linkage method and distance measure in the HCA was found to be the Ward linkage method and squared Euclidean distance measure in agreement with Hair *et al.* (2006). The number of relevant clusters was identified based on examination of similarity levels and dendrograms. Similarity in chemical composition amongst asphaltenes was assessed based on similarity and distance levels in the HCA results and analysis of the various variables that have significant loadings on the relevant PCs (Tabachnick and Fidell, 2007; Hair *et al.*, 2006; Brereton, 2003; Beebe *et al.*, 1998).

5.3 Results and Discussion

5.3.1 Assignment of bands

(a) Assignment of solid-state ^{13}C NMR absorption bands

The solid-state ^{13}C NMR spectra of the asphaltenes generally consist of two broad absorption bands at 0 – 60 ppm and 100 – 150 ppm (Figure 5.3 (a)) assigned to aliphatic carbon and aromatic carbon, respectively (Murphy *et al.*, 1982). The aromatic carbon consists of primary (methyl), secondary (methylene) and tertiary (methine) carbon. The aromatic carbon, on the other hand, consists of tertiary carbon (bonded a one hydrogen) and quaternary carbon (bonded to no hydrogen).

The dipolar dephased ^{13}C NMR spectra also consist of the two broad absorptions (Figure 5.3 (b)). The peak at 0 – 60 ppm is mainly due to quaternary aromatic carbon as the signals from the protonated tertiary carbon have been mostly removed by the dephasing programme.

Therefore, the peak is indicative of the degree of condensation in the aromatic ring system of the asphaltenes. The peak at 100 – 150 ppm in the dipolar dephased spectra (Figure 5.3 (b)), on the other hand, represents signals from the tertiary aliphatic carbons and mobile primary (methyl) carbons (Murphy et al., 1982).

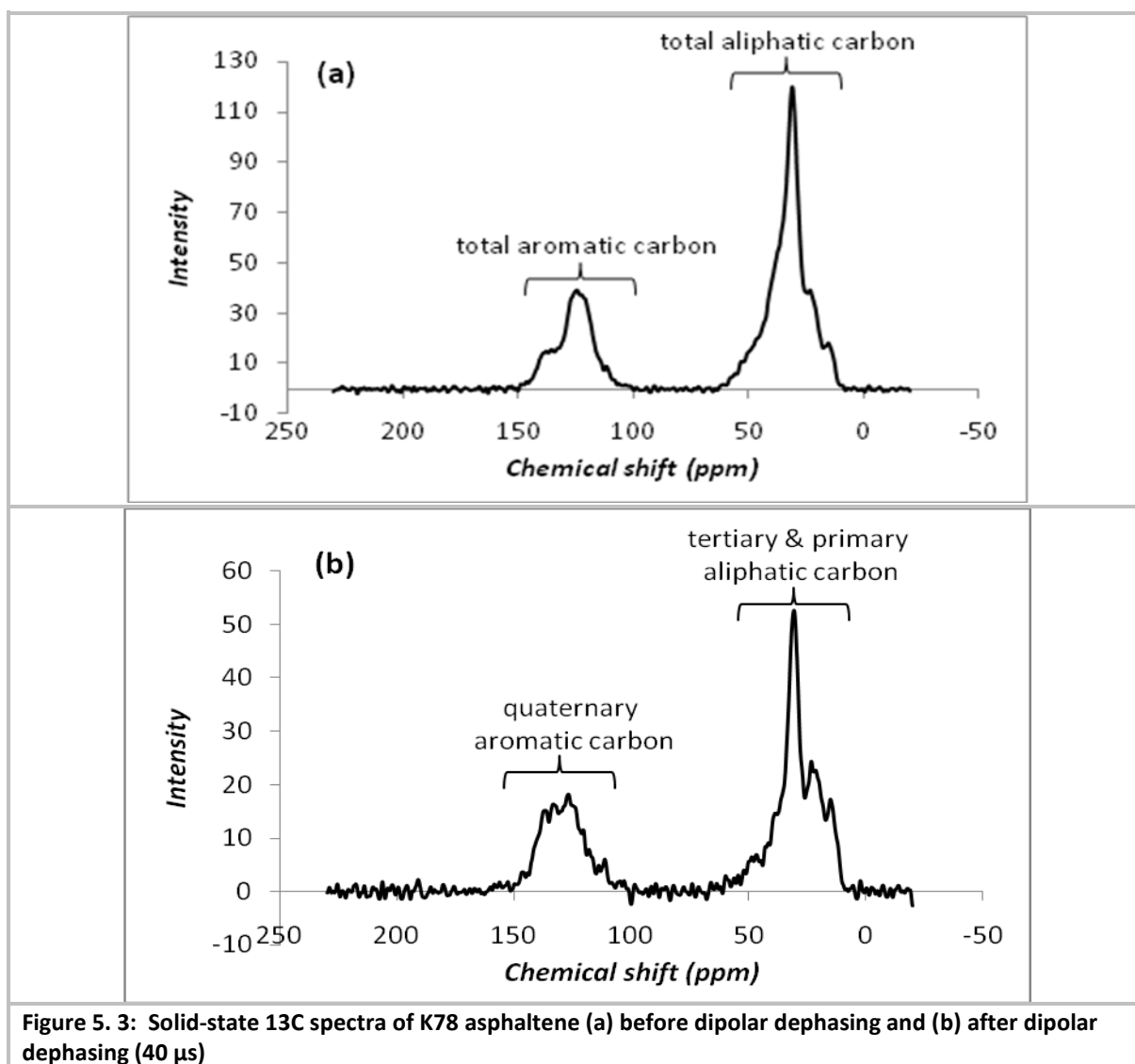


Figure 5. 3: Solid-state ^{13}C spectra of K78 asphaltene (a) before dipolar dephasing and (b) after dipolar dephasing (40 μs)

(b) Assignment of 3500 to 2750 cm^{-1} region

This region of the FTIR spectra of asphaltenes consists of a number of bands provided by various chemical functional groups. The broad absorption band between 3500 and 3100 cm^{-1} (Figure 5.4) is assigned to hydroxyl (O–H) and pyrrolic (N–H) stretching vibrations. The band is often sharp where the functional groups are isolated. However, if the groups are involved in polymeric intermolecular hydrogen bond and/or chelation with carbonyl (C=O) group (Nakanishi, 1962) a broad absorption band is observed as in Figure 5.4. In general, the band is weak in almost all petroleum asphaltenes analysed in this work (Figure 5.4 (a) & (b)). It is however prominent and strong in the spectra of asphaltenes from coals and black shales (Figure 5.4 (c) & (d)). This suggests the OH and NH functionalities are relatively more abundant in coal and black shale asphaltenes than is the case in petroleum asphaltenes.

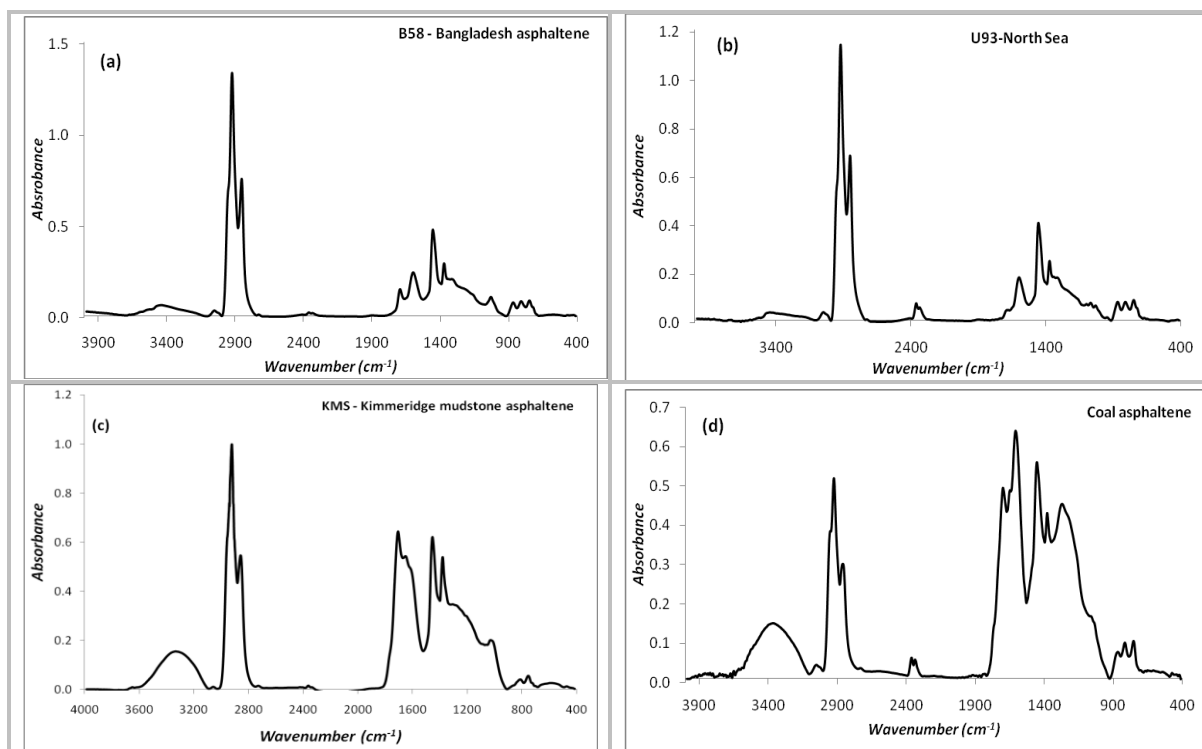


Figure 5. 4: Typical mid-infrared spectra of asphaltenes derived from (a) Bangladesh oil; (b) a Northsea oil; (c) a black shale asphaltene from Kimmeridge mudstone; and (d) a Northsea coal

The two relatively weak bands between 3100 and 3000 cm^{-1} are attributed to aromatic C–H stretching vibration. The bands are barely detectable in immature asphaltenes from black shales and coals (Figure 5.4 (c) & (d)). They are however relatively strong in spectra of the asphaltenes from petroleum, the Tanezzuft black shale and mature coal (e.g. (a), (b) & (d) in Figure 5.4). They often appear as a shoulder to the aliphatic C–H stretching aliphatic band or may occur below 3000 cm^{-1} in which case they may overlap with the aliphatic stretching bands. Winberley & Gonzalez (1961) observed that the band shifts from about 3000 to 3050 cm^{-1} as number of aromatic rings decreases (Yen *et al.*, 1984). The band at 3020 cm^{-1} may therefore indicate structures with 5 or more aromatic rings while that at 3050 cm^{-1} may be due to structures with 3 rings or less.

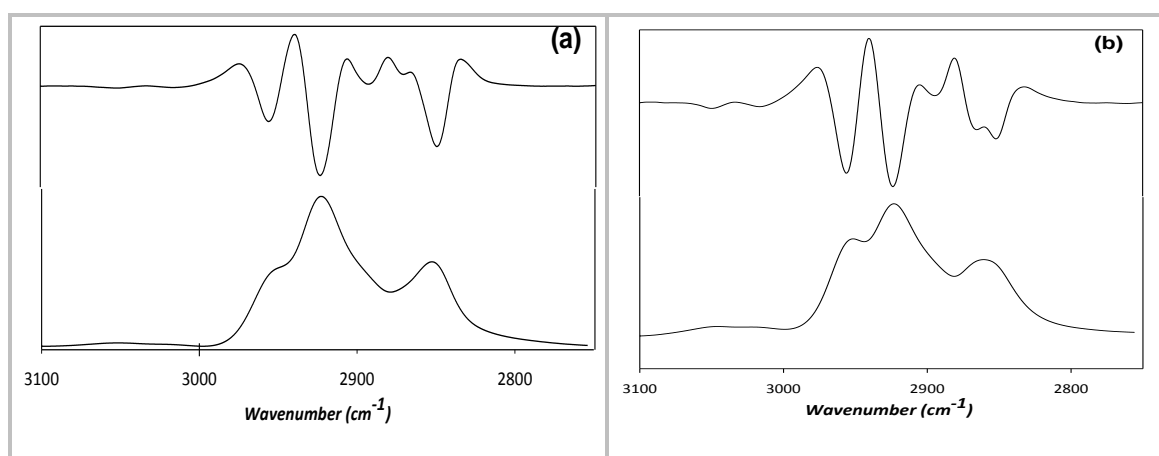


Figure 5. 5: Second derivative (top) of $3100 - 2750\text{ cm}^{-1}$ region of the mid-infrared spectrum of the asphaltenes from (a) Oman oil (O28) and (b) Tanezzuft black shale (T35) showing deconvolution of the superimposed bands in the region.

The 3000 to 2750 cm^{-1} region of the spectrum reveals three main bands at approximately 2920, 2925 and 2850 cm^{-1} (Figure 5.4). Second derivative of the region however shows five (5) bands at about 2954, 2923, 2897, 2869 and 2850 cm^{-1} (Figure 5.5). These bands are generally assigned to C–H stretching vibrations of aliphatic groups as shown in Appendix 5A. The first two bands at 2954 and 2923 cm^{-1} are assigned to asymmetric stretching vibrations due to C–H at 2° and 1° carbons (i.e. methylene, R_2CH_2 and methyl, RCH_3 groups respectively) while the last two bands at 2869 and 2850 cm^{-1} are due to the corresponding symmetric stretching modes of the respective two groups. The middle band at 2897 cm^{-1} is attributed to C–H stretching vibration at 3° carbon (i.e. methine, R_3CH) (Guiliano et al., 1990; Yen et al., 1984).

(c) *Assignment of 1800 to 925 cm^{-1} region*

This is a very complex region with at least eighteen bands as revealed by the second derivative of the region (Figure 5.6). The band at about 1770 cm^{-1} in spectra of coals and black shale asphaltenes is assigned to carbonyl (C=O) functionality in ester group (RCOOR) while the band between 1695 and 1715 cm^{-1} is attributed to carbonyl (C=O) functionality in carboxylic acid group. Both bands are prominent in black shale and coal asphaltenes. In petroleum asphaltenes the ester band is absent while the acid band occurs only as a shoulder to the aromatic band at about 1600 cm^{-1} in some others (Figure 5.4). The band at 1660 cm^{-1} , on the other hand, is assigned to highly conjugated carbonyl (C=O) group of the quinone-type (Ibarra et al., 1996; Guiliano et al., 1990).

Note however that definite assignment of the acid carbonyl band is difficult as C=O functionality in ketones also absorbs in the same region (Painter et al., 1981; Nakanishi, 1962). The later possibility is particularly reinforced in petroleum asphaltenes by the fact that carboxyl carbonyl group absorbs at about 1700 cm^{-1} or higher wavenumbers and are accompanied by a fairly broad band at 3500 to 3100 cm^{-1} due to hydroxyl (O–H) group which is not significant in the petroleum asphaltenes.

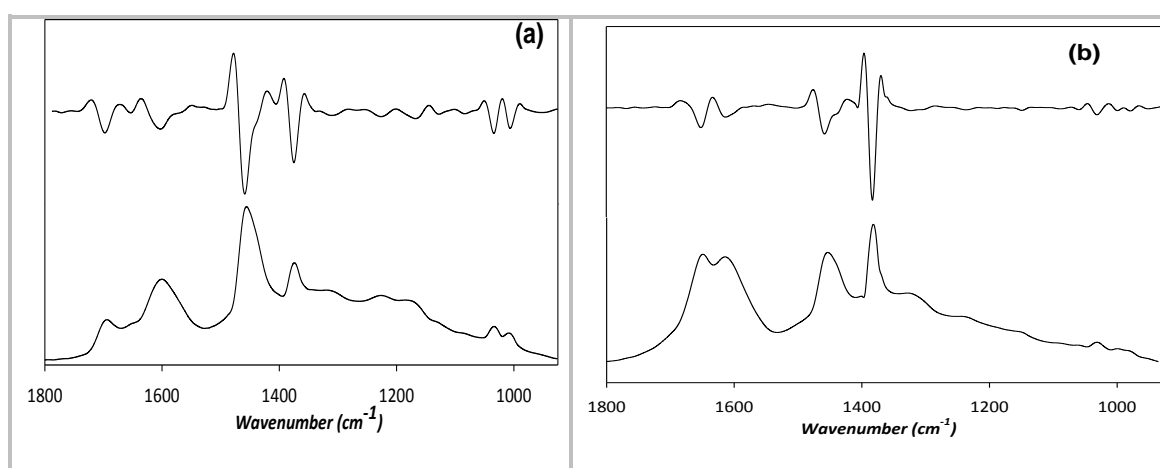


Figure 5. 6: Second derivative (top) of the 1800 – 925 cm^{-1} mid-infrared spectrum (bottom) of the asphaltenes from (a) Oman oil (O28) and (b) Tanezzuft black shale (T35) showing the deconvolution of superimposed bands in the region.

The four bands at about 1600, 1570, 1487 and 1439 cm^{-1} have been observed in coal spectra to intensify with coalification and thus are attributed to absorptions by aromatic C=C stretching vibrations and are therefore indicative of the aromatic ring system in the asphaltenes (Ibarra et al., 1996; Guiliano et al., 1990). The first three bands are enhanced by

conjugation with carbonyl (C=O) functionality (Ibarra *et al.*, 1996). Note however that positive correlations were observed between relative amounts of nitrogen in petroleum asphaltenes and the first three absorption bands respectively (Figure 5.7). This suggests a significant contributions from aromatic C=N absorption to the bands and thus indicates aromatic nitrogen is an important functionality in petroleum asphaltenes.

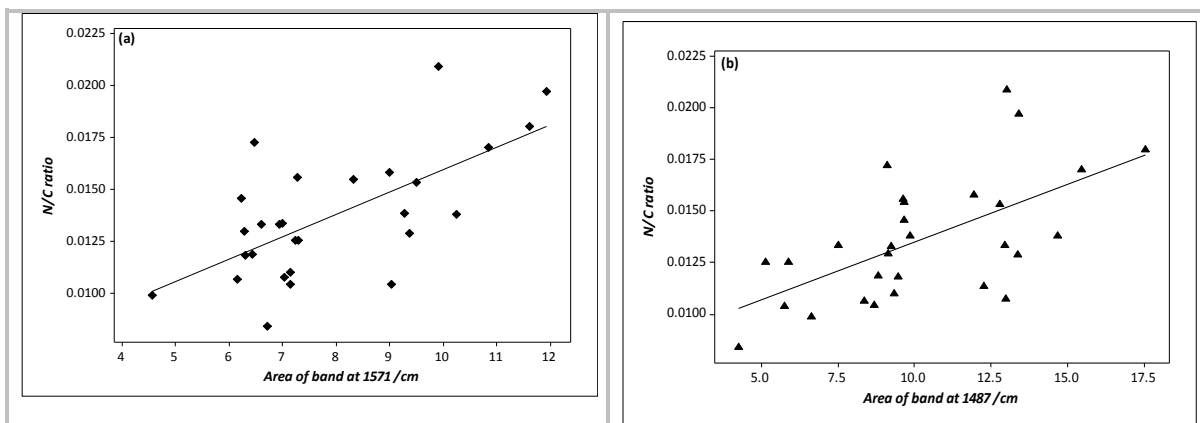


Figure 5. 7: Plot showing correlation between asphaltene N/C ratio and the absorption bands at (a) 1571 cm^{-1} ($R^2 = 0.42$) and (b) 1487 cm^{-1} ($R^2 = 0.32$) respectively indicating the bands have contributions from aromatic C=N stretching vibrations.

The band at 1459 cm^{-1} is assigned to asymmetric deformation by aliphatic methyl (CH_3-) and methylene ($-\text{CH}_2-$) groups. Similarly, the band at 1413 cm^{-1} is assigned to asymmetric methylene ($-\text{CH}_2-$) and/or OH group deformations. The intensity of the band at about 1375 cm^{-1} was observed to increase with coal rank and is consequently attributed to deformation vibrations by methyl (CH_3-) group attached to aromatic system. Likewise, the band at 1348 cm^{-1} is attributed to symmetric deformation vibrations of methyl (CH_3-) group attached to carbonyl (C=O) functionality (Ibarra *et al.*, 1996; Guiliano *et al.*, 1990). Note however that the two bands at 1414 and 1375 cm^{-1} correlate positively with nitrogen content of the asphaltenes (Figure 5.8). Consequently, the bands are likely by alkyl groups attached to nitrogen functionally possibly in tertiary amine structures as corroborated by presence of aromatic amine C–N absorption bands (see below).

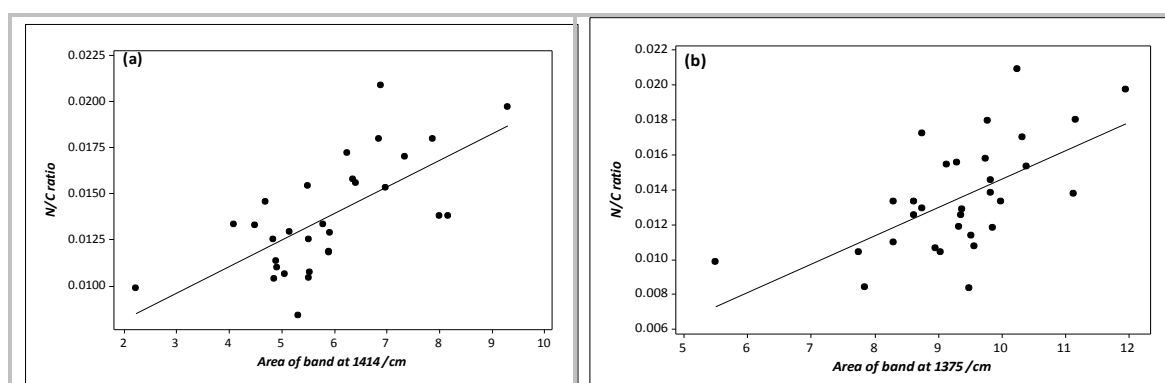


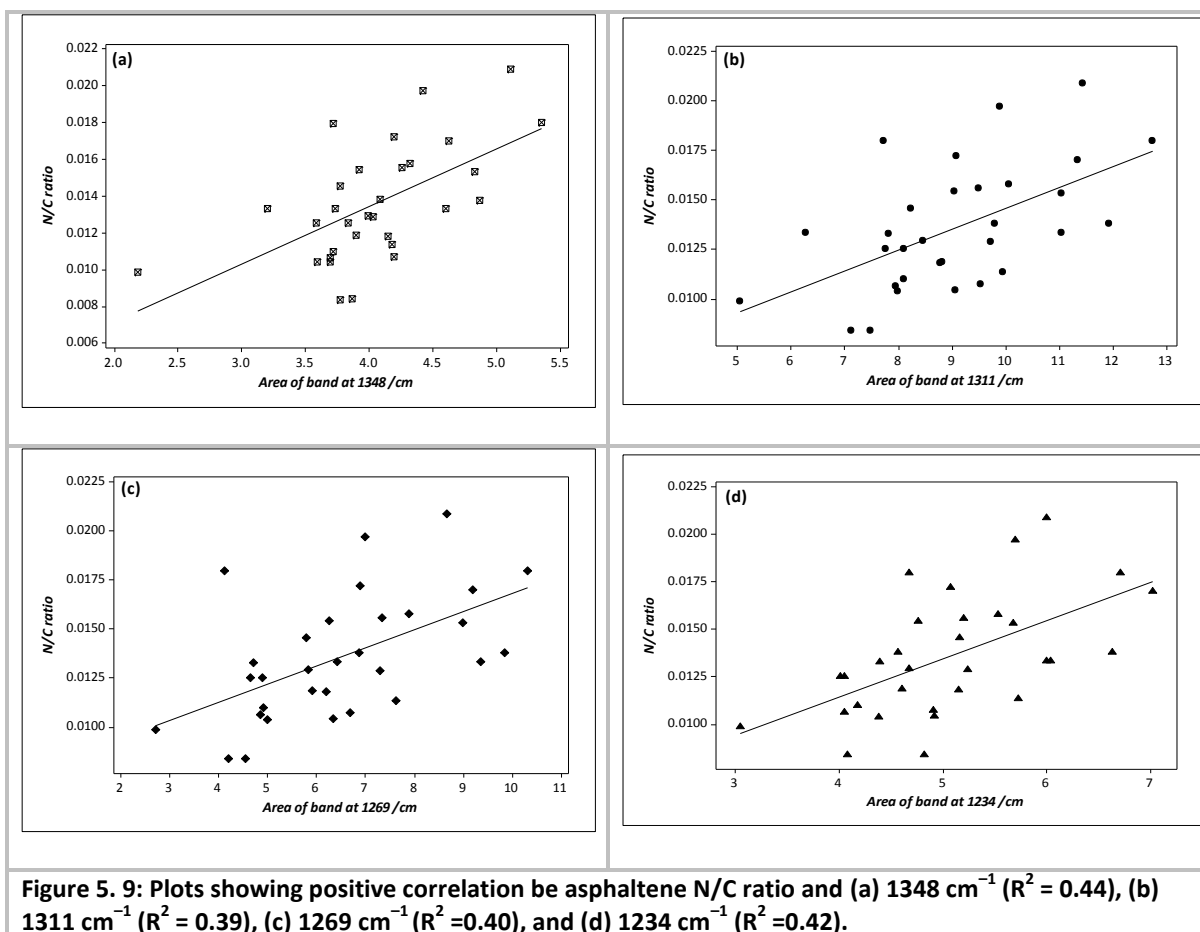
Figure 5.8: Plots showing correlation between asphaltene elemental N/C ratio against relative band areas of the bands at (a) 1414 cm^{-1} ($R^2 = 0.43$) and (b) 1375 cm^{-1} ($R^2 = 0.36$) indicating the bands are associated with nitrogen.

The bands between 1300 and 1000 cm^{-1} are difficult to assign because many groups absorb in the region (Painter *et al.*, 1981). Nevertheless, Ibarra *et al.* (1996) assigned these bands to

stretching vibrations by C–O groups from various functionalities including ethers, phenols, alcohols etc. (Appendix 5A). However, C–C stretching, O–H and –CH₂– deformations also absorb in this region in addition to S=O (sulphoxides, R₂S=O), SO₂ (from sulphones, R₂SO₂), and C–N (from aliphatic, R₃N, and aromatic, ArNR₂, amines) (Socrates, 1980; Nakanishi, 1962). The bands could also be due to mechanical coupling of these vibration (Painter *et al.*, 1981). Consequently, Painter *et al.* (1981) conclude that “it is likely that bands between 1000 and approximately 1300 cm⁻¹ cannot be described in terms of simple motions of specific functional groups or chemical bonds, but instead have complex, poorly defined, mixed character”.

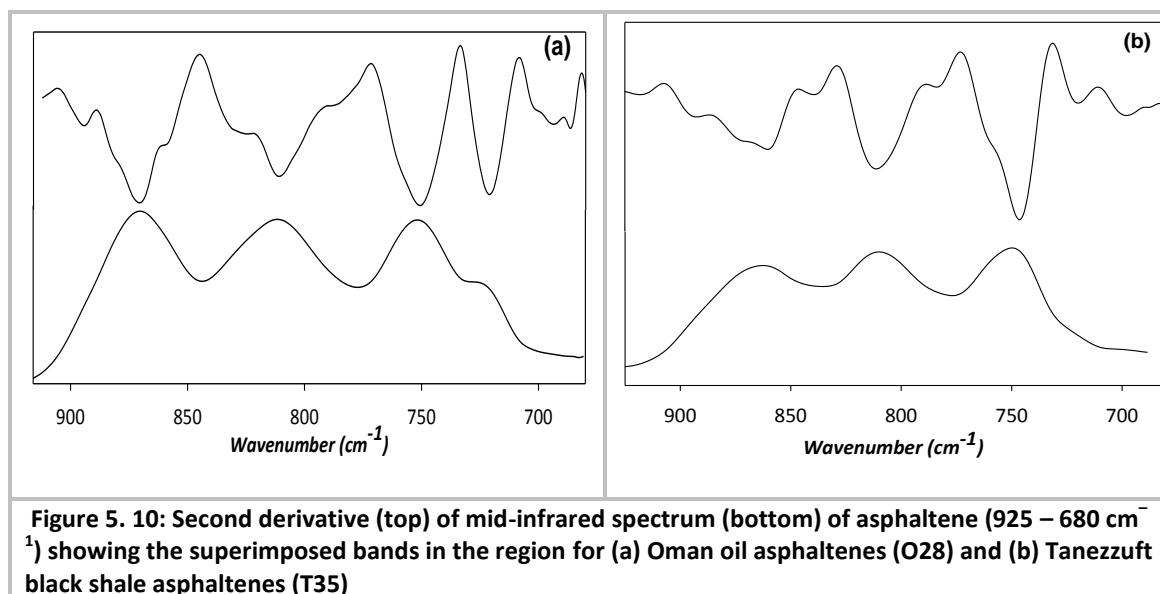
The band at 1035 cm⁻¹ resolves into two bands in the second derivative of the spectra (Figure 5.6). They have been assigned by Ibarra *et al.* (1996) to C–O stretching vibrations. Some other workers (Permanyer *et al.*, 2005; Lamontagne *et al.*, 2001; Boukir *et al.*, 1998) however have assigned them to stretching vibrations by sulphone (S=O) and sulphoxide (SO₂) functional groups. Correlation of the bands with S/C ratio however did not show any relationship between the parameters. This suggests the bands might not be due to the sulphur functionalities.

Nevertheless, four bands within the range show clear positive correlation with N/C elemental ratio (Figure 5.9). Studies of standard compounds have revealed that absorptions by stretching vibrations of C–N bond of tertiary aliphatic amines occur between 1230 and 1030 cm⁻¹ while those by aromatic C–N bond (i.e. C_{arom}–N) and aliphatic C–N bond (i.e. C_{aliph}–N) in aromatic amines absorb in the range 1360 – 1250 and 1280 – 1180 cm⁻¹, respectively (Nakanishi, 1962). Consequently, the three bands at 1348, 1311 and 1269 cm⁻¹ are assigned to C_{arom}–N. The fourth band at 1234 cm⁻¹ is assigned to C_{aliph}–N functionality of tertiary aromatic amines. The weakness of the correlation might be due to influence of bands of other functionalities that absorb in the region and the fact that the nitrogen is not exclusively fixed in these functionalities.



(d) Assignment of 925 to 700 cm^{-1} region

This region commonly contains three fairly strong absorption bands (Figure 5.4) which are generally assigned to out-of-plane deformations of aromatic C–H group (Yen *et al.*, 1984; Nakanishi, 1962). The bands reflect various degrees of substitution on the aromatic ring system (Ibarra *et al.*, 1996; Guiliano *et al.*, 1990; Yen *et al.*, 1984; Nakanishi, 1962). Yen *et al.* (1984) and Guiliano *et al.* (1990) have shown that the region can be clearly divided into: 890 - 850 cm^{-1} attributed to 1 isolated hydrogen; 830 - 815 cm^{-1} attributed to 2 adjacent hydrogens; 800 - 775 cm^{-1} attributed to 3 adjacent hydrogens; and 760 - 745 cm^{-1} attributed to 4 adjacent hydrogens on an aromatic ring system.



The three bands however consist of up to ten superimposed bands as revealed by second derivative of the region (Figure 5.10). These bands are curve fitted and assigned as defined in Appendix 5A (Ibarra *et al.*, 1996). The band at 724 cm⁻¹ is aliphatic rather than aromatic and is generally attributed to rocking vibration by methylene (-CH₂-) unit of long alkyl (greater than butyl) groups (Nakanishi, 1962). There is however disagreement on assignment of the band at about 830 to 840 cm⁻¹. Guiliano *et al.* (1990) assigned this to rocking vibration by cyclic methylene (-CH₂-) unit based on Kuehn *et al.* (1984) observation that the band correlate with evolution towards cyclic saturated structures. On the other hand, Ibarra *et al.* (1996) assigned it to out-of-plane vibration by 2 adjacent hydrogens on aromatic ring.

5.3.2 Coal asphaltene: evolution with maturity

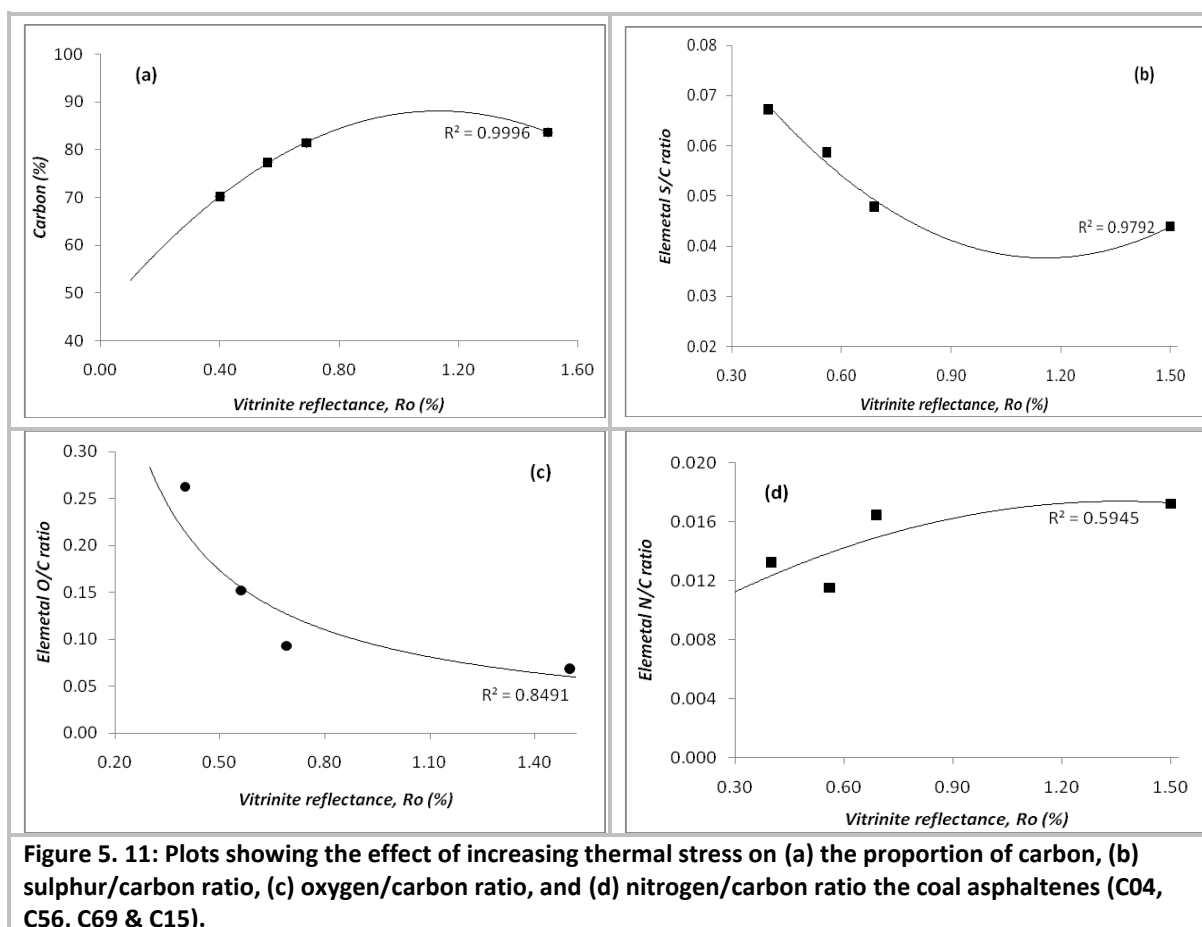
Table 5.2 shows the relative proportions of the major elements in the four coal asphaltene with carbon being over 70% of the total weight of the asphaltene and hydrogen being only about 6%. Although oxygen is significant, it appears to be dependent on the coal rank (maturity).

Table 5.2: Results of elemental analysis of the coal asphaltene showing the relative proportions of the five major elements (oxygen (O) was calculated by difference)

Sample	R _o	N (%)	C (%)	H (%)	S (%)	O (%)
C04A	0.40	0.93	70.18	5.76	4.72	18.41
C56A	0.56	0.89	77.35	5.48	4.54	11.74
C69A	0.69	1.34	81.47	5.70	3.90	7.59
C15A	1.50	1.44	83.62	5.51	3.67	5.76

The relative carbon content of the asphaltene increases with increasing maturity (Table 5.2, Figure 5.11 (a)). On the other hand, H/C, O/C as well as S/C ratios decrease with thermal maturity (vitrinite reflectance, R_o). The trends however appear to level off at relatively high maturities (R_o >1.0%) as the relative change in the respective ratios decrease (Figure 5.11). The relative amount of nitrogen (N/C) however increases, albeit more slowly than either oxygen or sulphur, with increasing maturity as shown in Figure 5.11 (d). Similar trends were observed by Rouxhet *et al.* (1980) with respect to thermal evolution of coals and kerogens. Li *et al.* (1997)

also observed enrichment in pyrrolic nitrogen in Duvernay Formation source rocks with increasing maturity. Although they attributed their observations to interaction of the nitrogen compounds with solid organic/mineral matter, the observation in this work has alternative explanation.



The observed gradual increase in nitrogen with maturity might be because of two dynamic processes during diagenesis of the organic matter. First the loss of other elements occurs more rapidly (Figure 5.11 (b) & (c)) than nitrogen (Figure 5.11 (d)) such that the net effect is enrichment in nitrogen content of the residual organic matter. Secondly, a significant proportion of the total nitrogen might be fixed in functional groups (e.g. aromatic pyridinic & pyrrolic nitrogen (Baxby et al., 1994)) that are relatively more stable than sulphur and oxygen functional groups. The overall observable effect is therefore gradual increase in the nitrogen content of the asphaltenes as shown in Figure 5.11 (d).

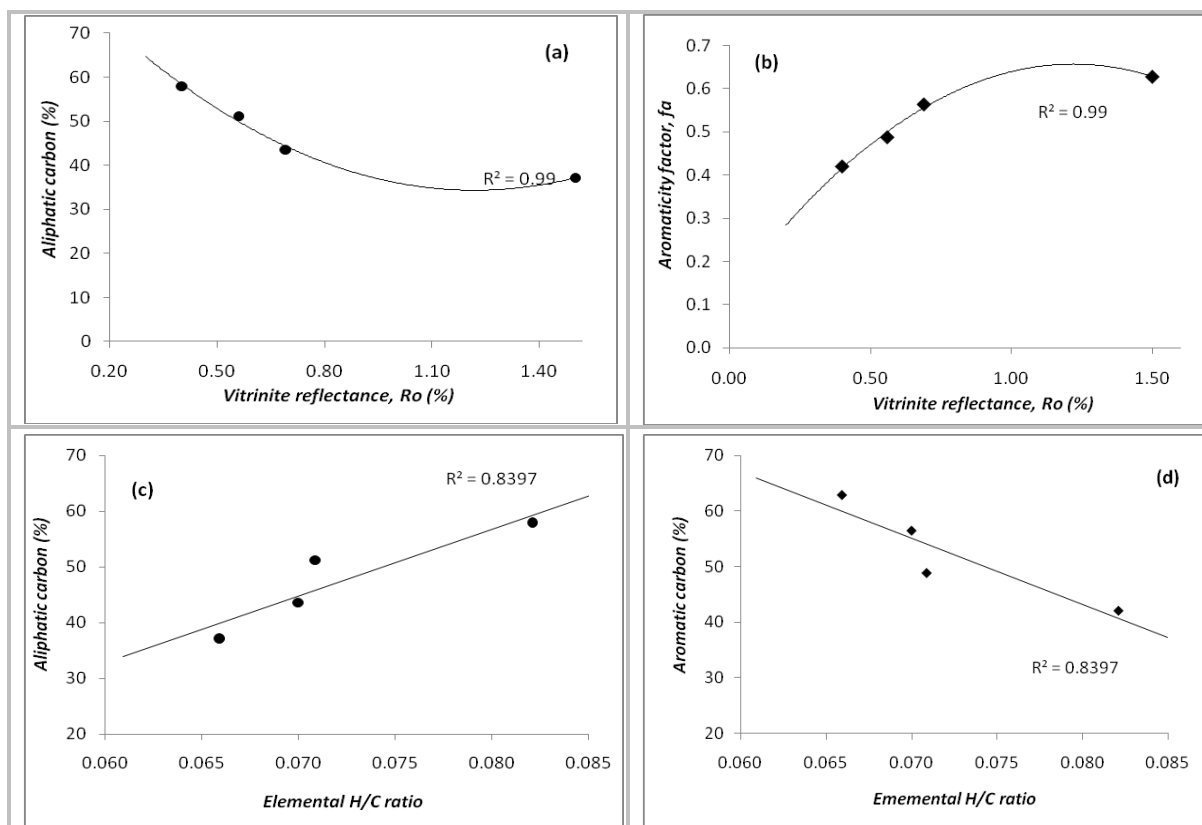


Figure 5. 12: Plots showing the relationship between vitrinite reflectance and (a) aliphatic and (b) aromatic contents; and between elemental hydrogen content and (c) aliphatic and (d) aromatic contents of the coal asphaltenes (C04, C56, C69 & C15).

The total carbon in the asphaltenes can be broadly grouped into aliphatic and aromatic carbons as observed from solid-state ^{13}C NMR analysis. The aliphatic carbon in the asphaltenes gradually decreases with increasing maturity to a near constant values at $R_o > 1.0\%$ (Figure 5.12 (a)). The aromatic carbon, on the other hand, increases with increasing maturity towards equilibrium value at R_o values greater than about 1.0% (Figure 5.12 (b)). This suggests formation of more aromatic structures from the aliphatic, possibly naphthenic structures with increasing maturity of the asphaltenes although dealkylation occurs as well (Rouxhet et al., 1980). This is supported by the inverse relationship between aromatic carbon content and H/C ratio (Figure 5.12 (d)) of the asphaltenes which suggests aromatisation is accompanied by hydrogen loss.

Although the aromaticity factor (f_a), indicating aromatic carbon content, of the asphaltenes increases with increasing maturity (R_o) (Figure 5.13 (b)), the fraction of quaternary carbon in the aromatic carbon ($f_a^{a,N}$) appears to be independent of maturity (Table 5.3). This suggests the degree of condensation of the aromatic ring system is independent of maturity with maturity range under investigation ($R_o = 0.40$ to 1.50%). Note, for example, the least mature C04 ($R_o = 0.40\%$) has more condensed aromatic structures than the most mature C15 ($f_a^{a,N} = 0.66$ against 0.57 , Table 5.3) although the later has greater proportion of aromatic carbon as reflected in their respective aromaticity factor, f_a (Table 5.3). Note however, the fraction aromatic hydrogen (H_a) and tertiary aromatic carbon (f_a^H) relative to the total carbon in the asphaltenes appear to increase with maturity (Table 5.3). These observations are consistent with results of Wilson and Vassallo (1985) in their study of distributions of carbon in coals.

They attributed this dealkylation of aromatic side chains and aromatisation of alicyclic moieties with increasing thermal stress (Wilson and Vassallo, 1985).

Table 5. 3: Structural parameters calculated from the results of the solid-state ^{13}C NMR analysis of the coal asphaltenes

Sample	R_o	fa	$f_a^{a,H}$	$f_a^{a,N}$	f_a^H	Ha
C04	0.40	0.42	0.34	0.66	0.14	0.17
C56	0.56	0.48	0.46	0.54	0.22	0.28
C69	0.69	0.56	0.47	0.53	0.26	0.28
C15	1.50	0.63	0.43	0.57	0.27	0.41

The thermal evolutions of various oxygen functionalities are monitored by following the change in relative amounts of the respective functionalities as represented by the normalised areas (A) of the bands. Thus the evolutions of relative proportions of the ester (A_{1768}), carboxyl (A_{1698}) and conjugated carbonyl (A_{1607}) groups with increasing maturity are presented in Figure 5.13. All these functionalities follow similar trend; decreasing with increasing maturity. The ester functional group (A_{1768}) decreases more sharply approaching zero with increasing maturity. The C–O functionalities, measured from the sum of the bands between 1,300 and 950 cm^{-1} , also decrease with increase in thermal maturity of the asphaltenes.

However, the thermal evolution does not seem to very much affect the broad band between 3100 and 3500 cm^{-1} (Appendix 5B). In fact, Rouxhet et al. (1980) observed that evolution of hydroxyl groups is preceded by carbonyl and aliphatic functionalities.

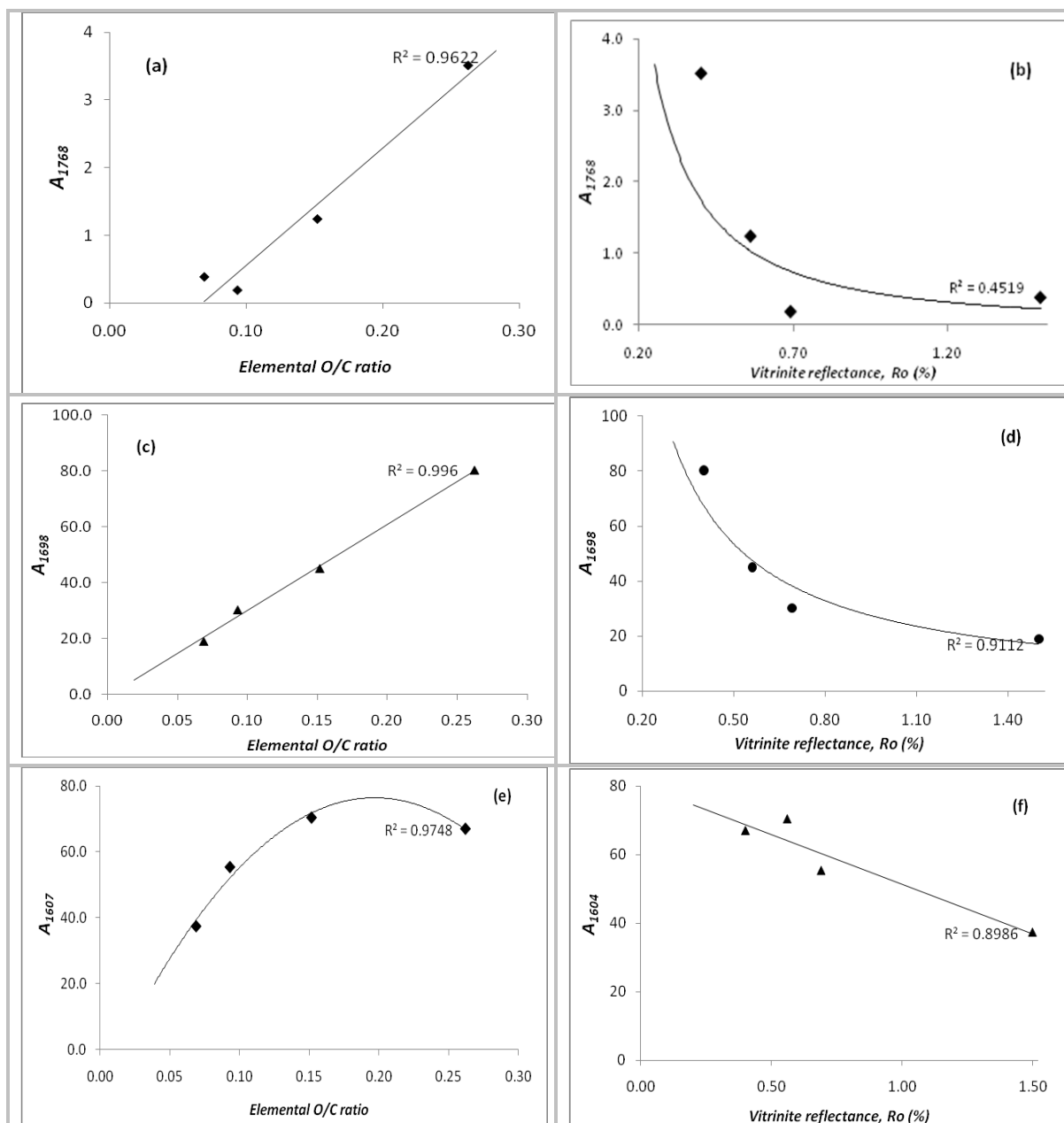


Figure 5.13: Plots showing the evolution of oxygen functionalities; (b) ester (A_{1768}), (d) carboxyl (A_{1698}) and (f) conjugated carbonyl (A_{1607}) in the coal asphaltenes with thermal maturity (vitrinite reflectance). (a), (c) and (e) show correlation of the respective functionalities with O/C ratio.

5.3.3 Black shale (source-rock) asphaltenes

In order to investigate the similarities and differences amongst asphaltenes isolated from source rock, bitumen samples from three different black shale samples namely Batra black shale, Kimmeridge mudstone and Tanezzuft black shale were analysed. The similarities and differences amongst the asphaltenes are quite clear from their spectra (Figure 5.14) even between asphaltenes from same black shale column (*cf.* B358 & B372, Figure 5.14). Deconvolution and curve-fitting of the spectra however gives deeper insight as discussed below.

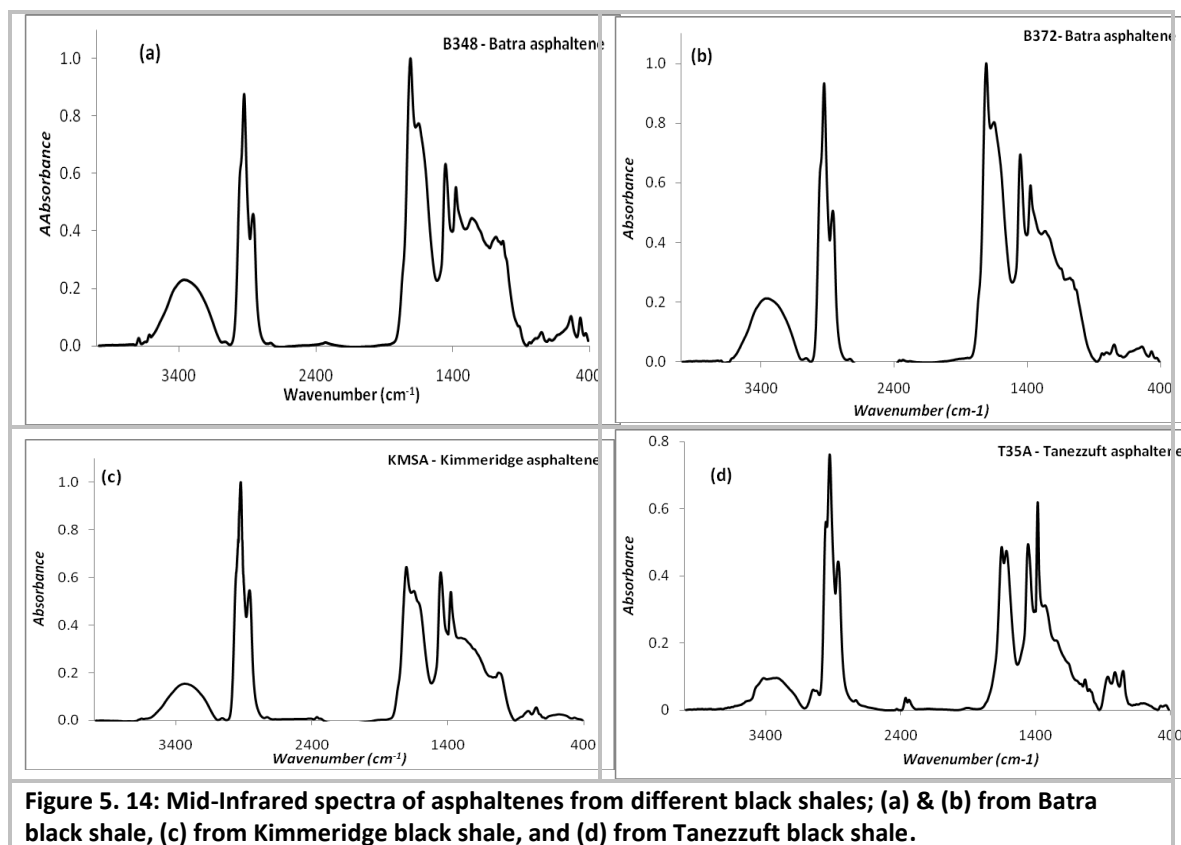


Figure 5. 14: Mid-Infrared spectra of asphaltenes from different black shales; (a) & (b) from Batra black shale, (c) from Kimmeridge black shale, and (d) from Tanezzuft black shale.

(a) Aliphatic functionalities

The aliphatic composition of the asphaltenes does not seem to vary very much particularly amongst the three immature asphaltenes from Batra black shale (B372 & B348) and Kimmeridge clay (KMSA). In these asphaltenes, the hydrogen content appears to be almost exclusively saturated hydrogen with relative proportion of aromatic hydrogen, $ha \leq 0.01$ (Table 5.4) compared to Tanezzuft asphaltene in which over 10% ($ha = 0.11$, Table 5.4) of the hydrogen is on aromatic rings as corroborated by ¹³C NMR data ($Ha = 0.17$, Table 5.5).

Similarly, the Tanezzuft asphaltene (T35A) appears to have greater proportion of long chain alkyl moieties as depicted in its higher R value (Table 5.4). The Batra asphaltenes have the lowest proportions of the long chain alkyl groups with R values being less than 1.4 compared to 2.44 for Kimmeridge and 2.94 for Tanezzuft asphaltenes. This is somewhat in agreement with the fractions of methyl, methylene and methine groups in the asphaltenes as measure by fCH_3 , fCH_2 and fCH respectively (Table 5.4). High fCH_2 coupled with low fCH_3 indicate relatively long chain alkyl groups. On the other hand, the values of fCH (Table 5.4) suggest Kimmeridge asphaltene (KMS) contains less branched alkyl structures than other asphaltenes as high fCH values indicate high tertiary carbon and therefore high branching.

(b) Oxygen functionalities

All the asphaltenes show prominent broad absorption between 3600 and 3100 cm⁻¹ by hydroxyl (O–H) and amine/pyrrolic N–H involve in polymeric hydrogen bonding. From the relative proportion of this band in black shale asphaltenes compared to petroleum asphaltenes

(Figure 5.14 and Figure 5.16), it is clear that the former have relatively greater proportions of hydroxyl, and possibly amine/pyrrolic, functional groups.

There is a clear difference amongst the source-rock asphaltenes particularly in the region between 1300 and 700 cm^{-1} . In all the asphaltenes the acid carbonyl band at 1700 cm^{-1} is quite intense. However, in immature asphaltenes (B348, B372 & KMS), it is the most intense in the region; being more intense than the aromatic C=C band at 1600 cm^{-1} . The spectra of the immature asphaltenes also show the presence of ester carbonyl group band at about 1750 cm^{-1} which seems to be more prominent in B348. The Batra asphaltene has generally greater proportion of carbonyl (C=O) than either T35 or KMS asphaltenes with the 1700 cm^{-1} being the dominant band (Figure 4.14).

There is also clear difference amongst the asphaltenes in the distribution of the C–O functionalities as exhibited by the bands between 1300 and 1000 cm^{-1} which are generally attributed to these functionalities. In general, the immature asphaltenes (B348 & KMS) have higher proportions of these functional groups than marginally mature T35 asphaltenes (Figure 5.14). This might however be source dependent as both B348 and B372 asphaltenes from Batra 'hot' shale appears to have higher proportion of these functionalities than the corresponding immature KMS asphaltenes from Kimmeridge mudstone (Figure 4.14).

Table 5.4: Showing values of asphaltene structural parameters calculated* for the mid-infrared data of the asphaltenes

Sample	B348	B372	KMS	T35
<i>CO Index</i>	0.71	0.69	0.66	0.49
<i>CO/Ar</i>	1.29	1.04	0.96	0.32
<i>fCO_e</i>	0.02	0.01	0.02	0.00
<i>fCO_a</i>	0.53	0.48	0.49	0.33
<i>fCO_c</i>	0.44	0.51	0.49	0.67
<i>C-O/C=O</i>	0.46	0.44	0.48	0.62
<i>C-O/CH_x</i>	1.95	1.66	1.27	0.88
<i>fCH₃</i>	0.40	0.39	0.31	0.26
<i>fCH₂</i>	0.44	0.40	0.61	0.60
<i>fCH</i>	0.16	0.21	0.08	0.14
<i>R</i>	1.37	1.25	2.44	2.94
<i>ha</i>	0.00	0.00	0.01	0.11
<i>hs</i>	1.00	1.00	0.99	0.89
<i>Pc</i>	0.14	0.26	0.14	1.32

*see Appendix 7 for equations used to calculate the parameters

(c) *Aromatic functionalities*

Aromatic structures also appear to vary amongst the asphaltenes. The asphaltene from marginally mature Tanezzuft black shale (T35) shows prominent absorption between 3100 and 3000 cm^{-1} from aromatic C–H stretching vibrations which is barely detectable in both the immature asphaltenes from Batra and Kimmeridge shales. This is in agreement with the aromatic C–H out of plane bands between 900 and 700 cm^{-1} which are intense in T35. A closer look at the relative intensities of the bands reveals that the band resulting from an isolated hydrogen (1H) is significantly lower than that from 4 and 5 adjacent hydrogens in the immature asphaltenes (B348 & KMS) compared to the marginally mature T35. This indicates greater degree of condensation in the marginally mature asphaltene (T35). This is substantiated by the values of *Pc*, a measure of degree condensation (Table 5.4). While the immature asphaltenes have values that are generally less than 0.3, the Tanezzuft asphaltene have a value of about 1.3 which is surprisingly higher than most of the petroleum asphaltenes (*cf.* Appendix 5C). Solid-state ^{13}C NMR data of this sample (T35) show 52% ($f_a = 0.52$, Table 5.5) of the carbon is present in aromatic moieties while aromatic carbon in petroleum asphaltenes is generally 40% or less (Figure 5.15). Most of the aromatic carbon (72%) in the Tanezzuft asphaltenes is present as quaternary carbon ($f_a^{a,N} = 0.72$, Table 5.5) indicating highly condensed ring system comparable to some petroleum asphaltenes (Table 5.5). Similarly, the relative proportion of aromatic hydrogen of the Tanezzuft asphaltene is significantly greater (over 10%) than in the other asphaltenes (<1.0%) as shown by their respective *ha* values (Table 5.4). This is corroborated by ^{13}C NMR data (*Ha* = 0.17, Table 5.5)

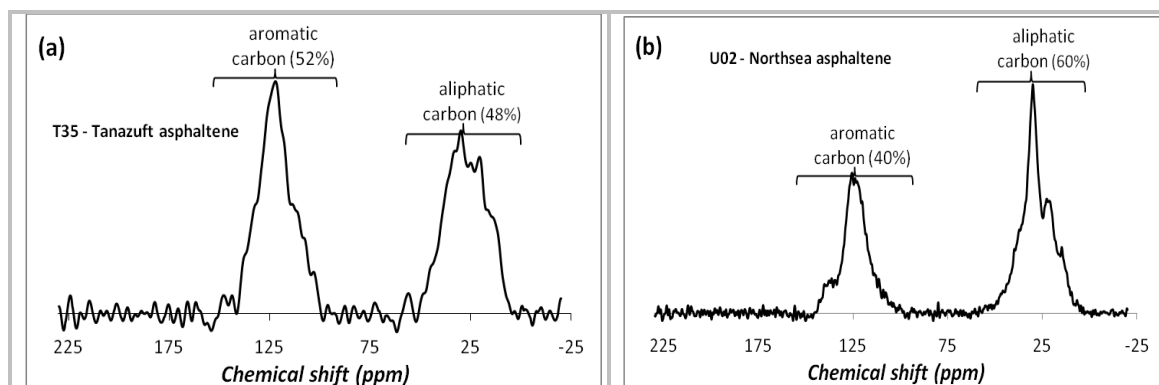


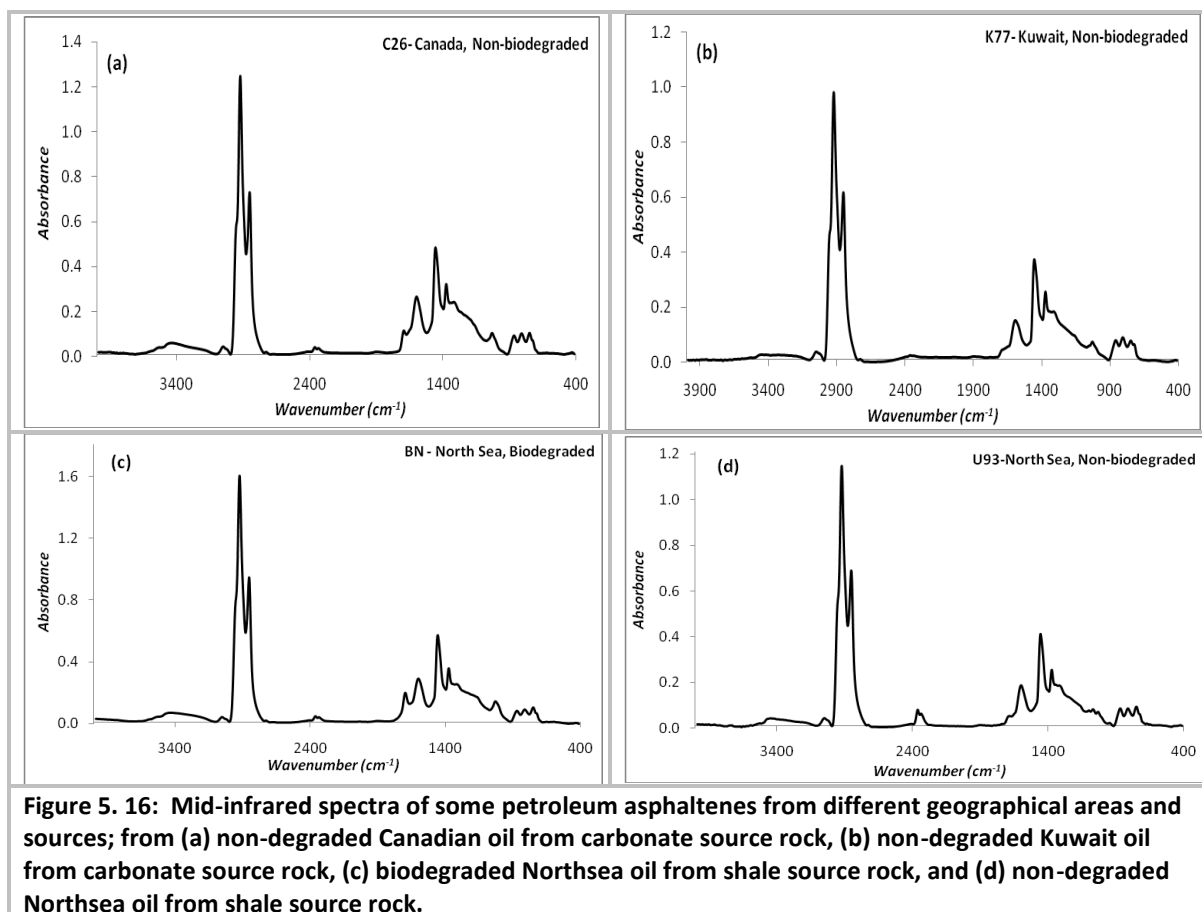
Figure 5. 15: Solid-state ¹³C NMR spectra of the asphaltenes from (a) sample T35, Tanezzuft black shale and (b) a Northsea oil (U02) from Flora oil field showing the marginally mature Tanezzuft asphaltenes contains relatively more aromatic carbon (52%) than the oil asphaltenes (40%).

The pronounced aromatic content of Tanezzuft black shale asphaltenes compared to other black shale asphaltenes, and even most petroleum asphaltenes (Figure 5.15), is believed to be a reflection of organic matter source rather than being a consequence of maturity. This is because the shale is only marginally mature with average 20S to 20R (C_{29} steranes) and 22S to 22R (C_{32} homohopanes) ratios of 0.51 and 0.54 respectively (see Chapter 3) in agreement with Rock-Eval maturity indices ($T_{max} = 432^{\circ}C$, $PI = 0.17$). Tanezzuft black shale has been observed to be particularly rich in graptolites (Aziz, 2000) which has been shown to consist mainly of aromatic structure (in fact more aromatic than vitrinite) with aliphatic groups (Bustin et al., 1989). This predominantly aromatic substance is likely to have influenced the composition of the asphaltenes.

In general, although the above observations are amongst asphaltenes from different black shales, a similar variability in the chemical functionalities was observed amongst asphaltenes from the same source rock unit (the basal Tanezzuft 'hot' shales) but from different depth intervals. Sixteen asphaltenes were taken and analysed by FTIR from the black shale samples from different intervals from the 470 m thick unit. The asphaltenes show significant aromatic content (similar to T35) that does not vary very much. The aliphatic content is also similar amongst the samples. The greatest variability is seen in the oxygen functionalities and particularly the carboxyl group and some C–O groups which may be related to the carboxyl functional group (Appendix 5C).

5.3.4 Petroleum asphaltenes

The mid-infrared spectra of asphaltenes from petroleum are generally very similar irrespective of their different sources (Figure 5.16). The prominent bands in the spectra are those resulting from aliphatic C–H stretching vibrations, aromatic C=C stretching and aromatic C–H out-of-bound vibrations. The band by C=O is prominent in some asphaltenes (Figure 5.16 (a) & (c)) and occurs only as a shoulder in some others (Figure 5.16 (b) & (d)). Nevertheless, for detailed analysis the spectra were deconvoluted and curve-fitted to resolve and semi-quantify the overlapping bands and are discussed below.



(a) *Aliphatic functionalities*

Absorption bands by aliphatic groups appear to be the dominant functionalities in petroleum asphaltenes (Figure 5.16) in contrast to black shale and coal asphaltenes where carbonyl groups dominate (*cf.* Figure 3.14). This is agreement with results from NMR analysis of 20 asphaltenes which show; the relative proportion of aliphatic carbon in asphaltenes is generally between 60-70% for asphaltenes from non-biodegraded oils. Asphaltenes from biodegraded oils have even higher proportions of the aliphatic carbon (>70%).

(b) *Oxygen & nitrogen functionalities*

Oxygen functionalities in petroleum asphaltenes are mainly carbonyl (C=O) groups from carboxylic acids and conjugated quinone-type carbonyl systems. Hydroxyl (O–H) groups from carboxylic functionalities, and possibly from phenols, are also present but in relatively low proportions compared to coal and black shale asphaltenes considering the relative proportion of the OH/NH broad band between 3600 and 3100 cm^{-1} (Figure 5.16).

The carbonyl (C=O) groups in the petroleum asphaltenes vary widely. In general, ester groups (band at 1770 cm^{-1}) are absent in all the asphaltenes and the carbonyl functionalities occur exclusively as carboxylic acid and conjugated quinones. The relative proportions of these groups in asphaltenes from oils vary widely. While in some samples, particularly most of the Northsea asphaltenes, the carboxyl carbonyl group (*fCOa*) is dominant by up to 70%, in others (e.g. C26/C30, K77/K78, and O28/O31) the conjugated carbonyl group (*fCOc*) dominates by

similar proportions (Appendix 5C). It is interesting to note that the conjugated carbonyl group is dominant in asphaltenes from oils generated from carbonate and marl source rocks (C26/C30, K77/K78, Q43/Q61, and O28/O31) with higher proportions in asphaltene from carbonate-sourced oils (e.g. C26/C30 & K77/K78) than marl-sourced oils. Most of the asphaltenes from oils generated from shale source rocks (e.g. the Northsea oils), on the other hand, have higher proportions of the carboxyl carbonyl groups. This observation is likely to be due to contrasting acidity of the carbonate (basic) and clay (acidic) mineralogy of the source rocks. Carbonates being basic could neutralise and adsorb acidic organic matter. Nevertheless, differential source and maturity could also play a role in the distribution of the functionalities (Ibarra et al., 1996) and this may explain why some Northsea asphaltenes have greater proportions of the conjugated carbonyl functionality.

Furthermore, asphaltenes from oils with common reservoir and source rock (e.g. C26/C30, NA1/NA2 and O28/O31) have similar proportions of the two types of carbonyl functionalities. On the other hand, where the asphaltenes are from different reservoirs (e.g. the Northsea oils, K77/K78, and Q43/Q61), the relative proportions of the carbonyl groups tend to vary possibly because the oils were generated from different source kitchens and/or experienced different thermal histories.

Previous FTIR studies have completely overlooked the importance of nitrogen functionalities in infrared spectra of asphaltenes (e.g. Yen et al. (1984)). Analysis of nitrogen functionalities in asphaltenes and other carbonaceous substances has been mainly undertaken using X-ray Absorption Near Edge Structure (XANES) from which it has been observed that pyrrolic and pyridinic nitrogen are the dominant nitrogen functionalities in petroleum asphaltenes with little or no saturated amines (Mitra-Kirtley et al., 1993b).

In this work nitrogen functional groups have been tentatively identified from the spectra of petroleum asphaltenes. In addition to aromatic ring nitrogen (see below), the nitrogen functionalities occur bonded directly to aromatic carbon ($C_{\text{arom}}\text{-N}$) and aliphatic (alkyl) carbon ($C_{\text{aliph}}\text{-N}$) in tertiary aromatic amines (Figure 5.17 (a) & (b)). These functionalities were only observed in petroleum asphaltenes through correlation of certain bands with N/C elemental ratio (Figure 5.7). The apparent absence of similar nitrogen functionalities in black shale asphaltenes might be because of the presence of significant proportion of oxygen functionalities, particularly O–H groups, such that any C–N bands are completely overwhelmed by C–O absorption bands in the same region.

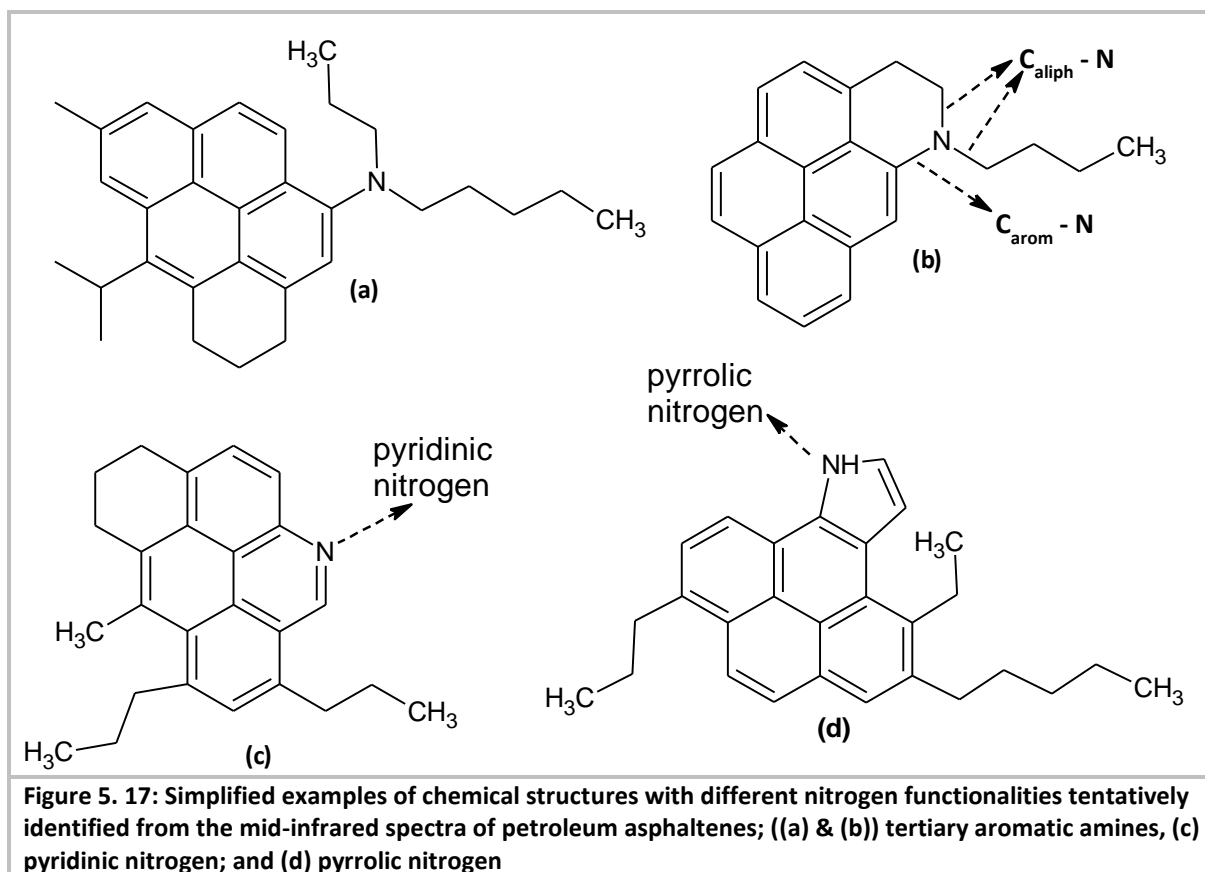


Figure 5.17: Simplified examples of chemical structures with different nitrogen functionalities tentatively identified from the mid-infrared spectra of petroleum asphaltenes; ((a) & (b)) tertiary aromatic amines, (c) pyridinic nitrogen; and (d) pyrrolic nitrogen

In general, the presence of these polar functionalities at the early stage of maturity, as is the case with respect to T35, and their relatively low presence in petroleum asphaltenes might be because of geochromatography and/or thermal maturity. Geochromatography during migration results in selective removal of polar compounds (e.g. carbazoles) from the migrating oil as a result of preferential chemisorption on carrier rock minerals (Bennett et al., 2002; Krooss et al., 1991). Oxygen- and nitrogen-based functionalities are particularly susceptible to geochromatography because of their acidic and basic character owing to the lone pair of electrons and possible hydrogen bonding. The effect of maturity on geomacromolecules based on studies on coals of different ranks show that oxygen-based functionalities and particularly hydroxyl groups are lost with increasing rank (maturity) of the coals (Ibarra et al., 1996).

(c) Aromatic functionalities

Results from solid-state ^{13}C NMR analysis of nineteen of the asphaltenes from oils reveal the aromaticity factor (f_a), indicating the relative proportion of aromatic carbon, of the sixteen petroleum asphaltenes varies between 0.24 and 0.40 and averages at 0.36. Generally, the asphaltenes from biodegraded oils have lower values of f_a than asphaltenes from non-degraded oils. The biodegraded samples (AR3, BN, CH and BN) have values between 0.23 and 0.29 and averages at 0.26 while the non-degraded samples have the f_a values between 0.27 and 0.40 and averages at 0.34 (Table 5.5).

Although the asphaltenes from the biodegraded oils have low proportion of aromatic carbon relative to the total carbon, the fraction ($f_a^{a,N}$) of non-protonated (quaternary) carbon in the aromatic moieties of the asphaltenes indicate most of the aromatic carbon in the degraded asphaltenes is present as quaternary carbon. The average value of this parameter is 0.79

(range = 0.70 to 1.00, Table 5.5) for the biodegraded asphaltenes while the non-degraded asphaltenes have 0.63 (range = 0.42 to 0.78, Table 5.5). This suggests a significantly greater degree of condensation in the the asphaltenes from the biodegraded oils than asphaltenes from the non-degraded oils.

There is wide variation in degree of condensation, as indicated by $f_a^{a,N}$ values (0.42 – 0.78) amongst the asphaltenes from the non-degraded oils (Table 5.5) even between samples with common source rock. For example, the asphaltenes from the two Canadian oils (C26 & C30), and the two Qatar oils (Q43 & Q61), respectively have significantly different $f_a^{a,N}$ values. Nevertheless, other samples with common source such as the two samples from Kuwait (K77 & K78), the two samples from Oman (O28 & O31), and five samples from the Northsea (U02, U07, U56, U59 and U89), respectively have similar values of the parameter. This observation is generally true with respect to other structural parameters from solid-state ^{13}C NMR data (Table 5.5).

Table 5. 5: Structural parameters calculated from the results of the solid-state ^{13}C NMR analysis of the petroleum and Tanezzuft (T35) asphaltenes (See section 5.1 for equations used to calculate the parameters)

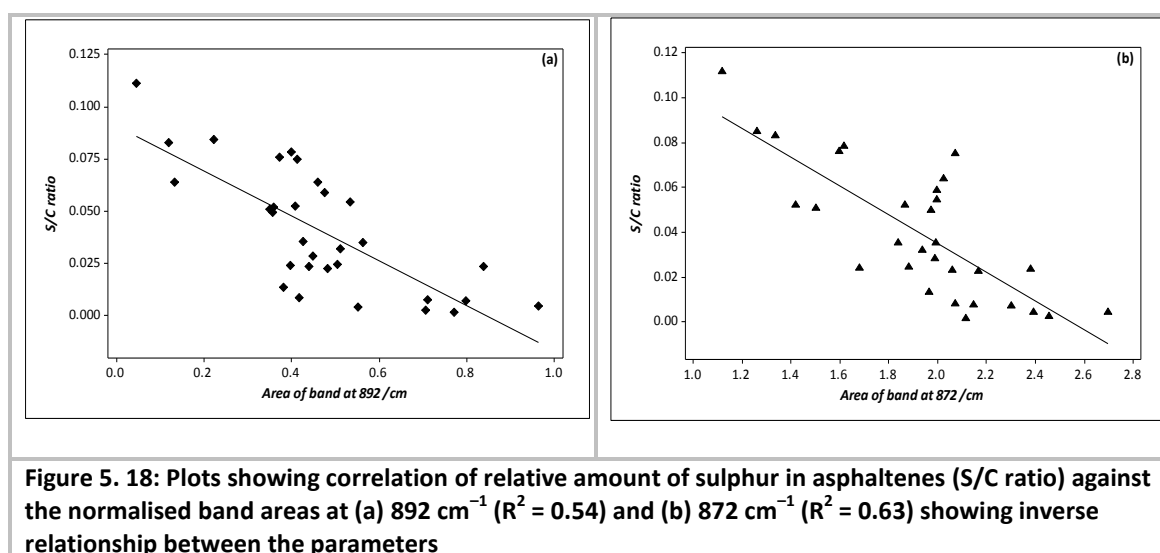
Sample	f_a	$f_a^{a,H}$	$f_a^{a,N}$	f_a^H	f_a^N	H_a
AR3	0.29	0.30	0.70	0.09	0.20	0.07
BN	0.27	0.30	0.70	0.08	0.19	0.07
C26	0.32	0.25	0.75	0.08	0.24	0.07
C30	0.39	0.36	0.64	0.14	0.25	0.13
CH	0.23	0.00	1.00	0.00	0.25	0.00
K77	0.32	0.40	0.60	0.13	0.19	0.12
K78	0.30	0.40	0.60	0.12	0.18	0.10
NB	0.24	0.25	0.75	0.06	0.18	0.05
O28	0.27	0.38	0.62	0.10	0.17	0.10
O31	0.34	0.37	0.63	0.13	0.22	0.12
PR1	0.29	0.45	0.55	0.13	0.16	0.11
Q43	0.29	0.58	0.42	0.17	0.12	0.15
Q61	0.36	0.34	0.66	0.12	0.23	0.16
U02	0.40	0.35	0.65	0.14	0.26	0.13
U07	0.32	0.40	0.61	0.13	0.20	0.13
U54	0.40	0.22	0.78	0.09	0.31	0.08
U56	0.36	0.37	0.63	0.13	0.23	0.14
U89	0.33	0.35	0.65	0.11	0.21	0.09
U59	0.39	0.34	0.66	0.13	0.26	0.12
T35	0.52	0.28	0.72	0.15	0.37	0.17

The FTIR results also show the aromatic groups in the petroleum asphaltenes are quite prominent as depicted by bands at $3100 - 3000 \text{ cm}^{-1}$ and $900 - 700 \text{ cm}^{-1}$ by aromatic C–H stretching and out-of-plane vibrations respectively and the presence of band at 1600 cm^{-1} by aromatic C=C stretching vibrations. The band at $3100 - 3000$ consists of two overlapping bands

at 3050 and 3017 cm^{-1} that are possibly due aromatic structures with 3 or less and 5 or more aromatic rings (Yen et al., 1984).

There is indication of heteroaromatic structures in asphaltenes from the infrared spectra. In particular, nitrogen in aromatic ring system appears to be important in asphaltenes to warrant correlating bands traditionally assigned to aromatic C=C vibrations to N/C elemental ratio thereby indicating the importance of the C=N group although both tend to absorb in the same region. This was however only observed in petroleum asphaltenes as attempt to correlate similar bands in Tanezzuft asphaltenes to the N/C ratio did not show any trend. This however might be because such bands are overshadowed by other more prominent bands possibly those by C–C, C–O etc.

It is noteworthy that the two bands at 892 and 872 cm^{-1} resulting from isolated hydrogen have been observed to inversely correlate with the relative proportion of sulphur in the asphaltenes (Figure 5.18). These bands indicate the degree of condensation and/or substitution on the aromatic ring system in the asphaltenes. The inverse relationship therefore suggests, aromatic ring condensation and/or substitution decrease with increase in sulphur content of the asphaltenes.



(d) *Effect of precipitation solvent on the precipitated asphaltenes*

The mid-infrared spectra of asphaltenes precipitated from the same non-biodegraded Northsea oil sample (U56) using *n*-pentane, *n*-hexane and *n*-heptane respectively are presented in Appendix 5D. As is the case in other petroleum asphaltenes the spectra generally show similar characteristic bands. Deconvolution (by curve-fitting) results are presented in Appendix 5D. The structural parameters are generally similar and appear to be independent of the solvent used in the precipitation of the asphaltenes. This is further corroborated by the solid-state ^{13}C NMR results (Table 5.6). The structural parameters of the asphaltenes are generally in agreement irrespective of the solvent used in the precipitation of the asphaltenes.

The values of the parameters are also in agreement with what were observed in other Northea asphaltenes (Table 5.5).

Table 5. 6: Structural parameters calculated from the results of the solid-state ^{13}C NMR analysis of the asphaltenes precipitated from the Northsea oil (U56) using *n*-pentane (U5), *n*-hexane (U6) and *n*-heptane (U7)

Sample	f_a	$f_a^{a,H}$	$f_a^{a,N}$	f_a^H	f_a^N	H_a
U5	0.37	0.40	0.60	0.15	0.22	0.14
U6	0.36	0.37	0.63	0.13	0.23	0.14
U7	0.33	0.42	0.58	0.14	0.19	0.14

However, this may appear to contradict the observations of Corbett & Petrossi (1978) and Long (1981) that the composition of asphaltenes vary with the kind of solvent used such that lower molecular weight solvents (e.g. *n*-pentane) precipitates greater amounts of resins with the asphaltenes than the higher molecular weight solvents (e.g. *n*-heptane). These differences however could have been removed through Soxhlet extraction of the asphaltenes which tend to 'clean' the asphaltenes by desorbing co-precipitated resins and waxes (see Chapter 4). It is therefore concluded that asphaltenes precipitated using *n*-pentane, *n*-hexane and *n*-heptane have similar structure and composition and the solvent employed in the precipitation of the asphaltenes has no significant effect on the composition of the asphaltenes provided appropriate measures were taken to remove co-precipitated materials.

5.3.5 Chemometric discrimination and correlation of asphaltenes

As seen above, petroleum asphaltenes generally have similar IR spectra and thus their discrimination based on visual examination of the spectra could be very difficult. However, with the aid of chemometric tools, infrared spectra could be used for such discrimination as has been applied to materials such as polymers (Beebe et al., 1998) and coal (Bona and Andrés, 2007). In this section unsupervised pattern recognition multivariate tools, including principal component analysis (PCA) and hierarchical cluster analysis (HCA), are used on the FTIR spectra of asphaltenes to explore the potential of identifying similarities and differences in chemical composition of the asphaltenes, and to correlate/discriminate amongst them based on these similarities and differences. Consequently, PCA was performed separately on three regions of the spectra namely 3100 – 2750, 1800 – 925, and 925 – 780 cm^{-1} to investigate the best region in correlating the samples.

(a) Analysis of 3100 – 2750 cm^{-1} spectral region

The principal component analysis of 3100 to 2750 cm^{-1} spectral region is summarised in Figure 5.19 (a) which shows that out of over 180 principal components (PCs) computed from the spectral data about 5 are the most important accounting for over 99% of the variance in the data. PC1 accounts for 72.1% while PC2 account for 14.4% variance and together they account for 86.5% of the variance in the data. This suggests score plot of PC1 against PC2 (Figure 5.19 (b)) could be useful in discriminating the asphaltenes and therefore the samples. The plot (Figure 5.19 (b)) however shows the asphaltene sample A39 from Abu Dhabi oil as an outlier. This asphaltene is quite different from all others in this study having prominent hydroxyl

absorption band. As outliers disproportionately affect PCA, this sample was removed and the analysis repeated.

Results of this analysis show the original multivariate data is reduced to about 6 important PCs accounting for 98.7% of the variance in the original data. Note that the elimination of A39 from the data set results in an increase in eigenvalues of PC2+ and consequently PC1 and PC2 together now account for only 71.2% of the variance. The loadings of various sections of the spectral region on PC1 show the most important contributors to this components are $3100 - 2995 \text{ cm}^{-1}$ and $2910 - 2750 \text{ cm}^{-1}$ which respectively correspond to aromatic C–H and aliphatic R_3CH , symmetric RCH_3 and R_2CH_2 stretching vibrations. On the other hand, the most important contributors to the second component (PC2) consist of the spectral region from $3000 - 2925 \text{ cm}^{-1}$ corresponding to asymmetric stretching vibrations of the aliphatic RCH_3 and R_2CH_2 groups.

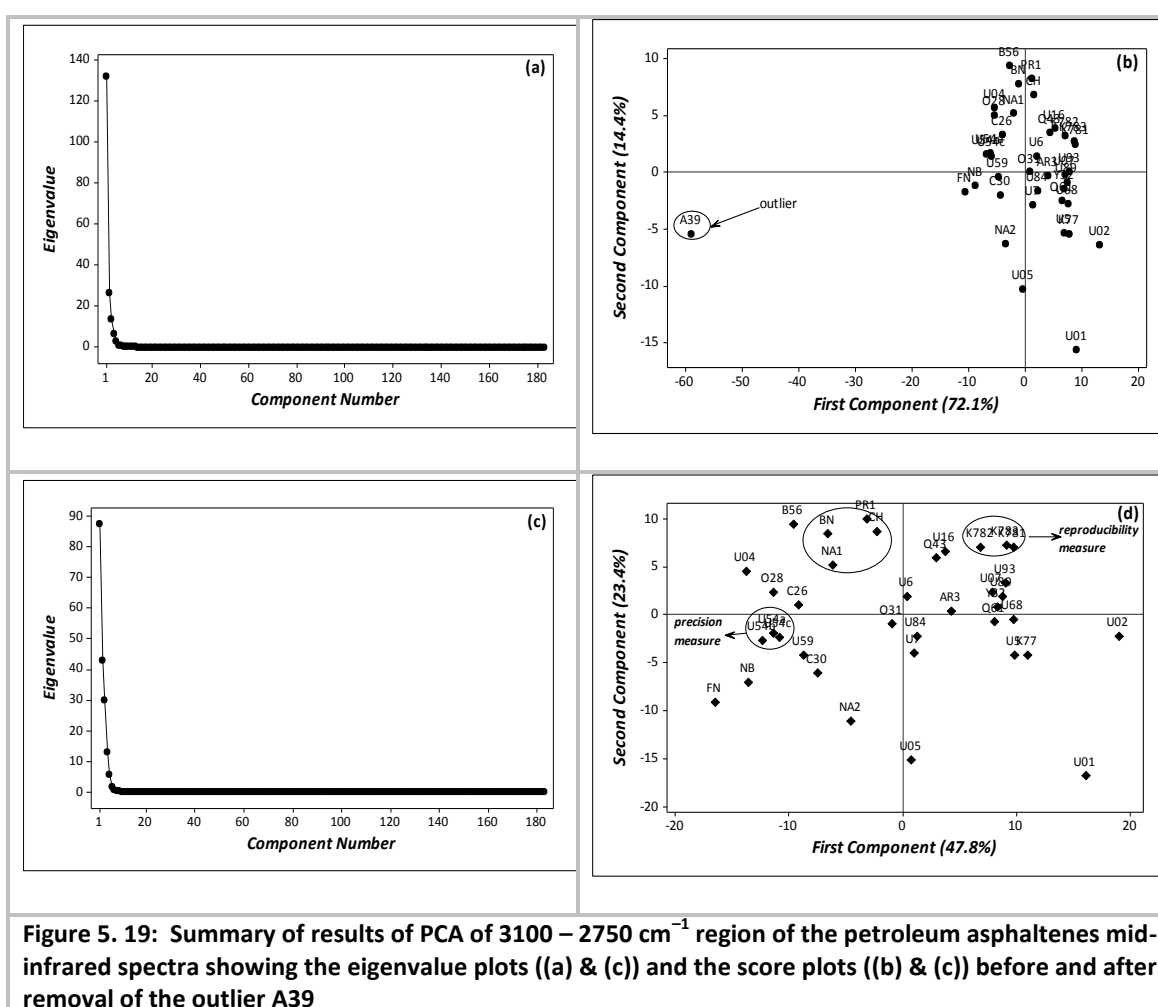


Figure 5. 19: Summary of results of PCA of $3100 - 2750 \text{ cm}^{-1}$ region of the petroleum asphaltenes mid-infrared spectra showing the eigenvalue plots ((a) & (c)) and the score plots ((b) & (c)) before and after removal of the outlier A39

Although the first two components (PC1 and PC2) account for about 71% of the variance in the data, the score plot of PC1 against PC2 shows no meaningful pattern attributable to the common source characteristic of the asphaltenes. Note the proximity of the samples in the plot indicates similarity in their chemical characteristics, and therefore chemical composition, described by the C–H vibrations. The only meaningful pattern is with respect to assessment of reproducibility of the measurements. Samples K781, K782 and K783 are triplicates of the Kuwait oil asphaltene (K78) prepared using the same procedures. The proximity of the samples

in the score plot indicates good reproducibility of the sample preparation method. The reliability of the instrument, on the other hand, was assessed by triplicate analysis of one sample (U54) at different points during the period of the analysis. These triplicate analyses are presented as U54a, U54b and U54c. The close proximity of these analyses on the score plot shows very good precision and therefore reliability of the measurements.

Furthermore, the proximity of BN, PR1, NA1 and CH in the plot is also noteworthy. These asphaltenes, although from different geographical regions, are biodegraded. The proximity may apparently reflect this although two other asphaltenes from biodegraded oils (U16 & NB) have significantly different scores on both PCs indicating they are significantly different from the other five samples. The asphaltenes from the two Northsea Kittiwake oils (U01 & U05) also have similar scores on PC1. The disparity between them is on their different on PC2 which although positive are significantly different.

Improvement in discrimination between the asphaltenes is achieved using hierarchical cluster analysis (HCA) using the principal components generated from PCA as independent variables in order to remove the negative influence of the multicollinearity of the original spectral data on the analysis (Hair *et al.*, 2006). For this purpose six significant PCs (PC1 to PC6), accounting for 98.9% of the variance in the data, were selected based on eigenvalues versus component number plot (Figure 5.19 (c)) for the HCA. This results in a general improvement in discrimination and classification of the samples.

A total of seven clusters were obtained although two of them (clusters 5 and 7, Figure 5.20) are one-sample clusters and represent unusual observations with respect to their scores on the PCs and therefore their 3100 – 2750 cm^{-1} IR spectral characteristics (Figure 5.20). These unusual observations are the asphaltenes from the Serbian (Pannonian Basin) biodegraded oil NA1 which was observed to have an unusual *n*-alkanoic acid distribution from results of the ruthenium ion catalysed oxidation (RICO) of the asphaltene (Chapter 6). The unusual FTIR character of this sample might be reflecting this 'usual' distribution of the alkyl side chain of the asphaltene compared to other oil asphaltenes.

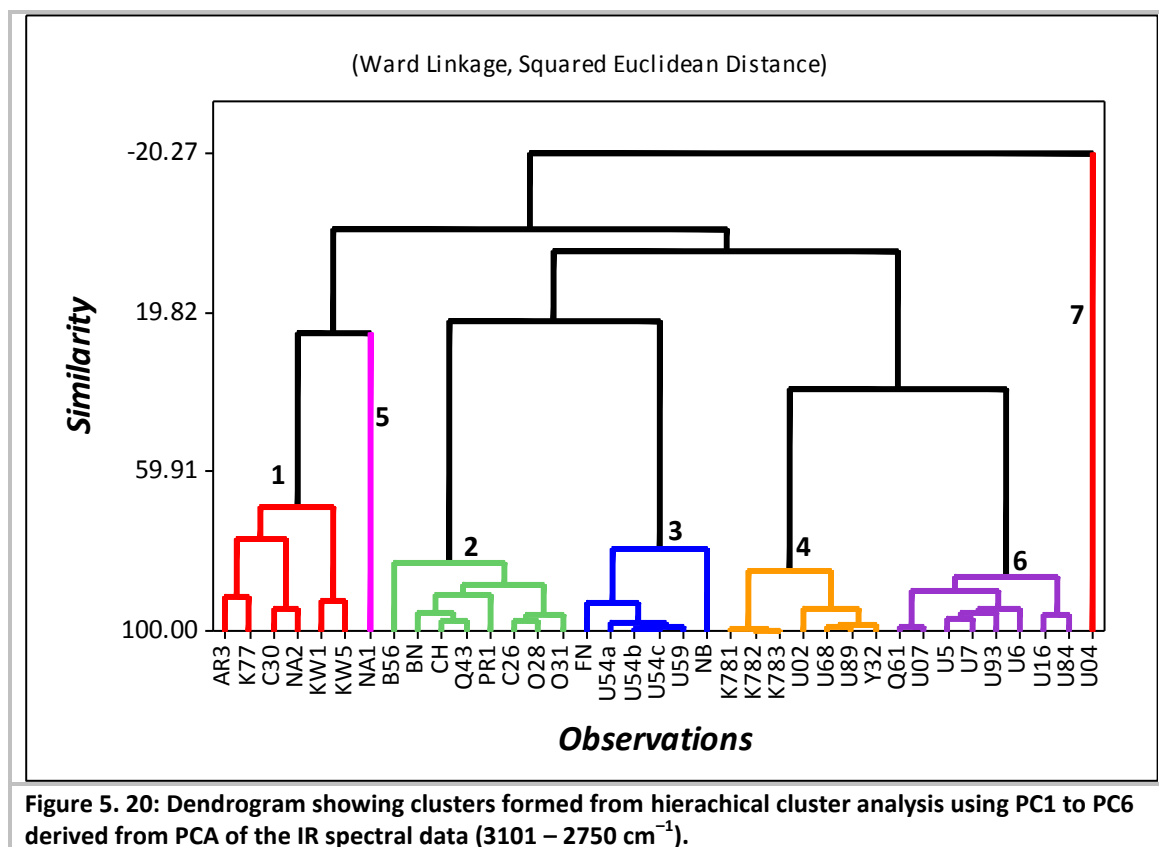


Figure 5. 20: Dendrogram showing clusters formed from hierarchical cluster analysis using PC1 to PC6 derived from PCA of the IR spectral data (3101 – 2750 cm^{-1}).

The dendrogram further shows the level of precision of the measurement and reproducibility of the analysis. The three measurements on sample U54 (i.e. U54a, U54b & U54c) are not only grouped in same cluster but have similarity level of over 98%. Similarly, the three samples prepared from K78 asphaltene (i.e. K781, K782 & K783) are also grouped together (cluster 4) with similarity of over 99%.

Furthermore, the three asphaltenes U5, U6 and U7 precipitated from U56 oil from Northsea using *n*-pentane, *n*-hexane and *n*-heptane respectively are grouped in the same cluster (cluster 6) with similarity amongst them of 94 to 97% indicating very similar chemical composition with respect to their scores on the PCs and therefore their C–H vibration signatures of their respective aliphatic and aromatic moieties.

In general, the asphaltenes from Northsea oils seem to be grouped together compared to other asphaltenes. Thus, with the exception of Q61 from Qatar and NB from Nigeria, clusters 6 and 3 exclusively consist of asphaltenes from the Northsea oils. Although this may be due to compositional similarity amongst the asphaltenes, it also could be because these asphaltenes form the bulk of the sample set. Other clusters are mixtures of asphaltenes from oils of different geographical regions and different sources. Cluster 1 for example consists of asphaltenes from the Gulf of Mexico (AR3), Middle East (K78), Canada (C30) and Northsea (U01 & U05). Similarly, cluster 2 is a combination of asphaltenes although both asphaltenes from the two Oman oils (O28 and O31) are grouped in this cluster with similarity of over 95%.

Notably, there are many asphaltenes from oils generated from the same source rock that are classified in different clusters. This suggests the asphaltenes are chemically (in terms of aliphatic and aromatic C–H signatures) more similar to other members of their groups than they are to asphaltenes with which they share common source rock but classified in different

clusters. For example, K77 is grouped in cluster 1 while K78 in cluster 4 and C30 in cluster 1 while same source C26 is grouped in cluster 2 although clusters 1 and 2, with distance between centroids of 2.66 are the closest clusters in the classification.

It is also clear from Figure 5.20 that biodegradation does not seem to influence classification of the asphaltenes. Asphaltenes from the biodegraded oils (AR3, NA1, CH, BN, NB and U16) are grouped in different clusters with other members that are not biodegraded. This suggests that the biodegraded oil asphaltenes are compositionally, in terms of aliphatic and aromatic C–H signatures, more similar to the non-biodegraded oil asphaltenes that are members of their clusters than they are to other biodegraded oil asphaltenes.

(b) Analysis of 1800 – 925 cm⁻¹ spectral region

This is a complex region consisting of bands by various kinds of functional groups such carbonyl C=O, aromatic C=C, aliphatic C–C and C–O in ether and ester groups. Figure 5.21 is the result of PCA on the spectral region from 1800 to 925 cm⁻¹. The PCA condense the information in the region into six significant principal components (PC1 to PC6) which cumulatively account for 96% of the variance in the data (Figure 5.21 (a)). PC1 and PC2 together account for 61.4% of the variance. The loadings of the original variables on the two PCs show that PC1 is a fair representation of all the wavenumbers covering 1700 to 1000 cm⁻¹ with all the major bands, except those at 1031 and 1006 cm⁻¹. PC2, on the other hand, has a more complex loading. The carboxylic and conjugated carbonyl (C=O) bands have significant but negative loadings as do the two bands at 1031 and 1006 cm⁻¹. Aromatic C=C and aliphatic bands between 1450 and 1300 cm⁻¹, however, have significant positive loadings on the PC.

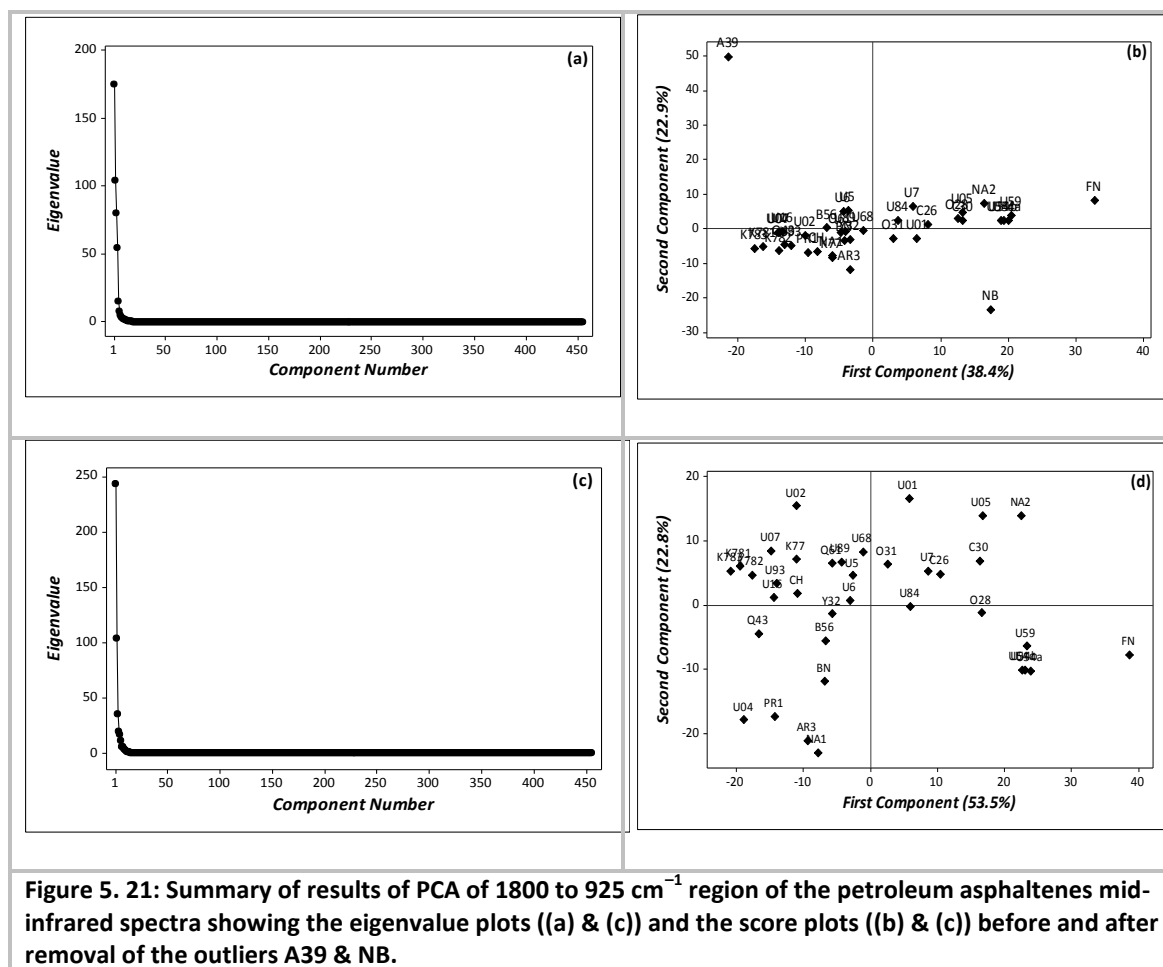


Figure 5. 21: Summary of results of PCA of 1800 to 925 cm^{-1} region of the petroleum asphaltene mid-infrared spectra showing the eigenvalue plots ((a) & (c)) and the score plots ((b) & (d)) before and after removal of the outliers A39 & NB.

The score plot of PC1 and PC2 is presented in Figure 5.21 (b). The plot shows the dimensional structure in the samples based 61.4% variance of the data. As in Figure 5.20, sample A39 and NB are possibly outliers and are thus removed from the data set. This increased the Eigenvalue, and therefore the proportion of the variance, of PC1. The first five PCs now cumulatively account for 92.1% of the variance, and PC1 and PC2 together account for 76.3% of the variance in the data. The score plot of PC1 and PC2 (Figure 5.21 (d)) is therefore a better representation of the information in the data than initially observed before the removal of the outliers and thus accounts for more dimensionality in the samples.

As in chemometric analysis of the 3100 – 2750 cm^{-1} region of the asphaltene spectra, the precision of the measurements and reproducibility of the analysis are respectively reaffirmed by proximity of the triplicates of samples U54 and K78 (Figure 5.22) on the PC1 versus PC2 space. The plot also shows four of the six biodegraded oil asphaltene are closely located which indicates similarity in chemical composition amongst the asphaltene. This is in addition to close proximity of the three K78 samples and the three U54 measurements in support of good repeatability and precision of the methods as observed in the analysis of the 3100 – 2750 cm^{-1} region.

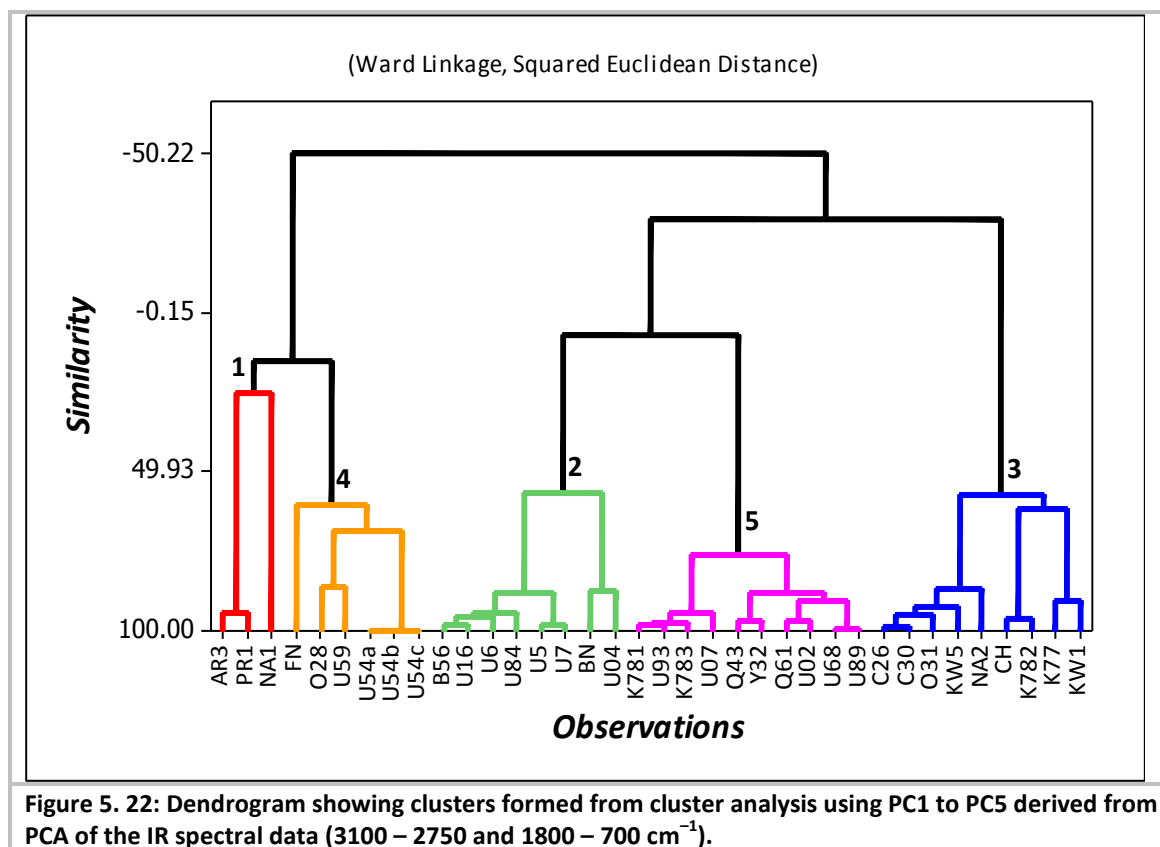


Figure 5. 22: Dendrogram showing clusters formed from cluster analysis using PC1 to PC5 derived from PCA of the IR spectral data (3100 – 2750 and 1800 – 700 cm^{-1}).

Note also in this score plot that U01 and U05 have similar plot scores on the PC2 although their scores on PC1 are significantly different thereby setting them significantly apart on the plot the reverse is however the case with respect to marine carbonate sourced C26 and C30 from Canada. Nevertheless, in general asphaltenes from Northsea oils, all of which are believed to be sourced from the Jurassic Kimmeridge Clay Formation, are scattered in nearly all sections of the score plot. This shows heterogeneity in the chemical composition of the samples as represented in the two PCs

As the first two PCs represent only about 76% of the variance, there is still significant information that has not been captured in the score plot above. Thus hierarchical cluster analysis (HCA) was done using scores of the asphaltenes on the first five orthogonal PCs. The analysis grouped the asphaltenes into five clusters of significant chemical heterogeneity and members of which are of similar chemical characteristics as represented by the PCs. The first cluster has three members all of which are biodegraded and two (AR3 and PR1) of which are from Gulf of Mexico and which are more similar to each other than they are to the asphaltene from the biodegraded Pannonian Basin oil (NA1).

The second cluster contains, with exception of B58 from Bangladesh, asphaltenes from Northsea oils sourced from Jurassic Kimmeridge Clay. U5, U6 and U7 are however from the same oil (U56) but precipitated using *n*-pentane, *n*-hexane and *n*-heptane respectively.

(c) *Analysis of 925 – 680 cm^{-1} spectral region*

The PCA of aromatic C–H out-of-bond vibration spectral region of the asphaltenes reduced the multivariate data with over 95% of the variance captured in the first four PCs (Figure 5.23). The first two PCs (PC1 & PC2) account for 85% of the variance. The score plot of the two PCs is

shown in Figure 5.23. From this sample A39 appears to be an outlier as observed in analysis of other spectral regions. It was therefore removed from the analysis.

The resulting PCA shows that PC1 and PC2 together now account for about 70% of the variance in the data. Loadings of the variables on the two PCs show that PC1 has nearly equal contributions from all the bands in the region. PC2 on the other hand has significant negative loading from bands between 900 and 860 cm^{-1} and between 775 and 735 cm^{-1} which are respectively by isolated hydrogen (1H) and four neighbouring hydrogens (4H) on aromatic system. The bands at 850 and 720 cm^{-1} resulting from 1H and alkyl chain greater than butyl have significant positive loadings on the PC. The PC might therefore be a presentation of degree of condensation and substitution on the aromatic ring systems in the asphaltenes.

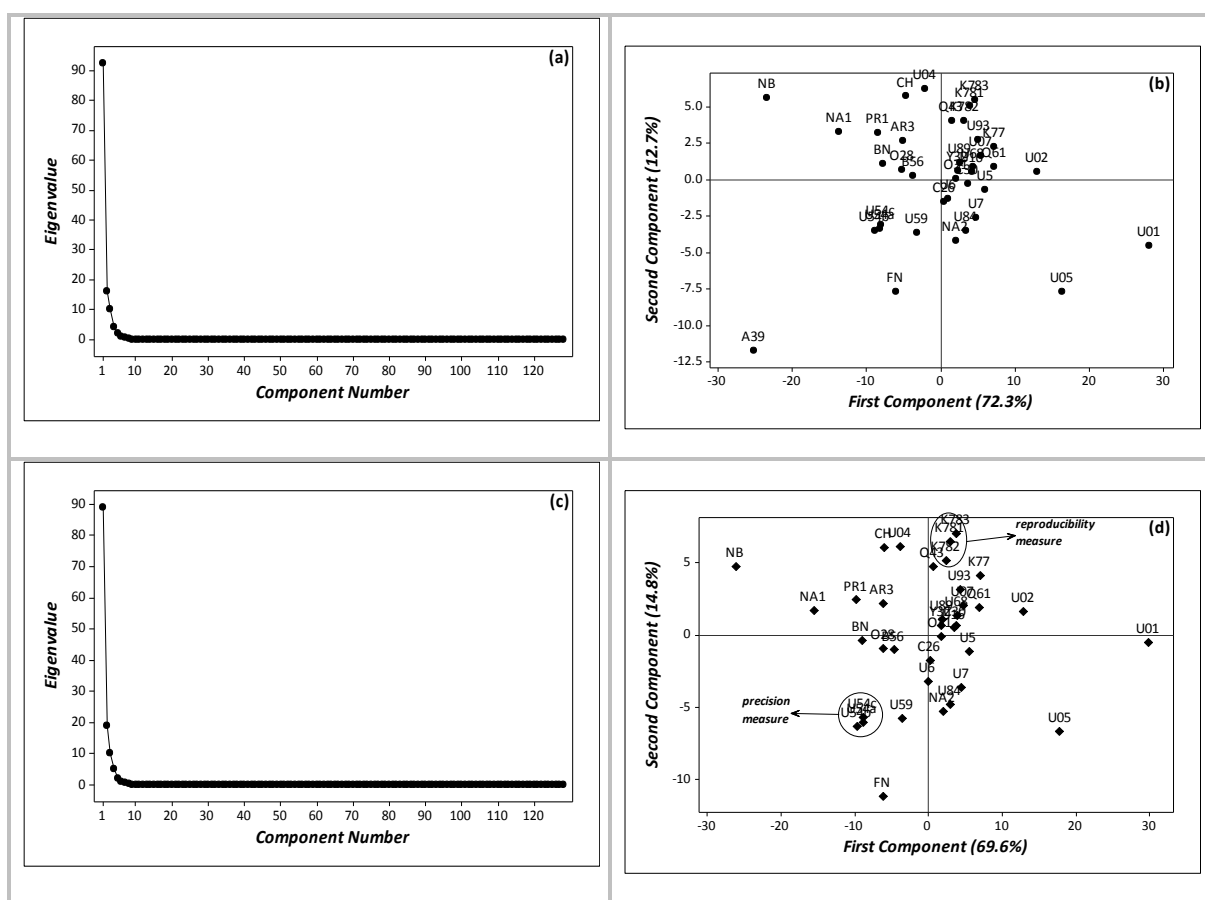
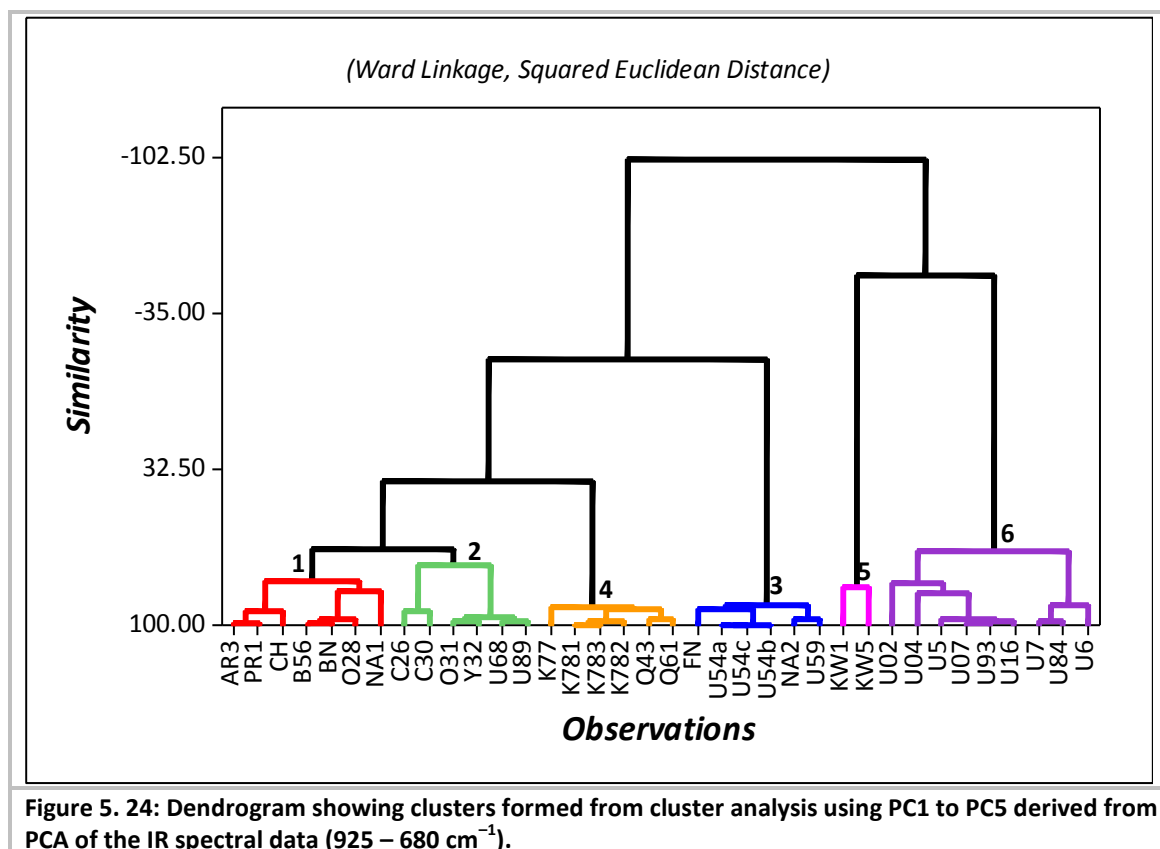


Figure 5. 23: Summary of results of PCA of 925 to 700 cm^{-1} region of the petroleum asphaltenes mid-infrared spectra showing the eigenvalue plots ((a) & (c)) and the score plots ((b) & (d)) before and after removal of the outlier A39.

The score plot of PC1 against PC2 displays the asphaltenes based on their respective scores as represented in the two PCs. As in analysis of the other spectral regions presented in earlier sections, precision and reproducibility measurements are very good as depicted by the proximity of the three U54 measurements and K78 samples respectively. Four of the six asphaltenes from biodegraded oils also plot fairly closely. Most other samples however have similar scores on PC1 and cluster together on the score plot thereby making difficult to discern any meaningful structure from the plot.



The first four PCs accounting for 96% of the variance in the data were used in HCA. The results of the analysis are summarised in Figure 5.24. Five clusters with significant heterogeneity and within cluster similarity level of at least 68% were obtained. Precision measurements (U54) are grouped in cluster 3 with over 99% similarity level. Similarly, repeatability samples (K78), grouped in cluster 4, have about 99% similarity level. Clusters 3, 5 and 6 consist exclusively of asphaltenes from Northsea oils, except that NA2 asphaltene from Pannonian Basin non-biodegraded oil is grouped in cluster 3. Cluster 4, on the other hand, consist of asphaltenes from Middle East (Qatar and Kuwait) oils all of which were sourced from marine carbonate/marl source rocks (see Chapter 3).

Clusters 1 and 2 consist of mixture of asphaltenes from different geographical regions and sources. The heterogeneous membership of these clusters is exemplified by the grouping in cluster 2 of the two asphaltenes (C26 & C30) from marine carbonate sourced Canadian oils and asphaltenes (U68 & U89) from marine shale sourced Northsea oils in addition to asphaltenes (O31 & Y32) from Oman and Yemen oils. Nonetheless, the clustering the level of similarity between same source asphaltenes is greater than other members of the cluster particularly with respect to C26/C30 and U68/U89 pairs. Note however that while O31 is grouped in cluster 2, its same source counterpart O28 is grouped in cluster 1. Although this may reflect different source kitchens with significant difference in organo-facies as reflected in the distribution of steranes in the maltene fractions of the two oils, the difference observed here may not be extremely significant considering the level of similarity of 67% between cluster 1 and 2 which is similar to the similarity level of 68% observed in cluster 6. It is interesting to note that cluster 1 consists of 5 of the 6 asphaltenes from biodegraded oils used in this study, although it also contains 2 asphaltenes (B56 & O28) from non-biodegraded oils.

Cluster 5 comprises exclusively the asphaltenes from the two Northsea Kittiwake oils. This shows the asphaltenes are compositionally, with respect to the substitution pattern on the aromatic ring systems, similar to each other. It is however not clear why the two asphaltenes are considerably different from other asphaltenes and particularly from those obtained from other Northsea oils. The significance of the difference is shown from the fact that the distance between cluster centroids (3.8 to 4.6) is highest wherever it is involved. The only recorded distinct feature of these samples is they have particularly high C_{35} homohopanes with C_{35}/C_{34} homohopane ratio of about 1.40 which is significantly higher than other Northsea oils which average at about 1.0. Since Kimmeridge Clay was generally deposited under stratified anoxic condition (Wignall, 1994; Tyson et al., 1979), the difference could be a reflection of the level of maturity when the oils were generated. The two Kittiwake oils (U01 & U05) are likely less mature than other Northsea oils to explain the pronounced C_{35} homohopanes and therefore just as A39 appears as an outlier in the analyses because of its advanced maturity, U01 and U05 appear to have 'unusual' characteristics because of their relatively low maturity.

(d) *Complete spectral analysis*

The three spectral regions are further analysed together to explore whether this could improve the discrimination of the asphaltenes. Results of the PCA show that fewer than 20 PCs account for 99% of the variance in the data. The first PC accounts for 42.1% of the variance and together with PC2 cumulatively account for 71.6% of the variance (Figure 5.25). The loadings of the variables on the two PCs are generally as described in the three sections above.

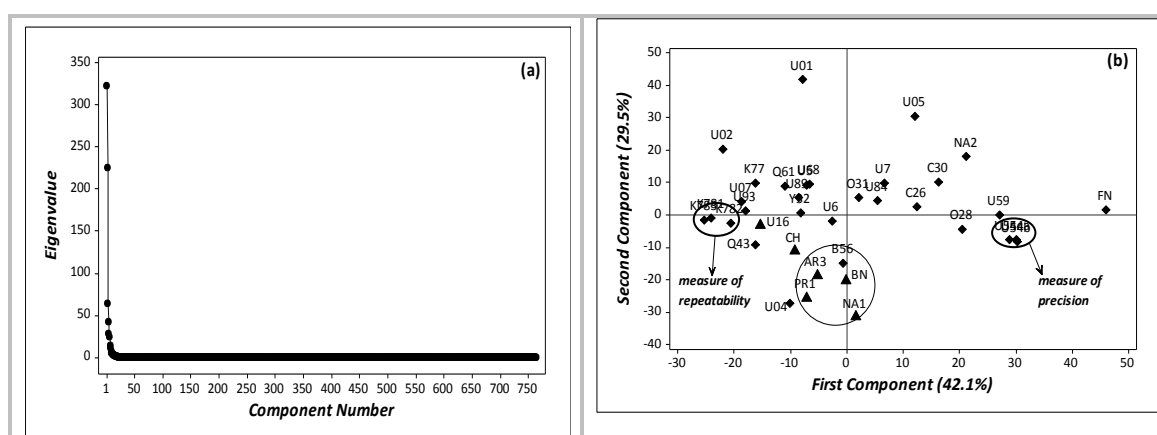


Figure 5. 25: Summary of results of PCA of 3100 – 2750 cm^{-1} and 1800 to 700 cm^{-1} regions of the petroleum asphaltenes mid-infrared spectra showing (a) the eigenvalue plots, and (b) the score plots. The outliers A39 & NB have been removed from the analysis.

Score plot of PC1 against PC2 is presented in Figure 5.25. As observed in the previous sections, U54 and K78 respectively plot closely indicating good precision and repeatability of the measurements and sample preparation methods adopted. Note that most of the samples have similar scores on PC1 and most of the differences amongst the asphaltenes is based on their scores on PC2. Nonetheless, it is interesting to note that 5 of the six asphaltenes (represented by solid triangles, Figure 5.25) from biodegraded oils have relatively high negative scores (> -10) on PC1 and low score (< -10) on PC2. The Kittiwake asphaltenes U01 and U05 have the highest (> 30) scores on PC2 and Veslefrikk asphaltene FN has the highest score (> 40) on PC1 thereby setting them apart on the plot.

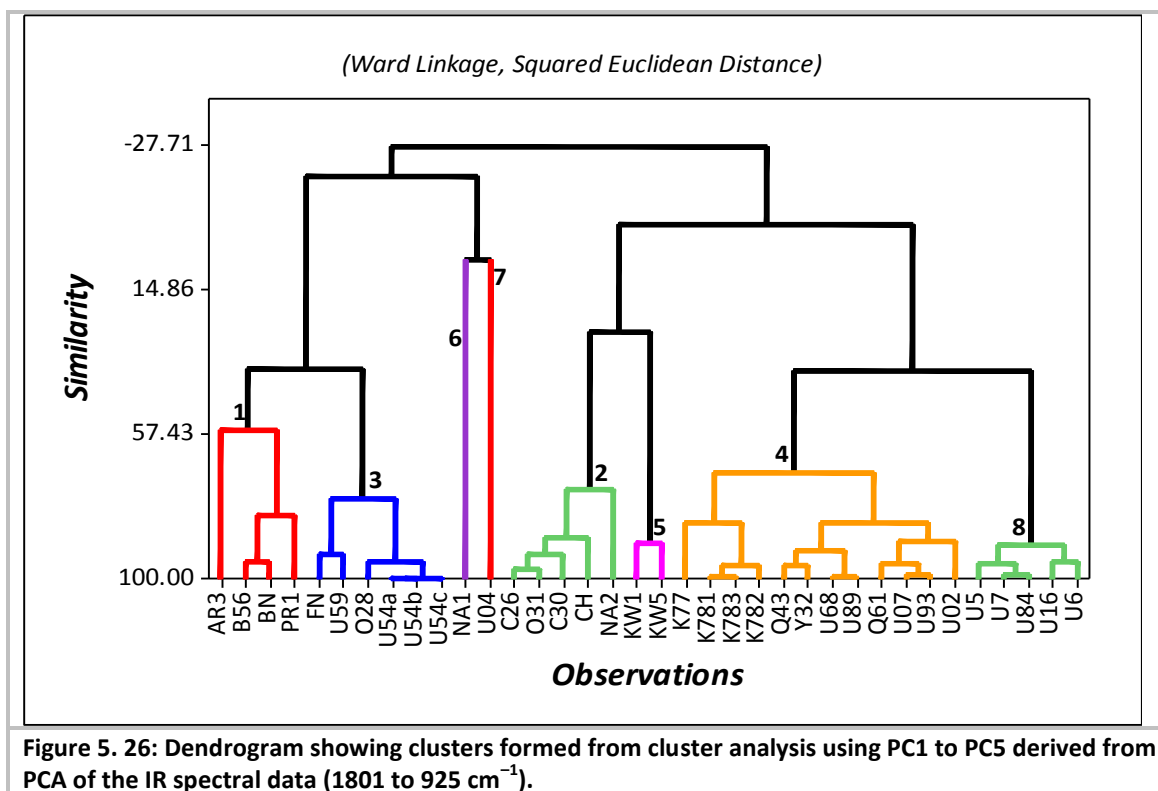


Figure 5. 26: Dendrogram showing clusters formed from cluster analysis using PC1 to PC5 derived from PCA of the IR spectral data (1801 to 925 cm^{-1}).

For HCA six significant PCs that cumulatively account for 92.3% of the information in the original variables were used. The results of the analysis give eight clusters (Figure 5.26) although two of them are one-sample clusters and represent unusual samples. These have been discussed in earlier sections. Nevertheless, U04 have negative scores on all the six PCs and NA1 has positive scores on PC2 to PC5 although other samples opposite scores.

Cluster 8 consists exclusively of asphaltenes from Northsea oils. Three of the asphaltenes (U5, U6 & U7) were precipitated from U56 Northsea oil using *n*-pentane, *n*-hexane and *n*-heptane respectively. The grouping of these asphaltenes in the same cluster and their level of similarity of 90% indicate near identical chemical composition irrespective of the solvent used in the precipitation of the asphaltene.

Members of clusters 1 and 4 come from wide variety of sources and depositional environments. Cluster 4 however has the highest within-cluster heterogeneity that may warrant identification of two groups; one consisting of the asphaltenes (K77 & K78), with similarity level of 84%, from marine carbonate-sourced Kuwait oils. The second consists of the two asphaltenes (Q43 & Q43) from Qatar oils, both sourced from marine marl source rock, and some asphaltenes from Northsea oils.

Cluster 3 consist of Northsea oils asphaltenes except O28 from one of the two Oman oils; the other being grouped in cluster 2. This may be because of differences in organic matter characteristics of the source kitchens of the two oils as suggested by distribution of the steranes from aliphatic fractions of the oils. As observed previously, cluster 5 is a two-sample cluster consisting of the asphaltenes from the Northsea Kittiwake oils. Cluster 2, on the other hand, consists of the three asphaltenes from Canada oils all of which were sourced from marine carbonate sources.

In general, statistical multivariate analysis of the similarities and differences amongst the different asphaltenes from different sources, depositional environment and geographical regions reveal that asphaltenes from a common source rock tend to show similar chemical composition as measured by FTIR and such asphaltenes are commonly classified in same groups. Misclassifications are however encountered and these could be attributable to differences in chemical composition because of maturity levels of the oils and/or subtle differences in organo-facies of different source kitchens. The results also show there no significant difference between asphaltenes precipitated by *n*-pentane, *n*-hexane and *n*-heptane. Furthermore, the chemical composition of the asphaltenes does not appear to reflect the depositional environment of the source rock which could be because the asphaltenes were formed early in the genesis of the organic matter. In addition, asphaltenes from biodegraded oils appear to exhibit significant similarity in the chemical composition resulting in some having similar IR spectral characteristics and therefore being classified in similar group.

5.4 Summary and Conclusions

Asphaltene are complex heterogeneous substances with high molecular weights and a wide range of molecular composition making it almost impossible to elucidate their chemical composition using traditional chromatographic/mass spectrometry techniques. However, bulk composition of complex materials such asphaltene may be investigated using FTIR particularly with the aid of curve-fitting tools to help resolve the complex overlapping bands that are commonly the product of the FTIR analysis of carbonaceous substances. These techniques together with chemometric tools were used to investigate the composition of the asphaltene from a variety of sources. The results obtained show that:

1. Asphaltene consists of complex chemical substances with diverse functionalities but principally saturated aliphatic and aromatic structures. Oxygen functionalities in the form of hydroxyl, carboxylic, ester and conjugated carbonyl are significantly present. Nitrogen functionalities mainly in form of aromatic tertiary amines, and aromatic pyridine- and pyrrole-type were also tentatively identified but only in petroleum asphaltene
2. Asphaltene from black shales generally have higher proportions of oxygen functionalities than petroleum asphaltene. Hydroxyl and carboxylic acid groups are particularly abundant and in fact are the dominant functional groups in some black shale asphaltene. Ester groups were detected only in black shale and coal asphaltene.
3. Aromatic structures are particularly prominent in petroleum asphaltene and only barely detectable in immature asphaltene from black shales. This however was observed to not only be maturity dependent but also be source dependent as asphaltene formed from aromatic-rich organic matter exhibit a high aromatic signature comparable to matured samples.
4. The relative proportion of carbonyl group in carboxylic and conjugated functionalities appears to be related to the depositional environment with asphaltene from oils sourced from carbonate and marl source rocks having greater proportion of conjugated carbonyl groups and the shale-sourced having greater proportion of the carboxylic carbonyl group.

5. The kind of light hydrocarbon solvent used in precipitation of petroleum asphaltenes does not appear to have a significant effect on the bulk composition asphaltenes so precipitated
6. Correlation/discrimination of asphaltenes based on their mid-infrared spectra with the aid of chemometric tools shows potential in correlating asphaltenes with similar chemical characteristics. However, as the composition of asphaltenes is dependent on their thermal histories, asphaltenes tend to evolve towards an equilibrium composition and asphaltenes with different source could be classified in the same group.

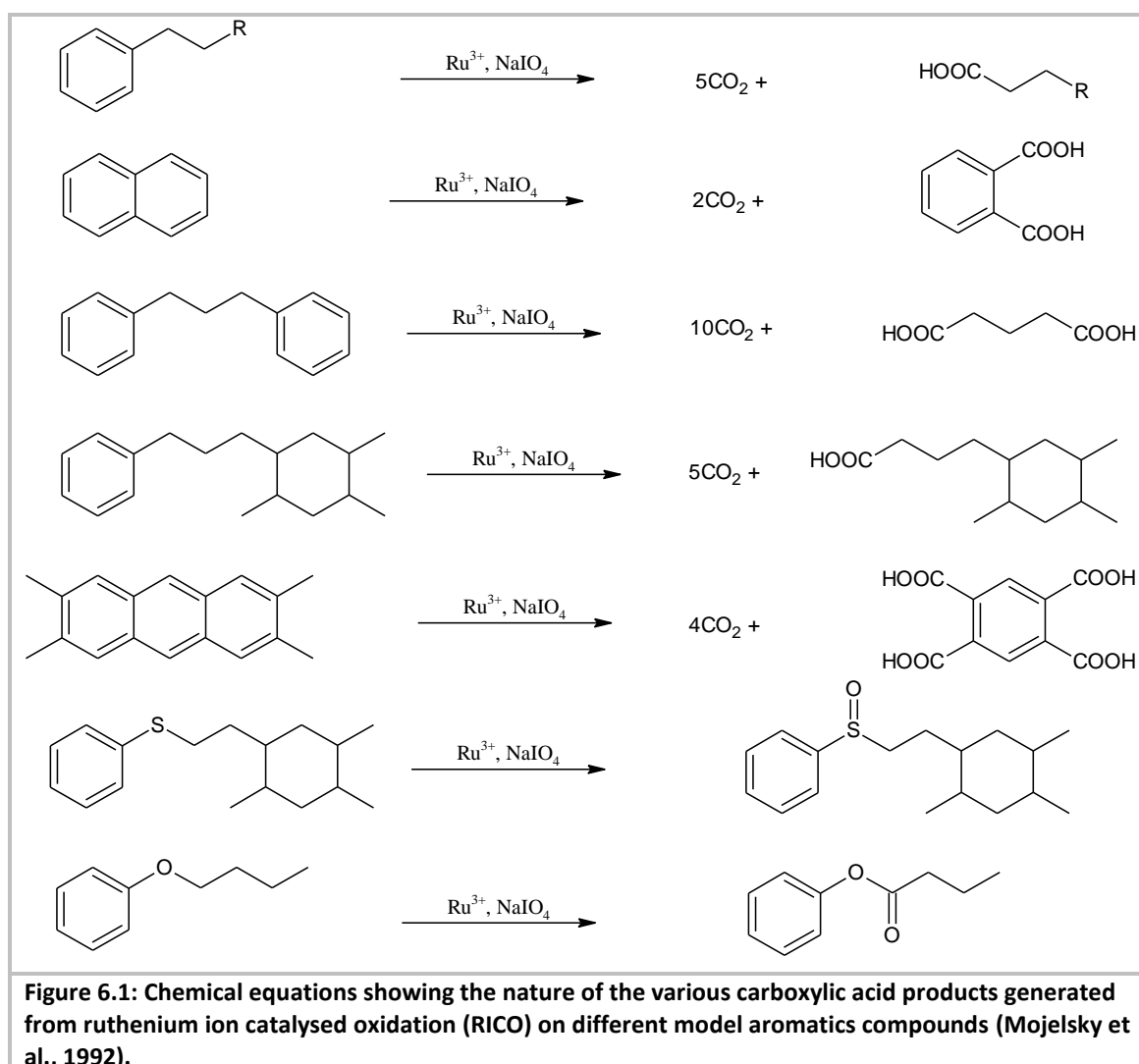
Chapter 6 Bound Biomarkers in Asphaltenes Released by Ruthenium Ion Catalysed Oxidation

6.1 Introduction

In Chapter 4 results were presented on the hydrocarbons (e.g. biomarkers) physically adsorbed/trapped in petroleum asphaltenes. In addition, asphaltenes are also known to contain biomarkers that are chemically bound to the asphaltene (aromatic) core via linkages such as the ester, ether, sulphide and carbon - carbon bond (see Section 2.5) and are therefore part of the asphaltene chemical structure of asphaltenes (Peng et al., 1997; Trifilieff et al., 1992).

The biomarkers bound in asphaltenes via carbon-carbon bonds appear to be formed during diagenesis rather than after the oil generation. While other bonds (i.e. ester and ether) could be formed in the reservoir from acids supplied through biodegradation for example (Aitken *et al.*, 2004), carbon-carbon bond formation in asphaltenes is most likely catalysed by clay minerals (Trifilieff et al., 1992) and therefore might have occurred in sediments during or immediately after deposition as a result of diagenesis.

There are many methods, such as permanganate, dichromate etc oxidation, for oxidative destruction of aromatic moieties (Barakat and Yen, 1988; Barakat and Yen, 1987). Ruthenium ion catalysed oxidation (RICO) using sodium periodate (NaIO_4) as oxidant is however particularly important. This technique was first used and reported by Djerassi and Eagle (1953). Since then the reagent, in its many forms, has been widely used in oxidation of various kinds of organic substrates ranging from alkenes to heteroatomic compounds (Kasai and Ziffer, 1983; Lee and van den Engh, 1973). The method involves using ruthenium ion (III) to catalyse fairly selective destruction (through oxidation) of the aromatic core to a carboxylic group without affecting any aliphatic appendages that may be attached to the aromatic ring system. The aliphatic groups are released as carboxylic acids (Figure 6.1).



RICO is a selective method in that the oxidation predominantly occurs at the α -aromatic ring carbon and so generates the alkyl group with carboxyl group from the degradation of the ring system. This has been confirmed by oxidation of pure compounds as illustrated in Figure 6.1. The figure, in addition, shows other bonds of interest, such as sulphide and ether, do not significantly interfere. For example, sulphides are converted to sulphones and sulphoxides, and ethers mainly to esters (Ilsley et al., 1986b; Gore, 1983).

Consequently, RICO has been widely used to elucidate structures of macromolecules including soil organic matter (Ikeya *et al.*, 2007); coal (Li et al., 2004; Blanc and Albrecht, 1991; Stock and Wang, 1986; Stock and Tse, 1983); kerogen (Blokker et al., 2006; Dragojlovic et al., 2005; Li et al., 2004; Boucher et al., 1991); asphaltenes (Peng et al., 1999a; Strausz et al., 1999a; Su et al., 1998; Mojelsky et al., 1992; Trifilieff et al., 1992); and other geopolymers (Ikeya et al., 2007; Blokker et al., 2006; Blokker et al., 2000).

The method has been successfully used to reveal that asphaltenes contain acyclic and cyclic aliphatic moieties, attached to aromatic moieties (Strausz *et al.*, 1999a). Peng *et al.* (1999a), for example, studied an immature asphaltene using RICO and observed that the oxidation products principally consists of *n*-alkanoic acids and diacids, as well as benzenepolycarboxylic acids. They also found biomarkers including hopanoic acids, steranoic acids and

gammaceranoic acid in the oxidation products. Most importantly, from the geochemical perspective, Peng *et al.* (1999a) were able to classify the oil, based on these biomarkers, as immature, possibly deposited in hypersaline lacustrine environment under suboxic conditions. Although this sort of information can be obtained from asphaltenes, there appears to be only two published work (Ma *et al.*, 2008; Guanjun *et al.*, 2003) that attempt to use asphaltene biomarkers to correlate oils.

Thus, the main aim of this part of the work is to use RICO to investigate the aliphatic content, and in particular bound biomarkers, in asphaltenes and explore the geochemical information that can be derived from these biomarkers. Specific objectives include:

1. to investigate the composition of the aliphatic moieties in asphaltenes from different sources and geographical regions
2. to investigate the significance of and the differences in molecular composition of the chemically bound biomarkers linked to asphaltenes from different sources, ages, geographical regions and palaeoenvironments of deposition
3. to investigate the evolution of the aliphatic moieties in asphaltenes with thermal maturation
4. to elucidate geochemical information that can be obtained from the chemically bound biomarkers
5. to analyse the relevance of such information in correlating/discriminating similar/different oils compared to information based on hydrocarbon biomarkers in the maltene fraction

6.2 Methodology

6.2.1 Selection and preparation of samples

Samples of crude oils were selected to cover different geographical regions, geological ages, sources and depositional environments (see Chapter 3) to enable the assessment of the influence of such variables on the information obtained. In order to study the influence of thermal maturation on the asphaltene biomarker, coal samples (C04, C56, C69 & C15) of different maturity (0.4 to 1.5% vitrinite reflectance) were also included in the study. The asphaltenes used were obtained from the oils and coals listed in Table 6.1.

Table 6. 1: List of samples used in the RICO bound biomarker studies presented in this Chapter

SN	Sample ID	Field	Source rock	Country
1	A32	-	Jurassic	Abu Dhabi
2	C26	Midale	Ordovician	Canada
3	C30	Midale	Ordovician	Canada
4	K77	Raudhatain	Jurassic	Kuwait
5	K78	Sabriyah	Jurassic	Kuwait
6	O28	Natih	Cretaceous	Oman
7	O31	Natih	Cretaceous	Oman
8	Q43	Al Shaheen	Jurassic	Qatar

9	Q61	Bul Hanine	Jurassic	Qatar
10	U02	Flora	Jurassic	UK
11	U54	Ettric	Jurassic	UK
12	U59	Bruce	Jurassic	UK
13	U68	-	Jurassic	UK
14	U89	Britannia	Jurassic	UK
15	B58	Habigong	Olig./Miocene.	Bangladesh
16	NBA	-	-	Nigeria
17	Y32	Hemiar	Jurassic	Yemen
18	NA1	Gaj	-	Serbia
19	NA2	-	-	Serbia
20	AR3	Confidential	Confidential	US
21	PR1	Confidential	Confidential	US

Bitumens were extracted from coal samples as described in Section 2.3.2. Asphaltenes were precipitated from bitumens and oils as described in Section 2.3.3. In order to minimise interference from co-precipitated hydrocarbon biomarkers from maltene fraction (Chapter 4), the asphaltenes were extracted with *n*-hexane for 10 days using the Soxhlet method as described in Section 2.3.3. The RICO procedure adopted and subsequent sample preparation are respectively described in Sections 2.3.6, 2.3.10 and 2.4.6.

6.2.2 Identification of compounds and data analysis

The carboxylic acid products from the RICO treatment of asphaltenes were analysed as methyl esters. However, the aromatic acids were not analysed because the available esterification method only allowed for analysis of organic phase products. The methyl esters were identified using their respective mass spectra and their relative retention times in mass chromatograms in comparison with published data as described in the text.

Concentrations of the compounds of interest were calculated (equation 6.1) using deuterated hexadecane-d₃₂ as the internal standard. The relative response factor was assumed to be one. The concentration (w_x) in mg/g asphaltenes was converted in number (n_x) per 100C or 1000C using equation 6.2.

$$w_x = \frac{A_x * w_s}{A_s * w_a} \quad 6.1$$

$$n_x = \frac{w_x * \%C}{12 * M_x} \quad 6.2$$

Where: A_x and A_s are the respective peak areas of the analyte and the internal standard; w_a and w_s are the respective weights of the asphaltenes and internal standard; %C is percentage

weight of carbon in the asphaltenes; and 12 and M_x are the molar masses of carbon and the analyte respectively.

6.2.3 Chemometrics

Although the importance of visual examination in comparing chromatographs and indices cannot be overemphasized particularly as different indices may have different weighting in decision making, chemometrics has the advantage of objectivity in finding subtle differences and similarities amongst the samples. This was therefore used in order to consider all variables simultaneously in comparing the samples.

The chemometric methods used for the purpose of pattern recognition are principal component analysis (PCA) and hierarchical cluster analysis (HCA). These multivariate tools are described in Section 5.2.3.

6.3 Results and Discussion

6.3.1 Method development and verification

The efficiency/yield of the method used for esterification of the RICO products (Section 2.3.10) was assessed using pure compounds (octadecanoic acid and aromatic benzene-1,2-dicarboxylic). The results show 99% of the stearic acid and 93% of the dibenzoic acid were converted to the corresponding esters. The method was therefore suitable for application in esterification of the RICO products. Nevertheless, only the aliphatic acids that partitioned into the organic phase of the RICO products were analysed. Aromatic acids partitioned into the aqueous phase and were therefore not amenable to the esterification method employed.

Carboxylic acids are known to be present in petroleum in varying proportions depending on the nature, maturity and geochemical history of the oil (Lochte and Littman, 1955). Thus, to ensure that the acids observed in products of RICO treatment of asphaltenes have no significant contribution from the free maltene acid pool, ten oils (consisting of both biodegraded and non-biodegraded oils) were analysed for free acid content. This was then compared to the asphaltene RICO products.

The results of the analyses show that the distribution of the free carboxylic acids in the maltenes is distinctively different from that in the asphaltene RICO products (Figure 6.2). The main *n*-alkanoic acids present in the maltenes are C₁₆ and C₁₈ homologues; other members up to C₃₀ are present but in relatively very low amounts ((*cf.* Figure 6.2 (a) & (b))). Steranoic acids (SA) are absent in both the biodegraded and non-biodegraded oils analysed. Hopanoic acids, on the other hand, are either absent or present in very low amounts in the non-biodegraded oils. Significant amounts of the hopanoic acids were however detected in the biodegraded oils. Nevertheless, unlike the hopanoic acids in the asphaltene RICO products, the hopanoic acids observed in the maltene fractions of the biodegraded oils consist predominantly of C₃₀ to C₃₂ homologues; homologues greater than C₃₂ are in general absent (*cf.* Figure 6.2 (c) & (d)).

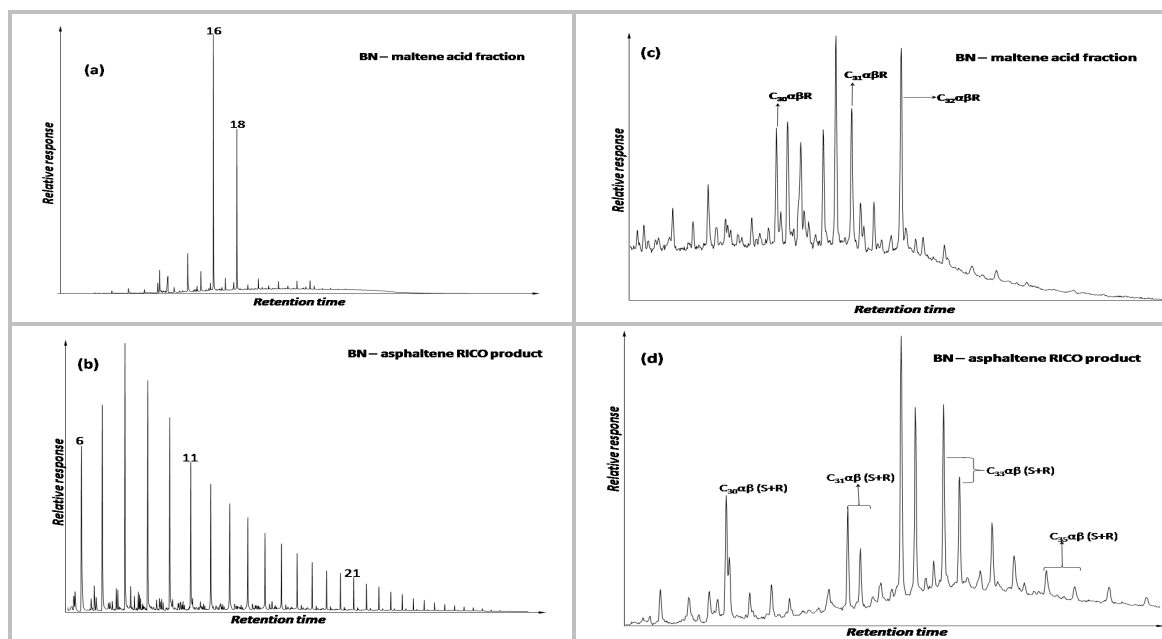
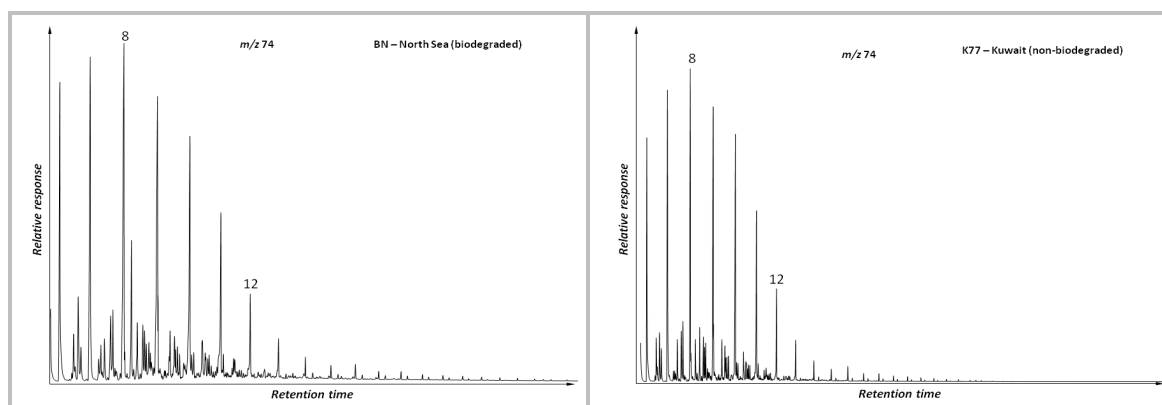
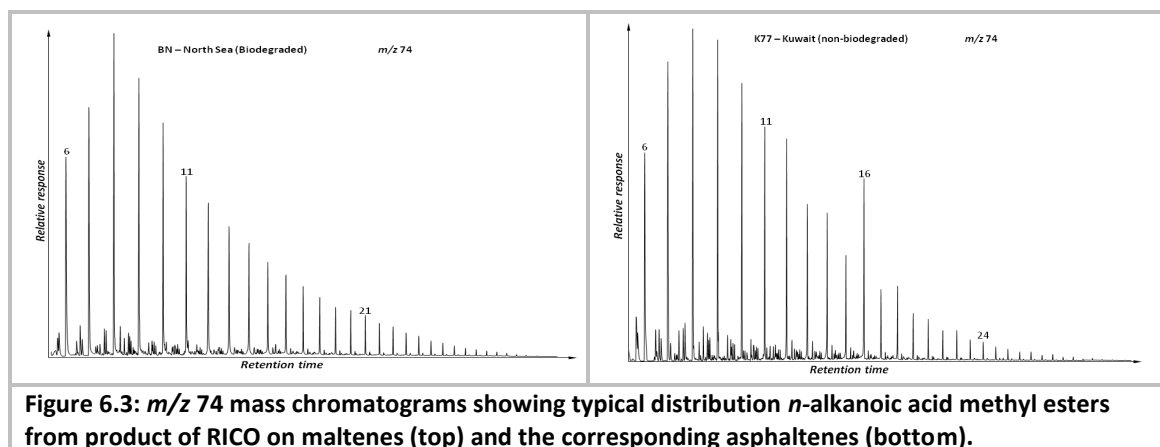


Figure 6.2: ((a) & (b)) m/z 74 mass chromatograms showing distribution of n -alkanoic acids in free maltene (a) and in product of RICO treatment of asphaltene (b); and ((c) & (d)) m/z 191 mass chromatograms showing typical distribution hopanoic acids the maltene (c) and in product of RICO treatment of asphaltenes (d) from the biodegraded oil (BN) from the Northsea.

Furthermore, to confirm that the bound biomarkers observed in the asphaltene RICO products are only significantly present in asphaltenes, maltene fractions from ten biodegraded and non-biodegraded, oils were subjected to RICO as well and the products analysed. The results (Figure 6.3) show that the maltene RICO products contain significant amounts of the n -alkanoic acids, but mainly consisting of the lower molecular weight homologues in range of C_6 to C_{13} ; C_{14+} homologues are present in relatively low amounts. This distribution is quite different from the distributions of the n -alkanoic acids observed in both maltenes and RICO products of asphaltenes. The most likely sources are the alkyl aromatic compounds in the maltenes. Hopanoic acids and steranoic acids, however, are generally not detected even from maltenes of biodegraded oils.

These results therefore clearly show that there was no significant contributions from free acids in the maltenes to the observed acids in the RICO products of asphaltenes; and that the acids observed in from the products of RICO treatment of asphaltenes are not likely to be from any co-precipitated components of the maltenes that might have remained in the asphaltenes even after the Soxhlet extraction of the latter.





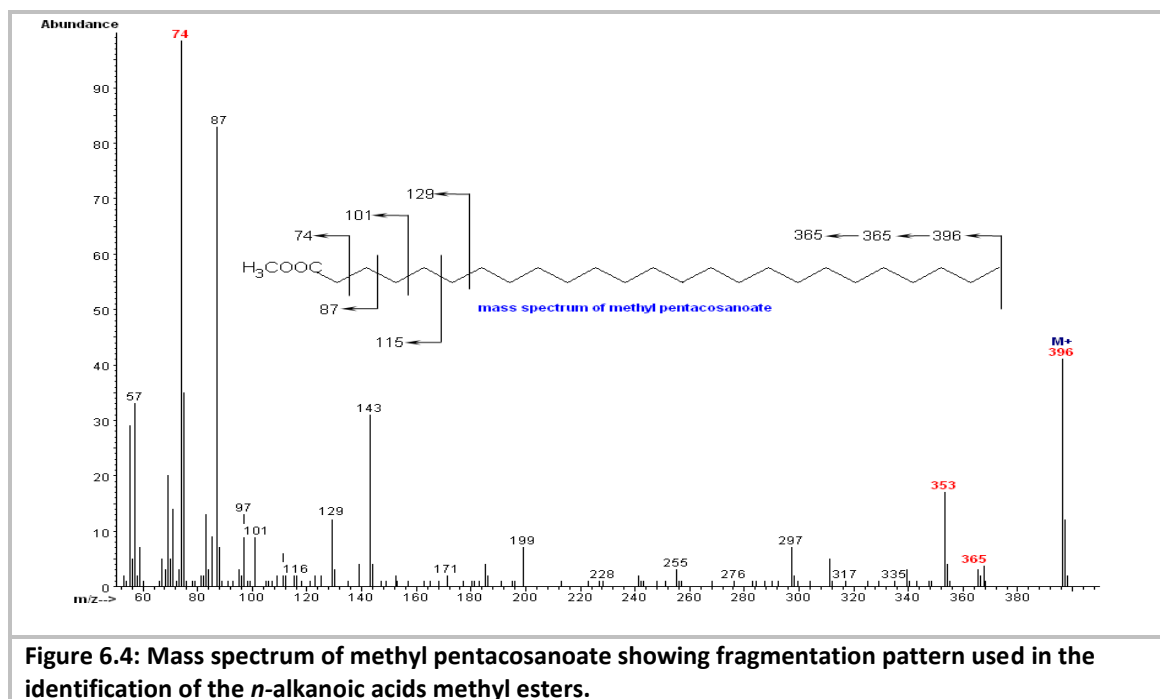
6.3.2 n -Alkanoic acids

(a) Identification of the n -alkanoic acids

n -Alkanoic acids are the major products of the RICO treatment of all the asphaltenes. The acids, as methyl esters, were identified from their respective mass spectra using the following outline fragmentation patterns (Christie, 2008):

- the molecular ion, $M^{+\bullet}$ = the corresponding n -alkane molecular ion + 44 from COO group
- $[M - 31]^{+\bullet}$ due to loss of a methoxy (CH_3O) group
- $[M - 43]^{+\bullet}$ due to loss of a C_3 unit lost via a complex rearrangement
- m/z 74 due to a McLafferty rearrangement ion confirming methyl ester
- m/z $[\text{CH}_3\text{OCO}(\text{CH}_2)_n]^{+\bullet} = 87, 101, 115, \dots$ showing there is no other functional group on the chain

As an example, Figure 6.4 is the mass spectrum of methyl n -pentacosanoate (C_{25} methyl ester) showing the important fragmentations used in identification of the compound.



(b) *Distribution of the n-alkanoic acids*

The *n*-alkanoic acids display a positively skewed unimodal distribution with homologues ranging from C₆ to C₃₅ with maxima typically between C₇ and C₁₀ (Figure 6.5). This distribution is similar to the observation of Strausz *et al.* (1999b) with respect to Boscan asphaltenes but is rather different from the observations of Trifilieff *et al.* (1992), Strausz *et al.* (1999a) and Peng *et al.* (1999a), which show maxima at C₁₄ to C₁₈ homologues. This could be because similar workup procedure to that used by the former was used in this work. Alkaline hydrolysis of the acids used by Strausz *et al.* (1999a) could result in loss of the lower molecular weight acids/esters. In addition, lengthy workup procedures involving chromatographic separations of the esters (Trifilieff *et al.*, 1992) could further result in significant loss of the volatile lower molecular weight homologues thereby shifting the observable maxima towards the higher molecular weight homologues.

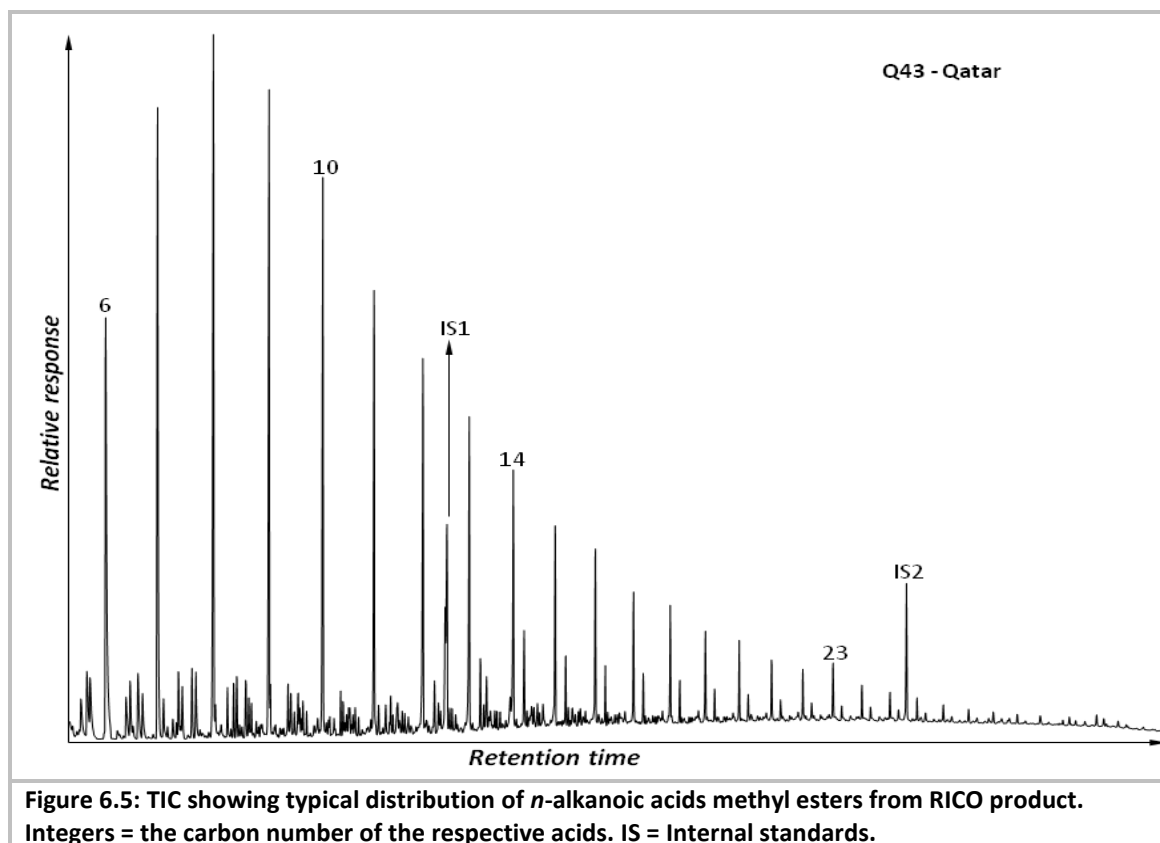


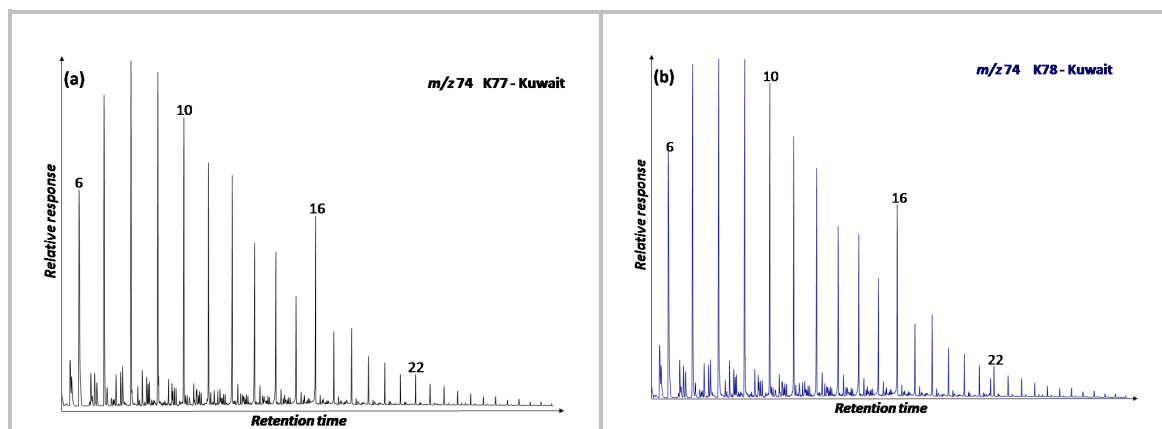
Figure 6.5: TIC showing typical distribution of *n*-alkanoic acids methyl esters from RICO product. Integers = the carbon number of the respective acids. IS = Internal standards.

The similarity in distribution of the *n*-alkanoic acids of all the asphaltenes analysed is further illustrated by range of values obtained from indices, such terrigenous-aquatic index (TAR), carbon preference indices (CPI & CPI1), and odd-even preference indices (OEP1 & OEP2) (Table 6.2), which are commonly used to characterise the distribution of *n*-alkanes from crude oils (Peters et al., 2005a). Peng et al. (1999a) observed a clear even-to-odd carbon preference in the *n*-alkanoic acids distribution from an immature asphaltenes. In this work, however, the values of all the *n*-alkanoic acid-based indices vary within a narrow range as indicated by small standard deviations of ± 0.13 for CPI. This may be a reflection of the effect of the thermal maturity of the samples.

Table 6.2: Some geochemical parameters describing the distributions of the *n*-alkanoic acids recovered following RICO treatment of asphaltenes

Sample	Location	TAR	CPI	CPI(1)	OEP(1)	OEP(2)
A39	Abu Dhabi	0.08	1.19	0.91	0.91	0.94
AR3	GoM	0.04	1.45	1.07	1.14	1.13
B58	Bangladesh	0.10	1.28	0.98	0.97	1.02
BN	Northsea	0.10	1.28	1.00	1.02	1.03
C26	Canada	0.14	1.22	1.00	1.02	1.00
C30	Canada	0.16	1.05	0.92	0.93	0.93
CH	Canada	0.09	1.24	0.99	1.02	1.02
K77	Kuwait	0.08	1.01	0.86	0.88	0.89
K78	Kuwait	0.08	0.99	0.84	0.86	0.86
NB	Nigeria	0.20	1.13	0.93	0.94	0.93
NA1	Serbia	0.20	1.35	1.07	1.08	1.07
NA2	Serbia	0.15	1.15	0.88	0.87	0.92
O28	Oman	0.12	1.16	0.93	0.98	0.90
O31	Oman	0.10	1.17	0.91	0.97	0.88
PR1	GoM	0.07	1.32	1.01	1.02	1.07
Q43	Qatar	0.08	1.25	0.97	0.99	1.00
Q61	Qatar	0.07	1.22	0.94	0.95	0.96
U02	Northsea	0.07	0.75	0.68	0.71	0.69
U56	Northsea	0.10	1.25	1.00	1.02	1.01
U79	Northsea	0.07	1.32	1.01	1.04	1.04
U93	Northsea	0.11	1.19	0.99	1.04	1.00
Y32	Yemen	0.09	1.32	1.03	1.03	1.05

Asphaltenes with a common source display a more striking similarity in the distribution of the *n*-alkanoic acids. For example, the Oman asphaltenes O28 and O31 from same reservoir (Natih) and field show no odd-to-even carbon predominance. This is also true for other asphaltene pairs such as Q43 & Q61 from Qatar (Figure 6.6), and Canadian asphaltenes, C26 & C30, from Midale reservoir and being from same source rock. Furthermore, asphaltenes, K78 and K77, from Kuwait, although obtained from different oil fields (Table 6.1), display similar distribution, with distinct even carbon predominance between the C₁₀ and C₂₃ homologues. Both also have a prominent C₁₆ homologue (Figure 6.6).



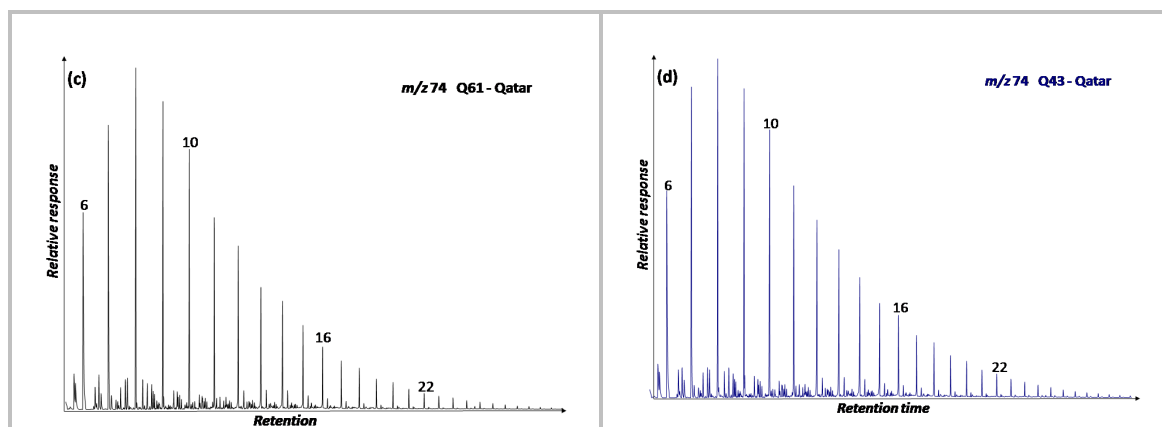


Figure 6.6: m/z 74 mass chromatograms showing striking similarity in distribution of n -alkanoic methyl esters from asphaltene following RICO treatment for pairs of same source oils. The integers = the total carbon atoms per molecule of the respective acids.

TAR compares the relative proportions of high molecular weight (waxy) acids (indicative of terrigenous organic matter input) to low molecular weight acids (indicative of marine organic matter input) (Peters et al., 2005a). Although this index is maturity dependent (Peters et al., 2005a), the observed low values (0.10 ± 0.03) (Table 6.2) apparently suggest predominance of marine organic matter input in all the oils in agreement with results obtained from analysis of hydrocarbon fractions of the oils as presented in Chapter 4.

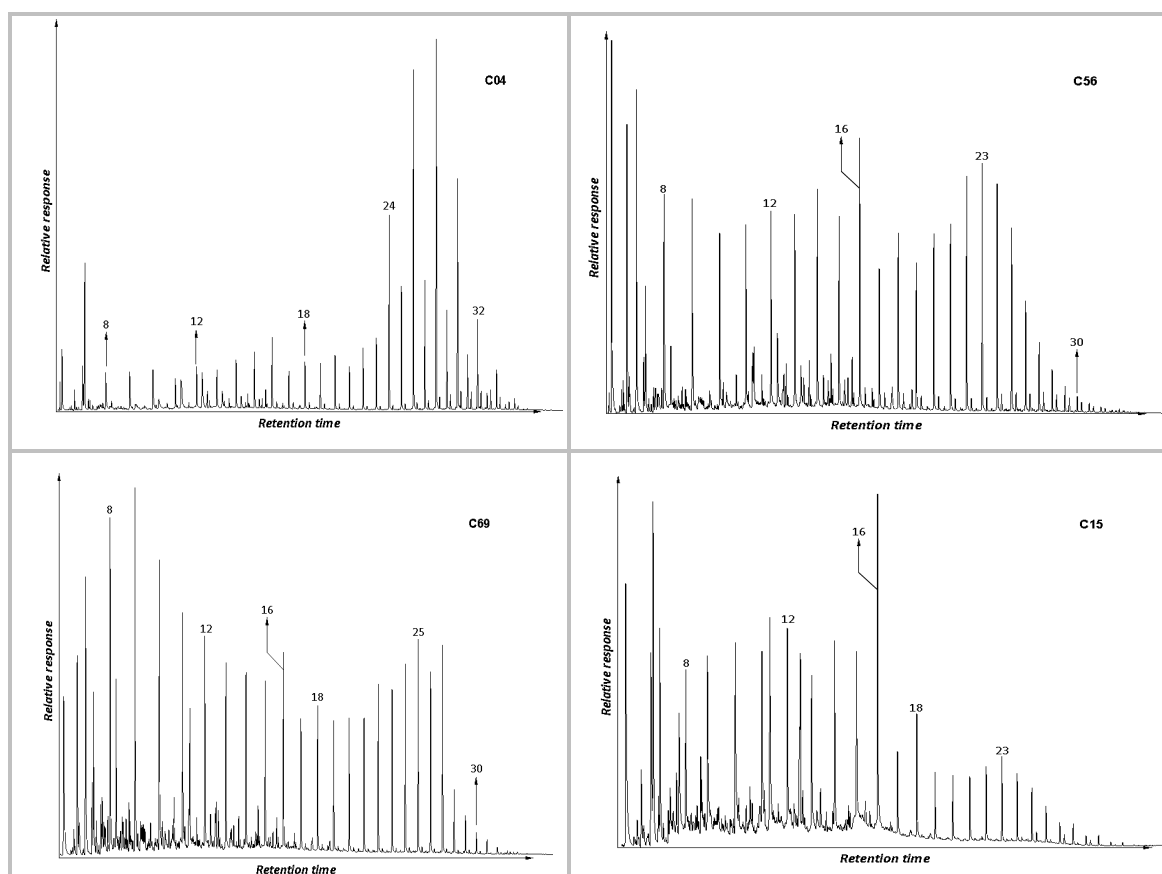


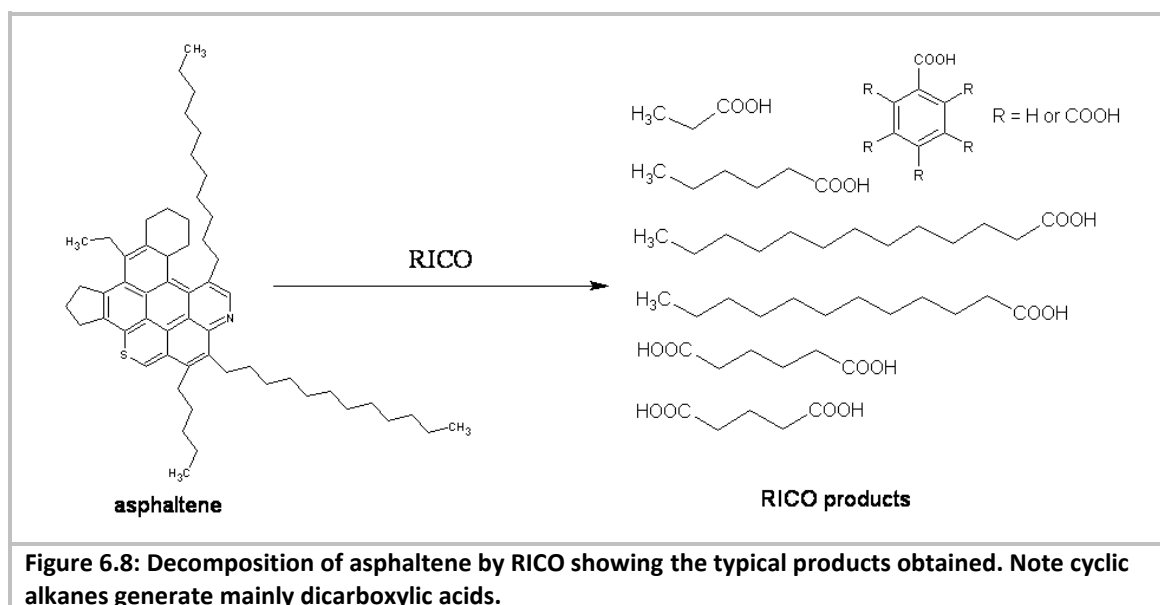
Figure 6.7: m/z 74 mass chromatograms showing variable distribution of the n -alkanoic acid methyl esters from RICO degradation products of coal asphaltene. The integers show the carbon number of the respective acids

Coal asphaltene display similar composition of n -alkanoic acids with homologues also ranging from C_6 to C_{36} (Figure 6.7) in the asphaltene RICO products in petroleum asphaltene. The

distribution of the homologues is, however, distinctly different. The immature coal asphaltene (C04, $R_o = 0.4\%$) shows dominance of the high molecular weight homologues (C_{24} to C_{30}) with strong predominance of even carbon number (Figure 6.7) homologues. The lower homologues ($<C_{24}$) are relatively small. The marginally mature C56 ($R_o = 0.56\%$), on the other hand, exhibits significant increase in the relative proportions of the lower homologues although the hump in the C_{20} to C_{26} homologues is still distinctive. The more mature asphaltene C69 ($R_o = 0.69\%$) shows a similar distribution of n -alkanoic acids as C56 but with increased relative proportions of the lower homologues. Sample C15 ($R_o = 1.5\%$), which is the most mature exhibit dominance of the lower homologues although there is prominent C_{16} as in sample C56.

(c) *Source of the n-Alkanoic acids*

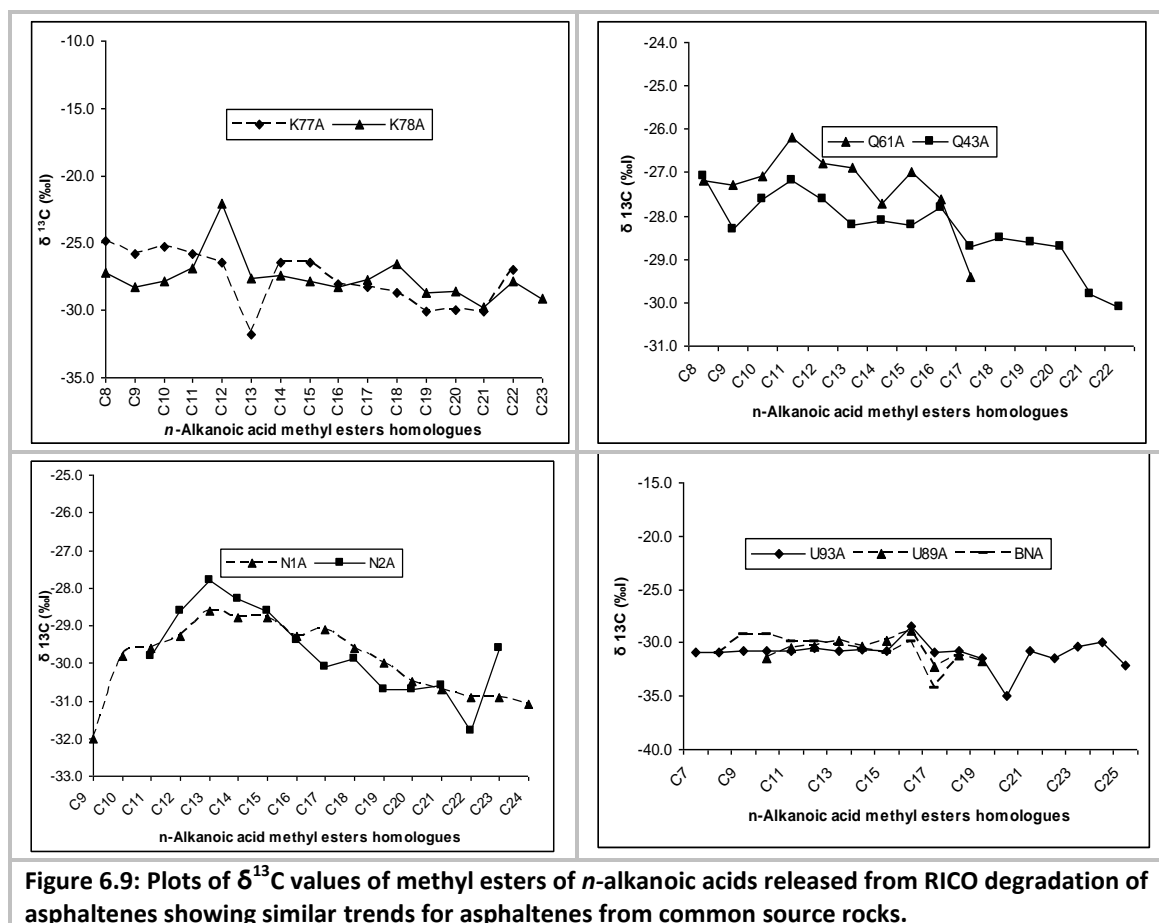
The n -alkanoic acids are mainly generated from the n -alkyl side chains attached to the aromatic units of the asphaltene macromolecules. The RICO results in degradation of the aromatic units with the aliphatic side chains being released as alkanolic acids as illustrated Figure 6.8 (Mojelsky *et al.*, 1992). However, although only C_{6+} n -alkanoic acids (Figure 6.5 and 6.7) were detected in the RICO oxidation products, the lower homologues also exist but in the aqueous phase of the product which was not analysed here. In fact, Strausz *et al.* (Strausz *et al.*, 1999b) observed that the C_1 to C_5 homologues are the dominant alkyl moieties (up to 50 to 70%) in asphaltene which may why the average chain length to about 4 to 7 (Strausz *et al.*, 1999b).



The relative amounts of the total n -alkanoic acids in the asphaltene oxidation products generally vary with different asphaltene from about 8.0 to 39 $\mu\text{g}/\text{mg}$ asphaltene. In general, some asphaltene with a common source (e.g. C30/C26 & K77/K78) have similar weights of the acids per weight of asphaltene. However, the Oman (O28 vs. O31) and Qatar (Q61 vs. Q43) asphaltene despite being respectively from same source rocks (see Chapter 3), have significantly different relative amounts (35 to 45 $\mu\text{g}/\text{mg}$ asphaltene) of the n -alkanoic acids. This variation could be due to one or more factors namely differences in: (a) organofacies of

source kitchens, (b) maturities of the asphaltenes, and (c) degree of preservation of the organic matter during diagenesis.

The results of the $\delta^{13}\text{C}$ analysis of the *n*-alkanoic acids from the asphaltene RICO products reveal that asphaltenes from the same source rock generally have similar $\delta^{13}\text{C}$ values. Most striking however are the similar $\delta^{13}\text{C}$ trends across the homologues exhibited by asphaltenes with common source rock. This was observed to be true even between asphaltenes from biodegraded and non-biodegraded oils (Figure 6.9).



The relative sulphur content of the asphaltenes fairly correlates positively ($R^2 = 0.62$, $p < 0.05$) with the relative amounts of the *n*-alkyl moieties (*n*-alkanoic acids) in the asphaltenes as shown in Figure 6.10. This suggests sulphur may play a role in the relative amount of aliphatic structures incorporated in the asphaltenes. It is known that good preservation of organic matter is facilitated by anoxic conditions (Tyson and Pearson, 1991; Demaison and Moore, 1980) – a situation where free hydrogen sulphide exists and extends into the water column thereby suffocating most of the more efficient grazing microbes (Tyson and Pearson, 1991). The observed positive correlation may therefore reflect increasing preservation and therefore increasing availability of the hydrogen-rich *n*-alkanoic materials for incorporation in the asphaltenes (and kerogen). However, as the model explains only about 62% of the variance in the data, other factors, possibly the nature of the original biomass, diagenesis and maturation, could be responsible for the unaccounted variance.

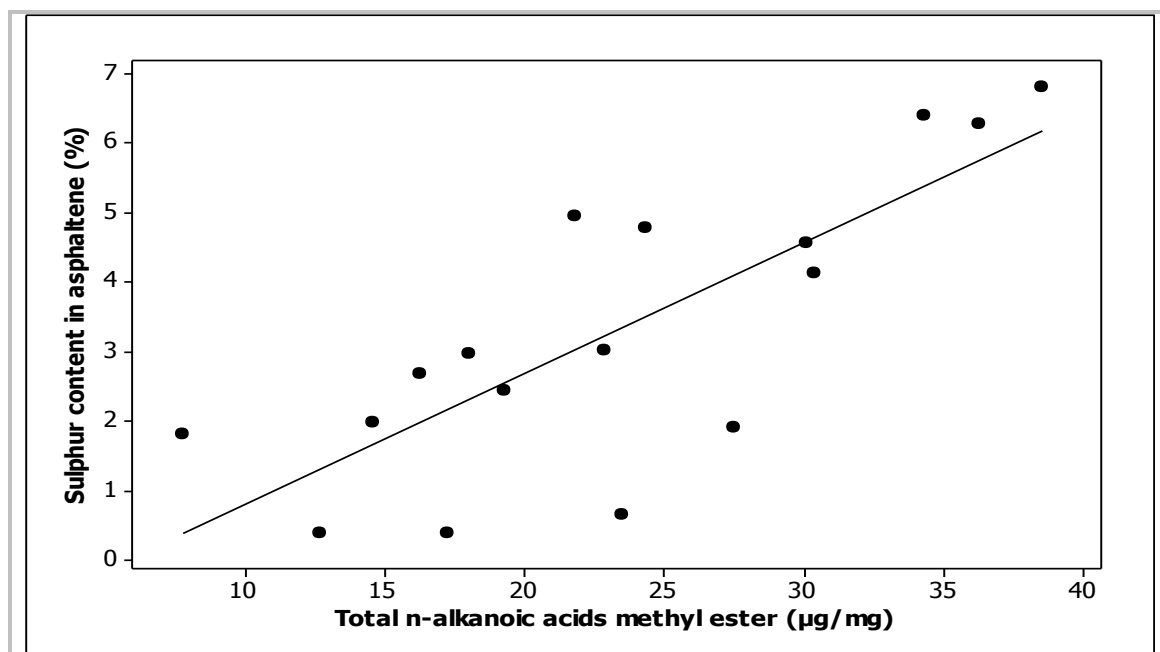


Figure 6.10: Linear plot of relative sulphur content of asphaltenes against the alkyl appendages in the asphaltene ($R^2 = 0.62$, $p < 0.05$).

6.3.3 α,ω -n-Alkandioic acids

(a) Identification of the α,ω -n-alkandioic acids

This class of compounds, as methyl esters, elute close to the *n*-alkanoic acids methyl esters. They were identified from their relative retention time and most importantly their mass spectra (Christie, 2006). The mass spectra of all the homologues show the following fragmentation characteristics:

- small, sometimes absent, molecular ion (M^{+*}) peak
- a prominent m/z $[M-31]^{+*}$ ion due to loss of methoxy (CH_3O) group
- m/z $[M-64]^{+*}$ due to loss of two CH_3O groups
- m/z $[M-73]^{+*}$ due to loss of CH_3OCOCH_2 group from McLafferty rearrangement ion
- m/z $[M-92]^{+*}$ due to loss of $CH_3O+CH_3OCOCH_2+2H$
- m/z $[M-105]^{+*}$ due to loss of $CH_3O+CH_3OCOCH_2+H$
- m/z $[M-123]^{+*}$ due to loss of $CH_3O+CH_3OCOCH_2+H_2O+H$
- series of ions m/z $[84 + 14n]^{+*}$, $n = 1, 2, 3, \dots$

Figure 6.11 is the mass spectrum of 1,13-dimethyl tridecanedioate showing the fragmentation pattern used in the identification of the homologues.

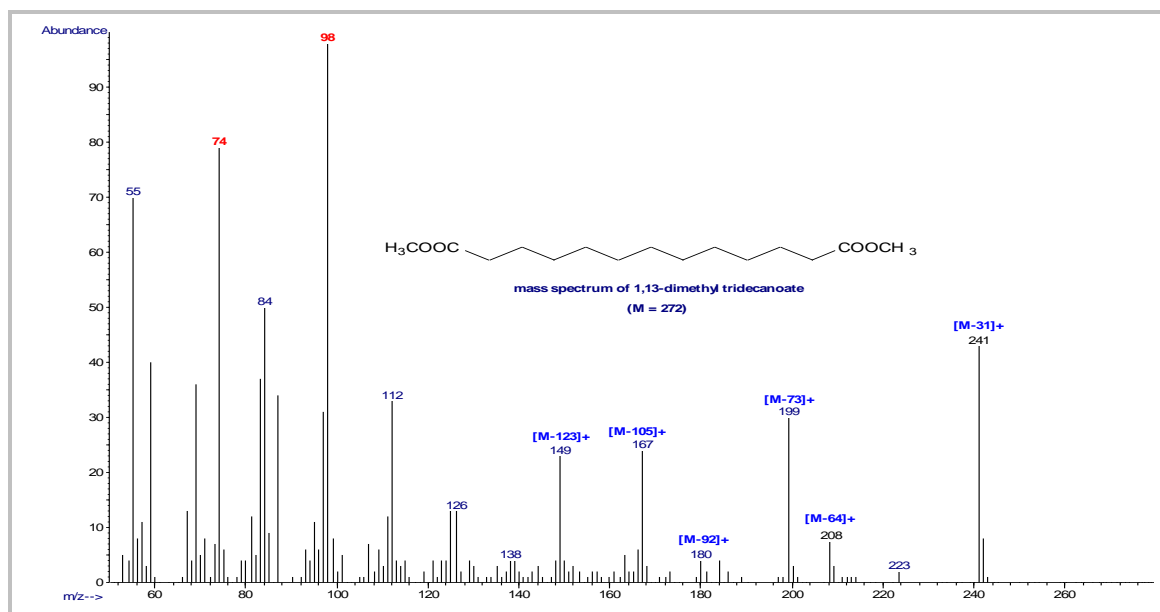


Figure 6.11: Mass spectrum of 1,13-dimethyl tridecanoate showing typical ions used in identification of the α,ω - n -alkandioic acids, methyl esters. Note the absence of molecular ion typical of the dibasic acids methyl esters.

(b) *Distribution of the α,ω - n -alkandioic acids*

The α,ω - n -alkandioic acids in the RICO product of the asphaltenes range from C_{10} to C_{36} displaying a positively skewed unimodal distribution with maxima at C_{11} to C_{14} homologues and gradual fall towards the high molecular weight members (Figure 6.12). Homologues below C_{10} are generally low in all the asphaltene RICO products which might be related to their solubility in the aqueous phase that was not analysed.

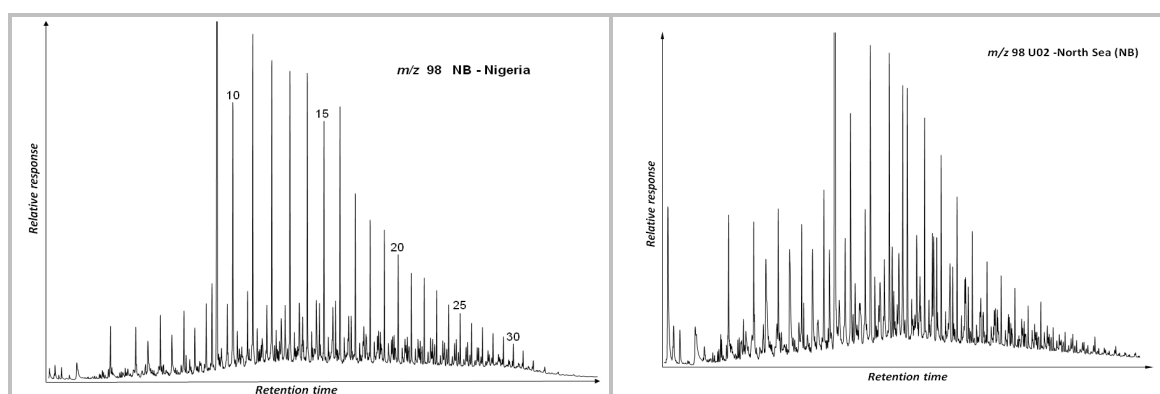


Figure 6.12: m/z 98 mass chromatogram showing typical distributions of α,ω -alkandioic acid dimethyl esters. Note slight predominance of the even homologues and conspicuous low proportions of the homologues less than the C_{10} homologue.

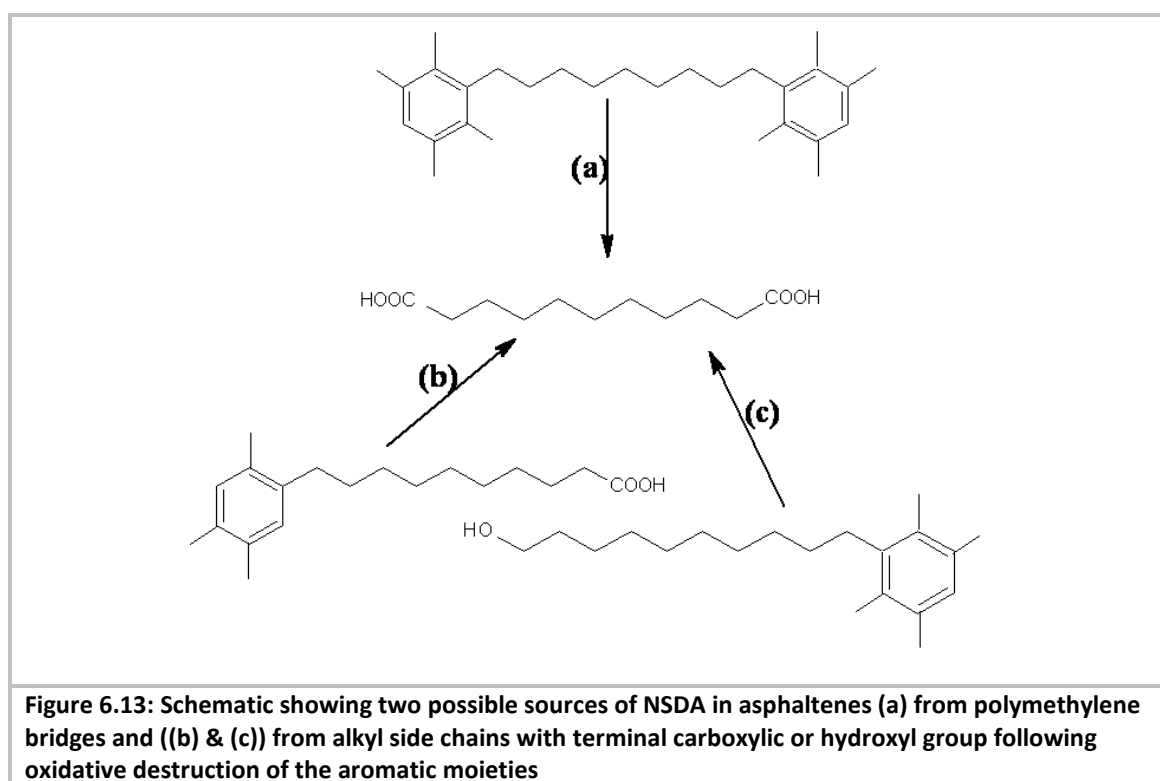
(c) *Source of the α,ω - n -alkandioic acids*

The n -alkandioic acids are believed to be derived from polymethylene bridges that link aromatic cores in asphaltenes (Mojelsky et al., 1992). The oxidative degradation of the cores yields the diacids (route (a) of Figure 6.13). This interpretation however advocates that

asphaltenes have polymeric, or at least oligomeric, structure where polymethylene bridges of different chain length interconnect condensed aromatic cores. As discussed in Section 1.3 of Chapter 1, this structure is rather controversial (Badre *et al.*, 2006) as it is claimed to be inconsistent with data obtained using various techniques (Mullins *et al.*, 2007).

However, alternative/additional sources of the diacids are alkyl side chains with terminal carboxyl or hydroxyl groups (Figure 6.13). The presence of these groups has been established from mid-infrared spectra of asphaltenes which invariably show the presence of absorption bands at 3100 – 3500 and 1700 cm^{-1} which can be assigned to hydroxyl and carboxyl groups.

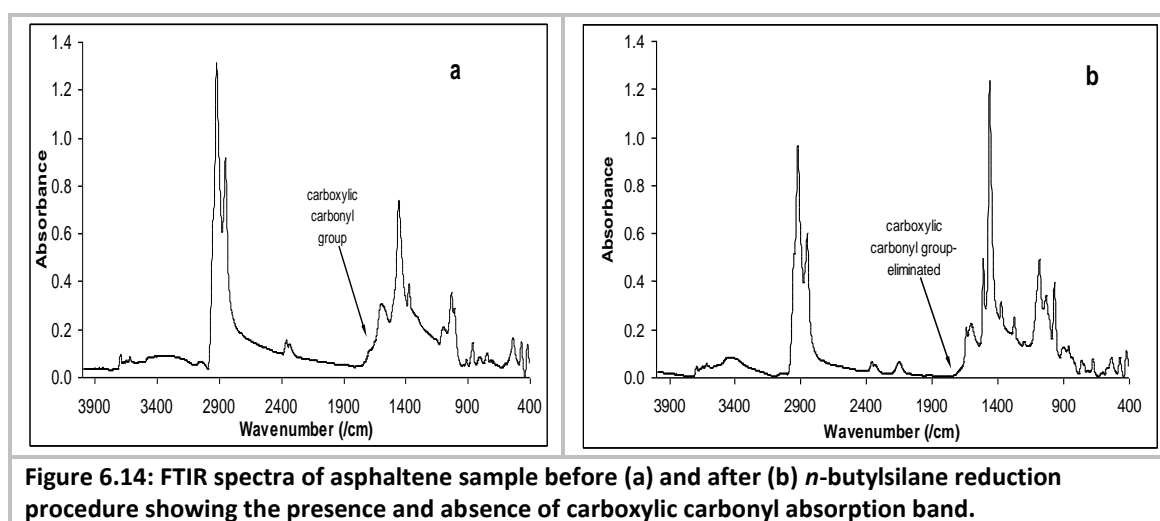
Furthermore, These alternative/additional sources for the diacids are supported by the predominance of the diacids over the monoacids in RICO products of immature asphaltenes (Peng *et al.*, 1999a) compared to mature asphaltenes which generally show much lower proportions of the diacids (Peng *et al.*, 1999a; Strausz *et al.*, 1999b). It has been shown in Chapter 5 of this thesis (see also Ibarra *et al.* (Ibarra *et al.*, 1996)) that the amounts of carboxyl and other oxygen functionalities fall with increasing maturity so that the more mature asphaltenes contain less proportion of the alkyl appendages with terminal carboxyl groups and therefore give less diacids in the RICO products.



Nevertheless, to further explore investigate the contributions of these alternative sources for the diacids, an experiment was designed to eliminate contributions from the alternative sources so that any diacids observed afterward might be from only the polymethylene bridges. An asphaltene sample (NB) was treated with a non destructive reduction procedure which completely reduces carboxyl and hydroxyl groups (Section 2.3.8). Figure 6.14 shows the mid-infrared spectra of the asphaltenes before and after the reduction process showing elimination of carboxylic group.

Results of the RICO treatment of the asphaltenes after reduction shows the presence of the α,ω -*n*-alkandioic acids albeit in lower proportions compared to before the reduction procedure. Although this does not imply polymeric structure for asphaltenes, it however suggests the existence of such linkage between at least a pair of aromatic units.

Furthermore, it has been observed that asphaltenes become more aromatic (Section 5.3.2) with increasing maturation. It is therefore reasonable to argue that bound saturated cyclic structures (such as hopanoids (see Section 6.3.5)) undergo aromatisation becoming part of aromatic units linked by polymethylene bridges. In fact, this may explain why hopanoic and steranoic acids were not observed in the C15 asphaltenes ($R_o = 1.5\%$) RICO products (Section 6.3.9).

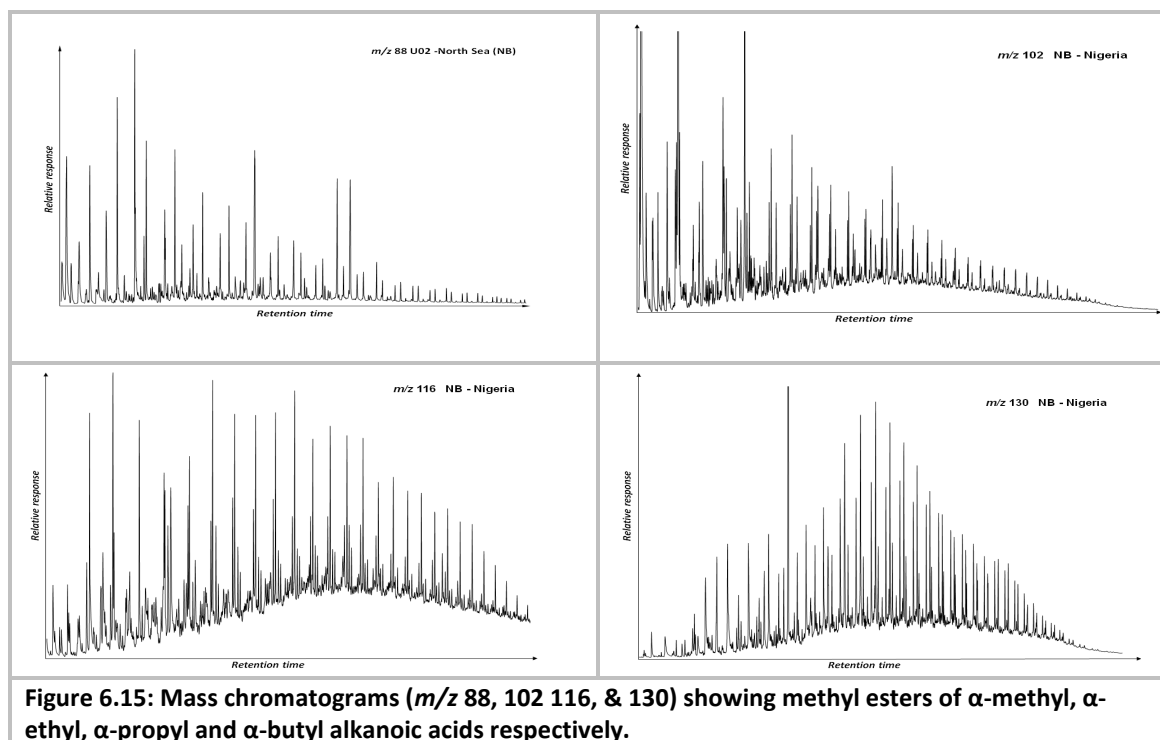


6.3.4 Branched alkanolic acids

Branched alkanolic acids were also detected in the oxidation products of RICO treatment of all the asphaltenes. They are however less abundant than the *n*-alkanoic acids and α,ω -*n*-alkandioic acids (Figure 6.15). The mass chromatograms representing the series were obtained from *m/z* 102, 116 and 130 for α -ethyl, α -propyl and α -butyl alkanolic acid methyl esters respectively (Peng et al., 1999a; Strausz et al., 1999a). The mass spectra were however weak and the assignment could not be confirmed.

The simple branched alkyl groups were possibly incorporated into the asphaltenes structure from their corresponding branched alcohols and/or unsaturated alkenes via Friedel-Craft-type alkylation (See Section 6.3.4 (c)).

It is interesting to note that isoprenoic acids, particularly pristanoic and phytanoic acids were not detected in the oxidation products of the asphaltenes. This could possibly be because they were not available in a form suitable for incorporation in asphaltenes via carbon-carbon bonds. The possible precursors for these compounds are in bound form (ester & ether) in their original compound and are not available for incorporation via carbon-carbon bonds.



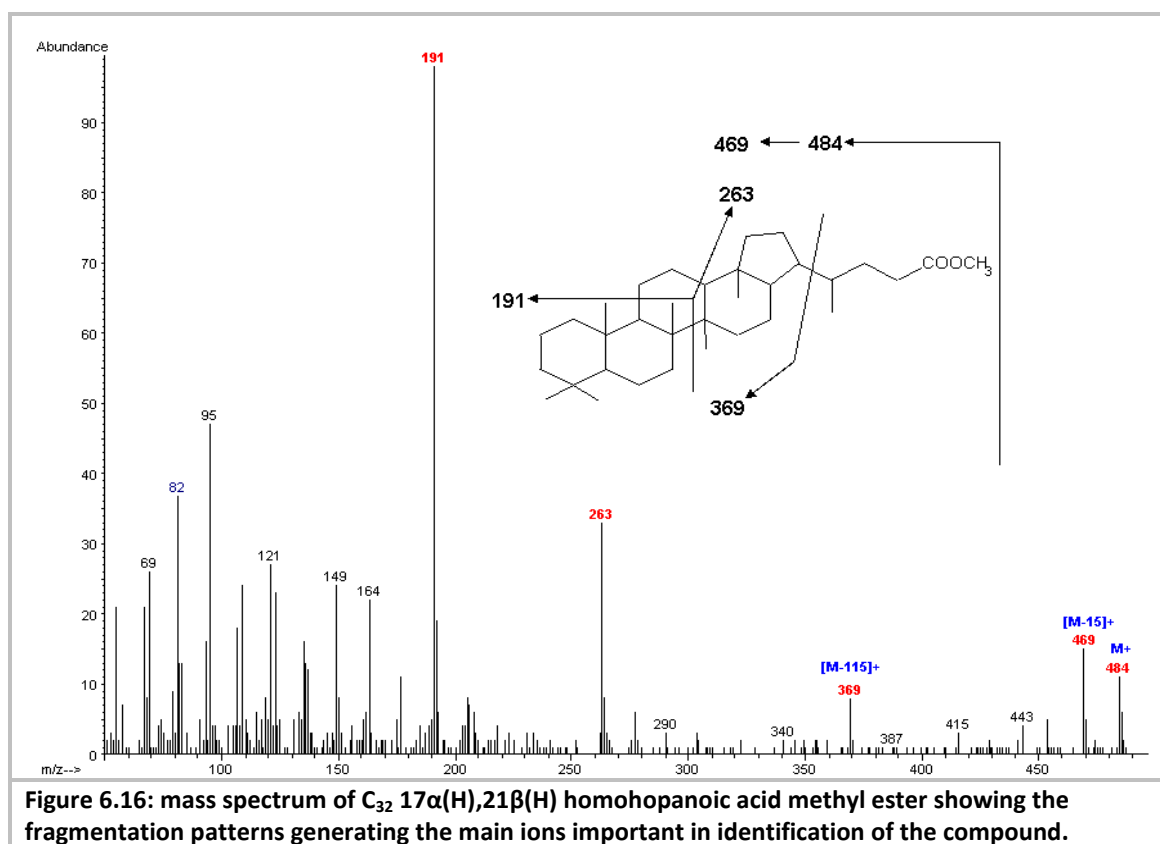
6.3.5 Hopanoic acids (HA)

(a) Identification of the hopanoic acids

Hopanoic acids are the major cyclic carboxylic acids in the products of RICO treatment of asphaltenes. The homologues of this group were identified from their mass spectra and relative elution pattern compared to published chromatograms (Bennett and Abbott, 1999; Peng et al., 1999a; Trifilieff et al., 1992; Jaffe et al., 1988). The mass spectra of the hopanoic acid methyl esters show the following fragmentation characteristics:

- the molecular ion peak $M^{+\bullet}$ = the molecular ion of the corresponding hopane + 46 from the additional OOCH_3
- $m/z [M^{+\bullet} - 15]$ from loss of CH_3 group
- a base peak m/z 191 from the cleavage in B ring as in the hopanes
- a prominent $m/z [148 + (\text{CH}_2)_n \text{COOCH}_3]^{+\bullet}$ where $n = 0, 1, 2, \dots$ for C_{30} to C_{36} corresponding to cleavage in the B ring
- as in hopanes, hopanoic acids methyl esters show $m/z [148 + (\text{CH}_2)_n \text{COOCH}_3]^{+\bullet} < 50\%$ of m/z 191 for $17\alpha(\text{H}), 21\beta(\text{H})$; and $> 50\%$ for $17\beta(\text{H}), 21\alpha(\text{H})$ and $> m/z$ 191 for $17\beta(\text{H}), 21\beta(\text{H})$ (Jaffe et al., 1988) respectively
- a relatively small m/z 369 due to the ring system (i.e. from loss of the side chain)
- as in hopanes, the elution order is $\text{C}_{30}, \text{C}_{31}, \text{C}_{32}, \dots$. In every homologue the $17\alpha(\text{H}), 21\beta(\text{H})$ elute before the $17\beta(\text{H}), 21\alpha(\text{H})$ and in every doublet 22S before 22R

Figure 6.16 is the mass spectrum of methyl esters of C_{32} $17\alpha(H),21\beta(H)$ hopanoic acid showing the major fragmentations useful in identification of the series. Figure 6.17, on the other hand, shows the elution pattern of the hopanoic acid methyl esters.



(b) *Distribution of the hopanoic acids*

As shown in Figure 6.17 the hopanoic acids from the RICO treatment of asphaltenes range from C_{30} to C_{36} homologues. The C_{28} hopanoic acid is also invariably present in all samples. The C_{32} hopanoic acids are the dominant homologues except in NA2 asphaltenes where C_{33} dominate (Table 6.3, page 190). There is a progressive decrease in abundance of the homologues from C_{32} to C_{36} with C_{32} & C_{33} generally being greater than C_{31} . The C_{36} homologue is only faintly detected in some asphaltenes (e.g. Figure 6.18) although it is relatively prominent in other (e.g. C_{26} & C_{30} asphaltenes from Canada).

The stereochemical configurations of the hopanoic acids consist of the $17\alpha(H),21\beta(H)$ and $17\beta(H),21\alpha(H)$ isomers. In some asphaltenes $17\beta(H),21\beta(H)$ isomers were also present. All the homologues from C_{30} to C_{36} hopanoic acids have the 22S and 22R epimers. In general, the $17\alpha(H),21\beta(H)$ and the 22S epimers are the more prominent isomers in each homologue. The C_{31} $17\beta(H),21\alpha(H)$ is significantly present in all the asphaltenes. In some other asphaltenes the $17\beta(H),21\alpha(H)$ diastereomer of the C_{30} and C_{32} homologues are also prominent.

Generally, there is a similarity in hopanoic acids distributions amongst the various asphaltenes analysed particularly with respect to the predominant homologues and isomers present. Nonetheless, hopanoic acids distributions from asphaltenes obtained from oils that have a common source rock are even more similar amongst themselves than they are to hopanoic acids distributions of asphaltenes obtained from oils of different source (Figure 6.18). Furthermore, it is important to note that although hopanes are almost completely removed from the maltenes of the Nigerian bitumen (NB) due to severe biodegradation (Chapter 3), the asphaltenes of the bitumen contains abundant hopanoic acids in the RICO product. In addition, gammaceranoic acid is prominent (peak G, Figure 6.17) although gammacerane was detected in the aliphatic hydrocarbon fraction.

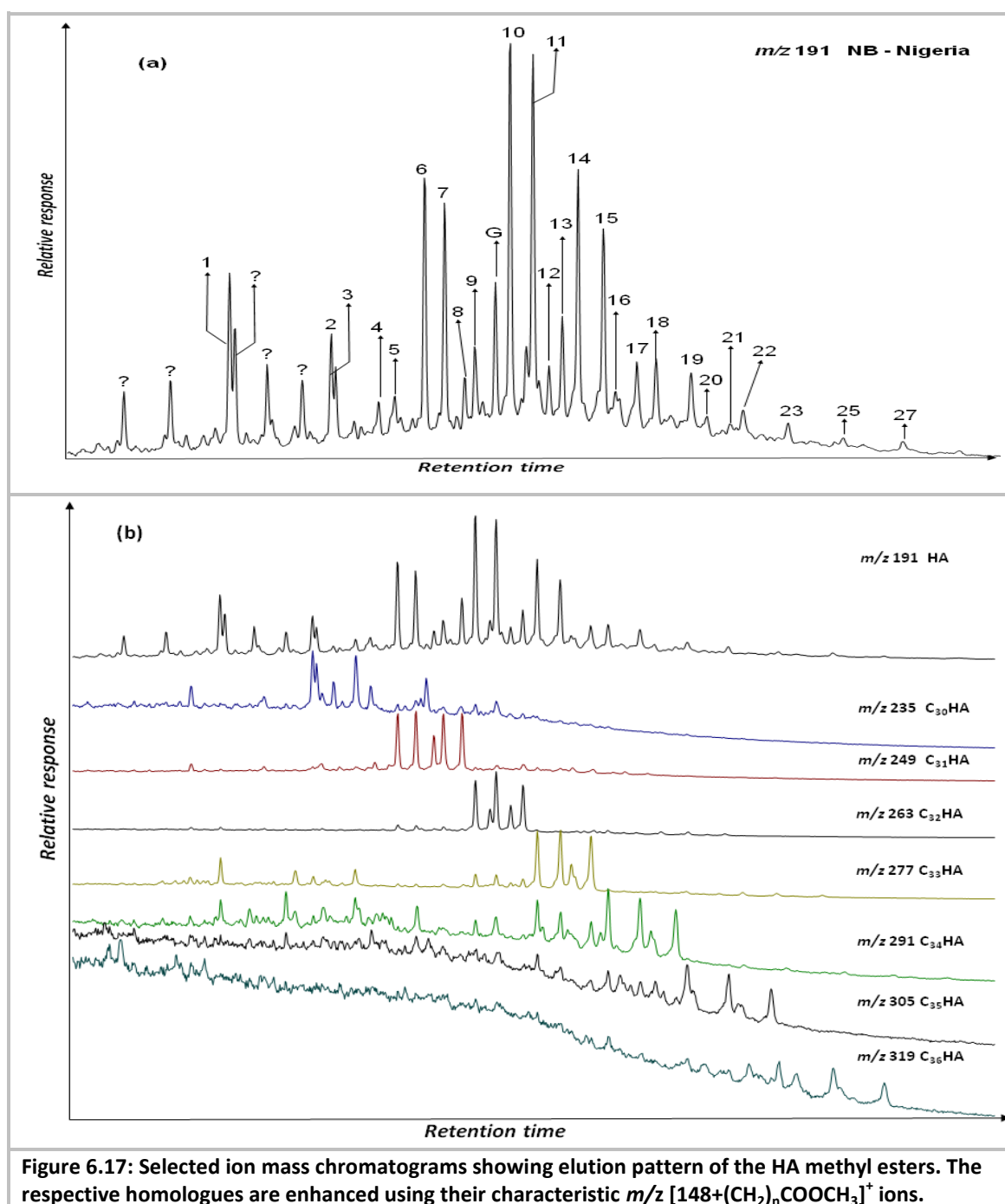


Figure 6.17: Selected ion mass chromatograms showing elution pattern of the HA methyl esters. The respective homologues are enhanced using their characteristic m/z $[148+(\text{CH}_2)_n\text{COOCH}_3]^+$ ions.

The products of RICO treatment of the coal asphaltene show the presence of the C₂₈ and C₃₀ to C₃₃ hopanoic acids with traces of C₃₄ homologue for C04, C56 and C69 asphaltene. No hopanoic acids were detected in C15 asphaltene. As in oil asphaltene, C₃₂ is dominant hopanoic acid in the RICO products of all the three coal asphaltene.

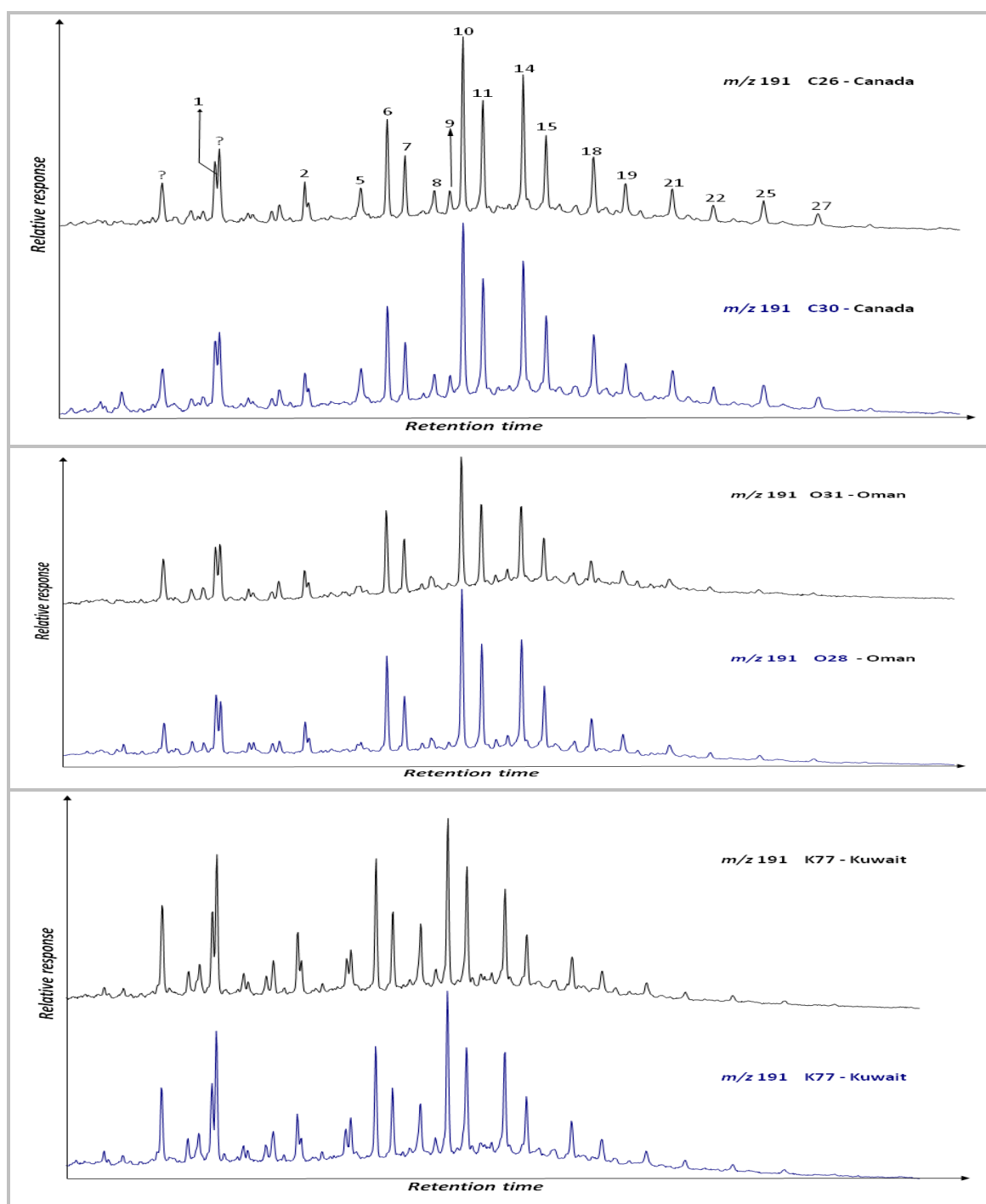
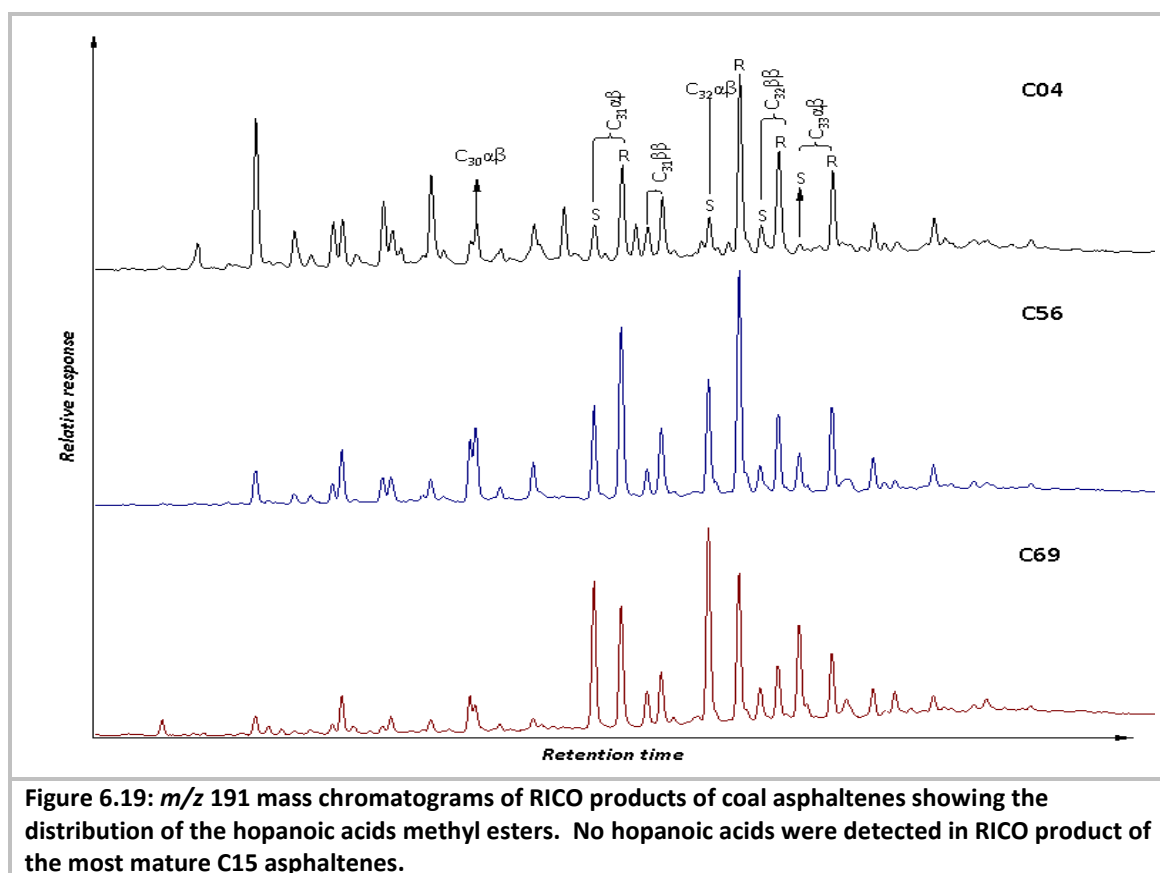


Figure 6.18: m/z 191 mass chromatograms of six different asphaltene RICO products showing similarity in distributions of hopanoic acids for asphaltene with a common source.

The main difference amongst the coal asphaltene, however, is in the distribution of isomers of the hopanoic acids. In the immature C04 asphaltene, the biological $17\beta(\text{H}),21\beta(\text{H})$ predominates followed by $17\alpha(\text{H}),21\beta(\text{H})$. The less stable $17\beta(\text{H}),21\alpha(\text{H})$ are also present. The 22S epimers are generally very small compared to the 22R epimers. In the mature C56 and C69 asphaltene, on the other hand, $17\alpha(\text{H}),21\beta(\text{H})$ are the dominant isomers and the $17\beta(\text{H}),21\alpha(\text{H})$ are practically absent. Unlike in C56 asphaltene, however, in C69 asphaltene, the 22S epimers are dominant over 22R for $17\alpha(\text{H}),21\beta(\text{H})$ isomers across the homologues. The

reverse is, however, the case for $17\beta(H),21\beta(H)$ isomers in all the two asphaltenes (Figure 6.19).



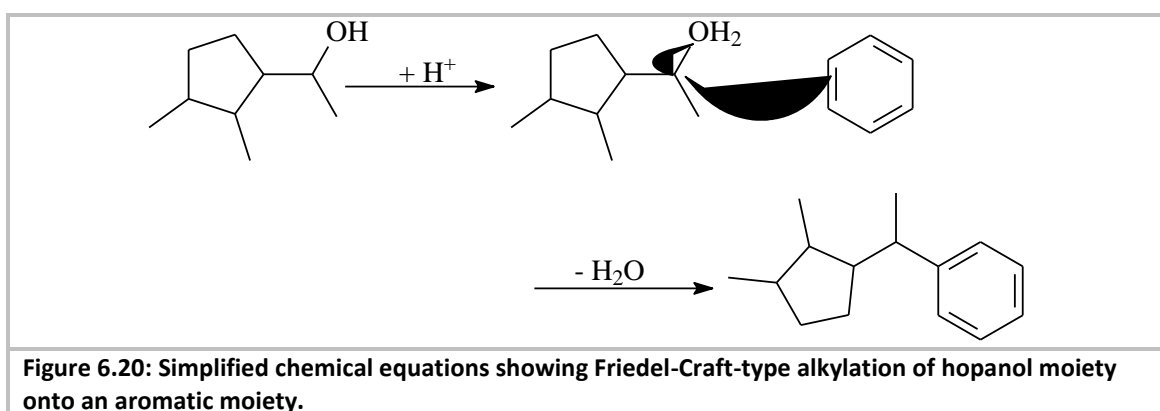
(c) *Source and incorporation of the hopanoic acids*

Hopanoic acids are, like other geohopanooids, molecular fossils of bacteriohopanepolyols (BHPs). BHPs are ubiquitous terpenoids synthesised mainly by prokaryotes (Rohmer et al., 1984) and thus found in various environmental settings (Talbot et al., 2008; Talbot and Farrimond, 2007). This class of natural products is found in wide range of structural variations although the most common is one with four functional groups at C32, C33, C34 and C35. BHPs with five (additional group on C31) or six functional groups (additional groups on C31 and C30) are also common in the environment. The hydroxyl group is the main functional group occupying these positions although, BHPs with other groups such as the amino or aminosugar functionalities at C35 have been observed (Talbot and Farrimond, 2007).

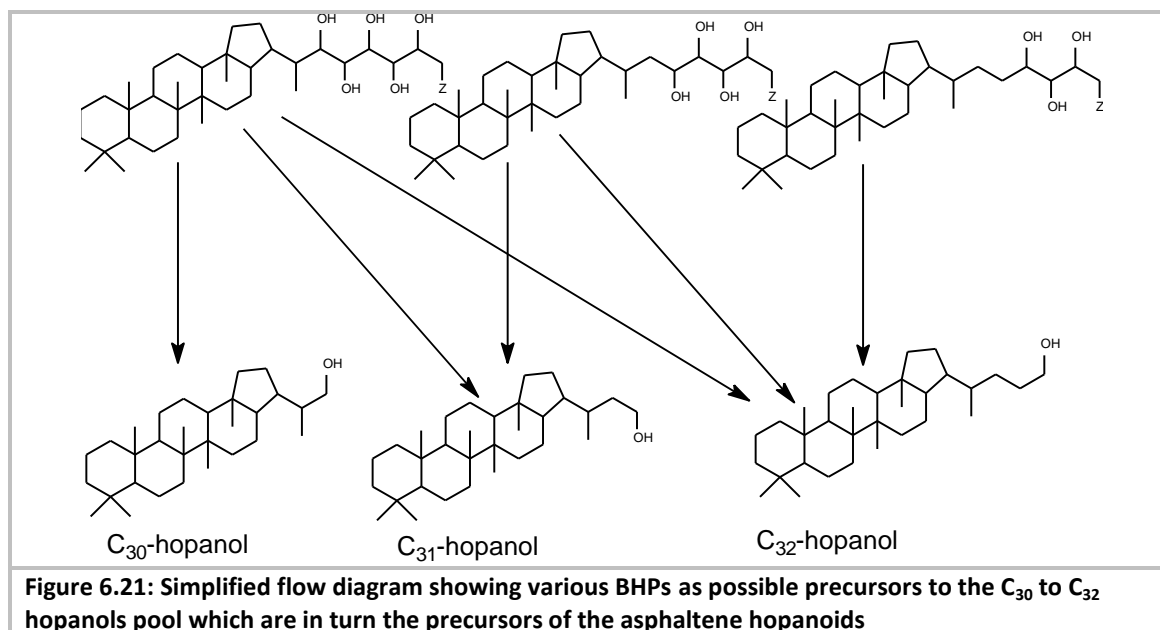
The diagenesis of the BHPs in the geosphere gives rise to a complex web of chemical reactions. This involves the formation of a complex mixture of geohopanooids including, amongst others, hopenes, hopanoic acids and hopanols with $17\beta(H),21\beta(H)$, $17\beta(H),21\alpha(H)$, and $17\alpha(H),21\beta(H)$ as well as 22R and 22S stereochemical configurations (Farrimond et al., 2002; Bennett and Abbott, 1999; Innes et al., 1998; Innes et al., 1997; Sinninghe Damsté et al., 1995b). Incorporation of hopanooids, and other biomarkers, into macromolecular materials such as kerogen and asphaltenes via formation of carbon-carbon, ether, ester and carbon-sulphur

linkages, has also been observed (Innes et al., 1997; Peng et al., 1997; Sinninghe Damste and De Leeuw, 1990).

The current hypothesis of the mode of incorporation of cyclic biomarkers in the asphaltene aromatic moiety is via Friedel-Crafts alkylation with clay minerals as catalyst (Trifilieff et al., 1992). The catalytic effect of clay minerals in alkylation and acylation reactions is well established (Cornélis et al., 1990; Laszlo, 1990; Clark et al., 1989). Various clay minerals have been observed to efficiently catalyse the coupling of an alcohol (e.g. benzyl alcohol) with an aromatic hydrocarbon (e.g. toluene) forming the corresponding alkylated compound (e.g. benzyl toluene) (Narender et al., 2006). In fact, Trifilieff et al. (1992) have shown that the clay mineral K-10 montmorillonite catalyses alkylation of cholestan-3 β -ol on benzene forming 3 β -phenylcholestane with about 40% yield. The resulting product on treatment by RICO gave 3 β -cholestanoic acid.



Consequently, it is reasonable to infer that hopanols can be alkylated on aromatic units in reaction similar to one illustrated in Figure 6.20. Terminal hopanols have been observed in sediments (Watson and Farrimond, 2000; Innes et al., 1998; Innes et al., 1997). Interestingly, the hopanol distribution is believed to reflect the different side chain functionalities of the precursor BHP (Innes et al., 1998). Therefore, if the hopanol distribution is further preserved through incorporation into asphaltenes, the hopanoic acids obtained from RICO treatment of the asphaltenes may reflect the original distribution of the hopanols and therefore the BHPs (considering the good selectivity of RICO). Thus, the C_{31} , C_{32} and C_{33} hopanoic acids distribution in the RICO products could be proxies for distributions of the hexa-, penta- and tetra functionalised BHPs present at the onset of diagenesis.



It seems that, it is feasible for hexa- and penta-functionalised BHPs to generate all the C₃₀₊ and C₃₁₊ hopanols respectively according to illustration in Figure 6.21. This could obviously explain the predominance of C₃₂ hopanoic acid in almost all the asphaltenes. It however fails to account for low C₃₃ relative to C₃₂ hopanoic acids. It is expected that if the above proposition holds, C₃₂ hopanol having more precursors than either C₃₀ or C₃₁ hopanols, would predominate during diagenesis and therefore more of it will be incorporated into asphaltenes resulting in greater proportions of C₃₃ hopanoic acids in RICO products of the asphaltenes. Consequently, the author maintains that the relative distribution of C₃₁, C₃₂ and C₃₃ hopanoic acids observed in asphaltenes RICO product is a proxy for distribution of functionalised BHPs prior to diagenesis. It should however be cautioned that substrate-to-oxidant ratio is important in the distribution of products from RICO; high ratio tends to generate significant amounts of the lower molecular weight acids (Ilsley et al., 1986a).

Finally, as shown in Section 6.3.1 the observed hopanoic acids, and other acids, in the asphaltenes RICO products are predominantly from oxidation of the asphaltenes and any contributions from free acids in the maltene is rather insignificant. This is further corroborated by the presence of C₃₆ homohopanoic acids in the RICO products and absence of its hydrocarbon equivalent (C₃₆ hopane) in the maltene fraction. RICO is known to add an extra carbon atom from the degraded aromatic moiety to the aliphatic moiety attached to the aromatic moiety (Mojelsky et al., 1992).

6.3.6 Steranoic acids (SA)

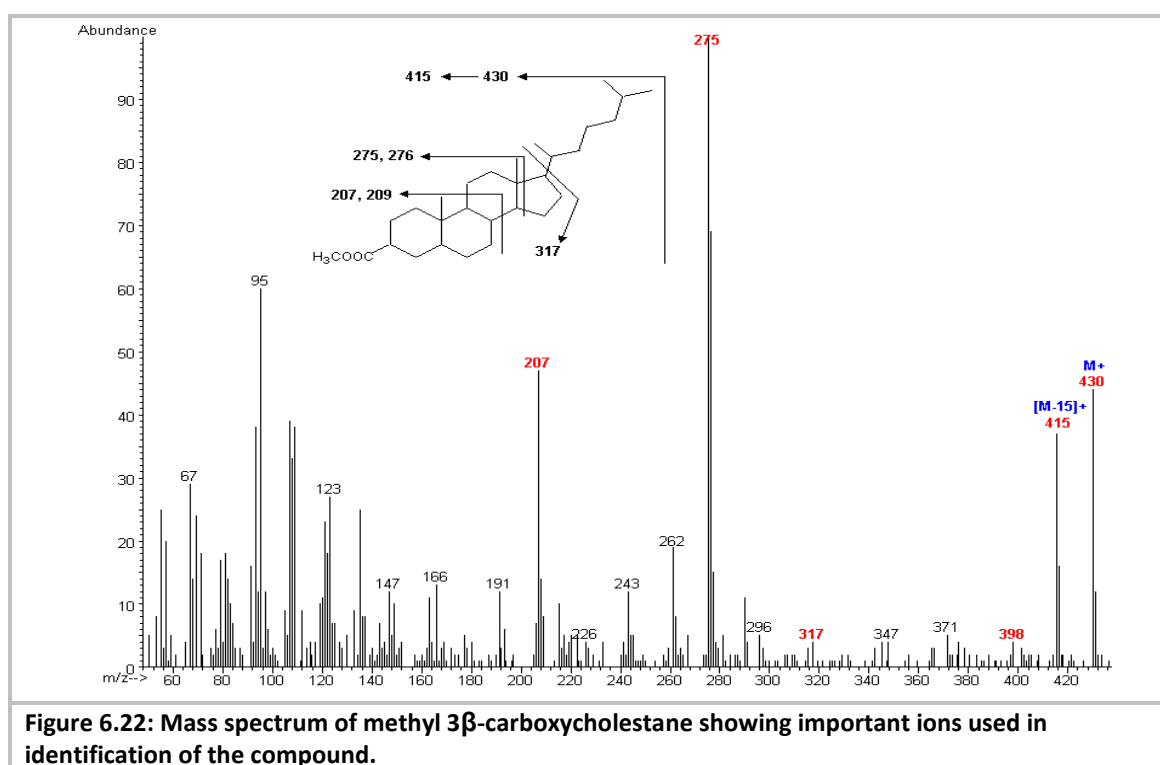
(a) Identification of steranic acids

The steranoic acids consist mainly of 3 β -carboxysteranes and those steranoic acids with carboxyl group on the side chain. Members of the latter type of steranoic acids (*m/z* 217 mass chromatogram) were not observed in the asphaltenes RICO products although they were detected in RICO product of Athabasca asphaltenes by Strausz et al. (1999a). The 3 β -carboxysteranes, on the other hand, were detected in the RICO products of all the asphaltenes analysed in this work. They were identified from their mass spectra and relative elution time

(Barakat and Rullkötter, 1995; Barakat and Rullkötter, 1994). In general, the following fragmentations are useful in the identification of the 3 β -carboxysteranes.

- the molecular ion peak M^{+*} = molecular ion of the corresponding sterane +58 from the additional COOCH_2 from the ester group
- an m/z [$M^{+*} - 15$] from loss of methyl (CH_3) group
- a base peak m/z 275/276 from the cleavage in D ring as in the steranes
- an m/z 317 is due to the ring system
- m/z 207 and m/z 290 are due to cleavages in C and D rings respectively
- as in steranes, m/z 275 > m/z 276 for 5 α (H),7 α (H),17 α (H), and m/z 275 < m/z 276 for 5 α (H),7 β (H),17 β (H)
- a similar elution pattern and the corresponding steranes

Figure 6.22 shows the mass spectrum of 3 β -carboxycholestane illustrating the typical fragmentations displayed by the steranoic acid methyl esters.



(b) *Distribution of the steranoic acids*

In general, the asphaltene RICO products comprise complex mixture of steranoic acids some of which could not be identified. However, regular steranoic acids tentatively identified consist of the homologues of 3 β -carboxysteranes. The mass spectra of these acids (as methyl esters) display m/z 275 (or m/z 276) as base peak and molecular ions of 430, 444 and 458 corresponding to C_{28} , C_{29} and C_{30} respectively. The C_{30} is the dominant homologue in most asphaltenes. Diasteranoic acids were not detected in the asphaltenes oxidation products.

Assuming the relative elution of the steranoic acids is similar to that of the regular steranes, the homologues appear to consist of 20S and 20R doublets of the 5 α (H),7 α (H),17 α (H), and 5 α (H),7 β (H),17 β (H) configurations. It is noteworthy however that the 5 α (H),7 β (H),17 β (H) are in low amounts in some of the samples (Figure 6.23).

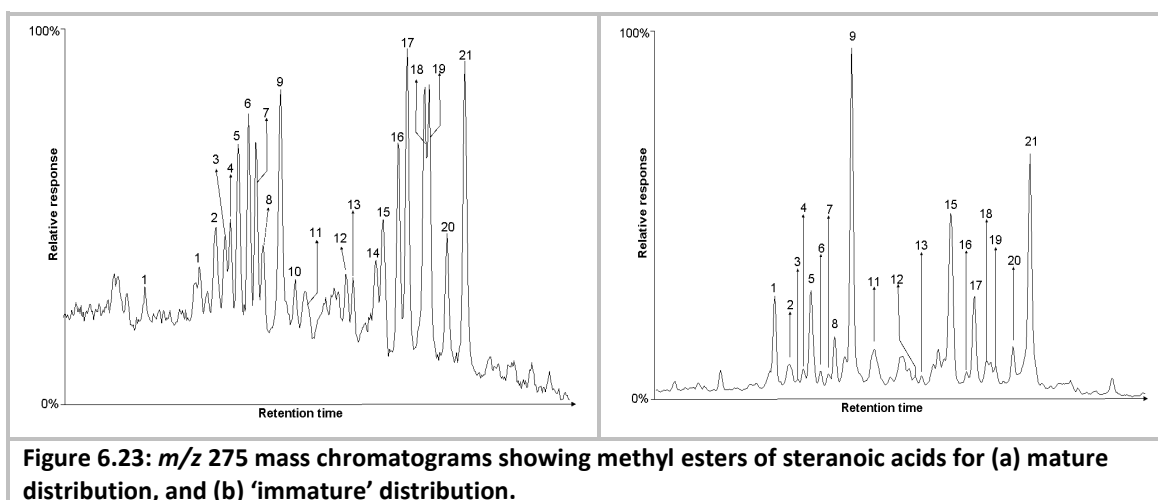


Figure 6.23: m/z 275 mass chromatograms showing methyl esters of steranoic acids for (a) mature distribution, and (b) 'immature' distribution.

Another class of steranoic acid present in the oxidation products are the A-ring methylated 4 α -methyl-3 β -carboxy-5 α (H)-sterane and/or 3 β -carboxymethyl-5 α (H)-steranes (Figure 6.24). These were detected from m/z 289 and they range from C₂₉ to C₃₁ homologues (Barakat and Rullkötter, 1994). They are mainly prominent in asphaltenes from biodegraded oils and especially the severely biodegraded bitumen NB from Nigeria. In general, these compounds have been observed as important components of RICO products of asphaltenes by other workers (Ma et al., 2008; Peng et al., 1999a).

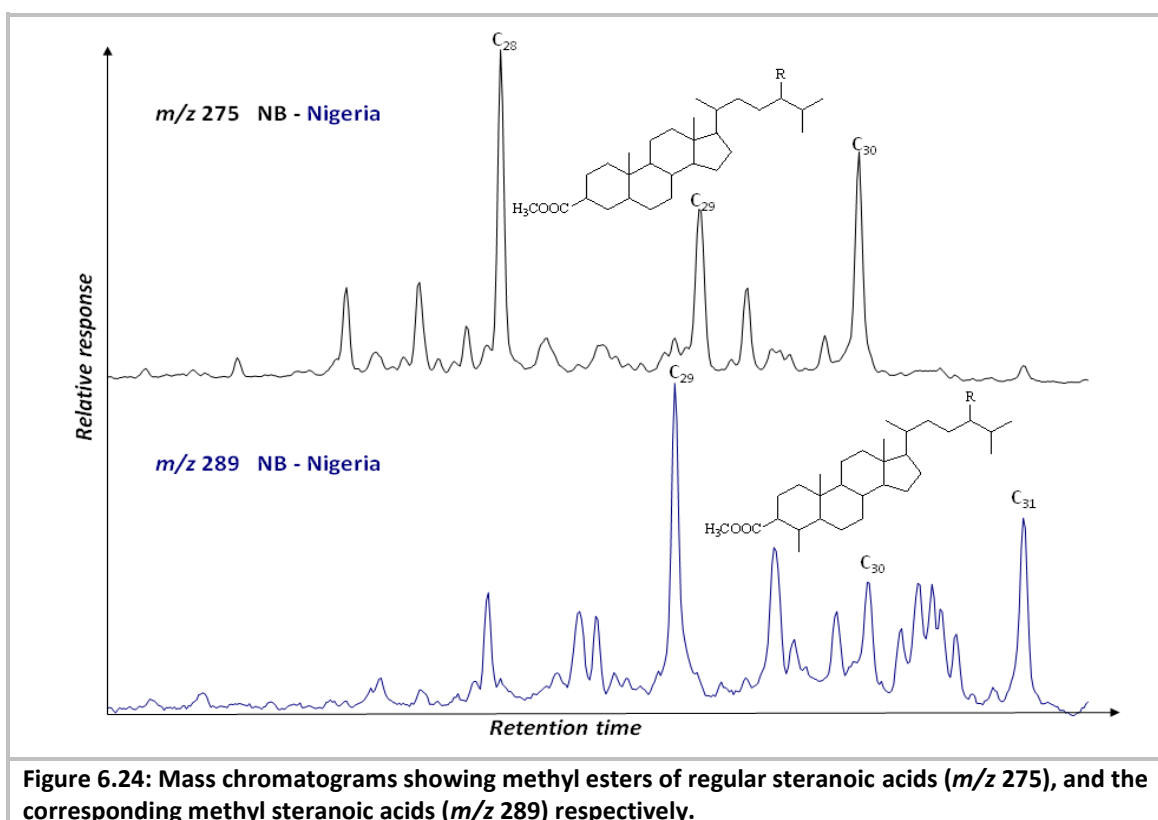


Figure 6.24: Mass chromatograms showing methyl esters of regular steranoic acids (m/z 275), and the corresponding methyl steranoic acids (m/z 289) respectively.

(c) Sources of the steranoic acids

The 3 β -carboxysteranes have been reported both as extractable 'free' compounds in sediments and oils, and as bound components of kerogen released by alkaline hydrolysis (Barakat and Rullkötter, 1995; Barakat and Rullkötter, 1994) indicating they are bound via ester linkages. The origin of these compounds is unknown as they have not been detected in biological systems and thus might be diagenetic products of biological steroids (Barakat and Rullkötter, 1995; Barakat and Rullkötter, 1994). Nonetheless, Barakat and Rullkötter (1994) hypothesised that the 3 β -carboxysteranes may represent unrecognised constituents of marine and freshwater algae, possibly as part of the resistant macromolecular cell wall structure of dinoflagellates, which have been selectively preserved in macromolecular structures and could be precursors of 3 β -methylsteranes observed in sediments and petroleum (Summons and Capon, 1988).

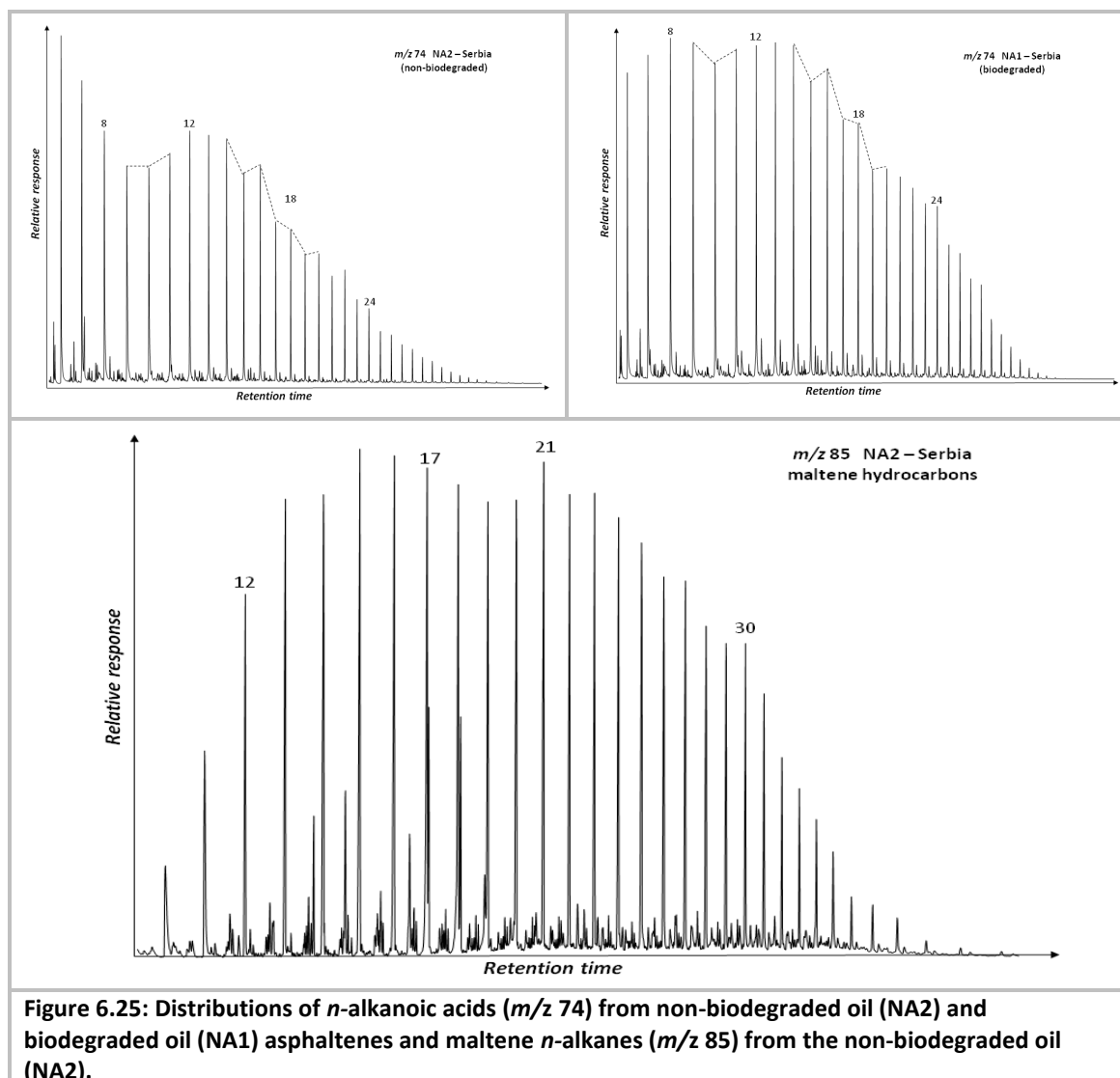
The 3 β -carboxysteranes observed in the RICO products of asphaltenes are however bound into the asphaltene structure via carbon-carbon bonds; they are unlikely to be the free 3 β -methylsteranes. This is because, firstly neither the 3 β -carboxysterane nor the 3 β -methylsteranes, the possible diagenetic products of the former, were detected in the maltene fractions of the oils analysed in this work. Secondly, Trifilieff et al. (1992) have shown that cholesterol could be incorporated into aromatic structures via carbon-carbon bonds and RICO on the product released 3 β -carboxycholetane as the main product.

It is therefore reasonable to conclude that sterols, an important component of cell wall structure of eukaryotes (Mackenzie et al., 1982), are the precursors of both steranes in maltene and the steroids in the asphaltenes. The asphaltene steroids were, in the early stages of diagenesis, incorporated into the asphaltenes via Friedel-Crafts-type alkylation.

6.3.7 Effect of biodegradation

The products of RICO treatment of asphaltenes from biodegraded oils have similar composition and distribution of *n*-alkanoic acids as asphaltenes from non-biodegraded oils. This is also true with respect to other acyclic components. For example, despite the obvious differences, there is clear similarity between relative distributions of the *n*-alkanoic acids homologues of biodegraded NA1 and non-biodegraded NA2 asphaltenes from the two Pannonian basin heavy oils (Table 6.1). This similarity is further emphasised by the fact that the *n*-alkanoic acids from the asphaltenes of NA1 display distribution that is strikingly similar to the *n*-alkane distribution of NA2 oil as shown Figure 6.25. This suggests the the potential of using distribution of asphaltenes *n*-alkyl moieties as replacement for the distribution of the *n*-alkanes in the maltenes where the *n*-alkanes are lost to biodegradation.

The similarity is also observed in the $\delta^{13}\text{C}$ of the *n*-alkanoic acid methyl esters. Asphaltenes from both biodegraded and non-biodegraded oils generated from the same source rock show similar *n*-alkanoic acids methyl esters $\delta^{13}\text{C}$ values and trend across the homologues as illustrated in Figure 6.9.



Furthermore, the hopanoic acid composition and distribution from the products of RICO treatment asphaltenes from biodegraded and non-biodegraded oils are also similar, to some extent. For example, both NA1 and NA2 asphaltenes have barely detectable hopanoic acids greater than C₃₄ homologue. Both also have prominent C₂₈ hopanoic acid content (Figure 6.26). Similarly, NA1 has a relatively small gammaceranoic acid peak (G, Figure 6.26) which is barely detectable in NA2 in agreement with the relative proportions of the compound in their respective hydrocarbon fractions. Nonetheless, there are differences in some cases. For example, while in the NA1 asphaltene, as in all other asphaltenes, C₃₂ hopanoic acid is the dominant homologue, in NA2 asphaltene C₃₃ hopanoic acid predominates. These similarities and differences between these heavy oils might indicate the fact that although the oils have same bulk source rock, their respective source kitchens might have subtle differences in organic facies.

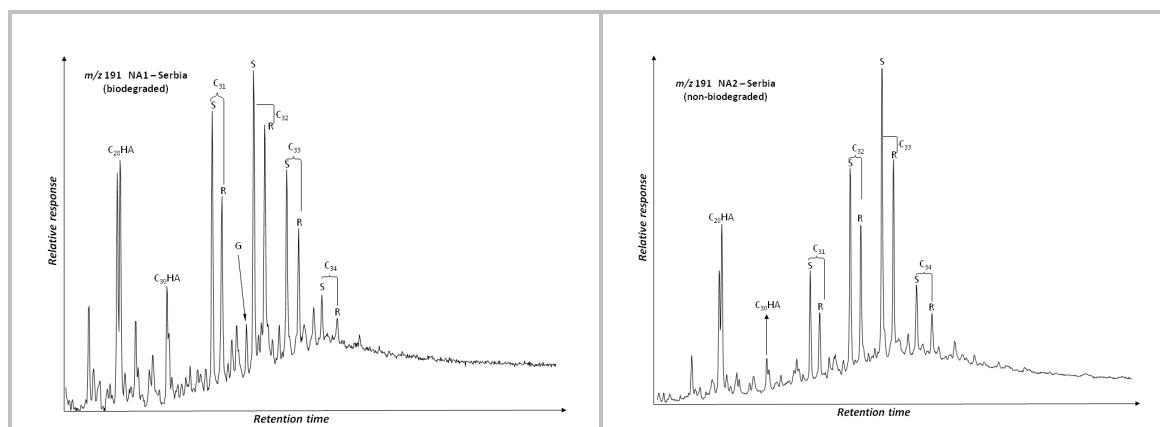


Figure 6.26: m/z 191 mass chromatogram showing HA distributions from products of RICO treatment of asphaltenes from Serbian biodegraded (NA1) and non-biodegraded (NA2) oils.

It is interesting to note that although the maltene hydrocarbons, including biomarkers, of the Nigeria bitumen (NB) were extensively biodegraded and are hardly detectable, as the m/z 191 mass chromatogram is dominated by the norhopanes (Chapter 3), the RICO product of the asphaltenes from NB contains abundant *n*-alkanoic acids as shown in Figure 6.27. The RICO product is also rich in hopanoic acids with mature distribution and prominent gammaceranoic acid (Figure 6.27). This suggests the source rock of the bitumen was deposited in anoxic, possibly hypersaline, setting (Sinninghe Damsté et al., 1995a) with hydrogen-rich kerogen; and the pre-biodegradation oil was rich in aliphatic hydrocarbon particularly the *n*-alkanes.

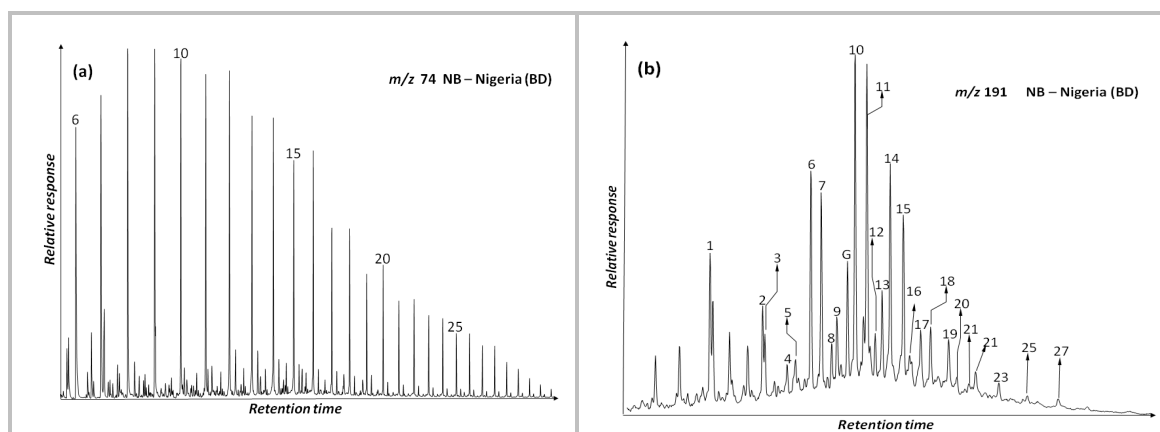


Figure 6.27: (a) m/z 74 mass chromatograms showing distributions of *n*-alkanoic acid methyl esters, and (b) m/z 191 mass chromatograms showing distribution of the hopanoic acid methyl esters from the RICO product of asphaltenes of the extensively biodegraded bitumen (NB) from Nigeria. (See Appendix 6C for assignment)

In general, biodegradation does not appear to change the bound acyclic and pentacyclic terpenoid composition of asphaltenes. The *n*-alkanoic acids and hopanoids are not only present but also exhibit a mature distribution that tends to mimic the maltene hydrocarbon composition. The observed mature distribution is not expected if there is any contribution from immature hopanoid pool from microbes responsible for the biodegradation activity.

Conversely, the bound steroids in asphaltenes seem to be affected by biodegradation. The composition and distribution of the 3β -carboxysteranes from RICO treatment of the asphaltenes from all the biodegraded oils exhibit an immature distribution. The distribution is dominated by the biological $5\alpha(\text{H}), 7\alpha(\text{H}), 17\alpha(\text{H})$ isomers and 20R epimers; the geological $5\alpha(\text{H}), 7\beta(\text{H}), 17\beta(\text{H})$ and 20S are very low in some samples and barely detectable in others.

(Figure 6.28). Similar distributions of the 3β -carboxysteranes from RICO products of asphaltenes from biodegrade oils have been reported by other workers (Ma et al., 2008; Trifilieff et al., 1992).

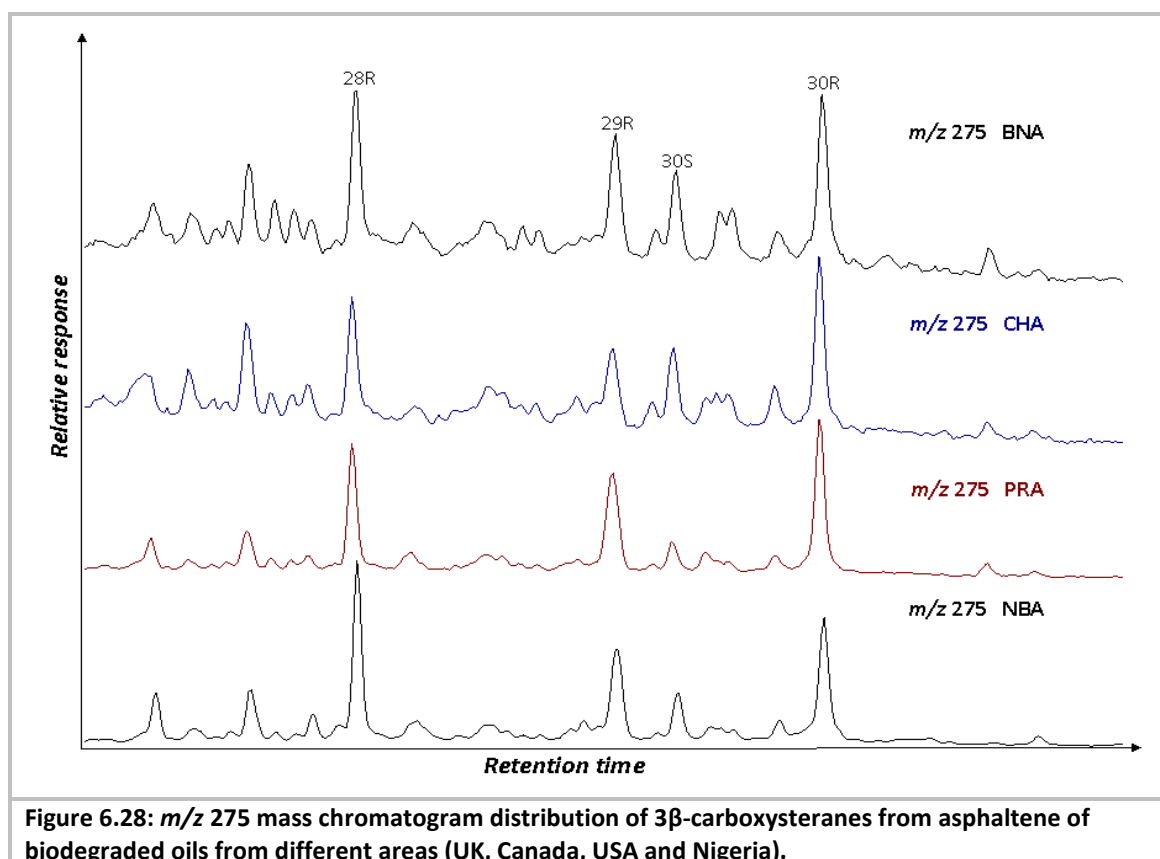


Figure 6.28: m/z 275 mass chromatogram distribution of 3β -carboxysteranes from asphaltene of biodegraded oils from different areas (UK, Canada, USA and Nigeria).

It is not yet clear why some asphaltenes, particularly those from biodegraded oils, exhibit immature distributions of the sterane acids. Some workers speculate that the asphaltenes protect the bound steroids from secondary alterations including maturation (Trifilieff et al., 1992). This is however unlikely for two reasons: (a) asphaltenes from most non-biodegraded oils exhibit mature distribution of the bound steroids; (b) bound hopanoid biomarkers in asphaltenes from both biodegraded and non-biodegraded oils exhibit mature distribution. If asphaltenes provide the claimed protection, it should be consistent in all asphaltenes and biomarkers. The fact that this is not the case; rather the phenomenon is consistently associated with biodegradation, strongly suggests the phenomenon is a latter in-reservoir occurrence most likely associated with biodegradation.

This is rather still puzzling. If biodegradation (and therefore microbes) is responsible for the alteration of the bound steroids in asphaltene, the alteration might occur through one or both of the following: (a) selective elimination of the geological isomers resulting in concentration and enhancement of the biological isomers. This is however problematic considering the observation that biodegradation results in preferential elimination of the biological isomers (Peters et al., 2005a); (b) selective addition of the biological isomers into the system so that the geological isomers are overwhelmed. This is also complicated; if clay minerals are required for incorporation of the steroids on the asphaltenes structure via carbon-carbon bond and for the fact that prokaryotes are responsible for biodegradation and should therefore enrich hopanoids rather than steroids which they do not synthesis.

It should however be noted that although this immature distribution is consistently observed in the asphaltenes from biodegraded oils, the distribution was also observed in oils that may otherwise be classified as non-biodegraded. These oils have normal *n*-alkanes content with no evidence of biodegradation. It is however possible that they are mixtures of biodegraded and non-biodegraded oils or biodegradation has set in although not yet significant enough to be detectable based on elimination of the *n*-alkanes.

6.3.8 Asphaltene versus maltene biomarkers

(a) *n*-Alkanoic acid versus *n*-alkanes

The major similarity between the asphaltene alkyl moieties, as revealed by composition and distribution of the *n*-alkanoic acids in the asphaltene RICO products, and the free *n*-alkane in the maltenes fractions of oils is the fact that both are dominated by the lower molecular weight homologues. The high molecular weight homologues are relative low and decrease sharply with increasing molecular weight. The distributions of *n*-alkanoic acids are generally similar to that of the corresponding *n*-alkanes in maltene; with the highest detectable homologues around C₃₃. Branched alkanes and alkyl groups are generally low.

However, although the free alkanes in the maltenes are easily removed by biodegradation, the alkyl moieties in the asphaltene do appear to be affected by biodegradation as evident from their distributions and $\delta^{13}\text{C}$ signatures.

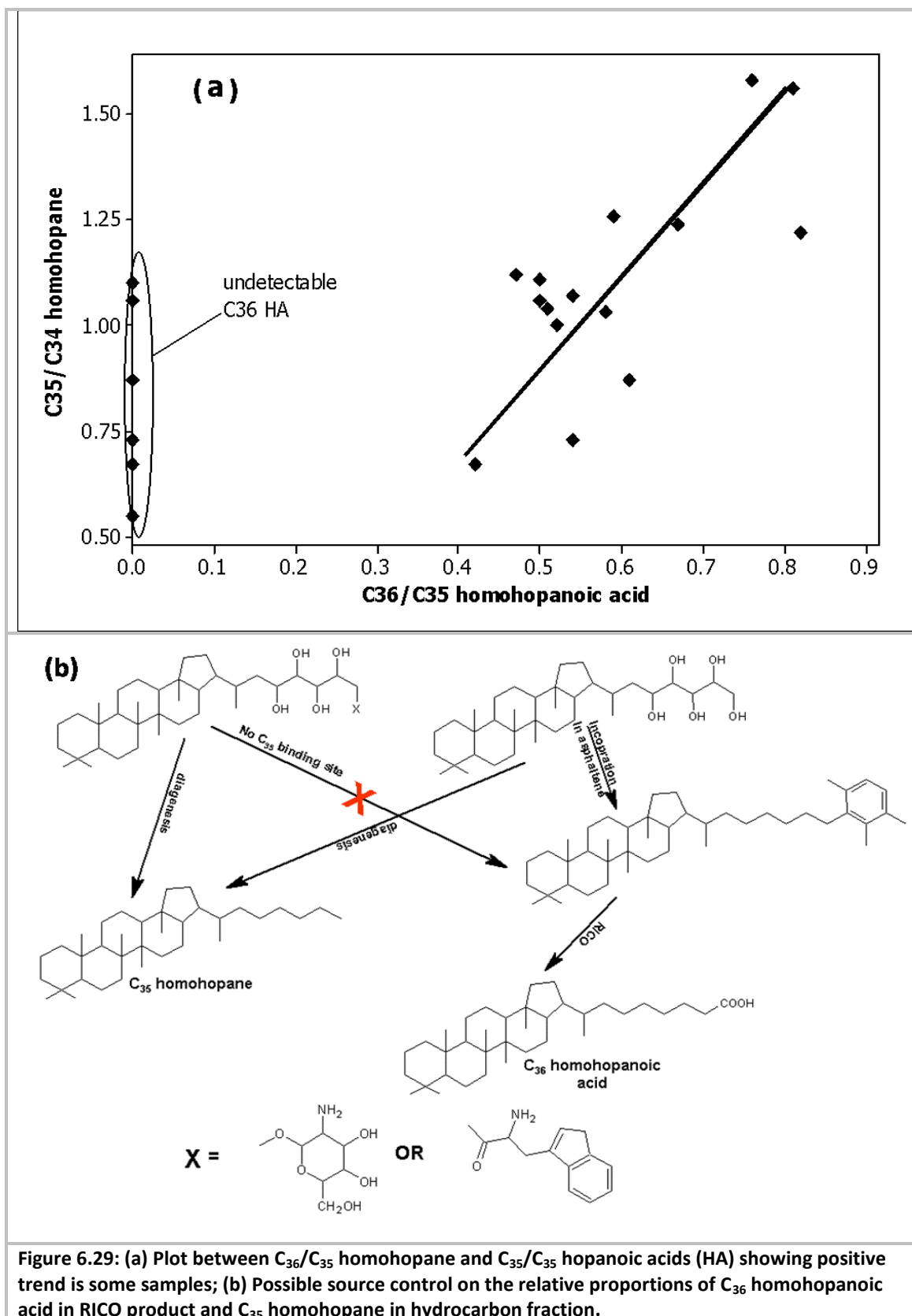
(b) *Hopanoic acids versus hopanes*

There are distinct differences between the free hopanes in maltenes and the hopanoic acids from RICO treatment of asphaltenes. For example, C₂₉ and C₃₀ hopanes are the dominant homologues in the maltenes, while C₃₂ hopanoic acid (not the corresponding C₃₀ and C₃₁ hopanoic acids) is the dominant homologue in the RICO products. This is possibly because no functionalised C₂₉ hopanoid capable of coupling onto aromatic structures occur naturally and thermal dealkylation of hopanoids during diagenesis and catagenesis ultimately generates C₂₉ norhopane. Furthermore, the asphaltenes RICO products contain C₃₆ hopanoic acid while C₃₆ homohopane is absent in the maltenes. This, as explained earlier, is due to addition of extra carbon (the primary or carboxyl group carbon) from oxidative degradation of the asphaltene aromatic moiety.

Table 6.3: Some biomarker-based parameters computed from RICO hopanoic and steranoic acid of asphaltenes

Sample	$C_{31}/(C_{31}-C_{36})\alpha\beta$ -HIA	$C_{32}/(C_{31}-C_{36})\alpha\beta$ -HIA	$C_{33}/(C_{31}-C_{36})\alpha\beta$ -HIA	$C_{34}/(C_{31}-C_{36})\alpha\beta$ -HIA	$C_{35}/(C_{31}-C_{36})\alpha\beta$ -HIA	$C_{36}/(C_{31}-C_{36})\alpha\beta$ -HIA	$C_{30}/C_{31}\alpha\beta$	$C_{32}/C_{31}\alpha\beta$	$C_{36}/C_{35}\alpha\beta$	$C_{28}/(C_{28}-C_{30})\alpha\alpha$ R-SA	$C_{29}/(C_{28}-C_{30})\alpha\alpha$ R-SA	$C_{30}/(C_{28}-C_{30})\alpha\alpha$ R-SA	$C_{29}/C_{30}\alpha\alpha$ R-SA
A39	0.17	0.38	0.30	0.15	0.00	0.00	0.43	1.50	0.00	0.00	0.00	0.00	0.00
AR3	0.33	0.45	0.16	0.06	0.00	0.00	0.49	0.99	0.00	0.34	0.29	0.37	0.80
B58	0.21	0.39	0.24	0.09	0.05	0.03	0.16	1.53	0.61	0.32	0.26	0.42	0.62
BN	0.14	0.40	0.26	0.11	0.06	0.04	0.03	2.19	0.67	0.30	0.28	0.41	0.68
C26	0.16	0.32	0.25	0.13	0.08	0.06	0.11	1.37	0.81	0.34	0.21	0.46	0.45
C30	0.15	0.34	0.24	0.12	0.08	0.06	0.13	1.51	0.76	0.33	0.19	0.48	0.40
CH	0.27	0.40	0.18	0.08	0.04	0.03	0.17	1.15	0.59	0.29	0.25	0.47	0.52
K77	0.22	0.38	0.22	0.10	0.05	0.03	0.13	1.13	0.58	0.31	0.27	0.42	0.65
K78	0.27	0.38	0.18	0.09	0.05	0.02	0.15	0.97	0.54	0.33	0.26	0.41	0.64
NA1	0.35	0.38	0.22	0.05	0.00	0.00	0.34	0.92	0.00	0.31	0.27	0.42	0.64
NA2	0.14	0.30	0.40	0.10	0.04	0.02	0.13	1.67	0.42	0.23	0.45	0.32	1.38
O28	0.21	0.39	0.25	0.09	0.04	0.02	0.08	1.63	0.51	0.33	0.38	0.29	1.29
O31	0.23	0.36	0.23	0.09	0.06	0.03	0.12	1.28	0.50	0.34	0.31	0.36	0.86
PR1	0.25	0.42	0.19	0.08	0.04	0.02	0.16	1.39	0.52	0.27	0.32	0.41	0.77
Q43	0.22	0.37	0.19	0.11	0.06	0.03	0.11	1.24	0.50	0.32	0.21	0.48	0.43
Q61	0.20	0.37	0.23	0.10	0.07	0.03	0.13	1.37	0.47	0.30	0.32	0.38	0.86
U02	0.30	0.35	0.21	0.08	0.07	0.00	0.17	0.95	0.00	0.41	0.27	0.33	0.82
U56	0.17	0.33	0.36	0.14	0.00	0.00	0.00	0.78	0.00	0.35	0.29	0.36	0.81
U79	0.22	0.43	0.24	0.07	0.04	0.00	0.10	1.61	0.00	0.32	0.29	0.40	0.72
U93	0.18	0.36	0.27	0.10	0.05	0.04	0.15	1.43	0.82	0.34	0.29	0.37	0.77
Y32	0.20	0.39	0.24	0.10	0.05	0.02	0.10	1.57	0.54	0.31	0.28	0.41	0.67

In general however, oils that have a relatively prominent C_{35} homohopane in the maltenes also exhibit prominent C_{36} hopanoic acid. As a result there is good positive correlation between C_{35}/C_{34} homohopane ratio from the maltenes and C_{36}/C_{35} hopanoic acid ratio in samples that have measurable C_{36} hopanoic acid (Figure 6.29 (a)). This relationship indicates a common precursor for the homohopanes (i.e. C_{34} & C_{35}) and the corresponding homohopanoic acids (i.e. C_{35} & C_{36}) from asphaltenes.



Despite this positive relationship, however, the C_{36}/C_{35} homohopanoic acids ratio (which is zero in some samples due to absence of C_{36} hopanoic acid) is less than C_{35}/C_{34} homohopane ratio in any give sample (Figure 6.29 (a); Table 6.3). This is believed to be a reflection of accessibility of C35 position of the precursor BHP for possible incorporation on to aromatic

structure in asphaltenes. The BHPs in which the C35 position is bound to a group other than -OH (or -NH₂) may not be available for C₃₅ Friedel-Crafts-type alkylation (Figure 6.29 (b)). Thus, the relative proportions of these types of BHPs, in addition to preservation condition, determine the amount of C₃₅ hopanoid incorporated into the asphaltenes which in turn determines the relative proportion of C₃₆ hopanoic acids observed in the RICO products.

(c) *3β-carboxysteranes versus steranes*

3β-carboxysteranes (C₂₈ to C₃₀) from asphaltenes also display similar distribution as the corresponding steranes (C₂₇ to C₂₉) from the maltene but mainly for oils that do not have 'biodegraded' oil (immature) steranoic acid signature' as shown in Figure 6.30. Nevertheless, C₂₉ steranoic acid homologue is consistently greater in the asphaltene RICO products compared to the corresponding C₂₈ sterane in the maltene hydrocarbon fraction (Figure 6.30).

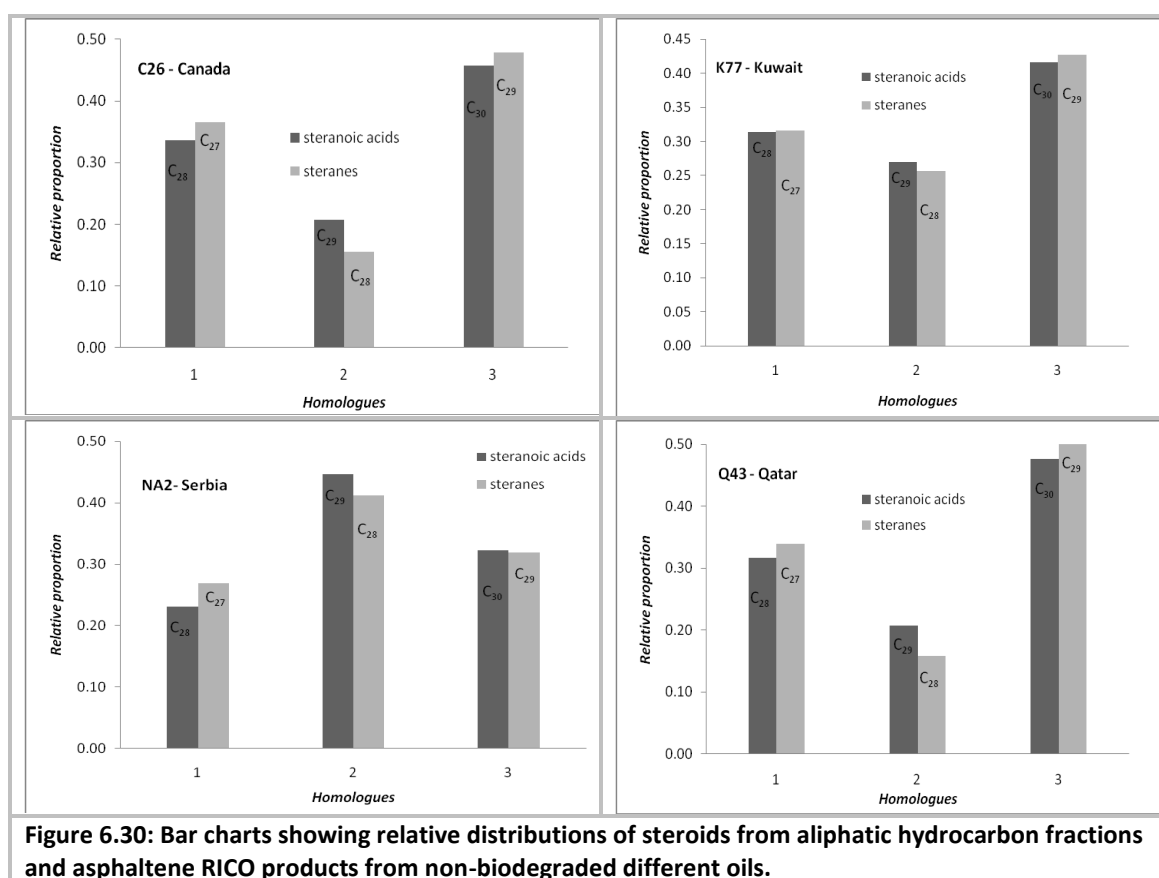


Figure 6.30: Bar charts showing relative distributions of steroids from aliphatic hydrocarbon fractions and asphaltene RICO products from non-biodegraded different oils.

However, for some of the oils particularly those that have immature steranoic acid distribution, the relative distributions of the steranoic acids from the asphaltene RICO products are rather different from the distribution of the corresponding steranes from the maltenes as shown in Figure 6.31. This further suggests the asphaltene-bound steroids (steranoic acids from RICO) might have different source from the maltene steranes.

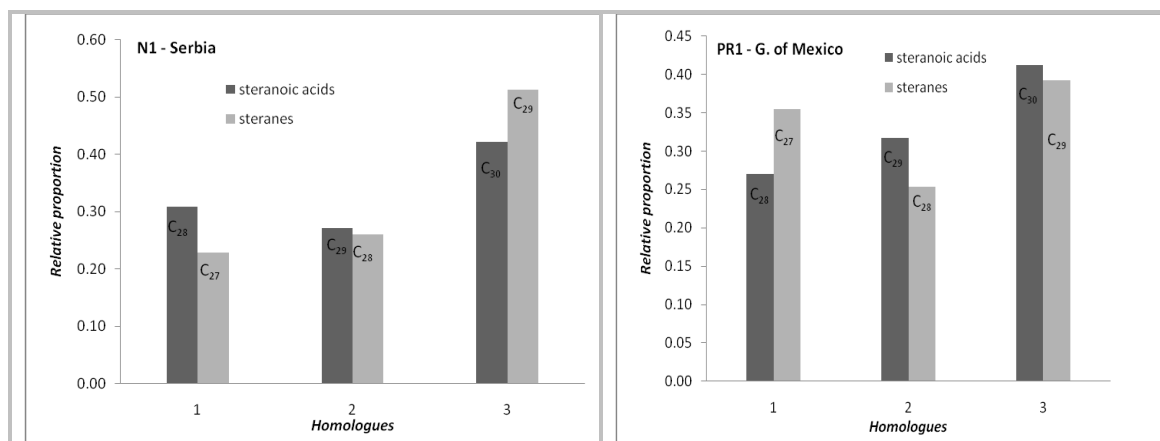


Figure 6.31: Bar charts showing relative distributions of steroids from aliphatic hydrocarbon fractions and asphaltene RICO products from non-biodegraded different oils.

(d) *Hopanoids versus steroids*

Figure 6.32 compares the regular steroid/hopanoic ratio calculated from both maltene and the asphaltenes RICO products. The plot shows a good positive correlation between the two ratios ($R^2 = 0.59\%$, $p < 0.05$) indicating both the maltene steranes and hopanes and asphaltene based steranoic and hopanoic acids have common precursors.

The plots further reveal that the sterane/hopane ratio is generally less than the corresponding steranoic acid/hopanoic acid ratio (Figure 6.32 (b)). In fact, the latter is greater than the former by up to a factor of about 3. This might be because of differences in the relative number of functionalities in the precursor steroids and hopanoids through which they are incorporated in asphaltene structures. For example, while bacteriohopanepolyols (BHPs) have 3 or more binding sites, steranes often have only one binding site. Thus, more of the hopanoids would be incorporated compared to the steroids. Consequently, the asphaltene based steroid/hopanoic ratio would be less than the maltene sterane/hopane ratio.

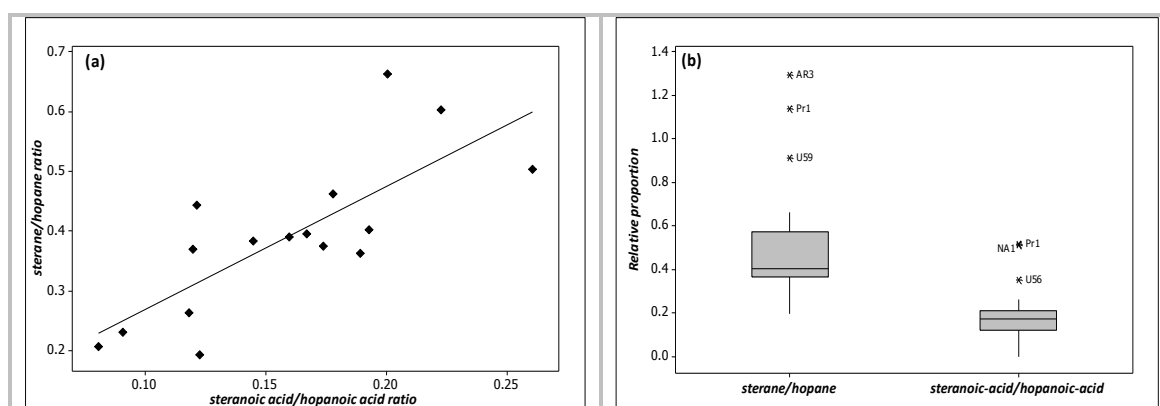


Figure 6.32: (a) Scatter plot of maltene hydrocarbon based sterane/hopane ratio versus asphaltene RICO based steranoic acid/hopanoic acid ratio ($R_2 = 0.59$); (b) box plot of the sterane/hopane and steranoic acid/hopanoic acid ratios showing the asphaltene-based ratio is less than the maltene-based ratio.

6.3.9 Effect of thermal maturation on asphaltene biomarkers

In general, analysis of products of RICO treatment of asphaltenes reveals that the distribution of aliphatic moieties of the asphaltenes changes with maturity in agreement with observations from mid-infrared spectra of the asphaltenes (Section 5.3.2). The distributions of *n*-alkanoic acids of the coal asphaltenes, for example, show lowest rank coal sample ($R_o = 0.40\%$) displays a dominance of the high molecular weight *n*-alkanoic acids. This however shifts towards lower molecular weight homologues as maturity increases to the highest rank coal C15 ($R_o = 1.5\%$) as shown in Figure 6.7. This is semi-quantitatively reflected in TAR, CPI and OEP which, although source parameters, are influenced by thermal maturity.

Similar redistribution of the *n*-alkane homologues in aliphatic hydrocarbon fractions resulting in alteration of CPI and OEP is attributed to generation of more stable lower molecular weight homologues from cracking of high molecular weight homologues (Peters et al., 2005a). The 'redistribution' of *n*-alkanoic acids however suggests with increasing thermal maturity the less stable high molecular weight alkyl side chains of the asphaltenes dealkylate and crack to free aliphatic hydrocarbons at a rate faster than the more stable lower molecular weight alkyl groups so that at higher maturity the latter tend to dominate. Therefore, the unimodal distribution of *n*-alkanoic acids from oil asphaltenes is possibly a reflection of the thermal effect. As the oils are mature ($R_o > 0.6\%$), they might have experienced enough thermal stress to cause redistribution of the alkyl side chains of the asphaltenes with dominance towards the lower homologues as observed (Section 6.3.2).

The effect of thermal maturity on the aliphatic moieties of asphaltenes is further revealed in the composition and distribution of the hopanoid acids in the coal asphaltenes RICO products. The proportions of the more thermally stable $17\alpha(H), 21\beta(H)$ and 22S isomers increase with maturity from C04 to C69 (Figure 6.19) as observed in free maltene hopanes (Section 3.3.2). This is shown by the thermal maturity parameters $\beta\beta/\alpha\beta$ and $22S/(22S+22R)$ (Table 6.4). Consequently, the HA from oil asphaltenes obviously have a mature distribution with dominance of the more stable geological $17\alpha(H), 21\beta(H)$ and 22S over the biological configurations (Table 6.4).

Table 6.4: Values of some maturity parameters based on hopanoic and steranoic acids from RICO products of asphaltenes

Sample	$\beta\beta/\alpha\beta C_{31}$	$22S(22S+22R)C_{31}$	$22S(22S+22R)C_{32}$	$22S(22S+22R)C_{33}$	$22S(22S+22R)C_{34}$	$22S(22S+22R)C_{35}$	$22S(22S+22R)C_{36}$	$\beta\beta/(\beta\beta+\alpha\alpha) C_{30}$	$20S/(20S+20R) C_{30}\alpha\alpha$
A39	0.49	0.60	0.56	0.64	0.54	0.00	0.00	0.00	0.00
AR3	0.35	0.49	0.49	0.63	0.58	0.00	0.00	0.15	0.20
B58	0.22	0.61	0.58	0.66	0.57	0.69	0.50	0.69	0.45
BN	0.32	0.60	0.59	0.65	0.56	0.60	0.59	0.33	0.32
C26	0.40	0.61	0.61	0.68	0.61	0.63	0.59	0.75	0.45
C30	0.45	0.60	0.56	0.68	0.57	0.65	0.61	0.63	0.42
CH	0.27	0.49	0.45	0.59	0.54	0.66	0.63	0.22	0.29
K77	0.54	0.64	0.59	0.66	0.58	0.64	0.57	0.54	0.42
K78	0.44	0.61	0.58	0.63	0.56	0.70	0.59	0.44	0.43
NA1	0.18	0.57	0.56	0.63	0.60	0.00	0.00	0.12	0.34
NA2	0.29	0.61	0.57	0.66	0.59	0.64	0.49	0.91	0.44
O28	0.14	0.61	0.59	0.66	0.62	0.71	0.50	0.40	0.47
O31	0.19	0.59	0.62	0.67	0.54	0.67	0.59	0.26	0.35
PR1	0.20	0.52	0.48	0.53	0.49	0.61	0.48	0.00	0.16
Q43	0.34	0.62	0.60	0.65	0.62	0.66	0.63	0.43	0.44
Q61	0.39	0.60	0.61	0.70	0.58	0.69	0.60	0.53	0.51
U02	0.24	0.65	0.58	0.65	0.60	0.62	0.00	0.00	0.37
U56	1.51	0.57	0.63	0.68	0.55	0.00	0.00	0.82	0.42
U89	0.21	0.58	0.58	0.62	0.54	0.69	0.00	0.00	0.27
U93	0.37	0.60	0.60	0.67	0.57	0.55	0.54	0.48	0.36
Y32	0.20	0.61	0.58	0.64	0.60	0.63	0.60	0.69	0.43

The isomerisation at C22 of bound hopanoids in asphaltenes appears to proceed without hinderance. In fact maturity assessment based on this isomerisation leads to the same conclusions as maltene based hopane isomerisation. Nevertheless, there is a difference between the biomarker maturity parameters from the two fractions. The asphaltene-based hopanoid maturity indices for C₃₃ and C₃₅ homologues are significantly higher (up to 0.70) compared to free hopane-based indices considering the equilibrium value is between 0.57 and 0.62 for the hopane-based indices (Peters et al., 2005a; Seifert and Moldowan, 1980). Similar values but lower (up to 0.66) were reported by Ma et al. (2008). It is not clear why this is the case but is likely to be due to some unknown compounds co-eluting with the 22S epimers.

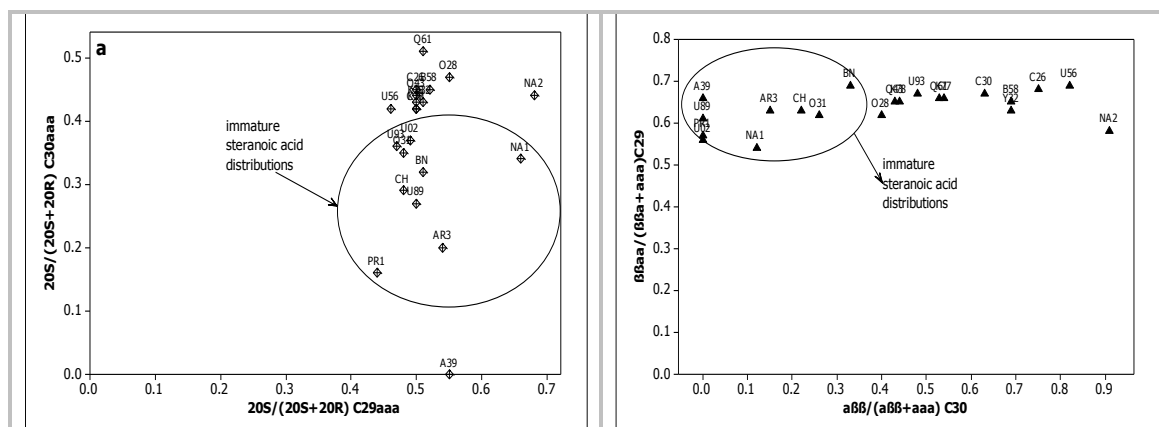


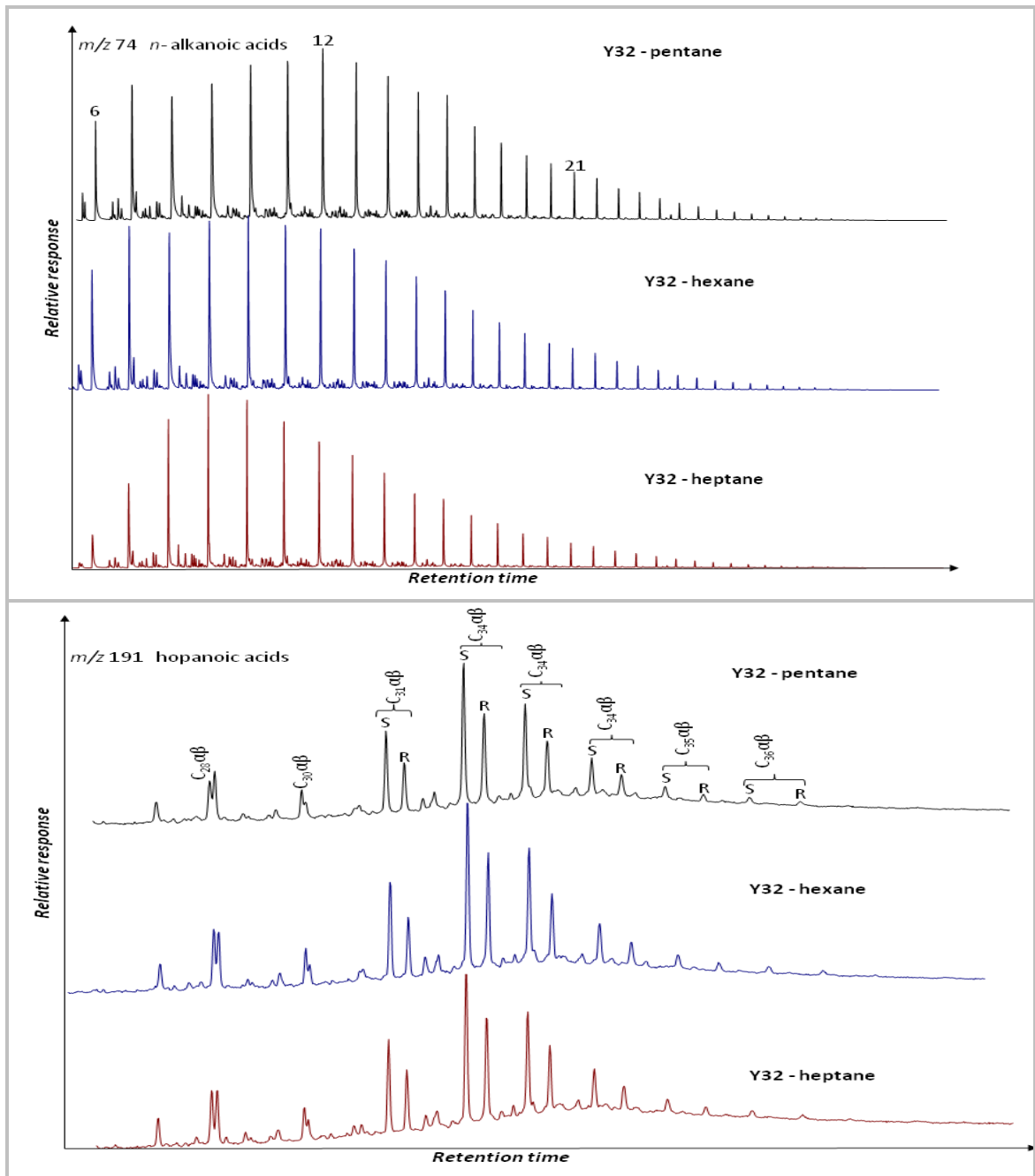
Figure 6.33: Trends in steranoic acids from asphaltene RICO product maturity parameters relative to aliphatic hydrocarbon steranes.

The absence of hopanoic acids in the RICO products of the most mature C15 coal asphaltene ($R_o = 1.5\%$) is likely to be due to the effect of thermal stress and accompanying aromatisation and thermal cracking that affects distribution of the aliphatic moieties. The coal probably has experienced enough thermal stress resulting in more or less complete loss of the bound hopanoids to the 'free' hopane pool through cracking. It is also possible that aromatisation of the cyclic aliphatic moieties occurs simultaneously with thermal cracking as observed from the results of FTIR analysis of the coal asphaltenes (Section 5.3.2).

Table 6.4 shows that the $20S/(20S+20R)$ steranoic acid (C_{30}) maturity parameter for the oils is generally below the equilibrium value of 0.52 (Peters et al., 2005a) although the steranes in the maltenes have reached equilibrium (Section 3.3.3). Even though most of the asphaltenes with the low maturity are either biodegraded or have immature steranoic acid distributions (Figure 6.33), some of the asphaltenes with mature steranoic acid distribution have relatively low steranoic acid-based $20S/(20S+20R)$ compared to the sterane-based parameter (Table 6.4). This is also true with respect to $\alpha\beta\beta/(\alpha\beta\beta+\alpha\alpha\alpha)$ maturity parameter Figure 6.33 (b)). In general, this shows that both steroid thermally dependent stereoisomerisations in asphaltenes are lagging behind the corresponding stereoisomerisations in free aliphatic hydrocarbon fractions.

6.3.10 Assessment of solvent effect on asphaltene biomarkers

It has been observed that the quality and quantity of asphaltene are partly depend on the solvent used for its precipitation (Long, 1981; Corbett and Petrossi, 1978). Consequently, it is reasonable to investigate the difference amongst the biomarker composition of asphaltenes precipitated using pentane, hexane and heptane. Thus, asphaltenes precipitated using these solvents were then subjected to RICO and the products analysed. Figure 6.34 compares the mass chromatograms of *n*-alkanoic, hopanoic and steranoic acid methyl esters from these treatments. This shows similar distributions irrespective of the precipitating solvent. Furthermore, various biomarker parameters computed from the data are presented in Appendix 5E. Values of these parameters further support that the results are independent of the solvent used to recover the asphaltene. These observations are in agreement with the bulk compositions of the asphaltenes as revealed by FTIR (Section 5.3.4).



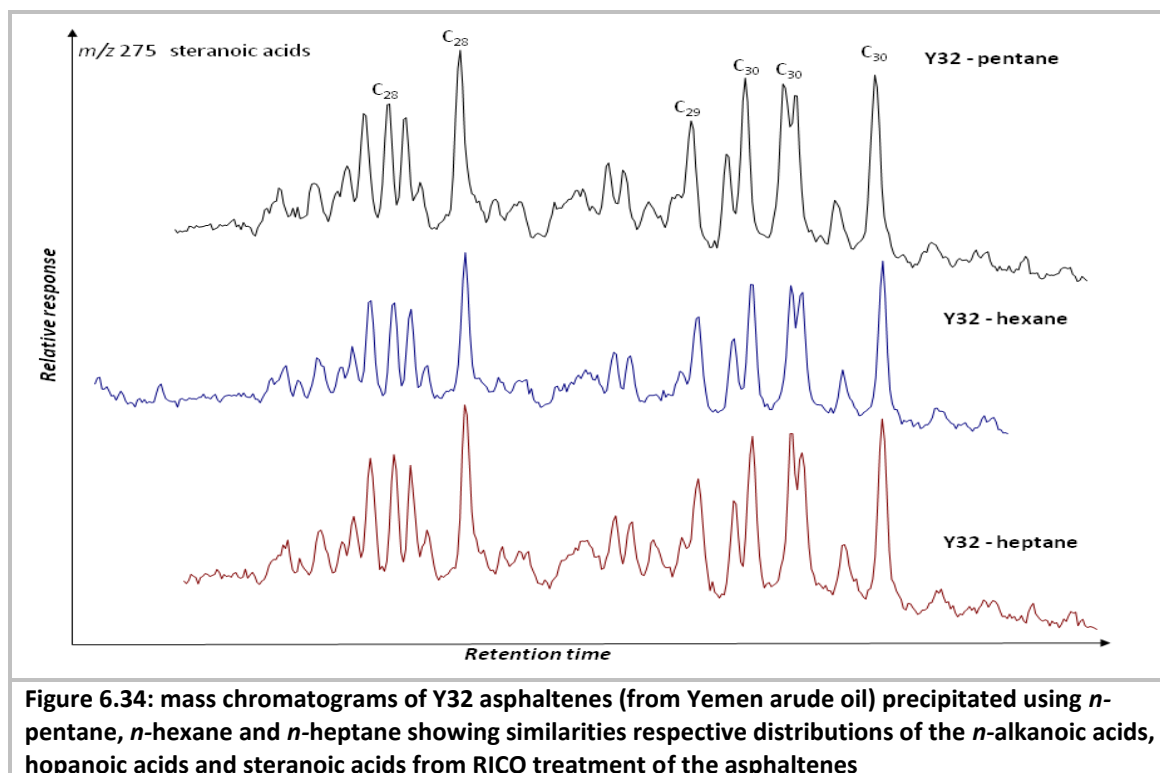


Figure 6.34: mass chromatograms of Y32 asphaltenes (from Yemen arude oil) precipitated using *n*-pentane, *n*-hexane and *n*-heptane showing similarities respective distributions of the *n*-alkanoic acids, hopanoic acids and steranoic acids from RICO treatment of the asphaltenes

This observation may appear to contradict the findings of Corbett & Petrossi (1978) and Alboudwarej et al. (2002) that the quality (e.g. molecular weight) of asphaltenes is dependent on the precipitating solvent (Section 1.2) such that the molecular weight of the precipitated asphaltene decreases from *n*-heptane to *n*-pentane. This was interpreted to indicate that the lower molecular weight solvents (*n*-pentane and *n*-hexane) precipitate a larger proportion of the lower molecular weight compounds that are otherwise components of maltene fraction (Long, 1981; Corbett and Petrossi, 1978) thereby 'diluting' the net molecular weight of the asphaltenes. The observation in this work that asphaltenes precipitated using the three different solvents exhibit similar distribution of biomarkers suggests the biomarkers are incorporated in the fraction (possibly higher molecular weight) of the asphaltenes that are precipitated out by all the solvents.

6.3.11 Correlation using asphaltenes biomarkers

Previous sections have shown that although asphaltenes are influenced by thermal maturation processes, in general asphaltenes from oils that have a common source rock exhibit similar molecular characteristics. The distributions of the *n*-alkanoic acids, hopanoic acids and steranoic acids are generally similar. Furthermore, the $\delta^{13}\text{C}$ isotopic signatures of the *n*-alkanoic acids are similar and follow similar trend across the carbon range. Despite this however, it has also been shown that often some asphaltenes that have the same source could have significant differences in the distributions of the biomarkers.

Nevertheless, it is worthwhile to investigate the extent the collective information derived from the molecular composition of RICO products of asphaltenes can be used to differentiate/correlate asphaltenes or oils into some meaningful groups possibly based on common source and depositional environment. Figure 6.35 is the results of principal component analysis (PCA) using the *n*-alkanoic acids based CPI and OEP data presented in

Table 6.2. The first two principal components (PC1 and PC2) account for about 97% of the variance with the four CPI and OEP parameters giving the highest contributions to PC1 and TAR to PC2. The figure shows some of the same source samples (e.g. K77 & K78 and O28 & O31) with a common source are closely grouped. Other samples (e.g. U02 & AR3, NA1) however plot away from rest of the groups showing these are distinctly different.

The classification is however more clearly shown in the dendrogram (Figure 6.35 (b)) from hierarchical cluster analysis based on the PC1 and PC2 from the PCA. AR3 and U02 are unusual asphaltenes as shown in Table 6.2. There is no distinct separation between asphaltenes from biodegraded and non-biodegraded oils. However, the Kuwait and Oman asphaltenes from a carbonate source rock form cluster 4. Most of the Northsea asphaltenes are in cluster 2 although the cluster also contains asphaltenes from other regions (Figure 6.35 (b)). The two Canadian (C26 & C30) asphaltenes from Midale oil field as well as the two Serbian asphaltenes (NA1 & NA2) are grouped in cluster 3 together with the Nigerian asphaltene (NB).

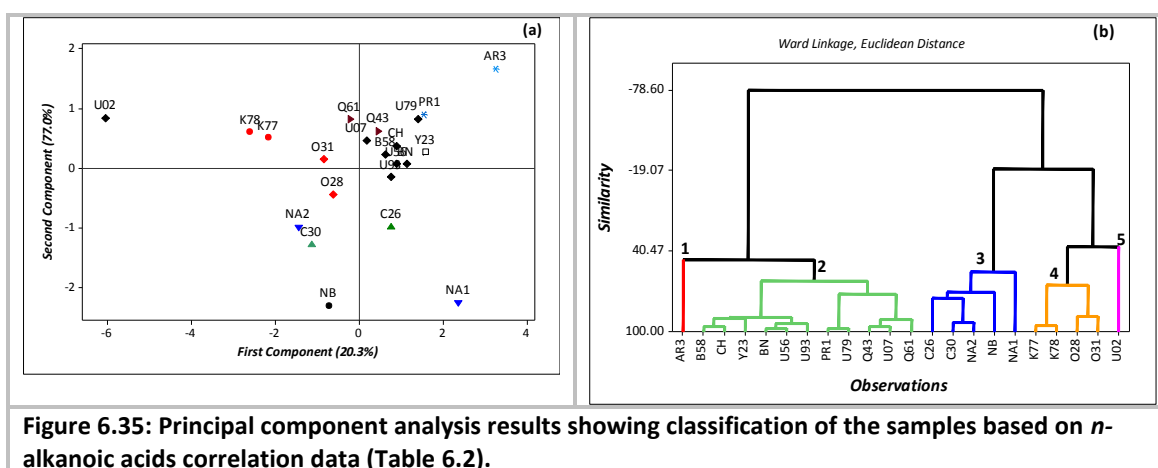
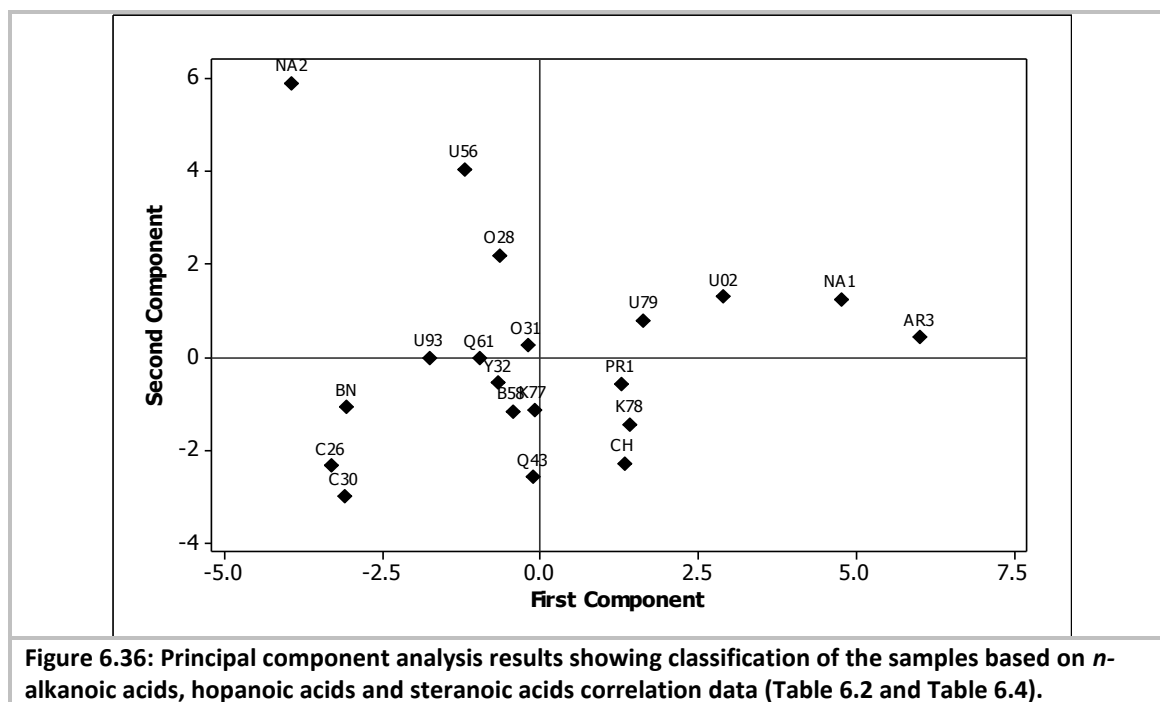


Figure 6.35: Principal component analysis results showing classification of the samples based on *n*-alkanoic acids correlation data (Table 6.2).

Furthermore, all the parameters calculated from *n*-alkanoic acids, HA and SA as presented in Table 6.2 and Table 6.4 were used for principal component analysis to discriminate amongst the samples. However, no significant improvement in grouping the samples based on any meaningful pattern was observed as is clear from Figure 6.36. It therefore seems visual inspection of relevant mass chromatograms in addition analysis of the *n*-alkanoic acids isotopic data is necessary for effective correlation/discrimination of oils using asphaltene bound biomarkers from RICO treatment products. This might be because not all the details are represented in the parameters calculated in addition to the fact that asphaltene molecular composition is not affected by diagenesis to the similar extent as are free maltene components.



6.4 Summary and Conclusions

Ruthenium ion catalysed oxidation of asphaltenes yields the aliphatic moieties of the asphaltenes with good selectivity and thus the composition of the product reflects the original aliphatic composition of the asphaltenes. Analysis of petroleum asphaltenes from various sources and coal asphaltenes of different maturity revealed:

1. The aliphatic moieties in asphaltenes are dominated by *n*-alkyl groups followed by α,ω -dicarboxylic acids. Other acyclic alkyl groups identified are branched alkyl groups.
2. Although the α,ω -dicarboxylic acids could be partly from polymethylene bridges between aromatic moieties, a significant proportion was due to alkyl groups with terminal hydroxyl and/or carboxylic groups
3. Generally, the $\delta^{13}\text{C}$ of *n*-alkanoic acids from RICO treatment of asphaltenes with common source show similar values and trend, and can be used to correlate samples of common source
4. Thermal evolution of asphaltenes follows a similar trend as the free aliphatic hydrocarbon fraction in terms of the distribution of the *n*-alkyl groups and isomerisation of biomarkers. The bound steroid isomerisation, however, lags behind the aliphatic hydrocarbon biomarker isomerisation
5. The asphaltene bound biomarkers have potential in the reflecting depositional condition anoxic/hypersaline condition through preservation of extended homohopanoids and gammaceranoid

6. The relative distribution of C₃₁ to C₃₃ homohopanoic acids from bound hopanoids in asphaltene could serve as proxies of relative distribution of hexa-, penta- and tetra-functionalised bacteriohopanepolyols
7. Biodegradation does not appear to affect the alkyl and hopanoid moieties even in extensively biodegraded petroleum. Thus the bound biomarker can be used as source of information lost with the loss of aliphatic hydrocarbon biodegradation
8. Asphaltene-bound steroid composition in all biodegraded oils consistently exhibit immature distribution. Non-biodegraded oils, on the other hand, show both mature and immature steroid distribution
9. Bound biomarkers have good potential in correlation of oils. This could be improved by using multivariate statistical methods such as principal component analysis. Better correlation can however be achieved with the help of compound specific carbon isotopic data.

Chapter 7 Summary and Future Work

7.1 Overall Conclusions

Occlusion of compounds in asphaltenes, in particular of biomarkers, is a very promising hypothesis particularly in the study of extensively biodegraded oils. The hypothesis is investigated to assess its validity or otherwise. Specifically, the extent of Soxhlet extraction required to remove adsorbed/co-precipitated components from asphaltenes, and the most suitable chemical degradation method for recovering the occluded compounds were investigated. Furthermore, simulation experiments were conducted to test the occlusion hypothesis and hydrocarbon compositions of the maltene adsorbed and occluded fractions were compared to investigate whether the differences amongst the fractions are statistically significant. Results of the investigation reveal the following:

The process of precipitation of asphaltenes from oils invariably results in co-precipitation of components, including hydrocarbons and resins, from the maltene fraction of the oil. Analysis of composition of asphaltenes therefore requires removal of the co-precipitated materials from the asphaltenes. This was observed to require Soxhlet extraction of the asphaltenes for several hours which vary with different asphaltenes. Although over 90% of the co-precipitated materials were removed from the asphaltenes in the first 48 hour of extraction, waxes in the range of C₃₆ to C₄₂ were observed in some asphaltenes even after 10 days of Soxhlet extraction which suggests there is no clear demarcation between the adsorbed (co-precipitated) and components or biomarkers that might have been occluded in the asphaltenes.

Hydrogen peroxide/acetic acid reagent was observed to significantly attack saturated hydrocarbons which makes it unsuitable for decomposing asphaltenes in order to release any biomarkers that may be occluded within them. Acidified potassium permanganate solution was found to be practically the most suitable reagent for this purpose. Nevertheless, comparative analysis of the saturated hydrocarbons in maltene, adsorbed and occluded fractions revealed clear differences in distributions of the *n*-alkanes amongst the fractions. However, the maturity and correlation indices calculated from the biomarkers of the fractions show no consistent systematic differences amongst the fractions. It therefore appears that the so-called occlusion of biomarkers by asphaltenes is most likely a consequence of co-precipitation which was dependent on the solubility properties of the waxes.

Mid-infrared and solid-state ¹³C NMR analyses of the asphaltenes revealed that petroleum asphaltenes consist predominantly of aliphatic moieties bonded to condensed aromatic structures with relative proportions of aromatic carbon in range of 30 to 40% for petroleum asphaltenes. Asphaltenes from biodegraded oils, however, are relatively less aromatic (25 to 27% aromatic carbon). The relative amounts of aliphatic and aromatic moieties in the asphaltenes from coal and black shales are dependent on the maturity and source of the organic matter.

Oxygen functionalities in asphaltenes are mainly in the form of hydroxyl, ether and carbonyl (ester, carboxyl and conjugated ketone) groups. Ester groups are generally absent in petroleum asphaltenes but were detected in coal and black shale asphaltenes. The carboxyl

group was detected in all the asphaltenes irrespective of source and geographical region. The carbonyl groups (particularly the carboxyl group) are the dominant functionalities in black shale and coal asphaltenes even at relatively high maturities. Nitrogen functionalities, in form of pyridinic and pyrrolic heteroaromatic systems as well as tertiary aromatic amines, were tentatively identified from the mid-infrared spectra of the petroleum and coal asphaltenes. In general, there were no significant differences in the bulk compositions of the asphaltenes precipitated using *n*-pentane, *n*-hexane and *n*-heptane.

Analysis of products of ruthenium (III) ion catalysed oxidation, a fairly selective chemical degradation of petroleum and coal asphaltenes, reveals the aliphatic moieties in the asphaltenes are dominated by *n*-alkyl groups followed by *iso*-alkyl groups. Alkyl dicarboxylic acids possibly generated alkyl groups with terminal carboxyl and hydroxyl groups as well as polymethylene bridges were also present. Relatively small amounts of naphthenic groups, mainly in form of homohopanooids and steroids, were also detected in the degradation products indicating that hopanooids and steroids were incorporated at the initial stages of diagenesis. The hopanooid moieties in the asphaltenes range from C₃₀ to C₃₆ homologues (each with 22S and 22R epimers) with dominance of the C₃₂ member except in one sample where C₃₃ is dominant. Both 17 α (H),21 β (H) and 17 β (H),21 α (H) isomers were observed. The C₃₆ homohopanooid in asphaltenes was observed to positively correlate with the C₃₅ homohopane in the hydrocarbon fraction of the maltenes indicating common precursor. The composition of the steroids in petroleum asphaltenes includes C₂₈ to C₃₀ regular steroids which were tentatively observed to consist of the 5 α (H),7 α (H),17 α (H), and 5 α (H),7 β (H),17 β (H) as well as 20S and 20R configurations. Other steroids tentatively identified are the methyl steroids including the C₂₉ to C₃₁ homologues.

The effect of organic matter source on the composition of asphaltenes could be significant depending on the thermal maturity of the asphaltenes. The distributions of the alkyl moieties in asphaltenes reflect the distribution of the *n*-alkanes in the maltene fractions. Similarly, the relative proportion of the C₃₅ homohopanooids in the asphaltenes correlates with the relative proportions of the C₃₅ homohopanes in the maltenes. This is also true with respect to the relative distribution of the steroids in many samples.

The prominence of bound C₃₆ hopanooids and gammaceranooid in some of the asphaltenes is also a clear indication of both organic matter source and depositional condition under which the organic matter was deposited. Furthermore, although mid-infrared spectra of petroleum asphaltenes are generally similar, multivariate statistical analysis of the spectra groups most of the asphaltenes based on their common sources. Deconvolution of the spectra revealed that the relative proportions of the carbonyl groups in carboxyl and conjugated functionalities appear to be related to the depositional environments. With few exceptions, asphaltenes from oils sourced from carbonate source rocks have greater proportion of conjugated carbonyl groups and the shale-sourced having greater proportion of the carboxyl group.

The effect of biodegradation is not yet fully established. Nevertheless, solid-state ¹³C NMR revealed that asphaltenes from biodegraded oils have relatively lower proportions of aromatic carbon compared to asphaltenes from non-biodegraded oils. Bound hopanooids were observed even in asphaltenes from extensively biodegraded oils. However, the bound steroids from

biodegraded oil asphaltenes consistently exhibit immature distribution. Non-biodegraded oils, on the other hand, show both mature and immature steroid distribution.

Furthermore, distinct differences were observed amongst asphaltenes from black shales, coals and crude oils. Unlike petroleum asphaltenes, the coal and black shale asphaltenes are dominated by oxygen functionalities although this might be related to the thermal maturities of the samples. However, asphaltenes from marginally mature Tanezzuft black shales show an aromatic content that is relatively greater than the relative aromatic content observed in petroleum asphaltenes which is a distinctive indication of organic matter contribution to the composition of the asphaltenes.

Thermal maturity was observed to affect the composition of asphaltenes. With increasing thermal stress, asphaltenes were observed to evolve towards an equilibrium structure or composition in which aromatic moieties become dominant over aliphatic moieties as a result of increasing condensation and dealkylation. Distribution of alkyl moieties shifts towards increasing proportions of the lower molecular weight homologues with increasing thermal maturity. The thermal stress also results in loss of oxygen functionalities from hydroxyl, ester and carboxyl groups. At the molecular level, isomerisation of bound hopanoids and steroids toward equilibrium composition was observed with increasing maturity. However, while isomerisation of bound hopanoids in asphaltenes appears to be in phase with the corresponding isomerisation of hopanes in the maltene fraction, the isomerisation of bound steroids lags significantly behind the corresponding isomerisation of the steranes.

Correlation/discrimination of asphaltenes based on their mid-infrared spectra with the aid of chemometric tools show potential in correlating asphaltenes with similar chemical characteristics. However, as the composition of asphaltenes is dependent on their thermal histories, asphaltenes tend to evolve towards an equilibrium composition and asphaltenes with different source could be classified in same group. Bound biomarkers have shown good potential in correlation of oils. This could however be improved by using multivariate statistical methods such as principal component analysis. Better correlation can however be done with the help of compound specific carbon isotopic data. In general, the $\delta^{13}\text{C}$ of *n*-alkanoic acids from RICO treatment of asphaltenes with common source show similar values and trend, and can be used to correlate samples of common source.

7.2 Future Work

Despite the work undertaken and presented in this thesis, there is additional work that needs to be done to further have a clearer understanding of chemical composition, origin and incorporation of biomarkers in asphaltenes. In light of my observations in the course of this work, it is my opinion that the following need further investigation:

1. The origin of the steranoic acids observed in RICO product of asphaltene from biodegraded oil should be established relative to the steranes in hydrocarbon fraction of the maltenes. This is necessary in order to unravel the dynamics of the development of the observed immature distribution of the steranoic acids in biodegraded oils. Comparative isotopic analysis of the steranoic acids and maltene steranes is a possible way through which this may be achieved

2. It is worthwhile to investigate the factors responsible for the slight but fairly consistent difference observed in 22S↔22R isomerisation between odd and even HA homologues. This can possibly be done through quantum mechanical modelling to investigate how carbon number affects the stability of the biological isomers particularly when attached to aromatic moieties in asphaltenes
3. Molecular investigation of aromatic moieties of asphaltene has been challenging because the chemical methods used tend to destroy them. Nevertheless, such work would be worthwhile as it will settle many issues with respect to the nature of the aromatic structures (e.g. number of rings) of asphaltene. This can be done by developing methods that selectively de-bridge the asphaltenes macromolecules without attacking the aromatic groups. A potential method is treatment of the asphaltenes with aqueous sodium dichromate solution at high temperatures (200 - 300 °C) in autoclave. The method has been observed to quantitatively oxidise methyl side chains of polynuclear aromatic compounds into carboxyl groups with negligible oxidation of the ring system (Friedman et al., 1965; Wiberg, 1965). Similar other methods have also been developed (Melchiorre *et al.*, 1965)
4. Comparative study of biomarkers derived from asphaltenes using RICO, hydrolysis, desulphurisation may be useful to evaluate the relative proportions of various biomarkers incorporated in asphaltenes. This could shed light on the preference and mode of incorporation of the bound biomarkers.
5. The conclusion reached in this work with regard to occlusion in asphaltenes that the observed apparent occlusion was due to coprecipitation mainly as a result of solubility of waxes can further be investigated by monitoring precipitation of standard waxes in oils. The occlusion can also be further investigated using severely biodegraded oils in which all hopane and sterane biomarkers in the maltene fraction are lost so that occlusion can be confirmed if the full range of the biomarkers were observed in the occluded fraction
6. Assignments of the bands from IR spectra of petroleum asphaltenes are generally done in comparison to mid-infrared spectra of coal which may have different composition and chemical environment. There is therefore the need to develop assignments specifically addressing the specific composition of asphaltenes. This is particularly emphasised by the observation in this work that some bands traditionally assigned to C–O might be due to C–N particularly in petroleum asphaltenes
7. There are many molecular entities in the RICO products of asphaltenes that have not been identified. The chemistry of these products could hold very important information in further understanding the nature of precursor molecules and mode of incorporation of such products in asphaltenes
8. Many compounds were observed in the lower retention time region of the m/z 191 mass chromatogram of derivatised RICO products that could not be identified but are possibly tricyclic and tetracyclic acids. Their relative distributions were observed to be

source dependent. Their identification could shade light and increase the application of RICO products in correlation studies

References

- Abdullah, F. H. and Connan, J. (2002) 'Geochemical study of some Cretaceous rocks from Kuwait: comparison with oils from Cretaceous and Jurassic reservoirs', *Organic Geochemistry*, 33, (2), pp. 125-148.
- Abdullah, F. H. A. and Kinghorn, R. R. F. (1996) 'A Preliminary Evaluation of Lower and Middle Cretaceous Source Rocks in Kuwait', *Journal of Petroleum Geology*, 19, pp. 461-480.
- Acevedo, S., Escobar, O., Echevarria, L., Gutierrez, L. B. and Mendez, B. (2004) 'Structural Analysis of Soluble and Insoluble Fractions of Asphaltene Isolated Using the PNP Method. Relation between Asphaltene Structure and Solubility', *Energy & Fuels*, 18, (2), pp. 305-311.
- Adams, M. J. (1991) 'Cluster Analysis with Infrared Spectra', *Analytical Proceedings*, 28, pp. 147 - 149.
- Adebiyi, F. M. and Omode, A. A. (2007) 'Organic, Chemical and Elemental Characterization of Components of Nigerian Bituminous Sands Bitumen', *Energy Sources, Part A: Recovery, Utilization, and Environmental Effects*, 29, (8), pp. 669 - 676.
- Aitken, C. M., Jones, D. M. and Larter, S. R. (2004) 'Anaerobic hydrocarbon biodegradation in deep subsurface oil reservoirs', *Nature*, 431, pp. 291-294.
- Al-Saad, H. and Ibrahim, M. I. A. (2005) 'Facies and palynofacies characteristics of the Upper Jurassic Arab D reservoir in Qatar', *Revue de Paléobiologie, Genève*, 24, (1), pp. 225-241.
- Al-Siddiqi, A. and Dawe, R. A. (1999) 'Qatar's Oil and Gasfields: a Review', *Journal of Petroleum Geology*, 22, (4), pp. 417-436.
- Alboudwarej, H., Beck, J., Svrcek, W. Y., Yarranton, H. W. and Akbarzadeh, K. (2002) 'Sensitivity of Asphaltene Properties to Separation Techniques', *Energy & Fuels*, 16, (2), pp. 462-469.
- Alsharhan, A. S. and Nairn, A. E. M. (1997) *Sedimentary Basins and Petroleum Geology of the Middle East*. Amsterdam: Elsevier.
- Ancheyta, J. (2007) 'Preface: Characterisation and Conversion of Asphaltenes', *Petroleum Science and Technology*, 25, (1-3), pp. 1-3.
- Ancheyta, J., Centeno, G., Trejo, F., Marroquin, G., Garcia, J. A., Tenorio, E. and Torres, A. (2002) 'Extraction and Characterization of Asphaltenes from Different Crude Oils and Solvents', *Energy & Fuels*, 16, (5), pp. 1121-1127.
- Andersen, S. I. and Birdi, K. S. (1991) *Journal of Colloid and Interface Science*, 142, pp. 497.
- Andersen, S. I. and Christensen, S. D. (2000) 'The Critical Micelle Concentration of Asphaltenes As Measured by Calorimetry', *Energy & Fuels*, 14, (1), pp. 38-42.
- Andersen, S. I. and Speight, J. G. (2001) 'Petroleum Resins: Separation, Character, and Role in Petroleum', *Petroleum Science and Technology*, 19, (1), pp. 1 - 34.

- Andreatta, G., Bostrom, N. and Mullins, C. O. (2007) 'Ultrasonic Spectroscopy of Asphaltene Aggregation', in Mullins, C. O., Sheu, E. Y. and Marshall, A. G.(eds) *Asphaltenes, Heavy Oils, and Petroleomics*. New York: Springer, pp. 231 - 257.
- Andreatta, G., Bostrom, N. and Mullins, O. C. (2005a) 'High-Q Ultrasonic Determination of the Critical Nanoaggregate Concentration of Asphaltenes and the Critical Micelle Concentration of Standard Surfactants', *Langmuir*, 21, (7), pp. 2728-2736.
- Andreatta, G., Goncalves, C. C., Buffin, G., Bostrom, N., Quintella, C. M., Arteaga-Larios, F., Perez, E. and Mullins, O. C. (2005b) 'Nanoaggregates and structure-function relations in asphaltenes', *Energy & Fuels*, 19, (4), pp. 1282-1289.
- Angle, C. W., Long, Y., Hamza, H. and Lue, L. (2006) 'Precipitation of asphaltenes from solvent-diluted heavy oil and thermodynamic properties of solvent-diluted heavy oil solutions', *Fuel*, 85, (4), pp. 492-506.
- Armstrong, H. A., Abbott, G. D., Turner, B. R., Makhlof, I. M., Muhammad, A. B., Pedentchouk, N. and Peters, H. (2009) 'Black shale deposition in an Upper Ordovician-Silurian permanently stratified, peri-glacial basin, southern Jordan', *Palaeogeography, Palaeoclimatology, Palaeoecology*, 273, (3-4), pp. 368-377.
- Aske, N., Kallevik, H. and Sjoblom, J. (2001) 'Determination of Saturate, Aromatic, Resin, and Asphaltenic (SARA) Components in Crude Oils by Means of Infrared and Near-Infrared Spectroscopy', *Energy & Fuels*, 15, (5), pp. 1304-1312.
- Augusti, R., Dias, A. O., Rocha, L. L. and Lago, R. M. (1998) 'Kinetics and Mechanism of Benzene Derivative Degradation with Fenton's Reagent in Aqueous Medium Studied by MIMS', *J. Phys. Chem. A*, 102, pp. 10723 - 10727.
- Aziz, A. (2000) 'Stratigraphy and hydrocarbon potentials of the lower Palaeozoic succession of licence NC 115, Murzuq Basin, SW Libya', in Sola, M. A. and Worsley, D.(eds) *Symposium on Geological Exploration in Murzuq Basin*. Amsterdam: Elsevier, pp. 349 - 368.
- Badre, S., Goncalves, C. C., Norinagab, K., Gustavsona, G. and Mullins, O. C. (2006) 'Molecular size and weight of asphaltene and asphaltene solubility fractions from coals, crude oils and bitumen', *Fuel*, 85, pp. 1 – 11.
- Barakat, A. O. and Rullkötter, J. (1994) 'Occurrence of Bound 3.beta.-Carboxysteroids in Geological Samples', *Energy & Fuels*, 8, (2), pp. 481-486.
- Barakat, A. O. and Rullkötter, J. (1995) 'Extractable and bound fatty acids in core sediments from the Nördlinger Ries, southern Germany', *Fuel*, 74, (3), pp. 416-425.
- Barakat, A. O. and Yen, T. F. (1987) 'Kerogen structure by stepwise oxidation : Use of sodium dichromate in glacial acetic acid', *Fuel*, 66, (5), pp. 587-593.
- Barakat, A. O. and Yen, T. F. (1988) 'Preliminary analysis of Monterey kerogen by mild stepwise oxidation with sodium dichromate in glacial acetic acid', *Geochimica et Cosmochimica Acta*, 52, (2), pp. 359-363.

- Baxby, M., Patience, R. L. and Bartle, K. D. (1994) 'The origin and diagenesis of sedimentary organic nitrogen', *Journal of Petroleum Geology*, 17, (2), pp. 211-230.
- Beebe, K. R., Pell, R. J. and Seasholtz, M. B. (1998) *Chemometrics: A Practical Guide*. New York: John Wiley & Sons, Inc.
- Behar, F. H. and Albrecht, P. (1984) 'Correlations between carboxylic acids and hydrocarbons in several crude oils. Alteration by biodegradation', *Organic Geochemistry*, 6, pp. 597-604.
- Bellamy, L. J. (1975) *The Infra-red Spectra of Complex Molecules*. London: Chapman and Hall.
- Bennett, B. and Abbott, G. D. (1999) 'A natural pyrolysis experiment -- hopanes from hopanoic acids?', *Organic Geochemistry*, 30, (12), pp. 1509-1516.
- Bennett, B., Chen, M., Brincat, D., Gelin, F. J. P. and Larter, S. R. (2002) 'Fractionation of benzocarbazoles between source rocks and petroleums', *Organic Geochemistry*, 33, (5), pp. 545-559.
- Bennett, B. and Larter, S. R. (2000) 'Quantitative Separation of Aliphatic and Aromatic Hydrocarbons Using Silver Ion-Silica Solid-Phase Extraction', *Anal. Chem.*, 72, (5), pp. 1039-1044.
- Bergmann, U., Groenzin, H., Mullins, O. C., Glatzel, P., Fetzer, J. and Cramer, S. P. (2003) 'Carbon K-edge X-ray Raman spectroscopy supports simple, yet powerful description of aromatic hydrocarbons and asphaltenes', *Chemical Physics Letters*, 369, (1-2), pp. 184-191.
- Berner, R. A. (1984) 'Sedimentary pyrite formation: An update', *Geochimica et Cosmochimica Acta*, 48, pp. 605 – 615.
- Berner, R. A. and Raiswell, R. (1983) 'Burial of organic carbon and pyrite sulphur in sediments over Phanerozoic time: a new theory', *Geochimica et Cosmochimica Acta*, 47, pp. 855 – 862.
- Bisutti, I., Hilke, I. and Raessler, M. (2004) 'Determination of total organic carbon - an overview of current methods', *TrAC Trends in Analytical Chemistry*, 23, (10-11), pp. 716-726.
- Blanc, P. and Albrecht, P. (1991) 'Parameters of "Macromaturity" (PMM): novel rank and type related indices from chemical degradation of macromolecular network of coals', *Organic Geochemistry*, 17, (6), pp. 913-918.
- Blokker, P., Schouten, S., de Leeuw, J. W., Sinninghe Damsté, J. S. and van den Ende, H. (2000) 'A comparative study of fossil and extant algaenans using ruthenium tetroxide degradation', *Geochimica et Cosmochimica Acta*, 64, (12), pp. 2055-2065.
- Blokker, P., van den Ende, H., de Leeuw, J. W., Versteegh, G. J. M. and Sinninghe Damsté, J. S. (2006) 'Chemical fingerprinting of algaenans using RuO₄ degradation', *Organic Geochemistry*, 37, pp. 871 – 881.

- Bona, M. T. and Andrés, J. M. (2007) 'Coal analysis by diffuse reflectance near-infrared spectroscopy: Hierarchical cluster and linear discriminant analysis', *Talanta*, 72, (4), pp. 1423-1431.
- Boucher, R. J., Standen, G. and Eglinton, G. (1991) 'Molecular characterization of kerogens by mild selective chemical degradation -- ruthenium tetroxide oxidation', *Fuel*, 70, (6), pp. 695-702.
- Boukir, A., Guiliano, M., Asia, L., El Hallaoui, A. and Mille, G. (1998) 'A fraction to fraction of photo-oxidation of BAL 150 crude oil asphaltenes', *Analisis*, 26, pp. 358 - 364.
- Bowden, S. A., Farrimond, P., Snape, C. E. and Love, G. D. (2006) 'Compositional differences in biomarker constituents of the hydrocarbon, resin, asphaltene and kerogen fractions: An example from the Jet Rock (Yorkshire, UK)', *Organic Geochemistry*, 37, pp. 369 – 383.
- Bray, E. E. and Evans, E. D. (1961) 'Distribution of n-paraffins as a clue to recognition of source beds', *Geochimica et Cosmochimica Acta*, 22, (1), pp. 2-15.
- Brereton, R. G. (2003) *Chemometrics: Data Analysis for the Laboratory and Chemical Plant*. Chichester: John Wiley & Sons Inc.
- Brincat, D. and Abbott, G. D. (2001) 'Some aspects of the molecular biogeochemistry of laminated and massive rocks from the Naples Beach Section (Santa Barbara-Ventura)', in Issacs, C. M. and Rullkoetter, J.(eds) *The Monterey Formation: From Rocks to Molecules*. New York: Columbia University Press, pp. 140 - 149.
- Buckley, J. S., Hirasaki, G. J., Liu, Y., Von Drasek, S., Wang, J. X. and Gill, B. S. (1998) 'Asphaltene Precipitation and Solvent Properties of Crude Oils', *Petroleum Science and Technology*, 16, (3), pp. 251 - 285.
- Bunger, J. W. and Li, N. C. (eds.) (1981) *Chemistry of Asphaltenes*. Washington, D.C.: American Chemical Society.
- Bustin, R. M., Link, C. and Goodarzi, F. (1989) 'Optical properties and chemistry of graptolite periderm following laboratory simulated maturation', *Organic Geochemistry*, 14, (4), pp. 355-364.
- Calemma, V., Iwanski, P., Nali, M., Scotti, R. and Montanari, L. (1995) 'Structural Characterization of Asphaltenes of Different Origins', *Energy & Fuels*, 9, (2), pp. 225-230.
- Calemma, V., Rausa, R., D'Antona, P. and Montanari, L. (1998) 'Characterization of Asphaltenes Molecular Structure', *Energy & Fuels*, 12, (2), pp. 422-428.
- Carman, G. J. (1996) 'Structural elements of onshore Kuwait', *GeoArabia*, 1, (2), pp. 239 - 266.
- Carnahan, N. F., Salager, J.-L., Anton, R. and Davila, A. (1999) 'Properties of Resins Extracted from Boscan Crude Oil and Their Effect on the Stability of Asphaltenes in Boscan and Hamaca Crude Oils', *Energy & Fuels*, 13, (2), pp. 309-314.

- Cassani, F., Gallango, O., Talukdar, S., Vallejos, C. and Ehrmann, U. (1988) 'Methylphenanthrene maturity index of marine source rock extracts and crude oils from the Maracaibo Basin', *Organic Geochemistry*, 13, (1-3), pp. 73-80.
- Castillo, J., Fernández, A., Ranaudo, M. A. and Acevedo, S. (2001) 'New Techniques and Methods for the Study of Aggregation, Adsorption, and Solubility of Asphaltenes. Impact of these Properties on Colloidal Structure and Flocculation.', *Petroleum Science and Technology*, 19, pp. 75 – 106.
- Cerný, J. (1996) 'Structural dependence of CH bond absorptivities and consequences for FT-i.r. analysis of coals', *Fuel*, 75, (11), pp. 1301-1306.
- Christie, W. W. (2006) *Preparation of Methyl Esters – Part 1*. Available at: www.lipidlibrary.co.uk/topics/ethests/index.htm (Accessed: 14 November).
- Christie, W. W. (2008) 'Mass spectra of methyl esters of fatty acids: Part 1. Normal saturated fatty acids', pp. 5. [Online]. Available at: <http://www.lipidlibrary.co.uk/ms/ms03/file.pdf> (Accessed: 25 Jan. 2009).
- Christy, A. A., Hopland, A. L., Barth, T. and Kvalheim, O. M. (1989) 'Quantitative determination of thermal maturity in sedimentary organic matter by diffuse reflectance infrared spectroscopy of asphaltenes', *Organic Geochemistry*, 14, (1), pp. 77-81.
- Cimino, R., Correria, S., Del Bianco, A. and Lockhart, T. P. (1995) 'Solubility and Phase Behavior of Asphaltenes in Hydrocarbon Media', in Sheu, E. Y. and Mullins, C. O.(eds) *Asphaltenes: Fundamentals and Applications* New York: Plenum Press.
- Clark, J. H., Kybett, A. P., Macquarrie, D. J., Barlow, S. J. and Landon, P. (1989) 'Montmorillonite supported transition metal salts as Friedel–Crafts alkylation catalysts', *J. Chem. Soc., Chem. Commun.*, 1989, pp. 1353 - 1354.
- Coelho, R. R., Hovell, I., Moreno, E. L., Lopes de Souza, A. and Rajagopal, K. (2007) 'Characterization of Functional Groups of Asphaltenes in Vacuum Residues Using Molecular Modelling and FTIR Techniques', *Petroleum Science and Technology*, 25, (1&2), pp. 41 - 54.
- Cole, G. A., Abu-Ali, M. A., Aoudeh, S. M., Carrigan, W. J., Chen, H. H., Colling, E. L., Gwathney, W. J., Al-Hajji, A. A., Halpern, H. I., Jones, P. J., Al-Sharidi, S. H. and Tobey, M. H. (1994) 'Organic Geochemistry of the Palaeozoic Petroleum System of Saudi Arabia', *Energy & Fuels*, 8, pp. 1425 – 1442.
- Corbett, L. W. and Petrossi, U. (1978) 'Differences in Distillation and Solvent Separated Asphalt Residua', *Ind. Eng. Chem. Prod. Res. Dev.*, 17, (4), pp. 342-346.
- Cornélis, A., Gerstmans, A., Laszlo, P., Mathy, A. and Zieba, I. (1990) 'Friedel-Crafts acylations with modified clays as catalysts ', *Catalysis Letters*, 6, (1), pp. 103-109.
- Costantinides, G. and Arich, G. (1967) 'Non-hydrocarbon compounds in petroleum', in Nagy, B. and Colombo, U.(eds) *Fundamental Aspects of Petroleum Chemistry*.Amsterdam: Elsevier, pp. 109–175.

- Creek, J. L. (2005) 'Freedom of Action in the State of Asphaltenes: Escape from Conventional Wisdom', *Energy Fuels*, 19, (4), pp. 1212-1224.
- Curiale, J. A., Cameron, D. and Davis, D. V. (1985) 'Biological marker distribution and significance in oils and rocks of the Monterey Formation, California', *Geochimica et Cosmochimica Acta*, 49, (1), pp. 271-288.
- Dean, W. E. and Arthur, M. A. (1989) 'Iron-Sulphur-Carbon Relationships in Organic-Carbon-Rich Sequences I: Cretaceous Western Interior Seaway', *American Journal of Science*, 289, pp. 708 – 743.
- del Rio, J. C., Martin, F., Gonzalez-Vila, F. J. and Verdejo, T. (1995) 'Chemical structural investigation of asphaltenes and kerogens by pyrolysis-methylation', *Organic Geochemistry*, 23, (11-12), pp. 1009-1022.
- Demaison, G. J. and Moore, G. T. (1980) 'Anoxic environments and oil source bed genesis', *AAPG Bulletin*, 64, (8), pp. 1179-1209.
- Didyk, B. M., Simoneit, B. R. T., Brassell, S. C. and Eglinton, G. (1978) 'Organic geochemical indicators of palaeoenvironmental conditions of sedimentation', *Nature*, 272, (5650), pp. 216-222.
- Djerassi, C. and Engle, R. R. (1953) 'Oxidations with Ruthenium Tetroxide', *J. Am. Chem. Soc.*, 75, (15), pp. 3838-3840.
- Donaggio, F., Corraera, S. and Lockhart, T. P. (2001) 'Precipitation onset and Physical Models of Asphaltene Solution Behavior', *Petroleum Science and Technology*, 19, pp. 129 – 142.
- Douglas, A. G. and Powell, T. G. (1969) 'The rapid separation of fatty acids from fossil lipids by impregnated adsorbent thin-layer chromatography', *Journal of Chromatography A*, 43, pp. 241-246.
- Dragojlovic, V., Bajc, S., Ambles, A. and Vitorovic, D. (2005) 'Ether and ester moieties in Messel shale kerogen examined by hydrolysis/ruthenium tetroxide oxidation/hydrolysis', *Organic Geochemistry*, 36, (1), pp. 1-12.
- Duyck, C., Miekeley, N., Porto da Silveira, C. L. and Szatmari, P. (2002) 'Trace element determination in crude oil and its fractions by inductively coupled plasma mass spectrometry using ultrasonic nebulization of toluene solutions', *Spectrochimica Acta Part B: Atomic Spectroscopy*, 57, (12), pp. 1979-1990.
- Ekulu, G., Nicolas, C., Achard, C. and Rogalaski, M. (2005) 'Characterisation of Aggregation Processes in Crude Oils Using Differential Scanning Calorimetry', *Energy & Fuels*, 19, pp. 1297 – 1302.
- Ekweozor, C. M. (1984) 'Tricyclic terpenoid derivatives from chemical degradation reactions of asphaltenes', *Organic Geochemistry*, 6, pp. 51-61.
- Ekweozor, C. M. (1986) 'Characterisation of the non-asphaltene products of mild chemical degradation of asphaltenes', *Organic Geochemistry*, 10, (4-6), pp. 1053-1058.

- Evdokimov, I. N., Eliseev, N. Y. and Akhmetov, B. R. (2006) 'Asphaltene dispersions in dilute oil solutions', *Fuel*, 85, (10-11), pp. 1465-1472.
- Farrimond, P., Griffiths, T. and Evdokiadis, E. (2002) 'Hopanoic acids in Mesozoic sedimentary rocks: their origin and relationship with hopanes', *Organic Geochemistry*, 33, (8), pp. 965-977.
- Friedman, L., Fishel, D. L. and Shechter, H. (1965) 'Oxidation of Alkylarenes with Aqueous Sodium Dichromate. A Useful Method for Preparing Mono- and Polyaromatic Carboxylic Acids', *J. Org. Chem.*, 30, (5), pp. 1453-1457.
- Galoppini, M. (1994) 'Asphaltene Deposition Monitoring and Removal Treatments: An Experience in Ultra Deep Wells ', *SPE*, Paper 27622, pp. 10.
- Gates-Anderson, D. D., Siegrist, R. L. and Cline, S. (2001) 'Comparison of Potassium permanganate and Hydrogen peroxide as Chemical Oxidants for Organically Contaminated Soil', *Journal of Environmental Engineering*, 127, pp. 337 - 347.
- Geng, W., Nakajima, T., Takanashi, H. and Ohki, A. (2009) 'Analysis of carboxyl group in coal and coal aromaticity by Fourier transform infrared (FT-IR) spectrometry', *Fuel*, 88, (1), pp. 139-144.
- George, G. N. and Gorbaty, M. L. (1989) 'Sulfur K-edge x-ray absorption spectroscopy of petroleum asphaltenes and model compounds', *Journal of the American Chemical Society*, 111, (9), pp. 3182-3186.
- Gonzalez, G., Sousa, M. A. and Lucas, E. F. (2006) 'Asphaltenes Precipitation from Crude Oil and Hydrocarbon Media', *Energy & Fuels*, 20, (6), pp. 2544-2551.
- Gordon, M. L., Tulumello, D., Cooper, G., Hitchcock, A. P., Glatzel, P., Mullins, O. C., Cramer, S. P. and Bergmann, U. (2003) 'Inner-Shell Excitation Spectroscopy of Fused-Ring Aromatic Molecules by Electron Energy Loss and X-ray Raman Techniques', *The Journal of Physical Chemistry A*, 107, (41), pp. 8512-8520.
- Gore, E. S. (1983) 'Ruthenium Catalysed Oxidations of Organic Compounds', *platinum Metals Rev.*, 27, (3), pp. 111-125.
- Grantham, P. J., Lijmbach, G. W. M. and Posthuma, J. (1990) 'Geochemistry of crude oils in Oman', *Geological Society, London, Special Publications*, 50, (1), pp. 317-328.
- Grantham, P. J., Lijmbach, G. W. M., Posthuma, J., Hughes Clarke, M. W. and Willink, R. J. (1988) 'Origin of Crude Oils in Oman', *Journal of Petroleum Geology*, 11, (1), pp. 61 - 80.
- Grantham, P. J. and Wakefield, L. L. (1988) 'Variations in the sterane carbon number distributions of marine source rock derived crude oils through geological time', *Organic Geochemistry*, 12, (1), pp. 61-73.
- Gray, J. (1993) 'Major Paleozoic land plant evolutionary bio-events', *Palaeogeography, Palaeoclimatology, Palaeoecology*, 104, pp. 153-169.

- Groenzin, H. and Mullins, O. C. (1999) 'Asphaltene Molecular Size and Structure', *J. Phys. Chem. A*, 103, (50), pp. 11237-11245.
- Guanjun, X., Dajiang, Z. and Wang, P. (2003) 'Using the biomarker bonded on the asphaltenes for biodegraded oil-source correlation', *Chinese Science Bulletin*, 48, (3), pp. 300-304.
- Guiliano, M., Mille, G., Doumenq, P., Kister, J. and Muller, J. F. (1990) 'Study of Various Rank French Demineralized Coals and Maceral Concentrates: Band Assignment of FTIR Spectra after Resolution Enhancement using Fourier Deconvolution', in Charcosset, H.(ed), *Advanced Methodologies in Coal Characterisation*. Amsterdam: Elsevier, pp. 399-417.
- Guillen, M. D., Iglesias, M. J., Dominguez, A. and Blanco, C. G. (1992) 'Semi-quantitative FTIR analysis of a coal tar pitch and its extracts and residues in several organic solvents', *Energy & Fuels*, 6, (4), pp. 518-525.
- Gutierrez, L. B., Ranaudo, M. A., Mendez, B. and Acevedo, S. (2001) 'Fractionation of Asphaltene by Complex Formation with p-Nitrophenol. A Method for Structural Studies and Stability of Asphaltene Colloids', *Energy & Fuels*, 15, (3), pp. 624-628.
- Haberhauer, G. and Gerzabek, M. H. (1999) 'Drift and transmission FT-IR spectroscopy of forest soils: an approach to determine decomposition processes of forest litter', *Vibrational Spectroscopy*, 19, (2), pp. 413-417.
- Hair, J. F., Black, W. C., Babin, B. J., Anderson, R. E. and Tatham, R. L. (2006) *Multivariate Data Analysis*. New Jersey: Pearson Prince Hall.
- Hallett, D. (2002) *Petroleum Geology of Libya*. Amsterdam: Elsevier.
- Hammami, A., Chang-Yen, D., Nighswander, J. A. and Stange, E. (1995) 'An experimental study of the effect of paraffinic solvents on the onset and bulk precipitation of asphaltenes', *Fuel Science and Technology International*, 13, (9), pp. 1167 - 1184.
- Hammami, A., Ferworn, K. A., Nighswander, J. A., OverĚš, S. and Stange, E. (1998) 'Asphaltenic Crude Oil Characterization: An Experimental Investigation of the Effect of Resins on the Stability of Asphaltenes', *Petroleum Science and Technology*, 16, (3), pp. 227 - 249.
- Hammami, A. and Ratulowski, J. (2007) 'Precipitation and Deposition of Asphaltenes in Production Systems: A flow Assurance Overview', in Mullins, O. C., Sheu, E. Y., Hammami, A. and Marshall, A. G.(eds) *Asphaltenes, Heavy Oils, and Petroleomics*. New York: Springer Science, pp. 617 - 660.
- Hayward, R. D., Martin, C. A. L., Harrison, D., Van Dort, G., Guthrie, S. and Padget, N. (2003) 'The Flora Field, Blocks 31/26a, 31/26c, UK North Sea', in Gluyas, J. G. and Hitchens, H. M.(eds) *United Kingdom Oil and Gas Fields, Commemorative Millenium Volume*. Vol. Memoir, 20 London: Geological Society, pp. 549 - 555.
- Herod, A. A., Bartle, K. D. and Kandiyoti, R. (2008) 'Comment on a Paper by Mullins, Martinez-Haya, and Marshall "Contrasting Perspective on Asphaltene Molecular Weight. This Comment vs the Overview of A. A. Herod, K. D. Bartle, and R. Kandiyoti"', *Energy & Fuel*, 22, pp. 4312-4317.

- Hofmann, P., Ricken, W., Schwark, L. and Leythaeuser, D. (2000) 'Carbon-sulfur-iron relationships and $\delta^{13}\text{C}$ of organic matter for late Albian sedimentary rocks from the North Atlantic Ocean: paleoceanographic implications', *Palaeogeography, Palaeoclimatology, Palaeoecology*, 163, (3-4), pp. 97-113.
- Holmgren, A. and Nord, B. (1988) 'Characterization of Peat Samples by Diffuse Reflectance FT-IR Spectroscopy', *Applied Spectroscopy*, 42, pp. 255-262.
- Honigs, D. E., Hirschfeld, T. B. and Hieftje, G. M. (1985) 'Near-Infrared Determination of Several Physical Properties of Hydrocarbons', *Analytical Chemistry*, 57, (2), pp. 443-445.
- Hughes, W. B. (1984) 'Use of thiophenic organosulfur compounds in characterizing crude oils derived from carbonate versus siliciclastic sources', in Palacas, J. G.(ed), *Petroleum Geochemistry and Source Rock Potential of Carbonate Rocks*. Tulsa, OK: American Association of Petroleum Geoscientists, pp. 181 - 196.
- Hunt, J. M. (1995) *Petroleum geochemistry and geology* New York W. H. Freeman
- Ibarra, J., Muñoz, E. and Moliner, R. (1996) 'FTIR study of the evolution of coal structure during the coalification process', *Organic Geochemistry*, 24, (6-7), pp. 725-735.
- Ikeya, Ishida, Ohtani, Yamamoto and Watanabe. (2007) 'Analysis of polynuclear aromatic and aliphatic components in soil humic acids using ruthenium tetroxide oxidation', *European Journal of Soil Science*, 58, pp. 1050-1061.
- Ilisley, W. H., Zingaro, R. A. and Zoeller Jr, J. H. (1986a) 'The reactivity of ruthenium tetroxide towards aromatic and etheric functionalities in simple organic compounds', *Fuel*, 65, (9), pp. 1216-1220.
- Ilisley, W. H., Zingaro, R. A. and Zoeller Jr., J. H. (1986b) 'The reactivity of ruthenium tetroxide towards aromatic and etheric functionalities in simple organic compounds', *Fuel*, 65, pp. 1216 - 1220.
- Innes, H. E., Bishop, A. N., Fox, P. A., Head, I. M. and Farrimond, P. (1998) 'Early diagenesis of bacteriohopanoids in Recent sediments of Lake Pollen, Norway', *Organic Geochemistry*, 29, (5-7), pp. 1285-1295.
- Innes, H. E., Bishop, A. N., Head, I. M. and Farrimond, P. (1997) 'Preservation and diagenesis of hopanoids in Recent lacustrine sediments of Priest Pot, England', *Organic Geochemistry*, 26, (9-10), pp. 565-576.
- Jaffe, R., Albrecht, P. and Oudin, J.-L. (1988) 'Carboxylic acids as indicators of oil migration--I. Occurrence and geochemical significance of C-22 diastereoisomers of the (17[β]H,21[β]H) C30 hopanoic acid in geological samples', *Organic Geochemistry*, 13, (1-3), pp. 483-488.
- Jennings, D. W. and Weispfennig, K. (2005) 'Experimental solubility data of various n-alkane waxes: effects of alkane chain length, alkane odd versus even carbon number structures, and solvent chemistry on solubility', *Fluid Phase Equilibria*, 227, (1), pp. 27-35.
- Jones, C. W. (1999) *Applications of Hydrogen peroxide and Derivatives*. Cambridge, UK: Royal Society of Chemistry.

- Jones, D. M., Douglas, A. G. and Connan, J. (1988) 'Hydrous pyrolysis of asphaltenes and polar fractions of biodegraded oils', *Organic Geochemistry*, 13, (4-6), pp. 981-993.
- Jones, D. M., Watson, J. S., Meredith, W., Chen, M. and Bennett, B. (2001) 'Determination of Naphthenic Acids in Crude Oils Using Nonaqueous Ion Exchange Solid-Phase Extraction', *Anal. Chem.*, 73, (3), pp. 703-707.
- Kasai, M. and Ziffer, H. (1983) 'Ruthenium tetroxide catalyzed oxidations of aromatic and heteroaromatic rings', *J. Org. Chem.*, 48, (14), pp. 2346-2349.
- Khadim, M. and Sarbar, M. (1999) 'Role of asphaltene and resin in oil field emulsion', *Journal of Petroleum Science and Engineering*, 23, pp. 213 - 221.
- Killops, S. and Killops, V. (2005) *Introduction to Organic Geochemistry*. Oxford: Blackwell Publishing.
- Kitson, F. G., Larsen, B. S. and McEwen, C. N. (1996) *Gas Chromatography and Mass Spectrometry: A Practical Guide*. San Diego: Academic Press.
- Knapp, D. R. (1979) *Handbook of Analytical Derivatization Reactions*. New York: John Wiley & Sons.
- Kokal, S. L. and Sayegh, S. G. (1995) 'Asphaltene: The Cholesterol of Petroleum', *SPE*, Paper 29787, pp. 169 - 181.
- Krooss, B. M., Brothers, L. and Engel, M. H. (1991) 'Geochromatography in petroleum migration: a review', *Geological Society, London, Special Publications*, 59, (1), pp. 149-163.
- Kuehn, D. W., Davis, A. and Painter, P. C. (1984) 'Relationships Between the Organic Structure of Vitrinite and Selected Parameters of Coalification and indicated by Fourier Transform IR Spectra', in Winans, R. E. and Crelling, J. C.(eds) *Chemistry and Characterization of Coal Macerals*. Washington, D.C.: American Chemical Society, pp. 99 - 120.
- Kunka, J. M., Williams, G., Cullen, B., Boyd-Gorst, J., Dyer, G. R., Garnham, J. A., Warnock, A., Wardell, J., Davis, A. and Lynes, P. (2003) 'The Nelson Field, Blocks 22/11, 22/6a, 22/7, 22/12a, UK North Sea', in Gluyas, J. G. and Hitchens, H. M.(eds) *Uninted Kingdom Oil and Gas Fields, Commemorative Millenium Volume*. Vol. Memoir, 20 London: Geological Society pp. 617 - 646.
- Lambert, J. B. and Mazzola, E. P. (2003) *Nuclear Magnetic Resonance Spectroscopy: An Introduction to Principles, Applications, and Experimental Methods*. New Jersey: Pearson Education Inc.
- Lamontagne, J., Dumas, P., Mouillet, V. and Kister, J. (2001) 'Comparison by Fourier transform infrared (FTIR) spectroscopy of different ageing techniques: application to road bitumens', *Fuel*, 80, (4), pp. 483-488.
- Langford, F. F. and Blanc-Valleron, M. M. (1990) 'Interpreting Rock-Eval pyrolysis data using of pyrolyzable hydrocarbons vs. total organic carbon.', *AAPG Bull.*, 74, pp. 799-804.

- Laszlo, P. (1990) 'Catalysis of organic reactions by inorganic solids', *Pure Appl. Chem.*, 62, (10), pp. 2027-2030.
- Lee, D. G. and Spitzer, U. A. (1969) 'Oxidation of ethylbenzene with aqueous sodium dichromate', *J. Org. Chem.*, 34, (5), pp. 1493-1495.
- Lee, D. G. and van den Engh, M. (1973) 'The Oxidation of Organic Compounds by Ruthenium Tetroxide', in Trahanovsky, W. S.(ed), *Oxidation in Organic Chemistry Part B*. Vol. 5 New York: Academic Press, pp. 177 -227.
- Leon, O., Rogel, E., Espidel, J. and Torres, G. (2000) 'Asphaltenes: Structural Characterization, Self-Association, and Stability Behavior', *Energy Fuels*, 14, (1), pp. 6-10.
- Leonard, J., Lygo, B. and Procter, G. (1995) *Advanced practical organic chemistry*. Glasgow: Blackie Academic & Professional.
- Leventhal, J. S. (1995) 'Carbon-sulfur plots to show diagenetic and epigenetic sulfidation in sediments', *Geochimica et Cosmochimica Acta*, 59, pp. 1207 – 1211.
- Li, C., Peng, P., Sheng, G. and Fu, J. (2004) 'A study of a 1.2 Ga kerogen using Ru ion-catalyzed oxidation and pyrolysis–gas chromatography–mass spectrometry: structural features and possible source', *Organic Geochemistry*, 35, pp. 531 – 541.
- Li, M., Yao, H., Stasiuk, L. D., Fowler, M. G. and Larter, S. R. (1997) 'Effect of maturity and petroleum expulsion on pyrrolic nitrogen compound yields and distributions in Duvernay Formation petroleum source rocks in central Alberta, Canada', *Organic Geochemistry*, 26, (11-12), pp. 731-744.
- Liao, Z. and Geng, A. (2002) 'Characterization of nC7-soluble fractions of the products from mild oxidation of asphaltenes', *Organic Geochemistry*, 33, (12), pp. 1477-1486.
- Liao, Z., Geng, A., Graciaa, A., Creux, P., Chrostowska, A. and Zhang, Y. (2006a) 'Saturated hydrocarbons occluded inside asphaltene structures and their geochemical significance, as exemplified by two Venezuelan oils', *Organic Geochemistry*, 37, (3), pp. 291-303.
- Liao, Z., Graciaa, A., Geng, A., Chrostowska, A. and Creux, P. (2006b) 'A new low-interference characterization method for hydrocarbons occluded inside asphaltene structures', *Applied Geochemistry*, 21, pp. 833 – 838.
- Liao, Z., Zhou, H., Graciaa, A., Chrostowska, A., Creux, P. and Geng, A. (2005) 'Adsorption/Occlusion Characteristics of Asphaltenes: Some Implication for Asphaltene Structural Features', *Energy & Fuels*, 19, (1), pp. 180-186.
- Lochte, H. L. and Littman, E. R. (1955) *The Petroleum Acids and Bases*. New York: Chemical Publishing Co. Inc.
- Long, R. B. (1981) 'The Concept of Asphaltenes', in Bunger, J. W. and Li, N. C.(eds) *Chemistry of Asphaltenes*. Washington D.C.: American Chemical Society.

- Lüning, S., Craig, J., Loydell, D. K., Štorch, P. and Fitches, B. (2000) 'Lower Silurian 'hot shales' in North Africa and Arabia: regional distribution and depositional model', *Earth Science Reviews*, 49, pp. 121 - 200.
- Ma, A., Zhang, S. and Zhang, D. (2008) 'Ruthenium-ion-catalyzed oxidation of asphaltenes of heavy oils in Lunnan and Tahe oilfields in Tarim Basin, NW China', *Organic Geochemistry*, 39, (11), pp. 1502-1511.
- Mackenzie, A. S., Brassell, S. C., Eglinton, G. and Maxwell, J. R. (1982) 'Chemical Fossils: The Geological Fate of Steroids ', *Science*, 217, pp. 491-504.
- Maddams, W. F. (1980) 'The Scope and Limitations of Curve Fitting', *Applied Spectroscopy*, 34, pp. 245-267.
- McCarthy, R. D. and Duthie, A. H. (1962) 'A rapid quantitative method for the separation of free fatty acids from other lipids', *J. Lipid Res.*, 3, (1), pp. 117-119.
- McKirdy, D. M., Aldridge, A. K. and Ypma, P. J. M. (1983) 'A geochemical comparison of some oils from Pre-Ordovician carbonate rocks', in Bjorøy, M., Albrecht, P. and Cornford, C.(eds) *Advances in organic geochemistry, 1981* New York: John Wiley & Sons, pp. 99 - 107.
- Melchiorre, J. J., Moyer, H. R. and Christman, L. J. (1965) '2,6-Naphthalenedicarboxylic Acid and Other Aromatic Acids via Nitrogen Dioxide-Selenium Oxidations', in *Selective Oxidation Processes*. Washington, D.C.: American Chemical Society, pp. 89-98.
- Mitra-Kirtley, S. and Mullins, O. C. (2007) 'Sulfur Chemical Moieties in Carbonaceous Materials', in Mullins, O. C., Sheu, E. E., Hammami, A. and Marshall, A. G.(eds) *Asphaltenes, Heavy Oils, and Petroleomics*. New York: Springer Science, pp. 157 - 188.
- Mitra-Kirtley, S., Mullins, O. C., Branthaver, J. F. and Cramer, S. P. (1993a) 'Nitrogen chemistry of kerogens and bitumens from x-ray absorption near-edge structure spectroscopy', *Energy & Fuels*, 7, (6), pp. 1128-1134.
- Mitra-Kirtley, S., Mullins, O. C., Van Elp, J., George, S. J., Chen, J. and Cramer, S. P. (1993b) 'Determination of the nitrogen chemical structures in petroleum asphaltenes using XANES spectroscopy', *J. Am. Chem. Soc.*, 115, (1), pp. 252-258.
- Mohamed, R. S., Ramos, A. C. S. and Loh, W. (1999) 'Aggregation Behavior of Two Asphaltenic Fractions in Aromatic Solvents', *Energy & Fuels*, 13, (2), pp. 323-327.
- Mojelsky, T. W., Ignasiak, T. M., Frakman, Z., McIntyre, D. D., Lown, E. M., Montgomery, D. S. and Strausz, O. P. (1992) 'Structural features of Alberta oil sand bitumen and heavy oil asphaltenes', *Energy & Fuels*, 6, (1), pp. 83-96.
- Moldowan, J. M., Peters, K. E., Carlson, R. M. K., Schoell, M. and Abu-Ali, M. A. (1994) 'Diverse applications of petroleum biomarker maturity parameters', *Arabian Journal for Science and Engineering*, 19, pp. 273 - 298.
- Moldowan, J. M., Seifert, W. K., Arnold, E. and Clardy, J. (1984) 'Structure proof and significance of stereoisomeric 28,30-bisnorhopanes in petroleum and petroleum source rocks', *Geochimica et Cosmochimica Acta*, 48, (8), pp. 1651-1661.

- Moldowan, J. M., Seifert, W. K. and Gallegos, E. J. (1985) 'Relationship between petroleum composition and depositional environment of petroleum source rocks', *AAPG Bulletin*, 69, (8), pp. 1255-1268.
- Moldowan, J. M., Sundararaman, P. and Schoell, M. (1986) 'Sensitivity of biomarker properties to depositional environment and/or source input in the Lower Toarcian of SW-Germany', *Organic Geochemistry*, 10, (4-6), pp. 915-926.
- Morgan, T. J., George, A., Alvarez, P., Herod, A. A., Millan, M. and Kandiyoti, R. (2009) 'Isolation of Size Exclusion Chromatography Elution-Fractions of Coal and Petroleum-Derived Samples and Analysis by Laser Desorption Mass Spectrometry', *Energy & Fuels*.
- Muhammad, A. B. (2004) *Organic Geochemistry of Batra Formation* thesis. Newcastle University.
- Mujica, V., Nieto, P., Puerta, L. and Acevedo, S. (2000) 'Caging of molecules by asphaltenes. A model for free radical preservation in crude oils', *Energy & Fuel*, 14, pp. 632–639.
- Mullins, C. O. (2007) 'Petroleomics and Structure-Function Relations of Crude Oils and Asphaltenes', in Mullins, O. C., Shue, E. Y., Hammami, A. and Marshall, A. G.(eds) *Asphaltenes, Heavy Oils, and Petroleomics*. New York: Springer Science, pp. 1 - 16.
- Mullins, O. C. (1990) 'Asphaltenes in crude oil: absorbers and/or scatterers in the near-infrared region?', *Analytical Chemistry*, 62, (5), pp. 508-514.
- Mullins, O. C. (2009) 'Rebuttal to Strausz et al. Regarding Time-Resolved Fluorescence Depolarization of Asphaltenes', *Energy & Fuels*, 23, (5), pp. 2845-2854.
- Mullins, O. C., Martinez-Haya, B. and Marshall, A. G. (2008) 'Contrasting Perspective on Asphaltene Molecular Weight. This Comment vs the Overview of A. A. Herod, K.D. Bartle, and R. Kandiyoti', *Energy & Fuel*, 22, pp. 1765 - 1773.
- Mullins, O. C., Shue, E. Y. and Marshall, A. G. (eds.) (2007) *Asphaltenes, Heavy Oils, and Petroleomics*. New York: Springer.
- Murphy, M. T. J. (1969) 'Analytical methods', in Eglinton, G. and Murphy, M. T. J.(eds) *Organic Geochemistry*. Berlin: Springer, pp. 74–88.
- Murphy, P. D., Gerstein, B. C., Weinberg, V. L. and Yen, T. F. (1982) 'Determination of Chemical Functionality in Asphaltenes by High-Resolution Solid-state Carbon- 13 Nuclear Magnetic Resonance Spectrometry', *Anal. Chem.*, 54, pp. 522-525.
- N'guessan, A., Carignan, T. and Nyman, M. (2004) 'Optimization of the Peroxy Acid Treatment of r-Methylnaphthalene and Benzo[a]pyrene in Sandy and Silty-Clay Sediments', *Environ. Sci. Technol.*, 38, pp. 1554 - 1560.
- N'guessan, A. L., Alderman, N. S., O'Connor, K., Abdul Rahim, A. Z. and Nyman, M. C. (2006) 'Peroxy-acid treatment of selected PAHs in sediments', *International Journal of Environment and Waste Management*, 1, pp. 61 - 74.
- Nakanishi, K. (1962) *Infrared Absorption Spectroscopy*. Tokyo: Nankodo Co Ltd.

- Nara, F., Tani, Y., Soma, Y., Soma, M., Naraoka, H., Watanabe, T., Horiuchi, K., Kawai, T., Oda, T. and Nakamura, T. (2005) 'Response of phytoplankton productivity to climate change recorded by sedimentary photosynthetic pigments in Lake Hovsgol (Mongolia) for the last 23,000 years', *Quaternary International*, 136, (1), pp. 71-81.
- Narender, N., Mohan, K. V. V. K., Kulkarni, S. J. and Reddy, I. A. K. (2006) 'Liquid phase benzylation of benzene and toluene with benzyl alcohol over modified zeolites', *Catalysis Communications*, 7, (8), pp. 583-588.
- Neves, G. B. M., De Sousa, M. D. A., Travalloni-Louvisse, A. M., Lucas, E. F. and González, G. (2001) 'Characterization of Asphaltene Particles by Light Scattering and Electrophoresis', *Petroleum Science and Technology*, 19, pp. 35 – 43.
- Nimmagadda, R. D. and McRae, C. (2006a) 'A novel reduction of polycarboxylic acids into their corresponding alkanes using n-butylsilane or diethylsilane as the reducing agent', *Tetrahedron Letters*, 47, (21), pp. 3505-3508.
- Nimmagadda, R. D. and McRae, C. (2006b) 'A novel reduction reaction for the conversion of aldehydes, ketones and primary, secondary and tertiary alcohols into their corresponding alkanes', *Tetrahedron Letters*, 47, (32), pp. 5755-5758.
- Nimmagadda, R. D. and McRae, C. (2007) 'Characterisation of the backbone structures of several fulvic acids using a novel selective chemical reduction method', *Organic Geochemistry*, 38, (7), pp. 1061-1072.
- Oh, K., Oblad, S. C., Hanson, F. V. and Deo, M. D. (2003) 'Examination of Asphaltenes Precipitation and Self-Aggregation', *Energy & Fuels*, 17, (2), pp. 508-509.
- Painter, P. C., Snyder, R. W., Starsinic, M., Coleman, M. M., Kuehn, D. W. and Davis, A. (1981) 'Concerning the Application of FT-IR to the Study of Coal: A Critical Assessment of Band Assignments and the Application of Spectral Analysis Programs', *Applied Spectroscopy*, 35, pp. 475-485.
- Pan, C., Geng, A., Liao, Z., Xiong, Y., Fu, J. and Sheng, G. (2002) 'Geochemical characterization of free versus asphaltene-sorbed hydrocarbons in crude oils: implications for migration-related compositional fractionations', *Marine and Petroleum Geology*, 19, (5), pp. 619-632.
- Peng, P., Fu, J., Sheng, G., Morales-Izquierdo, A., Lown, E. M. and Strausz, O. P. (1999a) 'Ruthenium-Ions-Catalyzed Oxidation of an Immature Asphaltene: Structural Features and Biomarker Distribution', *Energy & Fuels*, 13, (2), pp. 266-277.
- Peng, P., Morales-Izquierdo, A., Hogg, A. and Strausz, O. P. (1997) 'Molecular Structure of Athabasca Asphaltene: Sulfide, Ether, and Ester Linkages', *Energy & Fuels*, 11, (6), pp. 1171-1187.
- Peng, P., Morales-Izquierdo, A., Lown, E. M. and Strausz, O. P. (1999b) 'Chemical Structure and Biomarker Content of Jinghan Asphaltenes and Kerogens', *Energy & Fuels*, 13, (2), pp. 248-265.

- Pereira, J. C., Lopez, I., Salas, R., Silva, F., Fernandez, C., Urbina, C. and Lopez, J. C. (2007) 'Resins: The Molecules Responsible for the Stability/Instability Phenomena of Asphaltene', *Energy & Fuels*, 21, (3), pp. 1317-1321.
- Permanyer, A., Douifi, L., Dupuy, N., Lahcini, A. and Kister, J. (2005) 'FTIR and SUVF spectroscopy as an alternative method in reservoir studies. Application to Western Mediterranean oils', *Fuel*, 84, (2-3), pp. 159-168.
- Peters, K. E. (1986) 'Guidelines for evaluating petroleum source rock using programmed pyrolysis.', *AAPG Bulletin*, 70, pp. 318 - 329.
- Peters, K. E. and Moldowan, J. M. (1991) 'Effects of source, thermal maturity, and biodegradation on the distribution and isomerization of homohopanes in petroleum', *Organic Geochemistry*, 17, (1), pp. 47-61.
- Peters, K. E., Moldowan, J. M., Schoell, M. and Hemphkins, W. B. (1986) 'Petroleum isotopic and biomarker composition related to source rock organic matter and depositional environment', *Organic Geochemistry*, 10, (1-3), pp. 17-27.
- Peters, K. E., Walters, C. C. and Moldowan, J. M. (2005a) *The Biomarker Guide: Biomarker and Isotopes in Petroleum Exploration and Earth History*. Cambridge: Cambridge University Press.
- Peters, K. E., Walters, C. C. and Moldowan, J. M. (2005b) *The Biomarker Guide: Biomarkers and Isotopes in the Environment and Human History*. Cambridge: Cambridge University Press.
- Petersen, H. I., Rosenberg, P. and Nytoft, H. P. (2008) 'Oxygen groups in coals and alginite-rich kerogen revisited', *International Journal of Coal Geology*, 74, (2), pp. 93-113.
- Pinnock, S. J. and Clitheroe, A. R. J. (2003) 'The Captain Field, Block 13/22a, UK North Sea', in Gluyas, J. G. and Hitchens, H. M. (eds) *United Kingdom Oil and Gas Fields, Commemorative Millennium Volume*. Vol. Memoir, 20 London: Geological Society, pp. 431 - 441.
- Radke, M., Willsch, H., Leythaeuser, D. and Teichmüller, M. (1982) 'Aromatic components of coal: relation of distribution pattern to rank', *Geochimica et Cosmochimica Acta*, 46, (10), pp. 1831-1848.
- Ramljak, Z., Solc, A., Arpino, P., Schmitter, J. M. and Guiochon, G. (1977) 'Separation of acids from asphalts', *Anal. Chem.*, 49, (8), pp. 1222-1225.
- Rangel, A., Parra, P. and Niño, C. (2000) 'The La Luna formation: chemostratigraphy and organic facies in the Middle Magdalena Basin', *Organic Geochemistry*, 31, (12), pp. 1267-1284.
- Rohmer, M., Bouvier-Nave, P. and Ourisson, G. (1984) 'Distribution of hopanoid triterpenes in prokaryotes', *Journal of General Microbiology* 130, pp. 1137-1150.
- Rouxhet, P. G., Robin, P. L. and Nicaise, G. (1980) 'Characterization of kerogens and their evolution by infrared spectroscopy', in Durand, B. (ed), *Kerogen: Insoluble organic matter from sedimentary rocks*. Paris: Technip, pp. 163 - 190.

- Rubinstein, I., Sieskind, O. and Albrecht, P. (1975) 'Rearranged Sterenes in a Shale : Occurrence and Simulated Formation', *J. Chem. Soc., Perkin Trans. 1*, pp. 1833 - 1836.
- Rullkotter, J. and Michaelis, W. (1990) 'The structure of kerogen and related materials. A review of recent progress and future trends', *Organic Geochemistry*, 16, (4-6), pp. 829-852.
- Rullkötter, J. and Wendisch, D. (1982) 'Microbial alteration of 17 α (H)-hopanes in Madagascar asphalts: removal of C-10 methyl group and ring opening', *Geochimica et Cosmochimica Acta*, 46, (9), pp. 1545-1553.
- Saniere, A., Henaut, I. and Argillier, J. F. (2004) 'Pipeline transportation of heavy oils, a strategic, economic and technological challenge', *Oil & Gas Science and Technology- Revue De L Institut Francais Du Petrole*, 59, (5), pp. 455-466.
- Sarkawi, I., Abeger, G., Tornero, J. L. and Abushaala, E. (2007) 'The Murzuq Basin, Libya - A Proven Petroleum System', *3rd North African/Mediterranean Petroleum & Geosciences Conference & Exhibition*. Dath El-Imad Complex, Libya, February 26, 2007 to February 28, 2007. European Association of Geoscientist and Engineers, pp.
- Satya, S., Roehner, R. M., Deo, M. D. and Hanson, F. V. (2007) 'Estimation of Properties of Crude Oil Residual Fractions Using Chemometrics', *Energy & Fuels*, 21, (2), pp. 998-1005.
- Savitzky, A. and Golay, M. J. E. (1964) 'Smoothing and Differentiation of Data by Simplified Least Squares Procedures', *Analytical Chemistry*, 36, (8), pp. 1627-1639.
- Scalan, E. S. and Smith, J. E. (1970) 'An improved measure of the odd-even predominance in the normal alkanes of sediment extracts and petroleum', *Geochimica et Cosmochimica Acta*, 34, (5), pp. 611-620.
- Seifert, W. K. and Moldowan, J. M. (1980) 'The effect of thermal stress on source-rock quality as measured by hopane stereochemistry', *Physics and Chemistry of The Earth*, 12, pp. 229-237.
- Seifert, W. K. and Moldowan, J. M. (1986) 'Use of biological markers in petroleum exploration', in Johns, R. B.(ed), *Methods in Geochemistry and Geophysics*. Vol. 24 Amsterdam: Elsevier, pp. 261-290.
- Sfini, H. and Legrand, A. P. (1990) 'Qualitative and quantitative aspects of solid-state nuclear magnetic resonance spectroscopy measurements in coals', in Charcosset, H.(ed), *Advanced Methodologies in coal caharacterisation*. Amsterdam: Elsevier, pp. 115-133.
- Shedid, S. A. and Zekri, A. Y. (2006) 'Formation Damage Caused by Simultaneous Sulfur and Asphaltene Deposition', *SPE*, Paper 86553, pp. 58 - 64.
- Shepherd, M., MacGregor, A., Bush, K. and Wakefield, J. (2003) 'The Fife and Fergus Fields, Block 31/26a, UK North Sea', in Gluyas, J. G. and Hitchens, H. M.(eds) *United Kingdom Oil and Gas Fields, Commemorative Millenium Volume*. Vol. Memoir, 20 London: Geological Society, pp. 537 - 547.

- Sheu, E. Y. (2002) 'Petroleum Asphaltene-Properties, Characterization, and Issues', *Energy & Fuels*, 16, (1), pp. 74-82.
- Sheu, E. Y. and Mullins, O. C. (eds.) (1995) *Asphaltenes: Fundamentals and Applications*. New York: Plenum Press.
- Shue, E. Y. and Storm, D. A. (1995) 'Colloidal properties of asphaltenes in organic systems', in Shue, E. Y. and Mullins, O. C.(eds) *Asphaltenes: Fundamentals and Applications*.New York: Plenum Press, pp. 1 - 52.
- Sieskind, O., Joly, G. and Albrecht, P. (1979) 'Simulation of the geochemical transformations of sterols: superacid effect of clay minerals', *Geochimica et Cosmochimica Acta*, 43, (10), pp. 1675-1679.
- Singleton, K. E., Cooks, R. G., Wood, K. V., Tse, K. T. and Stock, L. (1985) 'Insights into coal structure from degradation with ruthenium tetroxide and tandem mass spectrometry', *Analytica Chimica Acta*, 174, pp. 211-223.
- Sinninghe Damste, J. S. and De Leeuw, J. W. (1990) 'Analysis, structure and geochemical significance of organically-bound sulphur in the geosphere: State of the art and future research', *Organic Geochemistry*, 16, (4-6), pp. 1077-1101.
- Sinninghe Damsté, J. S., Kenig, F., Koopmans, M. P., Köster, J., Schouten, S., Hayes, J. M. and de Leeuw, J. W. (1995a) 'Evidence for gammacerane as an indicator of water column stratification', *Geochimica et Cosmochimica Acta*, 59, (9), pp. 1895-1900.
- Sinninghe Damsté, J. S., Van Duin, A. C. T., Hollander, D., Kohnen, M. E. L. and De Leeuw, J. W. (1995b) 'Early diagenesis of bacteriohopanepolyol derivatives: Formation of fossil homohopanoids', *Geochimica et Cosmochimica Acta*, 59, (24), pp. 5141-5157.
- Smith, B. C. (1996) *Fundamentals of Fourier Transform Infrared Spectroscopy*. Florida: CRC Press LLC.
- Smith, L. G. (1991) 'Principal Component Analysis: An Introduction', *Analytical Proceedings*, 28, pp. 150 - 151.
- Socrates, G. (1980) *Infrared Characteristic Group Frequencies: Tables and Charts*. Chichester: John Wiley & Sons.
- Special, O. (1998) 'Worldwide Production Survey', *Oil & Gas Journal*, 96, (52), pp. 40 - 68.
- Speight, J. G. (1984) 'The Chemical Nature of Petroleum Asphaltenes', in *Characterisation of Heavy Crude Oils and Petroleum Residues*.Paris: Editions Technip, pp. 32 - 41.
- Speight, J. G. (1999) *The Chemistry and Technology of Petroleum*. New York: CRC.
- Speight, J. G. (2004) 'Petroleum Asphaltenes - Part 1: Asphaltenes, Resins and the Structure of Petroleum', *Oil & Gas Science and Technology*, 59, (5), pp. 467-477.
- Speight, J. G. and Moschopedis, S. E. (1981) 'On the Molecular Nature of Petroleum Asphaltenes', in Bunger, J. W. and Li, N. C.(eds) *Chemistry of Asphaltenes*.Washington D.C.: American Chemical Society, pp. 1 – 15.

- Standen, G., Boucher, R. J., Rafalska-Bloch, J. and Eglinton, G. (1991) 'Ruthenium tetroxide oxidation of natural organic macromolecules: Messel kerogen', *Chemical Geology*, 91, (4), pp. 297-313.
- Stewart, R. (1965) 'Oxidation by Permanganate', in Wiberg, K. B.(ed), *Oxidation in Organic Chemistry Part A*. Vol. 5 New York: Academic Press, pp. 443.
- Stock, L. M. and Tse, K. T. (1983) 'Ruthenium tetroxide catalysed oxidation of Illinois No. 6 coal and some representative hydrocarbons', *Fuel*, 62, pp. 974 - 975.
- Stock, L. M. and Wang, S.-H. (1986) 'Ruthenium tetroxide catalysed oxidation of coals : The formation of aliphatic and benzene carboxylic acids', *Fuel*, 65, (11), pp. 1552-1562.
- Stojanovic, K., Jovancicevic, B., Sajnovic, A., Sabo, T. J., Vitorovic, D., Schwarzbauer, J. and Golovko, A. (2009) 'Pyrolysis and Pt(IV)- and Ru(III)-ion catalyzed pyrolysis of asphaltenes in organic geochemical investigation of a biodegraded crude oil (Gaj, Serbia)', *Fuel*, 88, (2), pp. 287-296.
- Strausz, O. P., Mojelsky, T. W., Faraji, F., Lown, E. M. and Peng, P. (1999a) 'Additional Structural Details on Athabasca Asphaltene and Their Ramifications', *Energy & Fuels*, 13, (2), pp. 207-227.
- Strausz, O. P., Mojelsky, T. W., Lown, E. M., Kowalewski, I. and Behar, F. (1999b) 'Structural Features of Boscan and Duri Asphaltenes', *Energy & Fuels*, 13, (2), pp. 228-247.
- Strausz, O. P., Safarik, I., Lown, E. M. and Morales-Izquierdo, A. (2008) 'A Critique of Asphaltene Fluorescence Decay and Depolarization-Based Claims about Molecular Weight and Molecular Architecture', *Energy & Fuels*, 22, (2), pp. 1156-1166.
- Su, Y., Artok, L., Murata, S. and Nomura, M. (1998) 'Structural Analysis of the Asphaltene Fraction of an Arabian Mixture by a Ruthenium-Ion-Catalyzed Oxidation Reaction', *Energy & Fuels*, 12, (6), pp. 1265-1271.
- Sullivan, M. J. and Maciel, G. E. (1982) 'Structural resolution in the carbon-13 nuclear magnetic resonance spectrometric analysis of coal by cross polarization and magic-angle spinning', *Analytical Chemistry*, 54, pp. 1606 - 1615.
- Summons, R. E. and Capon, R. J. (1988) 'Fossil steranes with unprecedented methylation in ring-A', *Geochimica et Cosmochimica Acta*, 52, (11), pp. 2733-2736.
- Tabachnick, B. G. and Fidell, L. S. (2007) *Using Multivariate Statistics*. Boston: Pearson Education, Inc.
- Tabachnick, B. G. and Fidell, L. S. (2007) *Using Multivariate Statistics*. Boston: Pearson Education Inc.
- Talbot, H. M. and Farrimond, P. (2007) 'Bacterial populations recorded in diverse sedimentary bihopanoid distributions', *Organic Geochemistry*, 38, (8), pp. 1212-1225.

- Talbot, H. M., Summons, R. E., Jahnke, L. L., Cockell, C. S., Rohmer, M. and Farrimond, P. (2008) 'Cyanobacterial bacteriohopanepolyol signatures from cultures and natural environmental settings', *Organic Geochemistry*, 39, (2), pp. 232-263.
- Tekely, P., Nicole, D. and Delpuech, J. J. (1990) 'Heterogeneity of structure and motion in coals as revealed by ¹³C CP/MAS NMR', in Charcosset, H.(ed), *Advanced Methodologies in coal characterisation*. Amsterdam: Elsevier, pp. 135-147.
- Ten Haven, H. L., De Leeuw, J. W. and Sinninghe Damste, J. S. (1988) 'Application of biological markers in the recognition of palaeohypersaline environments', in Fleet, A. J., Kelts, K. R. and Talbot, M. R.(eds) *Lacustrine petroleum source rocks*. Oxford: Blackwell Scientific Publications for the Geological Society, pp. 123 - 130.
- Ten Haven, H. L., Rohmer, M., Rullkötter, J. and Bisseret, P. (1989) 'Tetrahymanol, the most likely precursor of gammacerane, occurs ubiquitously in marine sediments', *Geochimica et Cosmochimica Acta*, 53, (11), pp. 3073-3079.
- Terken, J. M. J. (1999) 'The Natih Petroleum System of North Oman', *GeoArabia*, 4, (2), pp. 157-180.
- Tissot, B. P. and Welte, D. H. (1984) *Petroleum formation and occurrence*. Berlin: Heidelberg: Springer-Verlag.
- Trifilieff, S., Sieskind, O. and Albrecht, P. (1992) 'Biological markers in petroleum asphaltenes: possible mode of incorporation', in Moldowan, J. M., Albrecht, P. and Philp, R. P.(eds) *Biological markers in sediments and petroleum*. New Jersey: Prentice Hall, pp. 350 - 369.
- Turner, B. R. and Richardson, D. (2004) 'Geological controls on the sulphur content of coal seams in the Northumberland Coalfield, Northeast England', *International Journal of Coal Geology*, 60, (2-4), pp. 169-196.
- Tyson, R. V. and Pearson, T. H. (1991) 'Modern and ancient continental shelf anoxia: an overview', in Tyson, R. V. and Pearson, T. H.(eds) *Modern and Ancient Continental Shelf Anoxia*. Vol. Geological Society Publication No 58 London: Geological Society, pp. 1 – 24.
- Tyson, R. V., Wilson, R. C. L. and Downie, C. (1979) 'A stratified water column environmental model for the type Kimmeridge Clay', *Nature*, 277, (5695), pp. 377-380.
- Vassallo, A. M., Wilson, M. A., Collin, P. J., Malcolm Oades, J., Waters, A. G. and Malcolm, R. L. (1987) 'Structural analysis of geochemical samples by solid-state nuclear magnetic resonance spectrometry. Role of paramagnetic material', *Anal. Chem.*, 59, (4), pp. 558–562.
- Venkatesan, M. I. (1989) 'Tetrahymanol: Its widespread occurrence and geochemical significance', *Geochimica et Cosmochimica Acta*, 53, (11), pp. 3095-3101.
- Vitorović, D. (1980) 'Structure elucidation of kerogen by chemical methods', in Durand, B.(ed), *Kerogen: Insoluble Organic Matter from Sedimentary Rocks*. Paris: Éditions Technip, pp. 301 - 338.

- Vitorovic, D., Djordjevic, M., Amblès, A. and Jacquesy, J. C. (1984) 'Multistage alkaline permanganate degradation of a type II kerogen', *Organic Geochemistry*, 5, (4), pp. 259-265.
- Waldo, G. S., Mullins, O. C., Penner-Hahn, J. E. and Cramer, S. P. (1992) 'Determination of the chemical environment of sulphur in petroleum asphaltenes by X-ray absorption spectroscopy', *Fuel*, 71, (1), pp. 53-57.
- Ward, J. J., Kirner, W. R. and Howard, H. C. (1945) 'Alkaline Permanganate Oxidation of Certain Condensed Cyclic Compounds Including coal', *Journal of Organic Chemistry*, 67, pp. 246 - 253.
- Watson, D. F. and Farrimond, P. (2000) 'Novel polyfunctionalised geohopanoids in a recent lacustrine sediment (Priest Pot, UK)', *Organic Geochemistry*, 31, (11), pp. 1247-1252.
- Watts, R. J., Haller, D. R., Jones, A. P. and Teel, A. L. (2000) 'A foundation for the risk-based treatment of gasoline-contaminated soils using modified Fenton's reactions', *Journal of Hazardous Materials*, B76, pp. 73-89.
- Watts, R. J. and Stanton, P. C. (1999) 'Mineralization of sorbed and napl-phase Hexadecane by catalyzed hydrogen peroxide', *Water Research.*, 33, (6), pp. 1405 -1414,.
- Wiberg, K. B. (1965) 'Oxidation by Chromic Acid and Chromyl Compounds', in Wiberg, K. B.(ed), *Oxidation in Organic Chemistry Part A*. Vol. 5 New York: Academic Press, pp. 443.
- Wiberley, S. E. and Gonzalez, R. D. (1961) 'Infrared Spectra of Polynuclear Aromatic Compounds in the C-H Stretching and Out-of-Plane Bending Regions', *Applied Spectroscopy*, 15, pp. 174-177.
- Wignall, P. B. (1994) *Black Shales*. Oxford: Oxford University Press.
- Will, J. M. and Peattie, D. K. (1990) *North sea oil and gas reservoirs-II : proceedings of the 2nd North Sea Oil and Gas Reservoirs conference*. Trondheim, Norway, May 8-11, 1989 The Norwegian Institute of Technology, Graham and Trotman.
- Wilson, M. A., Pugmire, R. J., Karas, J., Alemany, L. B., Woolfenden, W. R., Grant, D. M. and Given, P. H. (1984) 'Carbon distribution in coal and coal macerals by cross-polarization magic angle spinning carbon-13 nuclear magnetic resonance spectroscopy', *Anal. Chem.*, 56, pp. 933 943.
- Wilson, M. A. and Vassallo, A. M. (1985) 'Developments in high-resolution solid-state¹³C NMR spectroscopy of coals', *Organic Geochemistry*, 8, (5), pp. 299-312.
- Wilt, B. K., Welch, W. T. and Rankin, J. G. (1998) 'Determination of Asphaltenes in Petroleum Crude Oils by Fourier Transform Infrared Spectroscopy', *Energy & Fuels*, 12, (5), pp. 1008-1012.
- Xu, S. and Sun, Y. (2005) 'An improved method for the micro-separation of straight chain and branched/cyclic alkanes: Urea inclusion paper layer chromatography', *Organic Geochemistry*, 36, (9), pp. 1334-1338.

- Yarranton, H. W., Alboudwarej, H. and Jakher, R. (2000) 'Investigation of asphaltene association with vapor pressure osmometry and interfacial tension measurements', *Ind. Eng. Chem. Res.*, 39, pp. 2916 – 2924.
- Yen, T. F., Erdman, J. G. and Pollack, S. S. (1961) 'Investigation of the Structure of Petroleum Asphaltenes by X-Ray Diffraction', *Anal. Chem.*, 33, (11), pp. 1587-1594.
- Yen, T. F., Wu, W. H. and Chilingar, G. V. (1984) 'A Study of the Structure of Petroleum Asphaltenes and Related Substances by Infrared Spectroscopy', *Energy Sources, Part A: Recovery, Utilization, and Environmental Effects*, 7, (3), pp. 203 - 235.
- Zumberge, J. E. (1987) 'Terpenoid biomarker distributions in low maturity crude oils', *Organic Geochemistry*, 11, (6), pp. 479-496.